EUROPEAN SCIENCE FOUNDATION

NuPECC

Nuclear Physics European Collaboration Committee (NuPECC)

Nuclear Physics for Medicine

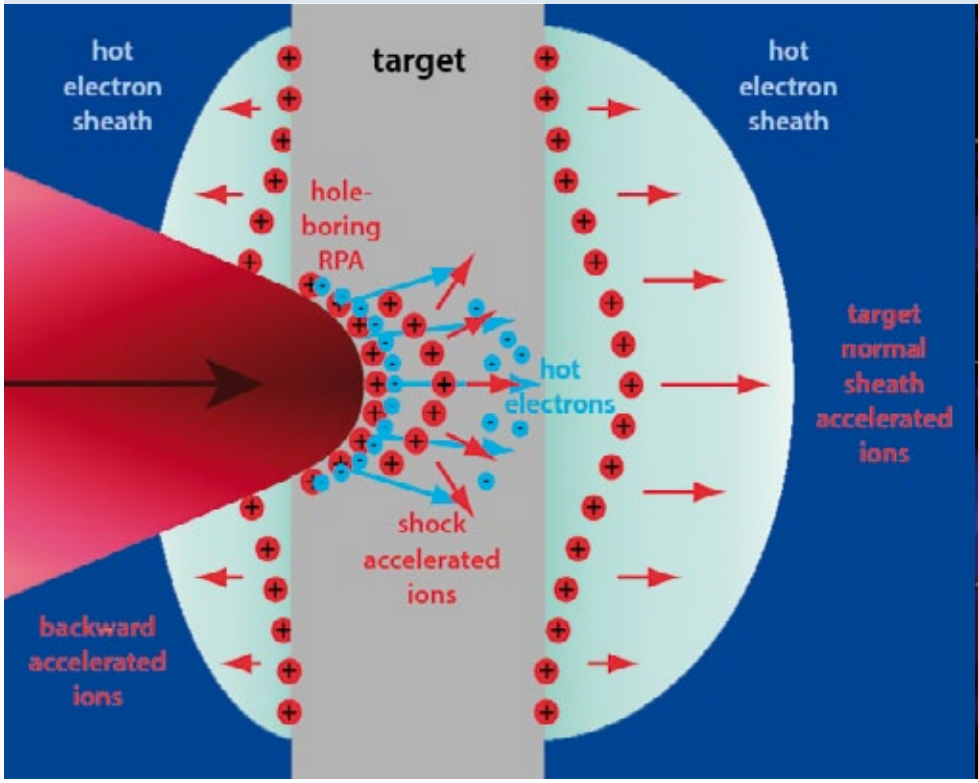

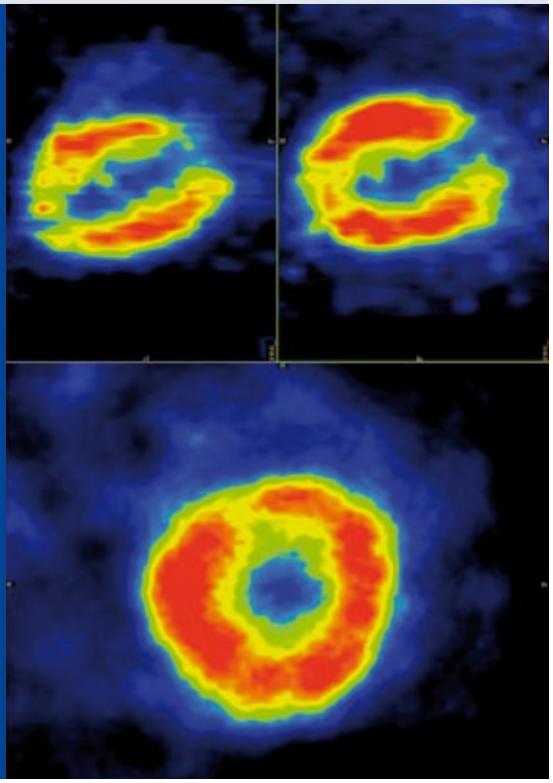

European Science Foundation (ESF)

The European Science Foundation (ESF) was established in 1974 to provide a common platform for its Member Organisations to advance European research collaboration and explore new directions for research. It is an independent organisation, owned by 66 Member Organisations, which are research funding organisations, research performing organisations and academies from 29 countries. ESF promotes collaboration in research itself, in funding of research and in science policy activities at the European level. Currently ESF is reducing its research programmes while developing new activities to serve the science community, including peer review and evaluation services.

www.esf.org

The European Science Foundation hosts six Expert Boards and Committees:

- The European Space Sciences Committee (ESSC)
- The Nuclear Physics European Collaboration Committee (NuPECC)
- The European Marine Board (EMB)
- The European Polar Board (EPB)
- The Committee on Radio Astronomy Frequencies (CRAF)
- The Materials Science and Engineering Expert Committee (MatSEEC)

In the statutory review of the Expert Boards and Committees conducted in 2011, the Review Panel concluded unanimously that all Boards and Committees provide multidisciplinary scientific services in the European and in some cases global framework that are indispensable for Europe's scientific landscape, and therefore confirmed the need for their continuation.
The largely autonomous Expert Boards and Committees are vitally important to provide in-depth and focused scientific expertise, targeted scientific and policy advice, and to initiate strategic developments in areas of research, infrastructure, environment and society in Europe.

Nuclear Physics European Collaboration Committee (NuPECC)

NuPECC is an Expert Committee of the European Science Foundation. The aim of NuPECC is to strengthen collaboration in nuclear science by promoting nuclear physics, and its trans-disciplinary use and application, in collaborative ventures between European research groups, and particularly those from countries linked to the European Science Foundation (ESF). NuPECC encourages the optimal use of a network of complementary facilities across Europe, provides a forum for discussing the provision of future facilities and instrumentation, and advises and makes recommendations to the ESF and other bodies on the development, organisation, and support of European nuclear research, particularly on new projects. The Committee is supported by its subscribing institutions which are, in general, member organisations of the ESF involved in nuclear science and research or research facilities.

www.nupecc.org

Nuclear Physics for Medicine edited by:
Faiçal Azaiez, Angela Bracco, Jan Dobeš, Ari Jokinen, Gabriele-Elisabeth Körner, Adam Maj, Alexander Murphy and Piet Van Duppen

For further information contact:

• **Professor Angela Bracco**
NuPECC Chair
Università degli Studi di Milano
Dipartimento di Fisica and INFN sez. Milano
Via Celoria 16 – 20133 Milano – Italy
Tel: +39 02 50317252
Email: bracco@mi.infn.it

• **Dr Gabriele-Elisabeth Körner**
NuPECC Scientific Secretary
c/o Physik-Department E12
Technische Universität München
85748 Garching – Germany
Tel: +49 172 89 15 011 / +49 89 2891 2293
Email: sissy.koerner@ph.tum.de

http://www.nupecc.org/index.php?display=staff/contacts

Cover pictures:
Top: Nuclei consist of protons (red) and neutrons (blue), which are each made up of three elementary quarks held together by gluons.
Below: (left) Advanced approaches to high intensity laser-driven ion acceleration, see page 123.
(Right) Image of an FDG-injected rat heart obtained in a small PET scanner for molecular imaging, see page 69.

ISBN: 978-2-36873-008-9

Contents

Foreword

Nuclear physics is a coin that has two sides: basic research and applications. Without basic research there would be little to be applied; applications resulting from basic research contribute to the wealth and health of society.

Modern medicine benefits tremendously from nuclear physics, both for diagnosis and for therapy. Therefore NuPECC initiated this report "Nuclear Physics for Medicine", with its three main sections: hadrontherapy, medical imaging and radioisotope production – topics that are actively and widely pursued in Europe and abroad.

Following the successful model of previous NuPECC reports, conveners were engaged by NuPECC members and Working Groups were set up for the three topics. NuPECC members and in particular NuPECC liaisons have followed and discussed thoroughly the various steps necessary to prepare this report. The draft reports were published on the NuPECC website and discussed at an open meeting in Paris on 18 November 2013. The input received from the community was incorporated, resulting in the report now at hand.

We wish you enjoyable reading!

Angela Bracco
NuPECC Chair

Gabriele-Elisabeth Körner
NuPECC Scientific Secretary

Introduction

The present report is one of the initiatives launched by NuPECC after the successful publication of its latest Long Range Plan "Perspectives for Nuclear Physics in Europe" in 2010 (see www.nupecc.org/pub/lrp10/lrp2010_final_hires.pdf). Thus it represents a contribution towards fulfilling the mission of this expert committee of the European Science Foundation.

While most nuclear physics phenomena are far beyond our daily experience there is a great variety of related techniques and applications such as those in medicine which have considerable impact on society.

The development of nuclear physics since the first discovery of the atomic nucleus by Rutherford in the early 20th century has been intimately tied to the development of new detection techniques, accelerators and to theoretical and simulation frameworks. A large number of these have found, and will increasingly find, applications in daily life, well outside the realm of nuclear physics and indeed of physics itself. Nuclear physics methods find increased applications within trans-disciplinary areas as diverse as energy, nuclear waste processing and transmutation, climate change containment, life sciences and cancer therapy, environment and space, security and monitoring, materials science, cultural heritage, arts and archaeology. Comprehensive surveys on the impact of nuclear physics were issued by NuPECC in 1994 and in 2003 with two reports on 'Impacts and Applications of Nuclear Physics in Europe' – see www.nupecc.org/pub/impact_applications_1994.pdf and www.nupecc.org/pub/impact_applications_interactions_2002.pdf, respectively. Since then nuclear physics has progressed and new ideas have emerged leading to developments of technological interest.

In the last Long Range Plan of NuPECC, issued in 2010, suggesting directions and a strategy in the field, one important recommendation concerns applications. In particular it was stated that further development of the nuclear physics skills base has to be pursued in view of current and future needs and these include of course the life sciences. One important question in this connection is: how can nuclear physics techniques improve medical diagnostics and contribute to cancer therapy? It is on this specific question that we have decided to focus and thus to issue this report prepared by a group of distinguished expert researchers, who have contributed a great deal and at a high level, to answer to these key questions.

It is important to stress that laboratories with focus on research in accelerator-based nuclear physics and on the related accelerator, detector, and isotope-production technology contribute (always indirectly but very often directly) to developments in nuclear medicine. Indeed not only can the best suited isotopes used for medical imaging and treatment be produced and developed with those accelerators, but the techniques used by nuclear physicists to peer "inside" the nucleus can be used to image and trace these agents inside the body to study human health and diseases.

In a multidisciplinary vision, the knowledge of nuclear physics provides fundamental support to the requests of many specialist physicians, such as oncologists, radiologists, radiotherapists, and nuclear medicine specialists, looking to guarantee early detection of disease and to select the most appropriate therapeutic strategies.

Life sciences projects in nuclear physics laboratories are literally saving lives every day. This is commonly the case in European laboratories, which also contribute by providing considerable expertise and advice to other centres which are fully dedicated to nuclear medicine. The new infrastructures in Europe for the production and study of radioactive beams offer in particular, because of their cutting edge technological advances, interesting opportunities for new developments from which nuclear medicine will benefit. NuPECC has decided to put emphasis on these aspects in this report.

In applying nuclear physics in medicine, constructive interaction with physicians is central. What do physicians ask of nuclear physics? And what is the medical and physical point of view of hadrontherapy, medical imaging and radioisotope production?

The answers to these questions are various and require some consideration and are addressed to some extent in this booklet.

In the footsteps of the alchemists

Paracelsus, a famous alchemist and medicus of the early 16th century stated: "Many have said of alchemy, that it is for the making of gold and silver. For me such is not the aim, but to consider only what virtue and power may lie in medicines." With the discovery of nuclear transmutation by Rutherford and Soddy and the first artificial transmutations by the Joliot-Curies, the alchemists' dream was eventually realised by nuclear physics and radiochemistry. Today, 500 years after Paracelsus, we may therefore conclude: "Many have said of nuclear physics, that it is for the making of new gold and silver (and other elements') isotopes. For us such is not the only aim, but also to consider what virtue and power may lie in these for medicine."

This report is organised into three chapters: the first on hadrontherapy, the second on medical imaging and the third on radioisotope production. These topics are interlinked but the underlying technological developments have their own history and peculiarities that will be stressed in these chapters. On the other hand the influence of new techniques and of particular improvements in each of these topics on the others is well stressed in the three chapters.

A principal theme of Chapter 1 is the progress made in radiation oncology in recent years driven by the use of hadrons (particles subject to the strong force) such as protons and atomic nuclei (ions). This frontier in radiation therapy, recognised and pursued worldwide, is illustrated together with new on-going developments. Key issues for hadrontherapy are the selectivity of the release of energy, the collimation of the particles, the availability of dedicated proton and/or ion accelerators, and the integration of diagnostic imaging results. One can see that the contribution of nuclear physics to hadrontherapy has been enormous in the past and can lead to further advances in the future. In this regard, exploitation of new technologies in the nuclear physics research will play a major role.

Chapter 2, devoted to imaging, illustrates how the techniques for producing images of various body parts using radioactive tracers have progressed over the years. The main point of this chapter is to emphasise how nuclear physics research has always been involved in medical imaging advances. Developments in medical imaging parallel advances in instrumentation for nuclear physics experiments, sharing methods, techniques, and manufacturers. Emphasis is given to the interplay of detector design and simulation and reconstruction models. A point of major focus is quality control in hadrontherapy. This chapter also briefly describes some applications in medical imaging of mass spectrometry, which is playing an important role in the modern facilities producing radioactive beams.

The focus of Chapter 3 is radioactive isotope production methods and their use for nuclear medicine. Particular attention is given to new and different strategies for producing isotopes for medical use. Indeed radionuclides are the essential fuel that is driving all nuclear medicine applications. With few exceptions the required radionuclides are not present in natural decay chains, so have to be produced by artificial transmutation driven by particle accelerators in nuclear physics facilities or reactors. It is important to stress that advances in the production of new radioactive isotopes come out of accelerator and research reactor centres that have nuclear physics research as their main goal, making this enterprise surely one of the important spin-offs from nuclear physics laboratories dealing with light and heavy ion accelerators.

In general, accelerator and research reactor centres play a key role in education and training of scientists and technical personnel for nuclear medicine activities. They certainly provide this sector with a very inspiring environment for new ideas and innovative techniques.

As a final remark it is worth noting that the booklet is not intended to be a position paper. Rather, it gives an updated overview of how fundamental nuclear physics research (in its broadest sense) has had and will continue to have an impact on developments in medicine.

With this document the NuPECC expert committee intends to inform the scientific community (beyond the nuclear physics community), funding agencies and policy makers in research of the latest developments in nuclear medicine driven by the technical efforts currently underway in nuclear physics facilities. As with previous Framework Programmes, it is important to be engaged in and committed to nuclear physics projects within Horizon 2020 that will enhance the mutual roles of fundamental and applied nuclear research.

Chapter I
Hadrontherapy

Conveners: **Marco Durante** (GSI) – **Sydney Galès** (Orsay, FAIR, ELI)

1.
Introduction

Two successive, comprehensive surveys of the impact of fundamental nuclear physics in medicine, or more precisely of the use of ionising radiation in the fight against cancer, were published by NuPECC in 1994 [1] and 2003 [2]. These reports have shown the very strong interface between physics, biology and medicine and the intense collaborations between physicists, biologists and physicians through the development of novel methods and instruments, which have had a large impact on our healthcare systems. In this spirit the present chapter on "hadrontherapy" gives an updated view on the current developments on the growing use of particle accelerators and associated equipment and methods in this field.

In 1946, accelerator pioneer Robert Wilson laid the foundation for hadrontherapy with his article in *Radiology* about the therapeutic interest of protons for treating cancer [3]. Today, cancer is the second highest cause of death in developed countries. Its treatment still presents a real challenge.

Hadrontherapy is an innovative cancer radiotherapy modality based on nuclear particles (protons, neutrons and light ions) for treatment of early and advanced tumours. Today proton therapy has grown into an advanced, cutting-edge clinical modality. Around 100,000 patients worldwide have been treated with protons since the establishment of the first hospital-based treatment centre in Loma Linda, California, in 1990. More than 10,000 have been treated with heavier ions, generally carbon. Various companies are now offering turn-key solutions for medical centres. Figure 1.1 shows the exponential grow of proton therapy centres around the world from 1950 to 2015.

The benefits of hadrontherapy are based both on physical (better ballistic accuracy) as well as biological reasons (especially for heavy ions), resulting in more accurate and efficient irradiation of the tumour, thereby reducing the dose to the surrounding healthy tissue and thus leading to a lower integral dose delivered to the whole body and lower

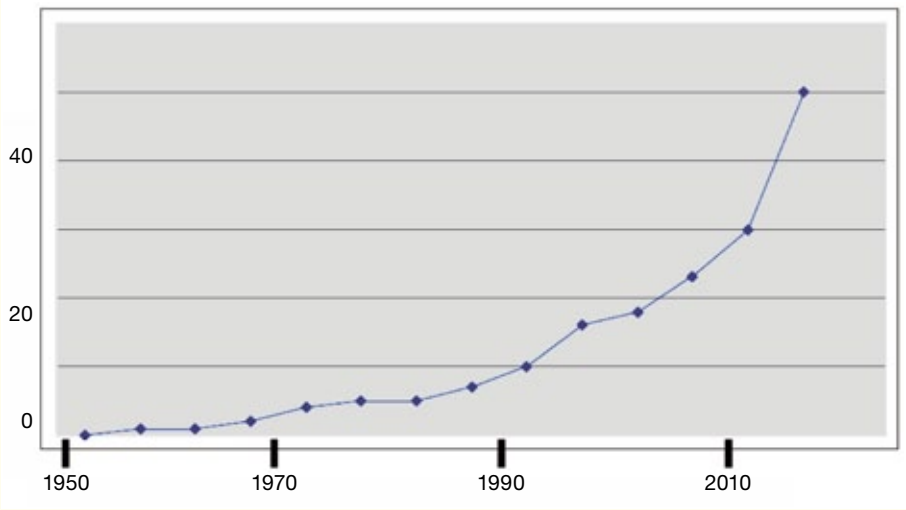

Figure 1.1.
Evolution of the number of proton therapy centres in the world between 1950 and 2015.

morbidity. Clinical interest in hadron therapy resides in the fact that it delivers precision treatment of tumours, exploiting the characteristic shape of the Bragg curve for hadrons, i.e. dose deposition as a function of depth of matter traversed. While X-rays lose energy slowly and mainly exponentially as they penetrate tissue, charged particles release more energy at the end of their range in matter – the Bragg peak. The Bragg peak makes it possible to target a well-defined region at a depth in the body that can be tuned by adjusting the energy of the incident particle beam, with reduced damage to the surrounding healthy tissue. The dose deposition is so sharp that new techniques had to be developed to treat the whole target. These fall under the categories of passive scattering, where one or more scatterers are used to spread the beam, or scanning, where a variable energy small pencil beam is moved through different slices of the tumour, reaching an unprecedented conformity of the target. To allow full flexibility in patient treatment, the accelerator should be coupled to an isocentric beam delivery system called "gantry".

Hadrontherapy is the epitome of a multidisciplinary and transnational venture: its full development requires the competences of physicists, physicians, radiobiologists, engineers and IT experts, as well as collaboration between research and industrial partners.

The history of hadrontherapy in Europe has been largely driven and influenced by nuclear physics. In the 1970s the European community was very much interested in pions, with a pilot project, PSI (Villigen, Switzerland). By the end of the 1980s it became clear that there was no clinical benefit to patients and that a cost-effective treatment was not possible because of the high cost of pion production. Pion therapy was terminated, and PSI switched to high-energy protons, building on their running proton therapy trial for ocular tumours. Proton therapy was already active in Russia, but it was not yet very popular in Western Europe. A few milestones toward its current widespread use (see Section 2, Figure 2.2) are summarised below.

• Pion therapy worldwide

Vancouver 1979–1994:	367 patients
Villigen 1980–1993:	503 patients
Los Alamos 1974–1982:	230 patients

• Proton therapy Villigen

1974: Ocular treatments 72 MeV
passive beam spread

1996: deep seated tumours 230 MeV ring cyclotron
Active beam delivery: horizontal magnetic deflection
Vertical: patient shift
Depth: degrader

• Other European therapy projects (no ocular treatments)

Russia: protons

1969	Moscow ITEP
1975	St. Petersburg
1999	Dubna

Sweden:

1989	Uppsala

France project:

1991	Creation of the Orsay Proton Therapy Centre (CPO), a hospital unit with exclusive use of the 201 Mev proton synchrocyclotron, under the auspices of a consortium comprising the Institut Curie, the Institut Gustave-Roussy (Villejuif), the Centre René-Huguenin (Saint-Cloud) and the Paris Public Hospitals (AP-HP).

- In November 2006: The Institut Curie officially launched an ambitious programme to extend its cancer treatment replacing the old synchrocyclotron with a 250MeV proton accelerator and a gantry
- Since 1991: More than 5,000 patients treated at the Centre between 1991 and 2010

2012	Launch of the project France Hadron for research and creation of infrastructures in particle therapy

German proposals and projects:

Heidelberg:

1973	MPI and DKFZ 200 MeV protons
1977	Large proposal same partners not funded by BMBF

Darmstadt / Heidelberg:

1982	Zero proposal: not finished
1988	First proposal Wannenmacher (Radiology Heidelberg) Lorenz (DKFZ), Kienle (GSI)
1990	Intermediate proposal for EU
1992	Second proposal (Wannenmacher, Specht

GSI, zur Hausen DKFZ)
The second proposal was never decided by BMBF but the partners started to construct the facility at GSI: The so called

GSI Pilot project:

- Start construction: May 1993 FZ Dresden joints the project
- December 1997 start treatment
- New options: 3 D scanner, biological treatment planning, in vivo PET
- End of project July 2008 after 440 patients treated

Heidelberg Ion beam Therapy HIT:

- September 1998 Proposal to BMBF
- 2003 positive decision by BMBF start construction at Heidelberg
- Layout and technical part: GSI
  medical part: Siemens
- Estimated total costs 35 Mio €
- 2009 start treatment: ca. 1500 patients treated up to now

München:

- Rinecker proton project proposal February 2002
- 2013: 1500 patients

Austria: MedAustron:

- May 1993 Austron project was proposed: spallation source for neutrons
- By the end of the 90s the idea of the neutron spallation source died but the medical project survived
- December 1998: Feasibility study I+II+III authors Pötter, Auberger; Regler
- 2006 New leadership Projekt Entwicklungs Gruppe PEG
- At present the synchrotron is installed and patient treatment is expected in 2 years

CERN:

EULIMA European light ion medical accelerator

- October 1987 start supported by EU Bruxelles
- Main contractor Centre A. Laccasagne, Nice: Pierre Mandrillon
- Univ. Catholique Louvain, MRC & Gray lab. IN2P3
- 1988 GSI became member

PIMMS proton ion medical machine study

- Members: MedAustron, TERA, CERN, Onkologie 2000 (Prague) CERN, GSI (not active)
- PIMMS was used for MedAustron at Wiener Neustadt and CNAO, Pavia

ENLIGHT European network light ion therapy: start 2002

- Currently the largest community of scientists interested in hadrontherapy, from different disciplines (http://enlight.web.cern.ch)

Exhibition **Hadrons for Health**, supported by CERN, TERA foundation, INFN, GSI and many local institutions, which was shown in the period 1995–2002 in more than 20 venues around Europe

In this chapter, a description of the world map of hadrontherapy centres and their development will be presented. Accelerator facilities have also evolved in recent decades, going from fundamental research laboratories, conceived and built mostly by academic research teams, to turn-key industrial ensembles. Innovations on very precise and new delivery and dosimetry, including range control and dosimetry, are under study. Very precise simulation and modelling of both beam characteristics and patient target area are nowadays used to ensure maximum efficiency associated with minimum irradiation of healthy surrounding tissue. Fundamental research on radiobiology will be discussed.

State-of-the-art techniques borrowed from particle accelerators and detectors are increasingly being used in the medical field for the early diagnosis and treatment of tumours and other diseases; medical doctors and physicists are now working together and are able to discuss global strategies. The revolution in image-guided radiation therapy (IGRT) will have an enormous impact in cancer therapy. While developing and optimising the next-generation facilities remains the community's primary goal, it is also of paramount importance that existing centres collaborate intensively and that researchers, clinicians and patients have protocols to access these structures. Hadrontherapy is a field in its infancy and in a clinical research phase with great potential.

References

[1] NuPECC, Impact and Applications of Nuclear Science in Europe: Opportunities and Perspectives. *NuPECC Report* 1994, ESF.

[2] NuPECC, Impact, Applications, Interactions of Nuclear Science. *NuPECC Report* 2003, ESF.

[3] R.R. Wilson. (1946). Radiological use of fast protons. *Radiology* **47**: 487–491.

2. Facilities in operation and planned

2.1 Historical development of hadron radiotherapy facilities

The rationale of using heavy charged particles in cancer radiotherapy was originally formulated in 1946 by Robert R. Wilson, the subsequent founding director of FermiLab, at that time working at Harvard University. He realised that by exploiting the high dose deposit (Bragg peak) at the end of the particle trajectory, the absence of dose beyond the particle range and the sharp lateral penumbra produced by heavy charged particle beams can be used to produce a dose distribution that is highly conformal to the target volume while sparing the surrounding healthy tissue. Patient treatment started in 1954 at the Radiation Laboratory in Berkeley with proton, deuteron and helium ion beams from the 184 inch synchrocyclotron. In Europe patient treatments with protons started in 1957 at the Gustaf Werner Institute in Uppsala, Sweden.

From the 1960s to the mid-1980s particle radiotherapy was based exclusively on accelerator facilities developed for nuclear physics, with beamlines and treatment rooms adapted to the needs of radiotherapy. Significant numbers of patients were treated at the Harvard Cyclotron Laboratory, the Gustav Werner Institute in Uppsala, the Paul Scherrer Institute in Villigen, the Institute of Theoretical and Experimental Physics (ITEP) in Moscow, the Joint Institute of Nuclear Research in Dubna, the Leningrad Institute of Nuclear Physics in Gatchina, the National Institute of Radiological Sciences, Chiba and the University of Tsukuba, Japan. At the National Accelerator Centre in South Africa, nowadays called iThembaLABS, 200 MeV protons have been used to treat cancer patients since 1993.

A new era in particle therapy started with the construction and installation of dedicated accelerators in hospital-based clinical centres. The first was the MC60 62.5 MeV proton cyclotron, delivered by Scanditronix, operating at the Clatterbridge Oncology Centre (UK) since 1989. The cyclotron has been used for fast neutron radiotherapy and proton therapy of eye melanoma and is still used (2013) for treatment of ocular tumours. The next major step was the installation at Loma Linda University (California, USA) of a dedicated 250 MeV proton synchrotron, developed by FermiLab, in 1990. It was the first dedicated clinical facility equipped with three rotating gantries.

A major step in particle therapy was the application of scanning beams, which allows "painting" the dose within the tumour volume. This technique results in a significant improvement of the conformity of the dose distribution with the target volume and is thus expected to improve treatment outcome. The first scanning systems were developed in the research facilities at PSI (Villigen, Switzerland) for protons and GSI (Darmstadt, Germany) for carbon ions and have been used to treat patients since 1996 and 1997, respectively. More recently scanning beams have started to be used on a routine basis in several clinical facilities, such as at the Rinecker Proton Therapy Center in Munich.

Since its start in 1954, nearly 110,000 patients had been treated with hadrontherapy by the end of 2012 [1]. Treatments with protons account for over 85% of the total, while treatments with carbon have been used in about 10% of the cases. In the remaining cases ions other than carbon and pions were used. Of the patients treated with protons more than 46% (43000) had ocular tumours. Patients treated with fast neutrons and boron neutron capture therapy (BNCT) are not included in these statistics.

2.2 Proton and carbon ion facilities in operation

2.2.1 Hadrontherapy centres

According to statistics of the Proton Therapy Cooperative Group [1] 39 proton and carbon ion therapy centres were operational at the end of 2012. In three centres only carbon ion treatment is applied (Lanzhou, Gunma, and Chiba), in another three centres both proton and carbon ion beams are used for treatment (Hyogo, Heidelberg and Pavia). Proton therapy is performed in 33 centres worldwide. In the first half of 2013 two ProCure centres in Seattle and Illinois as well as the WPE in Essen were opened and are treating patients with protons. A report of the Corporate Strategic Intelligence (CSIntel) on the market situation and perspectives for proton therapy around the world, published in October 2012 [2], lists 39 active proton and ion therapy facilities with a total of 106 treatment rooms.

Proton gantries are available in 23 centres in the USA, Japan and Europe. A carbon ion gantry is available only at the HIT facility at Heidelberg. In Europe gantries are used to treat patients at PSI Villigen, Rinecker Proton Therapy Center (PTC) in München, Orsay, Heidelberg, Prague and Essen.

In 34 proton therapy centres worldwide proton beams with energies around 200 MeV or higher are used. For treatment of ocular tumours six centres in Europe use proton beams with energies between 60 MeV and 74 MeV: Berlin (Germany), Catania (Italy), Orsay and Nice (France), Clatterbridge (UK), Kraków (Poland), PSI (Switzerland). The advantage of the lower energy cyclotrons is in particular the very sharp distal fall-off and lateral penumbra of the dose distribution. At the moment, no vendor is offering a dedicated low energy proton accelerator for treatment of eye tumours. The map of active proton and carbon ion therapy centres worldwide is shown in Figure 2.1, and a detailed map of those in Europe and Japan is presented in Figure 2.2.

The full list of currently operated and under construction facilities is published and regularly updated on the Proton Therapy Cooperative Group (PTCOG) web page [1].

2.3 Future facilities

2.3.1 Facilities in construction and commissioning

At the beginning of 2013 27 new proton therapy centres around the world were under construction or in the commissioning phase. In Europe five new centres with C-235 cyclotrons and scanning gantries are being installed or commissioned (Trento,

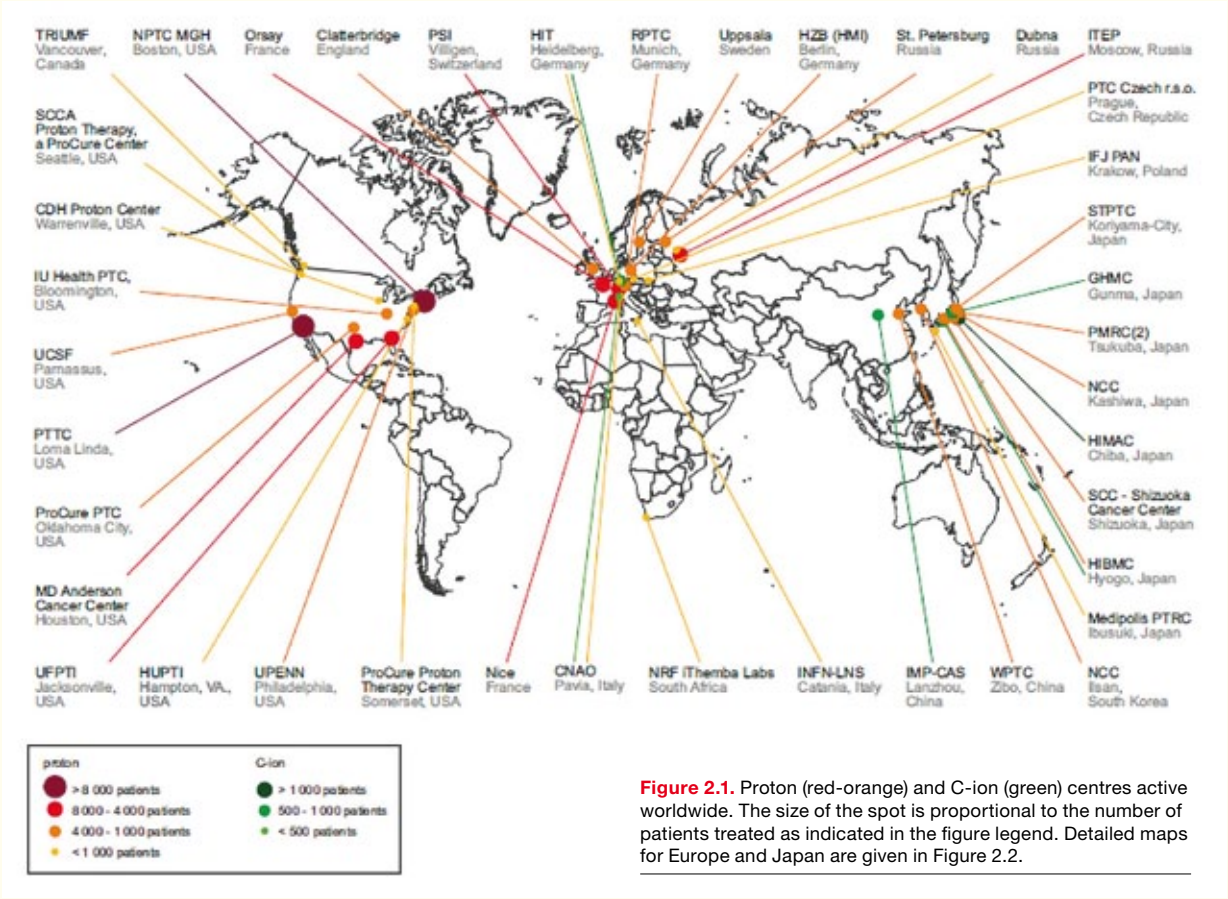

Figure 2.1. Proton (red-orange) and C-ion (green) centres active worldwide. The size of the spot is proportional to the number of patients treated as indicated in the figure legend. Detailed maps for Europe and Japan are given in Figure 2.2.

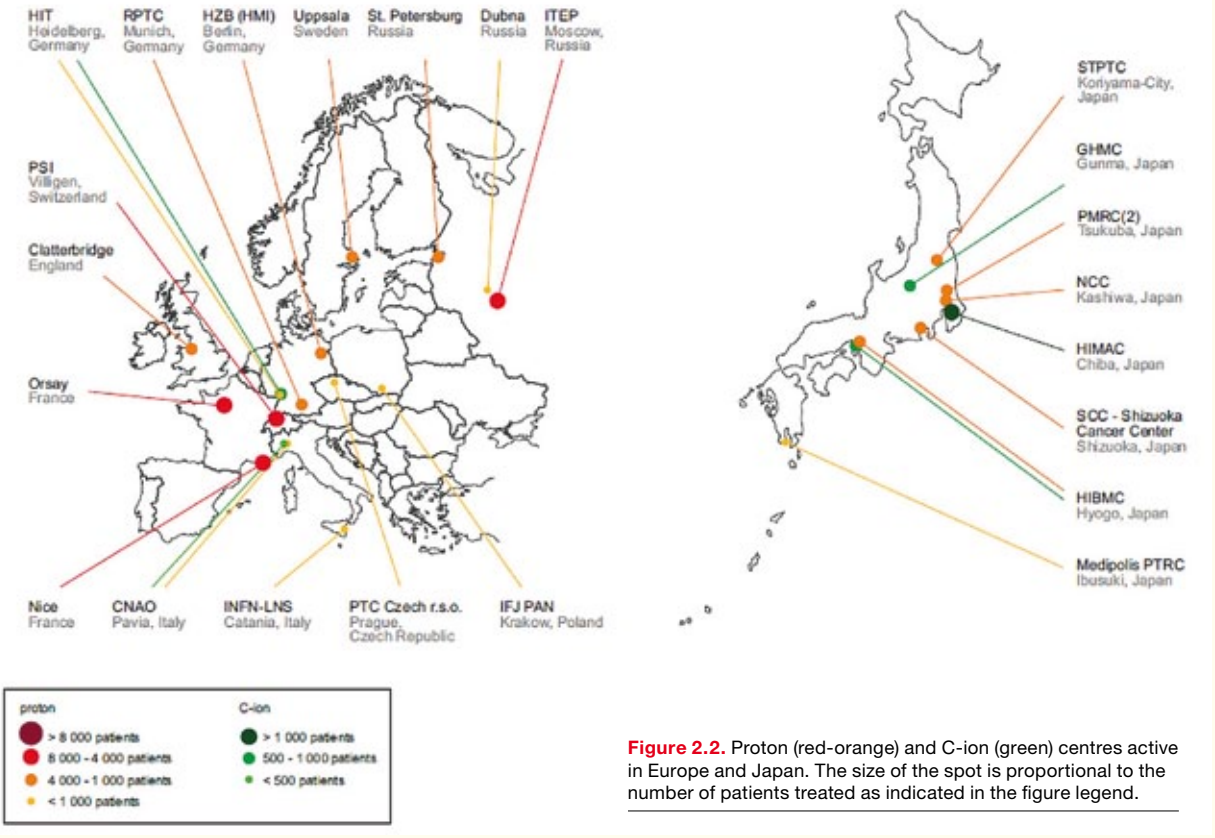

Figure 2.2. Proton (red-orange) and C-ion (green) centres active in Europe and Japan. The size of the spot is proportional to the number of patients treated as indicated in the figure legend.

Kraków, Dresden, Uppsala, Dimitrovgrad). They will start operation in 2013–2015.

Many of these novel facilities present unique innovations. The Oncoray proton therapy facility in Dresden is again based on the IBA Proteus 235 cyclotron, but has already included room for a laser-driven accelerator (Figure 2.3).

The proton therapy centre in Trento (ATreP) is the third in the world (after PSI in Villigen and the Rinecker centre in Munich) to rely only on Pencil Beam Scanning (PBS) as a treatment delivery technique. This gives ATreP probably the best PBS technical specifications available in terms of both spot size and spot position accuracy.

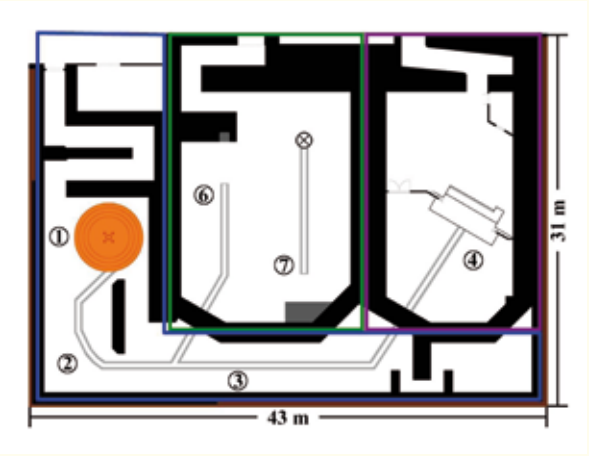

Figure 2.3. Layout of the Dresden proton therapy facility. Conventional proton accelerator and beam transport: cyclotron Proteus 235 (1); energy selection system (2); beam transport (3). Therapy room: isocentric gantry (4); universal nozzle, capacity < 500 pat. p.a. Experimental bunker: conventional p-beam (6); future: laser driven p-beam (7).

In addition to that, it is the first centre where it will be possible to choose among several proton spot sizes to find the best compromise between quality of the dose distribution and treatment delivery time. Some studies suggest that relying on larger spot sizes may allow better compensation for intrafraction motion, and ATreP will be the first where experimental verification of such a hypothesis will be possible. The so-called 'moveable snout' is another interesting innovation available for the first time in this centre. This functionality will allow the range shifter to be brought closer to the patients, thus improving the dosimetric quality of treatment where lower energies (below 70 MeV) are needed to cover the target. Last but not least, the project in Trento is placing great emphasis on the need for high-quality soft tissue imaging in the treatment room prior to treatment. It is now very likely that one of the rooms will have a diagnostic on-rail CT available for patient positioning, thus opening the door not only to treat indications where the bony anatomy is not a reliable surrogate of tumour position, but also to more sophisticated adaptive schemes, where the images acquired just prior to treatment are available for immediate dose

calculation and, when possible, treatment adaptation.

The CCB facility in IFJ PAN Kraków, also based on IBA Proteus 235 cyclotron and possessing two Pencil Beam Scanning gantries, will be operational in 2015. In addition to the therapy programme, the facility will pursue extensive basic studies in nuclear physics, medicine and biology.

The Marburg particle therapy facility, built by Siemens, did not start clinical operation even though it is practically completed because Siemens decided to quit the radiotherapy business. The future of the facility is at the moment very uncertain. In 2014 MedAustron in Wiener Neustadt will be completed. In Nice the acceptance of a superconducting 250 MeV synchrocyclotron ProteusOne with IBA compact gantry is scheduled for 2014. A proton therapy centre at the St. Petersburg Center of Nuclear Medicine of the International Institute of Biological Systems in Russia to be built by Varian is in the planning stage. In Poznań, Poland the PTC is planned to be completed towards the end of 2016. Two centres are planned to be operational by 2017 in Great Britain: at the Christie NHS Foundation Trust in Manchester and University College London Hospital (UCLH). In the Netherlands several proton therapy centres with a total treatment capacity of 2,200 patients per year are being planned; first treatments should take place in 2017. Four locations are being proposed: Amsterdam, Delft, Groningen and Maastricht. The site selection process will be completed in 2013. In Denmark, the construction of the National Center for Particle Radiotherapy (NCPRT) has been approved within the new Aarhus University Hospital. The location at the emerging new Aarhus University Hospital campus will enable easy and rapid construction of the centre, currently planning to enter operation in 2017. In addition to several new PTC in USA and Japan, new centres are planned in India, China, Korea, Taiwan and Saudi Arabia. In Europe, several other proposals have been submitted in Bulgaria (a synchrotron-based centre for protons and heavy ions), Romania (see http://www.icrsh.ro/), and Norway (also in this case, a centre planned for both protons and heavy ions).

2.3.2 New accelerators

According to the report of CSIntel [2], 255 proton therapy treatment rooms will be operational worldwide by 2017, while by 2020 this numbers is expected to increase to about 1,000 particle therapy treatment rooms. These developments in the market are stimulating active research and development towards cheaper and smaller accelerators and gantries.

Several new solutions are being proposed and will be soon introduced for customers. The MEVION S250 is the world's first superconducting synchrocyclotron proton therapy system from Mevion Medical Powered. Four such systems are under installation in USA. Optivus Proton Therapy offers the synchrotron based CONFORMA 3000 but the system has not been clinically used yet. ProTom comes into the market with a compact 330 MeV synchrotron, primarily developed in Russia and the Radiance 330 PT system. CPAC (Compact Particle Acceleration Corporation) has for several years been announcing a highly compact intensity-modulated proton therapy (IMPT) system powered by the dielectric-wall accelerator (DWA), but it remains in the development phase.

References

[1] Particle Therapy Co-Operative Group (PTCOG) webpage http://ptcog.web.psi.ch/

[2] Corporate Strategic Intelligence, *Proton Therapy Market Report*. CSIntell, 2012.

3. Accelerators

3.1 Introduction

The feasibility of radiotherapy with heavy charged particles, in the first instance protons but later on including heavier ions up to ^{40}Ar, first and foremost depends on the availability of accelerators delivering beams with the required characteristics. The historical development of accelerator technology, mainly guided by the needs of subatomic physics research and particle therapy, has led to the use of two distinct types of accelerator to produce the beams for particle therapy: in proton therapy compact isochronous cyclotrons are mainly used, although in some facilities synchrotrons are applied, while for therapy with heavier ions (essentially carbon) at present only synchrotrons are in use. This situation is to a large extent based on the accelerator types capable of delivering beams with the required energy that were available at the time experimental radiotherapy with protons and heavier ions started. Proton therapy started in the 1950s at synchro-cyclotrons, which could easily be replaced with isochronous cyclotrons without changing the techniques used to produce the dose distributions required. Radiotherapy with heavier ions, on the other hand, started in the 1970s and requires beam energies that were well beyond the capability of (synchro-)cyclotrons at that time.

3.2 Historical development

At the time Wilson proposed the use of heavy charged particles for radiotherapy no accelerators capable of producing beams with the required energy (about 230 MeV for protons and roughly 400 MeV/amu for carbon ions are needed to reach any location in the human body) existed. The synchro-cyclotron, based on the phase focusing discovered by Veksler and MacMillan, made it possible to pass the energy limit of the classical cyclotron, caused by relativistic effects, and to achieve for proton and helium beams the energies required to reach deep-seated tumours. The first patient treatment with protons took place in 1954 at the 188 inch synchro-cyclotron at Berkeley, USA, built to make the first explorations into the particle physics zoo. In 1957 the first patients were treated with the 200 MeV synchro-cyclotron at the Gustaf Werner Institute in Uppsala, Sweden. Protontherapy at the 160 MeV synchro-cyclotron at Harvard University, which became the first dedicated proton therapy facility, started in 1961 and continued until 2002.

The beam characteristics of the synchro-cyclotron (~100 Hz pulse rate, low intensity, fixed energy) limited its application to the treatment of static tumours, more in particular brain tumours.

To tailor the dose distribution to the target volume the size of the beam was strongly increased by a sophisticated scatter foil system followed by a rotating energy modulator wheel producing the required dose-depth distribution, a collimator to conform the beam to the tumour shape and a compensator to avoid dose being deposited beyond the tumour. It is relevant to mention that this technique is still being used at the majority of clinical proton therapy facilities today.

The step towards heavier ions, motivated by the radiobiological research of Tobias *et al.* at the Berkeley (Super-)HILAC, required yet another breakthrough in accelerator technology: the development of the heavy ion synchrotron, delivering a pulsed beam with pulse period of 1–10 s. First patient treatments were done at the Berkeley Bevalac with ions from helium to argon using a similar technique

to shape the dose distribution as used for the treatment with protons. Subsequently extensive research programmes on carbon therapy were also established at NIRS (Chiba, Japan), where some 7,000 patients have been treated since 1994, and GSI (Darmstadt, Germany), where over 400 patients have been treated in the period 1997–2009.

The very promising results obtained in particular for the treatment of radiation-resistant tumours with heavier ions have led to a significant effort in Japan and Europe to develop dedicated synchrotrons for carbon therapy that are suitable for installation in a clinical treatment centre. In Europe design studies were made by CERN, realised at CNAO (Pavia, Italy) and MedAustron (Wiener Neustadt, Austria), and GSI (Darmstadt, Germany), realised by Siemens at HIT (Heidelberg, Germany), Rhön Klinikum (Marburg, Germany) and Fudan University (Shanghai, China). In Japan three carbon therapy centres were built (NIRS, Chiba; Hyogo and Gunma) by different Japanese manufacturers, while several more are under construction.

The advent of highly sophisticated computer control of accelerators has enabled the development of much more sophisticated irradiation techniques:

- The narrow beam from the accelerator is actively scanned over the area to be irradiated by means of accurately tuned magnets. This so-called spot or raster scanning technique has been pioneered at the research facilities at PSI (Villigen, Switzerland) and GSI (Darmstadt, Germany) since the mid-1990s. It is now being transferred to clinical treatment centres and is gradually replacing the scattering technique developed at Harvard.
- The energy of the beam extracted from a synchrotron can be varied on a pulse-to-pulse basis or even within one pulse. By using this technique the penetration depth of the ions can be adjusted, which in combination with the spot/raster scanning technique results in a volume scan. This technique has been developed at GSI and is now also being applied at synchrotron based clinical centres for carbon and/or proton therapy: HIT (Heidelberg, Germany), CNAO, (Pavia, Italy), MDAnderson (Houston, USA). It will also be used at the MedAustron-facility (Wiener Neustadt, Austria), which is under construction.
- Cyclotrons deliver a fixed energy beam, so it is not possible to vary the penetration depth by varying the primary beam energy. Instead a variable thickness energy degrader in combination with an energy analysing system consisting of several magnets is used to tune the energy to the required value.

3.3 Microbeams

Low-energy accelerators have been used for many years for pre-clinical research in hadrontherapy. A large amount of data on the relative biological effectiveness (RBE) of charged particles has been gathered in low-energy van der Graaf, Tandem, or Linacs (see Chapter 7 and https://www.gsi.de/bio-pide for a database of RBE data including low-energy accelerators). A special case is the microbeam, where it is possible to target single cells (or sub-cellular structures) with a pre-defined number of charged particles. Complex imaging systems are necessary for positioning and visualising the cellular or sub-cellular targets, and the sub-micrometre accuracy in particle delivery is achieved either with collimators or, more frequently in the new machines, by magnetic focusing.

Microbeams started operation about 30 years ago, and have decisively contributed to fundamental new discoveries in radiobiology. The microbeam community holds regular meetings: the 11th meeting was held in Bordeaux (France) in October 2013 (http://www.cenbg.in2p3.fr/microbeam2013/) and the 12th will be in Fukui (Japan) in 2015 (http://www.microbeam-jp.org/iwm2015/). A list of the current active microbeam facilities employed for targeted irradiation of living cells is reported in Table 3.1.

3.4 Beam features for a hadrontherapy centre

The use of hadrons, particularly protons, in radiotherapy is a major innovation in the fight against cancer. However, the level of the definitions and specifications of a hadron beam is not yet as well defined as for other more conventional radioactive therapies. In this regard we should introduce the following definitions and specifications in accord with our experience and the data available in the literature. Increased selectivity ballistics of hadrons, compared with photons and electrons used in conventional radiation therapy, requires compliance with stringent specifications on the distribution of dose in order to achieve a highly conformal 3D therapy.

The general characteristics that each hadrontherapy centre must have are:

- ability to treat most cancers at any depth;
- treatment times as short as possible;
- high ability to discriminate between the volume to be treated and the healthy tissue that surrounds it and high dose uniformity in volume treated;

Table 3.1.
Charged particle microbeams for targeted irradiation of living cells. The list was constructed from the facilities reported at the last two microbeam workshops (period from 2010 to 2013). Table courtesy of Dr Philippe Barberet, CENBG, France.

	Laboratory	Location	Ion species	Energy range
Inside Europe	GSI	Darmstadt, Germany	C to U rarely p, He, Li	1.4–11.4 MeV/u
	SNAKE	Munich, Germany	p, He, Li, Be, B, C, O, F, Si, Cl, I	p: 4–28 MeV He: 1.4–10.5 MeV/u Li–O: 1–8 MeV/u Si, Cl: 1–4 MeV/u I: 05–2 MeV/u
	Ion Beam Centre	Surrey, UK	p to Ca	P: 4MeV He: 6MeV O: 12 MeV
	PTB	Braunschweig, Germany	p, He	2–20 MeV
	CENBG	Bordeaux, France	p, He	1–3.5 MeV
Outside Europe	RARAF	New York, USA	p, He	1–5 MeV
	JAERI	Takasaki, Japan	He, C, Ne, Ar	He: 12.5 MeV/u C: 18.3 MeV/u Ne: 13 and 17.5 MeV/u Ar: 11.5 and 13.3 MeV/u
	SPICE/NIRS	Chiba, Japan	p	3.4 MeV
	IMP	Fudan, China	p, He	6 MeV
	IMP	Lanzhou, China	C	Several to 100 MeV/u

- availability of treatment rooms with access for fixed and orientable beam lines;
- high accuracy (≤ 3%) in absolute and relative dosimetry;
- reliable control systems.

It is therefore necessary to define a beam of hadrons in terms of path, modulation of the Bragg peak, adjustment of the depth of penetration (range), dose rate, field size, uniformity and symmetry of the field, lateral penumbra and distal fall off.

The required characteristics of the hadron beams used for the treatment have a decisive influence in the choice of accelerator to use.

If one considers the dose curve as a function of depth, practical range defines the distance between the surface of the input beam of protons and distal point where the dose is reduced by 10%. It depends, usually, on the beam energy and materials along the beam line (tools for monitoring the beam, tools for adaptation range and beam modulation). The range of a beam of 250 MeV protons is approximately 38 cm in water. The equivalent energy demanded for a carbon ion beam is equal to 400 MeV/amu. The minimum range required for a line dedicated to the treatment of deep tumours is 22 cm in water. In the case of lines devoted to the treatment of shallow tumours such as in the eye, treatments require energy protons between 60 and 70 MeV, whose range is 3–3.5 cm in water. The range of the beam should be adjustable in steps of 0.2 mm in water for depths of less than 5 cm and in steps of at most 1 mm for depths larger than 5 cm. This can be achieved by either changing the energy of the beam or inserting an absorber in front of the patient (Range Shifter). The latter solution has the greater inconvenience in that it produces neutrons and light fragments (only in the case of ions) and that it deteriorates the geometric characteristics of the beam (emittance increase). Therefore it can only be used when the penetration depth of the beam is no more than 4–5 cm. When larger penetration depths are required it is highly preferable to reduce the beam energy with a properly shielded degrader outside the treatment room. This solution is always recommended in the case of using ions heavier than protons.

The longitudinal width of the Bragg peak is enlarged by varying the particle energy upon entrance in the patient's body in order to deposit a homogeneous dose throughout the tumour. This so-called Spread-Out Bragg Peak (SOBP) is defined as the distance between the proximal and distal points on the dose-depth curve where the dose is reduced to 95% compared to the value in the flat part of the SOBP. The SOBP width should be variable in 0.1–0.2 mm steps in water for beams with an energy lower than 70 MeV and in 1 to 2 mm steps for higher energy.

The field size should be different for fixed lines and lines with a rotating gantry. For fixed horizontal beams, used in the treatment of ocular tumours, field sizes between 5 and 35 mm in diameter are needed. For horizontal beams used to treat diseases of the head and neck, the field size requirements vary from 2x2 to 15x15 cm^2. For other lines of horizontal and vertical beam, as those with the gantry, field size requirements vary from 2x2 to 40x40 cm^2. In any case, it should be possible to adjust the field in steps of 1 mm with an overall accuracy of 0.5 mm.

The lateral penumbra (80%-20%) on entrance in the patient body should be as small as possible and, in any case, less than 2 mm. The penumbra is only due to the characteristics of the primary beam. Also the penumbra size at the maximum depth of treatment due to the spread of the beam in the tissue should be considered, although this contribution cannot be reduced or eliminated. In passive scattering systems the penumbra is not only determined by the primary beam characteristics but also by the scatterers and energy modulators. It can be reduced by using collimators, reducing the distance between collimator and skin and increasing the distance between the source and collimator. When using a variable primary energy the lateral penumbra is mainly influenced by the divergence of the pencil beam, which is determined by the optical properties of extraction system and the beam scanning pattern.

It should be also noted that a system of an active scanning beam uses a superposition of many beams at different energy and quality with a FWHM of between 0.5 and 1 cm, so the following aspects should be taken into consideration:

- the local dose rate can be extremely high because the local dose needed for the treatment could, in principle, be deposited all at once;
- the dose deposited in every elementary volume is obtained as a superposition of several beams; in order to achieve an accuracy of ±3%, an accuracy of 1% in the measurement of the dose of each beam is needed;
- the size of the beam spot can also be smaller than 0.5 cm FWHM. This must be considered in the design of the dose monitor, which should have a granularity and spatial resolution of less than a millimetre;
- the size of the beam and its position are two spatial parameters to be measured and verified during treatments.

Many factors, such as the intensity of the beam, the beam extraction system, the efficiency of beam transport and the technique used to vary the energy, influence the maximum dose rate to the target. For a field 40x40 cm^2 energy at maximum energy, the recommended dose rate interval should be 20 to 10 Gy min^{-1}. For a field 5x5 cm^2 at 70 MeV it is recommended to be 10 Gy min^{-1}. For treatment of ocular tumours, higher dose rates are required (15–20 Gy min^{-1}).

The macroscopic time structure of the beam may have consequences for the scanning systems and dosimetry equipment used. A cyclotron based system using passive scattering poses no specific problems as compared to conventional X-ray radiotherapy. In active scanning systems, on the other hand, rapid beam intensity fluctuations are a limiting factor for high accuracy dosimetry. For synchrotrons and pulsed linear accelerators the number of protons or ions per spill has consequences for the design of the scanning system and dosimetry tools.

3.5 Cyclotrons and synchrotrons: advantages and disadvantages

From the beginning of its history in Berkeley the cyclotron has been used for applications in the medical field. Operating at fixed magnetic field and constant energy its has a relatively simple design and operation. Moreover, the availability of superconducting technology makes it feasible to significantly reduce size and operating costs. Cyclotrons produce continuous beams with – if needed – high and easily controlled intensity and good stability. These characteristics make cyclotrons the accelerator of choice for an efficient system based on active scanning. Moreover, because the acceleration process is fast (typically <40 μsec) it is possible to switch the beam on and off rapidly. The beam intensity can be accurately adjusted on a millisecond timescale. The relatively small number of active components in typical cyclotrons for proton therapy make it an attractive accelerator from an economic point of view: the cost of construction and operation are up to now significantly lower than for synchrotons.

The main disadvantage of the cyclotron is its inability to rapidly vary the energy of the extracted beam, thus requiring external systems based on a passive degrader with an energy selection system. These systems, moreover, completely decouple the accelerator from the patient. They are typically made of graphite and are far from the treatment room. The production of neutrons is high but easily shielded and the activation is limited given the current low beam used in hadrontherapy. The degraders are sufficiently fast to allow varying the range with steps of 5 mm in less than 100 ms. This time is significantly shorter than that of the typical respira-

tory cycle (2–4 s). It is thus possible to implement treatment techniques controlled by the cycle of the patient's respiration (breathing active treatment).

Synchrotrons produce a pulsed beam with a macroscopic duty cycle of up to 50% of which the energy can be changed on a spill-to-spill basis. It has recently been shown by NIRS that the energy can be changed within a spill. The total weight of the machine is limited, but its dimensions are around 10 m and 30 m for protons and carbon ions, respectively. The beam intensity of synchrotrons is rather limited due to space charge effects at the beginning of the acceleration cycle and it is not easily stabilised. As compared to cyclotrons the operation of synchrotrons is rather complex, although modern computer-based control systems have strongly mitigated this difficulty. The ability to vary the beam energy eliminates the need for an additional degrader and energy selection systems.

3.6 Current status

Several companies in Europe, the USA and Japan are routinely delivering complete systems with accelerators and all other equipment.

IBA (Belgium) has over the last ten years installed some 15 systems worldwide; in Europe their isochronous cyclotron delivering 230 MeV protons has been installed in Essen (Germany), Orsay (France), Trento (Italy), Prague (Czechia), Krakow (Poland), Uppsala (Sweden) and Dresden (Germany).

Varian Medical Systems (USA/Germany) has installed a superconducting isochronous cyclotron delivering 250 MeV protons, developed in collaboration with NSCL (East Lansing, USA) and PSI (Villigen, Switzerland), at PSI and a complete facility with five treatment rooms at the RPTC (Munich, Germany). Several more systems based on this cyclotron are currently being installed.

Synchrotrons for carbon therapy based on a design developed at GSI have been installed at HIT (Heidelberg, Germany) and Rhön Klinikum (Marburg, Germany) by Siemens; a centre in Shanghai is under development. The synchrotron designed by a CERN-based collaboration and built and commissioned by INFN and a consortium of research institutes is operational at CNAO (Pavia, Italy) and is currently being installed at MedAustron (Wiener Neustadt, Austria). In Japan synchrotrons for carbon and/or proton therapy have been installed by different Japanese manufacturers in Chiba, Gunma, Hyogo, Koriyama, Shizuoka and Tsukuba. Several more are under construction. In the USA synchrotrons for proton therapy have been installed by Hitachi (Houston) and Fermilab (Loma Linda).

3.7 Future

A clinical particle therapy facility requires very large investments in equipment (accelerator, beamlines, gantries, etc.) and buildings. A proton therapy unit with two gantries based on a cyclotron typically requires an investment of 70–80 M€, while a facility for carbon therapy using a synchrotron may require a total investment in excess of 200 M€. Also the operation of such facilities is significantly more expensive than that of state-of-the-art conventional radiotherapy facilities with the same treatment capacity. Consequently, the treatment costs are a factor of between three (protons) and seven (carbon) times higher than for state-of-the-art conventional radiotherapy, which seriously compromises the market penetration of particle therapy. To remedy this situation the development of more compact, lower cost systems is essential. Both particle therapy equipment manufacturers and research institutes are exploring possibilities to achieve this goal.

The isochronous cyclotrons for proton therapy manufactured since about 2000 by IBA/Sumitomo (normal conducting) and Varian (superconducting) operate at a field of 1.7 and 2.4 T, respectively, which is rather conservative in comparison with the fields up to 5.3 T of the superconducting compact isochronous cyclotrons used in research institutes (NSCL, TAMU, INFN-LNS, KVI) since the 1980s. This indicates that substantial room for size and cost reduction exists.

In 2004 Mevion Medical Systems started the development of a 250 MeV proton synchro-cyclotron with a field of 9 T, using novel Nb_3Sn superconductor technology. This very compact cyclotron is mounted in the gantry, thus resulting in a very compact system. The first systems of this type are currently being commissioned at several locations in the USA.

IBA has undertaken the development of a 230 MeV proton synchro-cyclotron with a field of 5.6 T. This cyclotron, of which the prototype has delivered a first beam, will be coupled to a compact gantry with pencil beam scanning, resulting in a system with a footprint about twice as big as a treatment room for conventional radiotherapy. The pulse frequency of both machines is around 1 kHz, sufficient for the spot scanning technique that is becoming the standard in proton therapy.

Also Sumitomo has started the development of

a compact superconducting cyclotron with a 3.2 T central field and a compact gantry, while USA-based company ProNova has recently started the development of superconducting gantries.

A compact (<6 m diameter) synchrotron for protons has been developed by ProTom International and is now being commissioned for use in patient treatment at several locations in Europe and the USA. By combining fast acceleration (<300 ms up to maximum energy) with an extraction cycle of up to several seconds a relatively high duty cycle is achieved. Exploiting the 330 MeV maximum proton energy this accelerator is also suitable for radiosurgery and proton imaging.

Superconducting isochronous cyclotrons are also being considered for carbon therapy. Design studies have been carried out by INFN-LNS (Catania, Italy) and by Sumitomo for a machine delivering 300 MeV/amu carbon, sufficient to treat 75% of the relevant cases, while IBA in collaboration with JINR (Dubna, Russia) has designed a machine delivering 400 MeV/amu carbon. These machines can also deliver beams of helium, lithium and boron, while proton beams are produced by accelerating molecular hydrogen ions. In the INFN-LNS and IBA/JINR design proton beams of about 250 MeV are extracted by stripping extraction at a slighter smaller radius than that used for conventional extraction of carbon and other light ions.

The much smaller dimension and footprint of these machines as compared to the synchrotrons currently used for carbon therapy make them a very attractive option. Plans to construct a treatment facility based on the IBA/JINR and INFN-LNS designs are being developed by the ARCHADE-group (Caen, France) and in Catania.

A different approach is taken in the designs developed by Amaldi *et al.* (TERA Foundation and CERN) for both proton and carbon therapy. In these designs a compact isochronous cyclotron is used to deliver a proton or carbon beam that is post-accelerated to a variable energy by an independent cavity booster linac with a pulse frequency of 200 Hz. While in the initial design (Cyclinac, CABOTO) the S-band booster linac delivered the beam to a gantry, the latest design (TULIP) proposes to integrate the linac into the gantry, requiring the use of high gradient C-band or X-band accelerating structures. First tests have confirmed the feasibility of this scheme, and higher gradient accelerating structures are under development.

Fixed field alternating gradient (FFAG) synchrotrons are also being considered as variable energy post accelerators for particle therapy. These accelerators have a much higher repetition rate than conventional synchrotrons, while retaining the capability to change the energy at each pulse. A design study for a system with multiple independent extracted beams has been conducted in the RACCAM-project (Grenoble, France), while an electron model of an FFAG (EMMA) has been successfully developed at Daresbury (UK). Very significant R&D and prototype testing will still have to be done before the applicability of FFAG synchrotrons in particle therapy can be established.

Several completely new accelerator schemes are under development and may in the long run lead to still smaller sized accelerators, in particular for proton therapy.

The Dielectric Wall Accelerator, based on very high gradient pulses in a stack of insulating and conducting disks, would allow 200 MeV protons to be produced in a 2 m long linear accelerator rotating around the patient. The technology for this type of accelerator has been pioneered at the Lawrence Livermore National Laboratory and is now being developed further for proton therapy by the US company CPAC. Laser based acceleration schemes are developing rapidly and might eventually make it possible to accelerate the particles in even smaller volumes, but this technique is still in its infancy.

References

[1] U. Amaldi, B. Larsson Eds., *Hadrontherapy in Oncology*, Elsevier Science, ISBN 0-444-81918-5 (1994).

[2] U. Amaldi and G. Magrin, "Accelerators in Medicine", in *Accelerators and Colliders*, S. Myers and H. Schopper Eds., Springer, p. 488–513 (2013).

[3] *Reviews of Accelerator Science and Technology (RAST) vol. 2,* "Medical Applications of Accelerators", World Scientific (2009).

[4] M. Silari. (2011). Applications of particle accelerators in medicine. *Radiat. Prot. Dosim.* **146:** 440–450.

[5] W. Scharf, O. Chomicki. (1996). Medical accelerators in radiotherapy. *Physica Medica* **XII**: 199–210.

4. Beam delivery

4.1 Principle and interfacing

The beam delivery system is located downstream from the accelerator and is in charge of delivering the beam, in first instance to a phantom for quality assurance and then to the patient. It interfaces with the upstream system (ex: link with accelerator for high speed monitoring of current [1]) and the down-stream target (ex: feedback from the motion of the organ of the patient).

4.2 From the accelerator to the treatment rooms

The beam is transported from the accelerator "exit" to the treatment rooms by standard beamlines as also used in nuclear physics laboratories (dipoles, quadrupoles, stirrers, beamprofilers. etc.). The beam emittance could be in the range 2 to 5 pi.mm.mrad (normalised, 2σ). The beam is switched from one room to another via a dipole; the beam is thus only available for one room at a time. This constraint is acceptable during treatment hours because the time of irradiation is comparable with the duration of patient preparation and positioning but it is a limiting factor for longer quality assurance experiments.

The main specificity of particle therapy beamlines is the capacity to quickly adjust the tune of the several beam energies required for a patient's irradiations (from few seconds between highest/lowest energies to a 5 mm range change in less than 80 ms).

4.3 Beamline orientation in the treatment rooms

"Standard" radiation therapy machines consist of irradiation heads able to rotate 360° around a horizontally positioned patient. Due the magnetic rigidity of protons or carbons ions, the field of particle therapy has faced a real challenge. The first systems (1960–1990) were based on fixed beam lines forcing the pioneers to innovate (seated position, robotics solutions, specific immobilisation devices). In the 1990s the first full 360° solution appeared, called "gantry", a big mechanical structure rotating around the patient (weighing between 80 and 150 tons). Many papers describe the constraints or opportunities associated with gantries (cost of

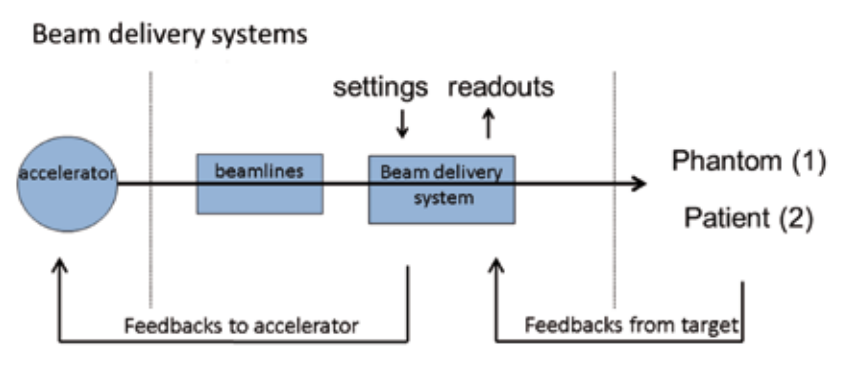

Figure 4.1.
Schematic of principle and interfacing of the beam delivery systems.

Figure 4.2. (a) Different kinds of gantry (Pedroni *et al.*). (b) Gantry (patient enclosure) at Institut Curie.

building, beam delivery principles). Nowadays, a broad range of solutions is still considered, from those where part of the motion is achieved by the patient positioner to the recent ones where the compact accelerator is embedded inside the gantry.

4.4 Beam delivery methods

There are two general methods to shape the beam to the tumour: the "passive scattering" technique, which was developed initially, and the more recent "scanning" techniques, which are expected to become the standard in the near future.

The "passive" method [2] consists of putting specific mechanical devices in the trajectory of the beam in order to "shape" it, using particle–matter interaction, to the tumour. The "scatterers" spread the originally Gaussian beam into a wide homogeneously distributed beam that is shaped to the tumour using patient-specific collimators. The dose-depth curve (the so-called "Spread-Out Bragg Peak", SOBP) required is then generated using energy "modulators", rotating wheels of varying thickness. Finally, longitudinal compensators, specific devices drilled for each field and each patient, achieve the last conformal shaping of the beam just before the skin of the patient. The limits of this technique are that it is not optimal in terms of the conformity of the dose deposition and that it results in additional dose to the patient due to the neutrons produced by the beam passing through the various components.

The active "scanning" technique exploits the physical proprieties of charged particles: a thin "pencil" beam coming directly from the beam-line (typical beam sizes at isocentre: 3–10 mm FWHM and minimum duration of 1 ms per spot) is transported to the patient to achieve small "spot" depositions of dose. The depth scanning is obtained by modifying the energy of the beam (directly for synchrotrons or through energy selection system for cyclotrons) for the different "slices" of the tumour. The scanning technique is a kind of 3D scanning of the treated volume. The main advantages consist

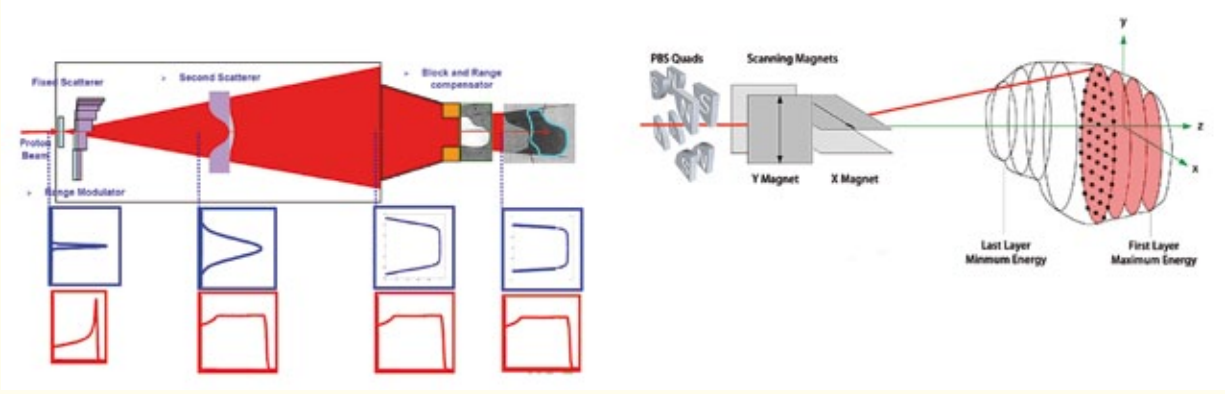

Figure 4.3. Passive (left) and active (right) beam delivery system (courtesy of IBA).

in a better conformity of the dose distribution to the target, the absence of patient-specific accessories and a much lower neutron dose. Constraints are, however, the complexity (speed, number of checks) and the sensitivity towards organ motion.

In both methods, non-invasive instrumentation, mainly ionisation chambers, is used to count and monitor the beam.

4.5 Beam delivery performances

Beyond the way to deliver the beam, the key question concerns the performance of the dose deposition. Besides the standards for conventional radiation oncology (field of 40 cm × 40 cm, average dose rate of 2 Gy/min for a tumour of one litre) the lateral and distal penumbras of the beams are the important criteria. The last trend is to converge towards the "Gamma Index" factor used in modern photon techniques. The reference papers on IMPT, Intensity Modulated Proton Treatment [3] describe the expectations and further challenges. But these performances must also be linked with the associated system and procedures: Treatment Planning System (model and method of commissioning), CT scanner and on-site imaging, and method and tools for regular quality assurance measurements.

4.6 Other considerations

Other issues are linked to beam delivery systems: control software and IT systems mainly in the context of high speed scanning techniques, radiation protection of the patient and modelling of the particle interactions in the beam delivery system or upstream, and safety and reliability. These combinations of new, innovative technologies can be associated with a significant level of risk.

4.7 Perspectives and challenges

The beam delivery system is the core point of development of particle therapy [5]; the charge particle nature of protons and carbon ions allows dynamic sweeping the beam [6-7]. But the promised Eldorado has to confront certain compromises: very thin and fast beams vs uncertainties of physiological and moving organs, advanced and innovative techniques vs high expectations in patients throughput linked with the cost of the facilities, systems developed and set by the industry vs research & development by academic institutions.

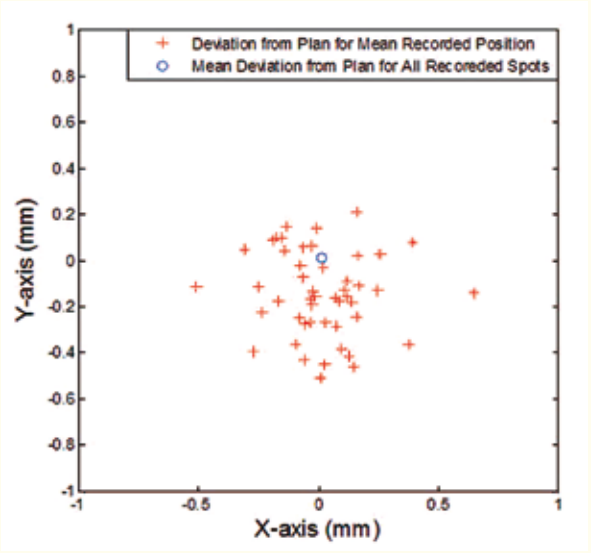

Figure 4.4. Displacement from the planned position of the mean recorded position for each spot position and mean displacement from the planned position for all recorded spots at one specific energy (163.9 MeV) [4].

References

[1] J. M. Schippers. (2009). Beam delivery systems for particle radiation therapy: current status and recent developments, *Rev. Accel. Sci. Tech.* **02:** 179.

[2] B. Gottschalk, Reference Document on Passive Scattering, http://ptcog.web.psi.ch/archive_sw_and_docs.html

[3] A. Lomax *et al.* (2005). Intensity Modulated Proton Therapy at PSI: Things we have learnt (and are still learning), *Radiother. Oncol.* **76:** S54–S55.

[4] H. Li *et al.* (2013). Use of treatment log files in spot scanning proton therapy as part of patient-specific quality assurance. *Med. Phys.* **40:** 021703.

[5] A. R. Smith. (2009). Vision 20/20: Proton therapy. *Med. Phys.* **36:** 556–568.

[6] T. Furukawa *et al.* (2010). Performance of the NIRS fast scanning system for heavy-ion radiotherapy. *Med. Phys.* **37:** 5672–5682.

[7] T. Haberer *et al.* (1993). Magnetic scanning system for heavy ion therapy, *Nucl. Instr. Meth.* **A330**: 296–305.

5. Dosimetry

5.1 Introduction

The primary quantity used in radiation therapy, including proton and heavy ion therapy, is absorbed dose to water, D_w. The basic output calibration of a clinical beam is a direct determination of the dose or dose rate in water under specific reference conditions, that is referred to as reference dosimetry. Primary dosimetry techniques for clinical proton and ion beams are based on calorimetry but the clinical reference instruments of choice are ionisation chambers.

In order to standardise the reference dosimetry between different therapy centres international protocols are established. The International Code of Practice published by IAEA (TRS-398) [1] for the determination of D_w in external beam radiotherapy uses the $N_{D,W}$ calibration factor in water determined by calibration of a dosimeter in standardised conditions in a water phantom:

$$D_{W,Q} = M_Q \; N_{D,W,Q_0} \; k_{Q,Q_0}$$

where M_Q is the reading of the dosimeter at beam quality Q, corrected for the influence of quantities other than beam quality and k_{Q,Q_0} is the correction for the beam quality, Q.

The goal of dosimetry in hadron radiotherapy [2] is not only the reference dosimetry but also delivery of tools for acceptance, testing and commissioning of treatment beam lines and treatment planning systems, periodic quality assurance checks and finally the verification of dose delivery. Therefore, specialised dosimetry tools for hadron therapy have been developed, frequently originating from research in instrumentation in nuclear physics.

5.2 Dosimetry tools for hadron radiotherapy

5.2.1 Reference dosimetry

Ionisation chambers (IC), for reference dosimetry in water phantoms are nowadays broadly offered by commercial companies. The most frequently used are the cylindrical ionisation chambers built out of graphite or A150 plastic with active volume around 0.6 cm^3 (Farmer chamber), cylindrical thimble chambers (0.125 cm^3) or plane parallel Markus chamber (0.02 cm^3). Frequently, the active volume of ionisation chambers is filled with air and the response is corrected for the atmospheric pressure. Watertight covers are available, which allow use of the chamber in water. For practically all chambers available on the market TRS-398 lists the correction for the radiation quality k_Q. Since dose is a quantity legally prescribed by a radiation oncologist, practically all reference therapeutic dosimeters used in clinics, consisting of an IC and an electrometer, are available with CE Medical or/and FDA certificates.

5.2.2 Relative dosimetry

The aim of relative dosimetry is to relate dose under non-reference conditions to the dose under reference conditions. In general no conversion coefficients or correction factors are required in measurements since it is only the comparison of two dosimeter readings, one of them being in reference conditions. Relative dosimetry is used to determine beam properties such as dose profiles (e.g. penumbras), percentage depth dose, tissue maximum ratios, output factors and others. A number of radiation detectors is routinely applied in relative dosimetry of proton and carbon ion beams, usually coupled to the scanners working in air or in water

phantoms such as miniature (thimble) ionisation chambers, Markus chambers, dosimetric diodes, diamond detectors or MOSFET detectors.

There are some specific needs of dosimetry for proton and ion therapy as compared to conventional MV X-rays radiotherapy.

One is to determine the depth dose distribution in water and the range of the beam, i.e. to measure the Bragg peak. This can be performed by scanning with a detector along the z-axis in a water phantom but for routine measurements this method is often too time consuming. One solution is a set of plane-parallel chambers (multi-layer ionisation chamber), separated by the absorbing layers in such a way that the entire structure has effectively the same stopping power (range) as the corresponding water phantom. Such a device is supplied by IBA-Dosimetry under the name Zebra. An alternative solution for quick depth dose measurements is offered by the PeakFinder Water Column (PTW, Freiburg). One beam monitor is installed at the entrance of the sealed water column and the second is the thin Bragg Peak monitor moving within the column. A single measurement takes a few minutes.

The sharp gradient of depth dose distributions and the application of scanning beams stimulated the development of two and three dimensional dosimetry (2D and 3D) systems. One of the important tools for scanning beams is a matrix of ionisation chambers, able to work as beam profile monitors or for 2D dose distribution in water. The INFN group in Torino has developed and built a pixelated parallel plate ionisation chamber to be used as a monitor for the proton therapy beam line. This system has been used among others at the proton therapy line at Orsay. The sensitive area of the detector is 160 x 160 mm^2, with the anode segmented in 1024 square pixels arranged in a 32 x 32 matrix; the area of each pixel is 5 x 5 mm^2. The detector is placed on the beam line just upstream of the last collimator to monitor the beam shape and to measure the stability and reproducibility of the delivery system. The matrix of ionisation chambers is commercially offered by IBA-Dosimetry as MatriXX and by PTW as Octavius detector 729, where the "729" stands for the number of cubic ion chambers available in the matrix. New developments based on ionisation chambers with a micro pattern readout (Micro Pattern Gaseous Detectors, MPGD) are on-going.

Another group of devices used to verify beam profiles is based on scintillators read by CCD cameras. Scintillation screens have been used to determine profiles of charged particle beams since the beginning of the use of accelerators. At HMI Berlin a system of a scintillator with CCD camera has been used since 2005 to determine lateral dose profiles of proton beams for eye treatment. A similar system is used for measurements of proton profiles at IFJ PAN. IBA introduced on the market Lynx, the 30 x 30 cm^2 scintillator with CCD camera, particularly dedicated for daily QA of the scanning beams.

5.2.3 Out-of-field dose

In order to study the out-of-field doses and to investigate the significance of secondary and scattered radiation additional tools may be necessary; especially if the goal is to assess the contribution from different types of secondary radiation. In hadrontherapy the production of neutrons (and heavier fragments in carbon therapy) may be important to quantify for each specific beam line and collimator setting. The low dose areas are mainly related to an increased risk of late effects, including radiation-induced secondary cancers.

There is a fundamental difference between the passive scattering beam lines and the scanning beam lines in terms of out-of-field dose. In passive beam delivery systems there are a number of filters and collimators in which secondary radiation is produced, while in active scanning systems, beam interactions with the patients themselves are in principle the only significant source of secondary radiation. The out-of-field doses can vary by several orders of magnitude. Particle fluence measurements (neutron, protons and heavier fragments) are needed in order to estimate this additional dose.

At GSI the fragmentation of the carbon ion pencil beam has been studied with a TOF-setup using scintillators for timing signals in combination with a BaF_2-detector. For in-phantom measurement quantifying the neutron dose and out-of-field doses in general, passive detectors such as CR-39 etch detectors and thermoluminescence detectors have been applied. More advanced (but more bulky) neutron detector systems include Bonner sphere systems, WENDI-2 detectors, as well as small SRAM-detectors. In addition, Monte Carlo simulations play an important role in this field due to the challenges in experimental measurements.

5.3 R&D

Real-time measurement of the 3D dose distribution is mandatory especially for fast scanning beams and repainting techniques. Extremely high-granularity tracking calorimeters for the detection of charged and neutral radiation will be able to determine the

Bragg-peak position as well as the lateral 2D dose distribution. Such a compact detector will be a single device performing tracking, particle identification and energy (range) measurements simultaneously. It consists of many (~50) layers of thin Si-pixel sensors sandwiched between absorbing layers. Typical pixel sizes are 5μm × 5μm or 20μm × 20μm. Because of the extremely large number of cells (~10^{14}) the device will be able to cope with a large particle flux without saturation effects. Various Si-pixel technologies are currently being studied, e.g. radiation-hard 3D sensors (SINTEF) and Monolithic Active Pixel Sensors (MAPS, Strasbourg).

References

[1] International Atomic Energy Agency, *Absorbed Dose Determination in External Beam Radiotherapy*, Technical Report Series No. 398, IAEA, 2000.

[2] C.P. Karger, O. Jäkel, H. Palmanas, T. Kanai (2010). Dosimetry for ion beam radiotherapy, *Phys. Med. Biol.* **55**: R193–R234.

6. Moving targets

6.1 Introduction

Cancer of organs affected by breathing motion such as lung or liver causes a large fraction of all deaths by cancer, and typically these cancers also show a very poor prognosis. The time scale of this motion is seconds, i.e. intrafractional. Other organs are affected e.g. by bowel motion with a time scale of minutes to days, typically regarded as interfractional.

For successful treatment of moving organs, the motion has to be assessed through volumetric imaging and has to be factored into dedicated treatment plans and strategies for motion compensation. During dose delivery, precise monitoring of the actual patient motion can control and adapt the previously optimised plan. The collected data during delivery permits precise 4D-dose recalculation useful for quality assurance and adaptive treatment schemes.

Besides the geometric motion of the target, in hadrontherapy range changes caused indirectly by the motion also have to be considered. Also lateral motion can change the radiological depth when different tissues have to be traversed by the beam to reach the target. This effect is especially severe in the lung, where low-density lung tissue can be replaced by soft tissue of either tumour or adjacent organs.

In scanned beam delivery, interference effects between target and tumour motion also have to be considered, the so-called interplay effect. This causes severe, highly variable deviations of the delivered dose.

6.2 Imaging moving organs

Treatment planning is typically based on a time-resolved, quasi-static 4D-CT scan. A CT is needed to estimate the water-equivalent path length (WEPL). The 4D-CT due to high exposure captures only a snapshot of breathing, and thus is not truly

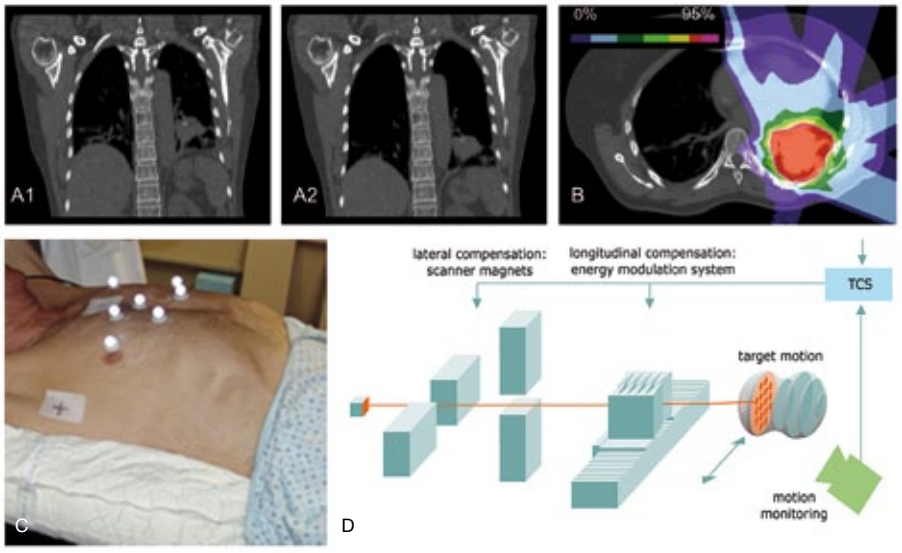

Figure 6.1.
Schematic treatment of moving targets, based on a 4D-CT (panel A1: end-exhale, A2: end-inhale); a treatment plan is calculated (B). The patient is positioned and his breathing motion monitored (C); the dose is delivered with a motion compensation scheme, here shown for tracking (D).

representative for the motion trajectory expected under treatment. Also for adaptive treatment with repeated imaging, other modalities would be of use. A possibility to explore is a static CT for the WEPL, and a prolonged 4D-MRI for motion maps.

6.3 Motion detection

6.3.1 Marker-based tumour motion detection

A widely applied strategy for tumour motion detection relies on implanted markers, which are detected by single or multiple X-ray imaging for localisation in 2D or 3D. Achievable accuracy is a few millimetres, especially if multiple views are used. A non-ionising, real-time alternative uses implanted transponders, continuously detected by external electromagnetic receivers. Although typical applications are in prostate cancer radiotherapy, the use of transponders is expected to expand to clinical application for moving lesions anywhere in the body.

Marker implantation for tumour motion detection is widely debated, especially for lung tumours, also related to marker migration and stability. The dense markers lead to difficult-to-compensate range deviations, with documented critical dosimetric deviations up to 82%. Low atomic number materials together with specific implantation criteria (perpendicular to the beam axis) may reduce dose perturbation, but markers raise serious concerns, particularly in scanned dose delivery.

6.3.2 Markerless imaging for target localisation

Fluoroscopy maybe used for continuous tumour localisation without implanted markers, with a documented accuracy of 2–3 mm in 2D. However, additional dose delivered to the patient deserves specific attention for continuous imaging of moving structures, particularly for pediatric patients.

Non-ionising alternatives include ultrasound for real-time detection with millimetre accuracy. The main drawback is that image quality is operator-dependent and remote imaging during treatment delivery requires the design of a stable holder of the ultrasound probe to apply a steady contact force with the patient. In-room MRI for high-contrast imaging in real-time during treatment may offer unique opportunities, although compatibility with high energy particle beams represents a serious challenge for application in hadrontherapy.

More futuristic solutions include the so called *theranostics*, where a low-dose, high energy particle beam maybe used for transmission measurements through the patient, resulting in range-dependent images (particle radiography/tomography). Higher beam energies than those used for treatment are required. Current studies are limited to the optimisation of appropriate detectors and preliminary experimental acquisitions.

6.3.3 External surrogates and correlation models

The localisation of external fiducials with non-ionising energies for patient-set-up correction and immobility verification has been applied for years. Point-based and surface-based external localisation has been used for motion detection and continuous localisation of internal moving structures. Surface abdominal motion is well correlated with the superior–inferior motion of inner anatomical structures due to breathing. Surface detection techniques to capture the whole thoraco-abdominal skin surface in a snapshot provide redundant information from which robust tumour motion can be achieved.

The use of external surrogates for target motion detection requires the use of external/internal correlation models, capable of interpreting non-linear correlation and hysteresis. Piece-wise linear/polynomial correlation as well as machine learning methods have been proposed with different level of complexity. All studies show that the correlation is patient-specific and time-dependent, thus requiring a frequent verification of model estimation and on-line adaptation of correlation parameters to encompass intra-fraction breathing irregularities.

6.4 Motion mitigation strategies

6.4.1 Margins

The clinical target volume can be expanded by margins to encompass the target motion, forming the internal target volume (ITV), often taken from a 4D-CT. In contrast to photon therapy, the above-mentioned range changes also have to be included in the margins, for which several strategies have been explored. Adaptive strategies update the ITV from consecutive 4D-CT scans between fractions. The strategies for the realisation of the ITV differ substantially between scanned and passive delivery.

The ITV technique does not require online motion monitoring and no additional hardware, making it comparatively simple to deliver. On the other hand, the ITV increases the target size and thus decreases the dose conformity, one of the big advantages of particle therapy.

6.4.2 Motion reduction

A straightforward strategy is to reduce the amplitude of target motion. This can be achieved e.g. by

Table 6.1. Overview of strengths and weaknesses of the motion mitigation techniques. ITV and rescanning as well as gating are already in clinical use, also in combination, while 4D-optimisation is in the early research phase, so that the entries should be seen as the potential of this technique.

Technique	Robustness	Conformity	Delivery requirements	Motion monitoring
ITV + rescanning	++	–	+	–
Gating	+	+	–	+
Tracking	–	++	++	++
4D-optimisation	+	++	+	++

abdominal compression, but also by rectal balloons as used in prostate cancer.

A different approach also resulting in a reduced residual motion is gating. The beam is delivered only if the target is within a pre-defined range, the so-called gating window. This generally leads to elongated treatment times, as depending on the size of the gating window only a certain fraction of the breathing cycle is available for irradiation.

6.4.3 Motion compensation

For scanned delivery, the beam can be adjusted to track the target motion. Motion lateral to the beam can be followed by adjusting the scanner magnets. Changes in WEPL are more difficult to compensate and require a range shifter. Precise motion monitoring can either supply tracking vectors directly, or detect a motion phase of a 4D-CT to use pre-computed motion maps. Changes in WEPL can currently be assessed only from 4D-CTs, though this could potentially change with the theranostics concept.

A promising alternative, but still in early stages of research, is 4D-optimisation. In essence, treatment plans are computed on all 4D-CT phases, incorporating tumour motion and WEPL changes directly. This potentially results in conformal target coverage also for complex motion patterns that are not adequately addressed by tracking. Also no specific hardware is required for WEPL changes, but computational costs are high.

6.4.4 Interplay

To counter interplay in scanned beam delivery, rescanning or repainting can be used. As the interplay is highly variable, depending on the exact temporal and spatial correlation of the two motions, applying a fraction of the dose multiple times leads to averaging of the dose errors. Several concepts exist, such as slice-by-slice, volumetric, or breath-controlled with different schemes to effectively break correlations between motion and delivery. The rescanning also increases the robustness of the method, as other variable errors are also averaged.

Similar to rescanning, fractionation also leads to averaging of random dose errors, though inhomogeneous fraction doses have to be accepted.

6.4.5 Dose calculation

Time-resolved dose calculation requires several input parameters available often only after irradiation. The timing and beam positions of dose delivery has to be correlated to actual, measured patient motion, which in turn has to be mapped onto a 4D-CT for range estimation. This kind of precise re-calculations can be helpful for adaptive treatment schemes and quality assurance, but also – using artificial inputs – for research simulations.

6.5 Summary

Several motion compensation and detection strategies are available, with gating and the ITV as comparatively simple options already in clinical use, especially for passive delivery. Scanned delivery for moving targets is more complex due to interplay and is only in the beginning of clinical implementation. Robustness of both motion compensation and monitoring remains an issue of ongoing research.

References

[1] C. Bert, M. Durante. (2011). Motion in radiotherapy: particle therapy, *Phys. Med. Biol.* **56**: R113–R144.

[2] M. Riboldi, R. Orecchia, G. Baroni. (2012). Real-time tumour tracking in particle therapy: technological developments and future perspectives. *Lancet Oncol.* **13**: 383–391.

[3] S. Mori, S. Zenklusen, A.C. Knopf. (2013). Current status and future prospects of multi-dimensional image-guided particle therapy, *Radiol. Phys. Technol.* **6**: 249–272.

7. Radiobiology

7.1 Introduction

Biologically-optimised treatment plans are often discussed in radiotherapy [1]. Use of radiobiological parameters for tumour control probability (TCP), normal tissue complication probability (NTCP), individual sensitivity and so on can indeed lead to optimisation of the physical treatment plan for a given tumour and for an individual patient. Clinical implementation of biologically-optimised plans is often hampered by the uncertainties in radiobiology. The issue is even more severe with particle therapy, where the relative biological effectiveness (RBE) of the beam is different from X-rays, depends on several parameters, and can change within the patients' body. Radiobiology of charged particles goes, however, far beyond RBE and may represent a major improvement of hadrontherapy compared to X-ray therapy. Modern DNA damage and repair measurement techniques now allow an unprecedented insight into the molecular damage induced by fast ions (Figure 7.1). These studies show that densely ionising radiation induces a high fraction of clustered DNA damage, which is more difficult to repair and triggers a different intra- and inter-cellular signaling cascade compared to sparsely ionising radiation. These effects are now the mainstream research topic in particle radiobiology [2].

7.2 RBE

RBE is a complicated radiobiological concept depending on several factors: measured endpoint, dose, dose rate, dose per fractionation, number of fractions, particle charge and velocity, oxygen concentration, cell-cycle phase. Data mining of RBE values from experiments performed in the past 50 years with different ions always show a large variance (Figure 7.2). The spread in RBE values cannot

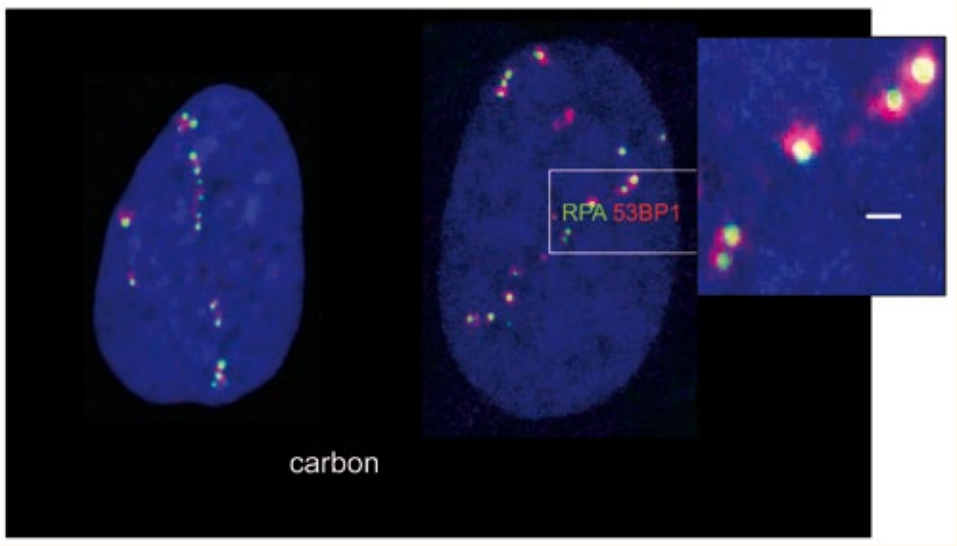

Figure 7.1. Co-localisation of DNA repair proteins along tracks of heavy ions in human cells. The pictures show the recruitment of the replication protein A (RPA) and the tumour suppressor p53-binding protein 1 (53BP1) to DNA damage streaks generated by C or U-ions accelerated at GSI in Darmstadt, Germany (courtesy of Gisela Taucher-Scholz).

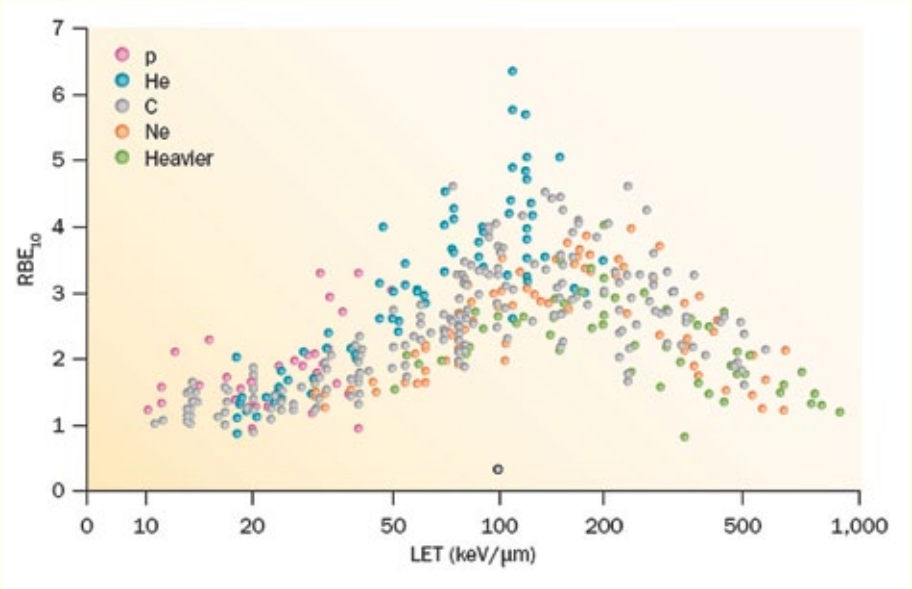

Figure 7.2.
RBE versus linear energy transfer (LET) from published experiments on in vitro cell lines. RBE is calculated at 10% survival, LET values are given as keV/µm in water. Different colours indicate different ions, from protons to heavy ions. Data points are extracted from the Particle Radiation Data Ensemble (PIDE) database (*www.gsi.de/bio-pide*) which currently includes 855 survival curves for cells exposed to photons (α/β ratio ranging 1–30) and ions.

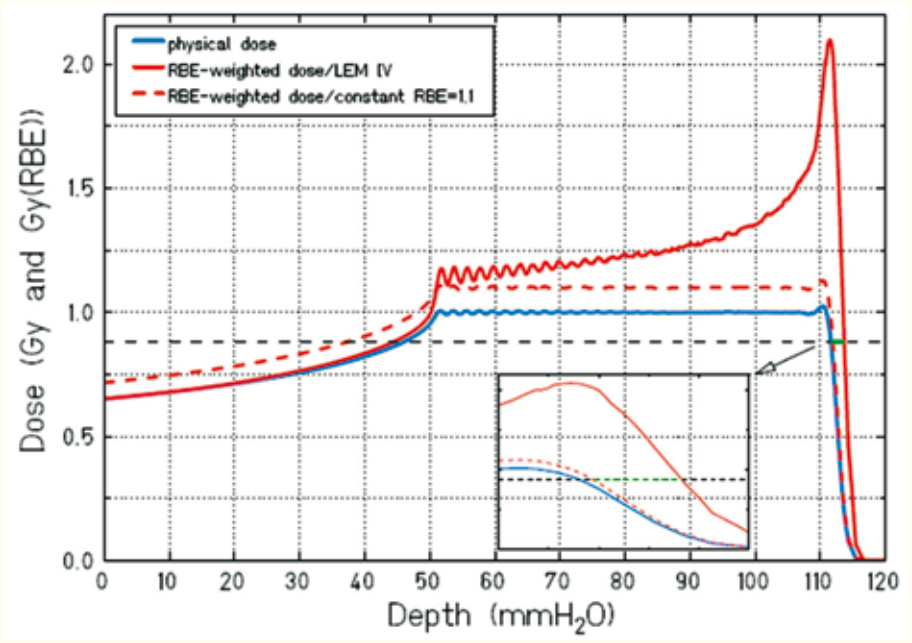

Figure 7.3.
Biological range extension due to a variable RBE with depth in proton therapy. The dashed line indicates the corrected physical SOBP using the conventional RBE=1.1. The orange line represents the correction using with the LEMIV model. The black dashed line the is the 80% of the prescribed RBE-weighted dose. The inset shows a zoom of the distal penumbra, and the green line the increased range predicted by the biological model. (Image and calculation courtesy of Rebecca Grün, GSI.)

be reduced by more in vitro experiments, just repeating what has been done for years. Dose escalation trials are performed in each facility using heavy ions, as it is currently done at HIT and CNAO, following the experience at NIRS. For proton beams, a RBE of 1.1 is used in clinical practice for both plateau and spread-out Bragg peak (SOBP). This is a reasonable and sound value, although in the very distal part of the SOBP the RBE increases, and the range of values goes from 0.7 to 1.6 at mid-SOBP. Even though the RBE issue is less problematic with protons than for heavy ions, perhaps a biological treatment plan taking into account the increase in the distal proton SOBP may reduce complications at the field edges. In fact, the increased RBE of slow protons translates in an extension of the effective range of the proton beam (Figure 7.3).

There is a lot of emphasis on RBE uncertainties in hadrontherapy, but in reality patients have been treated safely in several centres and in Lanzhou (China) they are treated for superficial and deep tumours with C-ions without any correction for RBE, i.e. using a flat SOBP in physical dose. Rather than focusing on more RBE measurements, research should focus on the newly emerging radiobiology which may open new scenarios in hadrontherapy and provide novel biology-guided applications in the clinics.

7.3 Cancer stem cells

It is now established that the tumour is a tissue, and that stem cells and stromal compartments play a

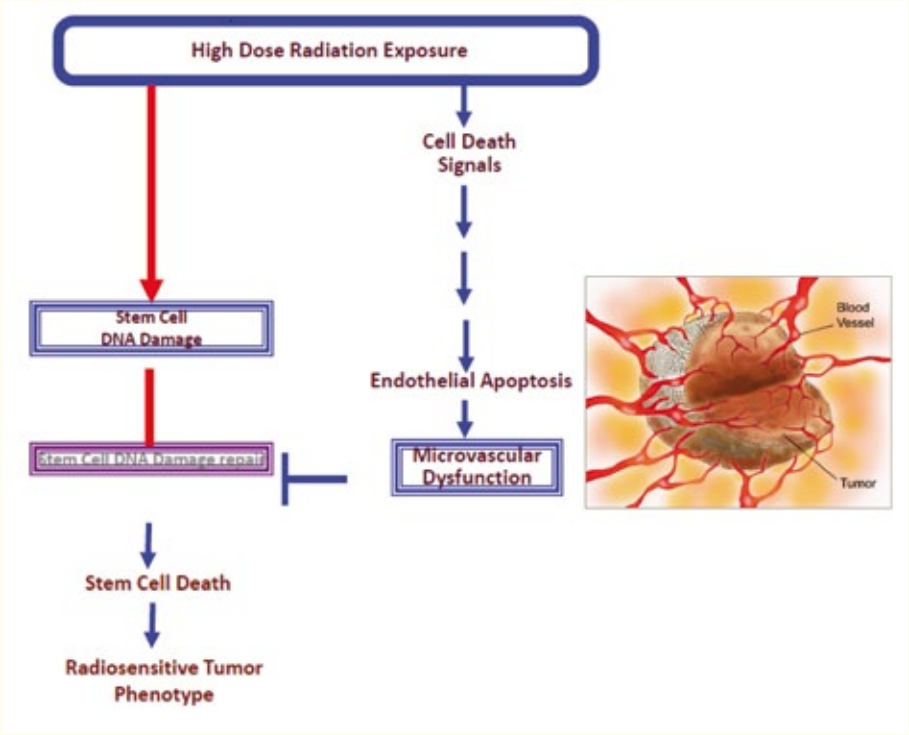

Figure 7.4.
Two modes of cell death following high-dose radiation exposure. In addition to the conventional DNA damage pathway, it is hypothesised that very high dose, such as those used in stereitactic ablative radiotherapy, elicits vascular damage, which contributes to cell death [3].

decisive role in its growth and homeostasis. Cancer stem cells are resistant to radiation and hypoxia, and therefore heavy ions may represent an ideal tool to destroy this compartment, which is responsible for both local recurrence and metastasis. Recent in vitro studies show indeed that carbon ions are more effective than X-rays in killing stem cells from colon and pancreas cancers. Moreover, preliminary results indicate an increased effectiveness of low-energy protons in eliminating cancer stem cells from colon and mammary human cancer cells in vitro (studies reviewed in ref. [3]).

7.4 Hypofractionation

Radiotherapy is now clearly going towards hypofractionation. Stereotactic body radiation therapy (SBRT) and ion therapy are both pushing hypofractionation toward the region of 1–3 fractions (oligofractionation) with a very high dose/fraction (up to 25–30 Gy). Treatment technology in conventional radiotherapy has in fact advanced so much in recent years, improving tumour localisation with high-quality imaging and achieving greater conformity using high-resolution collimators. This makes it possible to deliver single high doses to tumours, sparing organs at risk and maintaining the dose to the normal parallel organs below the tolerance dose. In addition, at very high dose, vascular injury, i.e. damage to the endothelial cells supplying the cancer tissue with oxygen and nutrients, may become a dominant pathway for tumour suppression (Figure 7.4). Damage to the tumour stroma at high doses has been elegantly shown by the Memorial Sloan Kettering Cancer Center (MSKCC, NY, USA) researchers, who found that vascular endothelial cell apoptosis is rapidly activated above 10 Gy per fraction [3], and that the ceramide pathway orchestrated by acid sphingomyelinase is a major pathway for the apoptotic response. In later clinical work involving the use of single fraction high-dose spinal SBRT, investigators from the same institution recorded pronecrotic response after doses in the range of 18–24 Gy, a radiographic change consistent with a devascularising effect. Particle radiobiology research at high doses is needed to support and guide oligofractionation in hadrontherapy. Indications of suppressed angiogenesis with C-ions even at low doses suggest that vascular damage may be particularly effective with protons or heavy ions.

7.5 Combined therapies

Even though local control is generally very high with hadrontherapy, in most malignancy radiotherapy must be combined with systemic therapies to control metastasis and increase survival. Combined radio and chemotherapy protocols are already used in many cancers, such as glioblastoma multiforme (GBM) or pancreatic cancer. However, very few radiobiology studies specifically address the potential synergistic interaction of drugs and ion irradiation. In vitro experiments on GBM have

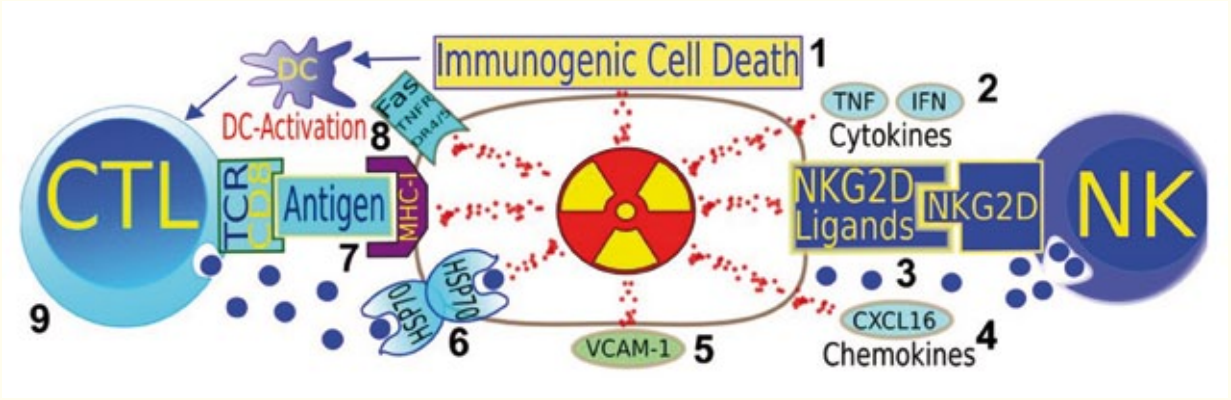

Figure 7.5. Pathways where radiation can synergise with immune adjuvant therapy for cancer. 1, Immunogenic cell death is promoted by ionising radiation, through dendritic cell activation and, consequently, T-cell expansion. 2, Cytokines play a role in radiation therapy success. 3, NKG2D-ligands, sensitising stressed cells to natural killer cells (innate immunity) are upregulated by radiation. 4, Chemokines can be induced by radiation, attracting effector T-cells to the tumour. 5, Radiation-induced interferon-gamma dependent upregulation of cell adhesion molecule also influences antitumour immunity. 6, Heat shock proteins sensitise to cytotoxic granzymes. 7, Radiation can lead to enhanced expression of MHC-I and to de novo expression of neoantigens. 8, Death receptors can be upregulated by irradiation. 9, CD8 T-cells are essential for the success of radiotherapy. (Image courtesy of Norman Reppingen, TU Darmstadt.)

provided useful indications on the combination of different drugs with C-ions.

Equally important is the combination of particle therapy with immunotherapy (reviewed in [4]), which is now rapidly gaining access in clinics with great expectations for cancer cure. Abscopal effects, defined as shrinkage of metastatic lesions far from the irradiation field during radiotherapy of a primary malignancy, have been reported for many years but although immune related effects were assumed to play a role, this was hitherto not immunologically proven. In March 2012, a melanoma patient at MSKCC received immune adjuvant anti-CTLA4 therapy for one year resulting in disease progression, requiring focal irradiation of her spinal metastasis (28.5 Gy, 6 MV X-rays in 3 fractions). In the CT scan four months after irradiation, disappearance of multiple metastases from the irradiation field occurred. Changes in cellular and molecular parameters indicate a comprehensive immune reaction against the tumour. More cases of abscopal effects with anti-CTLA4 treatment concurrent with radiotherapy were reported later, including one complete response (no cancer visible in PET scan). This is clear clinical evidence of immune-mediated abscopal effects, formerly observed in different animal models.

These studies beg the question of whether abscopal effects, and combined immunotherapy and radiotherapy, can be enhanced by charged particles (Figure 7.5). Carbon ions significantly reduced lung metastasis count in LM8 osteosarcoma mouse models and a model of squamous cell carcinoma in immune competent C3H mice. A recent study showed that heavy ion irradiation could confer tumour rechallenge resistance which was dependent on CD8+ T-Cells and influenced by NK cells in this system, showing synergy with dendritic cell treatment approaches – a new, very impressive and encouraging outcome for future protocols combining immunotherapy and hadrontherapy.

References

[1] A. Brahme (Ed.), Biologically Optimized Radiation Therapy. *World Scientific* ISBN: 978-981-4277-75-4 , 2014.

[2] J.S. Loeffler, M. Durante. (2013). Charged particle therapy – optimization, challenges and future directions. *Nat. Rev. Clin. Oncol.* **10:** 411–424.

[3] Z. Fuks, R. Kolesnick (2005). Engaging the vascular component of tumor response. *Cancer Cell* **8:** 89–91.

[4] M. Durante, N. Reppingen, K.D. Held. (2013). Immunologically augmented cancer treatment using modern radiotherapy. *Trends Mol. Med.* **19**: 565–582.

8. Modelling

8.1 Introduction

As described above in Section 7 'Radiobiology', various kinds of living cells can be effectively killed by accelerated ions, i.e. protons or heavier nuclei. The unique property of such particles is that the maximum in their linear energy transfer (LET) is reached at the end of their range in the medium (Bragg peak). This makes it possible to irradiate the target volume occupied by a tumour while sparing surrounding healthy tissues (see Section 9 "Treatment planning"). A reliable estimation of the biological dose distribution delivered to a patient is required for successful treatment. In calculations of biological dose from carbon ions it is important to take into account their elevated relative biological effectiveness (RBE) [1], in particular, close to the Bragg peak. A key starting point in evaluating the biological (i.e. RBE-weighted) dose delivered by a therapeutic ion beam to a specific sub-volume (voxel) is to calculate the energy and flux of primary and secondary particles propagating through this voxel. For calculating RBE biophysical models like LEM developed at GSI or the radiobiology model from NIRS can be applied (see [1] and Sections 7 and 9).

8.2 Monte Carlo modelling in hadrontherapy

The well-known Monte Carlo (MC) codes FLUKA, Geant4, MCNPX, PHITS and SHIELD-HIT were initially designed for simulations in particle and nuclear physics. However all of them are successfully used now in the field of hadrontherapy to model propagation of therapeutic beams of protons, neutrons or ions in various materials and tissues. As one can see in Figure 8.1, the number of papers devoted to MC modelling in hadrontherapy is growing, especially in the last five years, with their total number approaching 900. They can be classified according to several major tasks.

First, when the beam is transported to the patient through range modulators, ridge filters, scatterers and collimators in the case of passive beam delivery, one should simulate the radiation fields created due to interactions of beam particles with these components. This includes also the estimation of the dose due to secondary neutrons and the radiation background in the treatment room. The MC models are especially useful for evaluating the importance of low doses when event-by-event fluctuations are large.

Second, the dose delivered to the patient can be directly calculated from a voxel-based 3D image, coupled with a biophysical model to account for

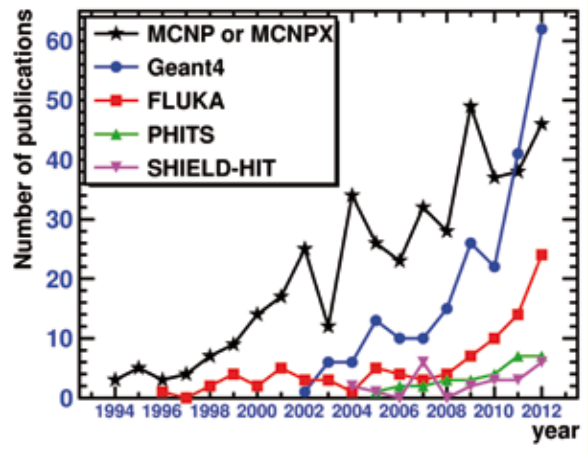

Figure 8.1. Annual number of publications related to hadrontherapy, where respective Monte Carlo codes/tools were used. Estimated from the Web of Science database (Thomson Reuters) in October 2013.

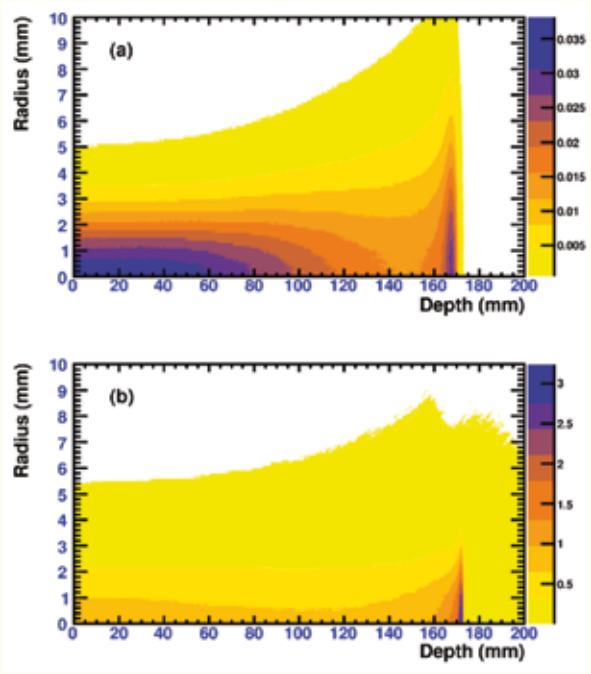

Figure 8.2. MCHIT/Geant4 results [I. Pshenichnov et al. (2008). *Nucl. Instr. Meth. B* **266**: 1094–1098] for spatial dose distributions in MeV/mm^3 per beam particle, for 4 mm FWHM pencil beams of (a) 170 MeV protons and (b) 330 A MeV ^{12}C ions in polymethylmethacrylate. Note the different dose scales in two panels.

RBE and compared to the dose calculated by other (e.g. analytical pencil-like beam) methods. In particular, such a validation may be necessary in the presence of metallic implants in the patients' body or for other quality assurance tasks (see Section 9). MC modelling includes detailed simulation of nuclear reactions induced by nucleons and nuclei in implants, as well as enhanced multiple scattering in such dense materials.

Third, since the resulting dose distribution is calculated in clinical environments by a Treatment Planning System (TPS) as a superposition of thin pencil-like beams, a library of pencil beam profiles can be created or validated with the help of MC codes.

Fourth, MC codes are indispensable for calculating the yields of unstable positron-emitting (PE) nuclei or prompt gammas to validate the range of protons and nuclei in human tissues in vivo.

Basically, in MC modelling a trajectory of each primary and secondary particle is calculated as a collection of short steps during particle propagation in the medium. The energy loss due to ionisation is calculated at each step and various nuclear reaction channels are simulated by the MC sampling method. Some examples of modelling of nuclear reactions relevant to proton and carbon ion therapy are given below. Several research groups (see e.g. [2,3]) have validated and benchmarked Monte Carlo codes/tools for simulating the propagation of protons and carbon nuclei in tissue-like materials and also in voxel-based anthropomorphic phantoms. Since this research field is rapidly growing (see Figure 8.1) only some key topics will be mentioned below with the aim of underlining major achievements and open issues.

In order to illustrate general trends in this field of research, the Monte Carlo model for Heavy-Ion Therapy (MCHIT) [4] based on the Geant4 toolkit is used here. The main task of any model is to reproduce the spatial distribution of energy deposition with sub-mm accuracy. The strength of a Monte Carlo model is that not only 1D depth-dose curves can be reliably calculated, but also 3D dose distributions in tissues. In Figure 8.2 an example of such distributions for proton and carbon beams is given. In particular, the effect of lateral scattering can clearly be seen, which is much stronger for protons than for ^{12}C. The advantages of the MC method are especially evident for modelling radiation fields in the beam penumbra where the contribution of secondary fragments and neutrons is essential.

8.3 Secondary neutrons

Secondary neutrons are produced by proton and carbon-ion beams in materials of beam-line elements, collimators, range modulators and also in the treatment volume. Such neutrons propagate further in surrounding tissues, air and shielding of the treatment room and can deposit energy very far from their production points. In order to evaluate the impact of secondary neutrons on a patient, a simple cubic (40 cm^3) water phantom irradiated by a proton or a carbon-ion beam was simulated with MCHIT [4]. The fraction of the total dose inside the phantom volume, which is specifically due to secondary neutrons produced by carbon nuclei, was estimated as ~1%. This value is similar to the one estimated for a proton beam and thus should not provide a serious hazard to the patient during treatment. The MCHIT model allows calculation of doses from secondary neutrons delivered at any distance from the treatment site. The model was validated with experimental data for secondary neutrons produced by 200 A MeV ^{12}C beam in a 12.78-cm thick water phantom. As one can see in Figure 8.3, general good agreement with the data is obtained. However, the yields of relatively slow neutrons (with energy below 150 MeV) emitted at large angles (20° and 30°) are overestimated by the model, and we conclude that there is still room to improve the fragmentation models of Geant4 with respect to production of secondary neutrons.

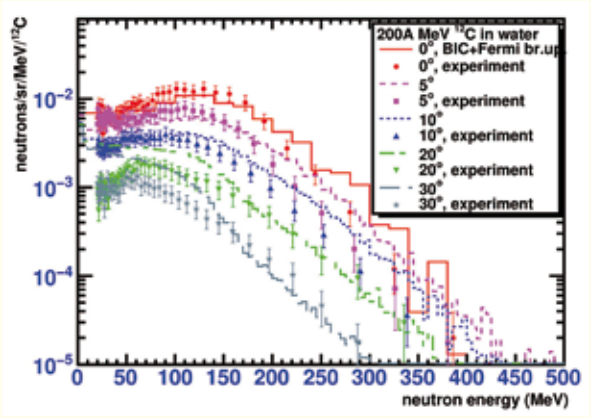

Figure 8.3. Energy spectra of neutrons produced by 200 A MeV ^{12}C beam in a water phantom at 0°, 5°, 10°, 20° and 30° to the beam axis. Histograms present MCHIT/Geant4 results obtained with the Light-Ion Binary cascade model connected with the Fermi break-up model. [From I. Mishustin *et al.* (2010). *Eur. Phys. J. D* **60**: 109–114.]

8.4 **Fragmentation**

As demonstrated by measurements with beams of 400A MeV ^{12}C nuclei propagating in a water phantom, up to 70% of projectiles undergo fragmentation before they reach the depth of the Bragg peak (Figure 8.4). ^{12}C projectiles stop at this depth, but earlier produced fragments (especially protons and alpha particles) propagate further beyond the Bragg peak. The attenuation of the ^{12}C beam and build-up of hydrogen, lithium, beryllium and boron fragments are accurately reproduced by MCHIT with the Quantum Molecular Dynamics (G4QMD) model for nucleus–nucleus collisions and the Fermi breakup model for nuclear de-excitation (Figure 8.4). Since Li, Be and B fragments along with ^{12}C projectiles provide the main contribution to the total dose, the depth-dose distribution is also well reproduced. At the same time the yield of helium fragments is underestimated, presumably due to neglecting the cluster structure of ^{12}C, which would otherwise enhance the emission of alpha particles in the fragmentation of ^{12}C. This indicates a direction for further development of nucleus–nucleus collision models, which may eventually include nuclear structure effects. Similar results on yields of nuclear fragments were obtained with FLUKA (see T.T. Böhlen *et al.* (2010). *Phys. Med. Biol.* **55:** 5833–5847) with its own set of nuclear reaction models.

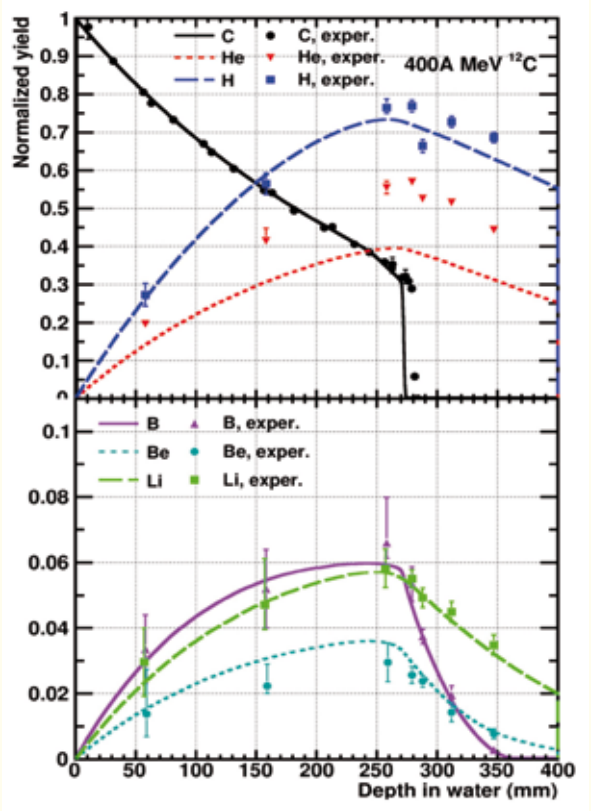

Figure 8.4. Attenuation of ^{12}C beam (black) and build-up of secondary fragments (from H to B, see the legend) in nuclear reactions induced by 400A MeV carbon nuclei in water. Points – experimental data [E. Haettner *et al.* (2006). *Radiat. Prot. Dosim.* **122**: 485–487], lines – simulations with MCHIT/Geant4 using QMD and Fermi breakup models.

8.5 **Simulations of PET images**

For treatment verification in hadrontherapy it is possible to exploit the production of unstable PE nuclei, ^{10}C (with the half-life of 19.26 s); ^{11}C (20.39 min); ^{13}N (9.97 min); ^{14}O (1.18 min) and ^{15}O (2.04 min), in nuclear reactions induced by therapeutic proton and carbon-ion beams. Such nuclei emit low-energy positrons which travel a few millimetres in tissue before they annihilate with electrons. The emission of characteristic pairs of annihilation photons can be detected with a PET scanner during the irradiation or 10–20 min afterwards. Since the momenta of photons from a single annihilation event are strongly correlated, a spatial distribution of positron-emitting nuclei can be reconstructed by tomographic methods and compared with the distribution calculated for the planned dose. Precise modelling of production of PE nuclei is thus one of the key issues of this method. Examples of calculated distributions of PE nuclei produced by protons and ^{12}C nuclei in tissue-like materials can be found elsewhere [2,3]. Fragments of target nuclei, ^{11}C and ^{15}O created by protons in tissues are evenly distributed along the beam path with a sharp fall-off close to the Bragg peak. In contrast, the maximum of β^+-activity created by ^{12}C nuclei is located close to the Bragg peak. This is because of projectile fragments, ^{10}C and ^{11}C, created in peripheral nucleus–nucleus

collisions, which have velocities close to the projectile velocity.

Two models, GATE/Geant4 and FLUKA, were compared recently with respect to modelling of PE nuclei production by protons and carbon ions in a common irradiation set-up [2]. The β^+-activity profiles calculated with these two codes for ^{12}C projectiles agree better than for protons. A similar comparison, but only for protons, was performed for FLUKA, Geant4, MCNPX and PHITS [3]. FLUKA gives the most accurate description of measured β^+-activity profiles for proton beams by using built-in approximations of measured cross sections for production of PE nuclei. The predictions of internal nuclear reaction models of FLUKA, Geant4, MCNPX and PHITS for yields of PE nuclei deviate from each other and from experiment. There is a clear need to improve nuclear reaction models used in these codes, especially for a better description of (p,n) reactions on carbon and oxygen. At the same time more data are needed for production of ^{11}C and ^{15}O by nuclear beams in various light materials to test and improve nucleus–nucleus collision models.

8.6 Summary

Monte Carlo modelling of proton and ion-beam cancer therapy is a powerful tool to establish the links between the physics of processes at the nuclear and atomic scales and radiation fields in the media. While a general agreement of simulation results obtained with FLUKA, Geant4, PHITS, SHIELD-HIT and MCNPX with experimental data is reached, none of the existing codes/tools can serve as an universal "best-choice tool". A wide international collaboration between theoretical and experimental groups is needed to foster the collection of more detailed and accurate data on nuclear reactions relevant to ion-beam therapy and improving their theoretical description.

References

[1] E. Blakely, J. Hendry, P. DeLuca, R. Gahbauer, B. Michael, A. Wambersie and G. Whitmore (Editors), *Relative biological effectiveness in ion beam therapy*, International Atomic Energy Agency and International Commission on Radiation Units and Measurements, Technical reports series No 461, Vienna, 2008.

[2] C. Robert, G. Dedes, G. Battistoni, T.T. Bohlen, I. Buvat, F. Cerutti, M.P.W. Chin, A. Ferrari, P. Gueth, C. Kurz, L. Lestand, A. Mairani, G. Montarou, R. Nicolini, P.G. Ortega, K. Parodi, Y. Prezado, P.R. Sala, D. Sarrut and E. Testa. (2013). Distributions of secondary particles in proton and carbon-ion therapy: a comparison between GATE/Geant4 and FLUKA Monte Carlo codes. *Phys. Med. Biol.* **58**: 2879–2900.

[3] E. Seravalli, C. Robert, J. Bauer, F. Stichelbaut, C. Kurz, J. Smeets, C. Van Ngoc Ty, D.R. Schaart, I. Buvat, K. Parodi and F. Verhaegen. (2012). Monte Carlo calculations of positron emitter yields in proton radiotherapy. *Phys. Med. Biol.* **57**: 1659–1674.

[4] I. Pshenichnov, I. Mishustin and W. Greiner. (2005). Neutrons from fragmentation of light nuclei in tissue-like media: a study with the GEANT4 toolkit. *Phys. Med. Biol.* **50:** 5493–5507.

9. Treatment planning

9.1 Introduction

The treatment planning process is a crucial step in the overall treatment procedure in radiation oncology and takes place prior to the first fraction being delivered to a patient. The aim is to simulate the dose distribution to the tumour and the surrounding normal tissue and organs at risk which would result from an intended treatment. From this dose distribution, tumour and organ specific parameters, or biological parameters, can be extracted in order to enable the prediction of the best knowledge treatment outcome, both with respect to local control and treatment-related toxicity. These simulations of such a treatment are performed with the support of a so-called treatment planning system (TPS).

In modern radiation oncology – irrespective of which beam quality is used for therapy (photons, particles, radioactive nuclides) – the treatment planning software runs on powerful computers. In the age of three-dimensional conformal therapy, developments in TPS made for proton beam therapy have set benchmarks for photon beam therapy. Due to the physical selectivity of protons and their strong range sensitivity to tissue variations, both in terms of dimension and density, the requirement for true three-dimensional (3D) treatment planning and dose calculation was soon realised and pursued. Consequently, the first 3D TPSs were used clinically in proton beam therapy. Only later, and driven by these developments, were 3D TPSs introduced into photon beam therapy. Figure 9.1 illustrates a typical dose distribution display of a TPS for photon beam and particle beam therapy.

9.2 The treatment planning process

The treatment planning process consists of several sub-tasks with strong mutual dependencies.

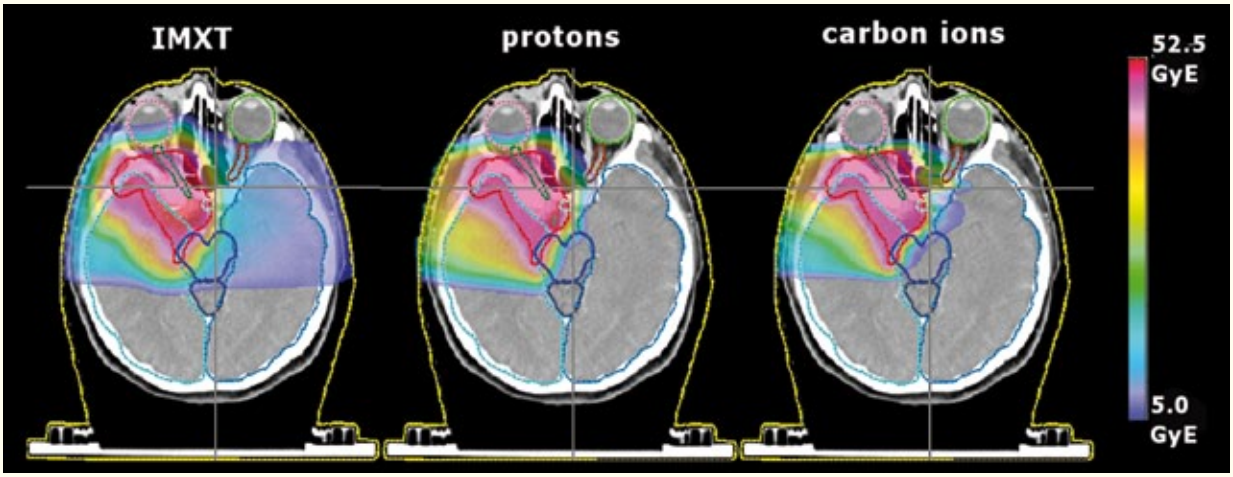

Figure 9.1. Dose distribution comparison for meningioma patients. From left to right, IMRT with photons based on 5 fields, scanned proton and carbon ion beam therapy.

Before treatment planning, during which the actual radiation fields are designed, a patient undergoes cross-sectional imaging in order to enable reconstruction of the patient's anatomy in 3D in treatment positions. In today's state-of-the-art radiation oncology practice, computer tomography (CT) is the basic imaging modality that serves treatment planning because it enables the calibration of grey-scale or Hounsfield units against various physical parameters that are required for heterogeneity modelling in dose calculation. In particle beam therapy this parameter is the stopping power of the relevant particle, while for photon and electron beam therapy it is the electron density.

CT Imaging in treatment positions implies that prior imaging positioning aids or immobilisation devices are defined and individually casted for the patient. Over recent decades, dedicated immobilisation devices have been developed for the various anatomical regions (brain, head-and-neck, thorax, abdomen, pelvis, extremities). In general, immobilisation devices used in particle beam therapy and in photon beam therapy are rather similar as they serve the same purpose. However, the important aspect when imaging the patient in treatment position is that potential attenuation effects of the treatment beam related to those devices can be accounted for when performing dose calculations with the TPS. Furthermore the selection of the most appropriate beam incidence needs to be based on the actual anatomic situation and patient geometry as intended for the treatment session. Special attention needs to be paid to situations if there are metals present in the patient, such as dental fillings, prostheses, or other implants, as they usually cause several artefacts. In special treatment situations, or for pathologies where the soft tissue contrast of CT is not sufficient, additional imaging series are performed using magnetic resonance imaging (MRI), which provides superior soft tissue contrast, or positron emission tomography (PET), in which tumour metabolism is taken into account for target definition. All additional images are then co-registered to the CT for structure segmentation.

Structure segmentation is a sub-process in treatment planning. This process defines the tumour, the volume to be irradiated (planning target volume – PTV), organs at risk (OAR) and other structures which must be taken into account in creating an optimal treatment plan. Structure segmentation is a manual process and as such prone to inter- and intra-observer uncertainties. The inter-observer uncertainties in target definition, which is a medical task, is probably the largest uncertainty in radiation oncology at present. Recent developments in imaging technology, for example the use of multimodality imaging information and in particular the use of PET, which complement pure morphologic CT information with functional information, have contributed significantly to reducing the inter-observer uncertainties in target definition. For more than forty years, the International Commission on Radiation Units and Measurements (ICRU) has defined and published recommendations for prescribing, recording and reporting radiation treatments. A common theme in all of these ICRU documents is the particular focus given to volume definition in order to establish a common language in radiation oncology. Several recommendations address the specific issues of photon (ICRU Reports 50, 62 and 83), electron (Report 71) and proton beam (Report 78) therapy.

The next step in the treatment planning process is the definition of treatment parameters. In this chapter the selection or combination of particle species, like protons, carbon ions or helium ions, will not be considered as a degree of freedom in treatment planning. However, with the upcoming particle therapy facilities for proton and carbon ion therapy that are based on synchrotrons, combined modality treatments, or selecting a specific particle type depending on indication, is feasible. In addition to making medical decisions on the dose per fraction and the total dose to be delivered, the treatment planner has to select beam directions, include aspects of treatment plan robustness against motion, and consider tolerance doses of OAR. Based on these parameters the dose is calculated and the treatment plan undergoes optimisation until a clinically useful and acceptable dose distribution is obtained. In this optimisation process, the treatment intent needs to be translated into treatment parameters such as maximum doses permitted to certain organs or subvolumes of organs, and required minimum doses to target (tumour) structures.

Treatment plan optimisation differs between the two beam delivery methods, i.e. passively scattered beams and scanned pencil beams (see Chapter 4 on Beam Delivery). For passively scattered beams, treatment plan optimisation is mostly based on human intelligence and a manual trial and error process. Optimisation parameters are beam shape and size, spread out Bragg (SOBP) peak length, beam incidence, beam weight, etc. This process is similar to treatment plan optimisation in standard 3D conformal radiotherapy with high energy photon beams. In contrast, scanned beam delivery is based on inverse planning or computerised treatment plan optimisation, in which particle fluence patterns are determined by algorithms that are

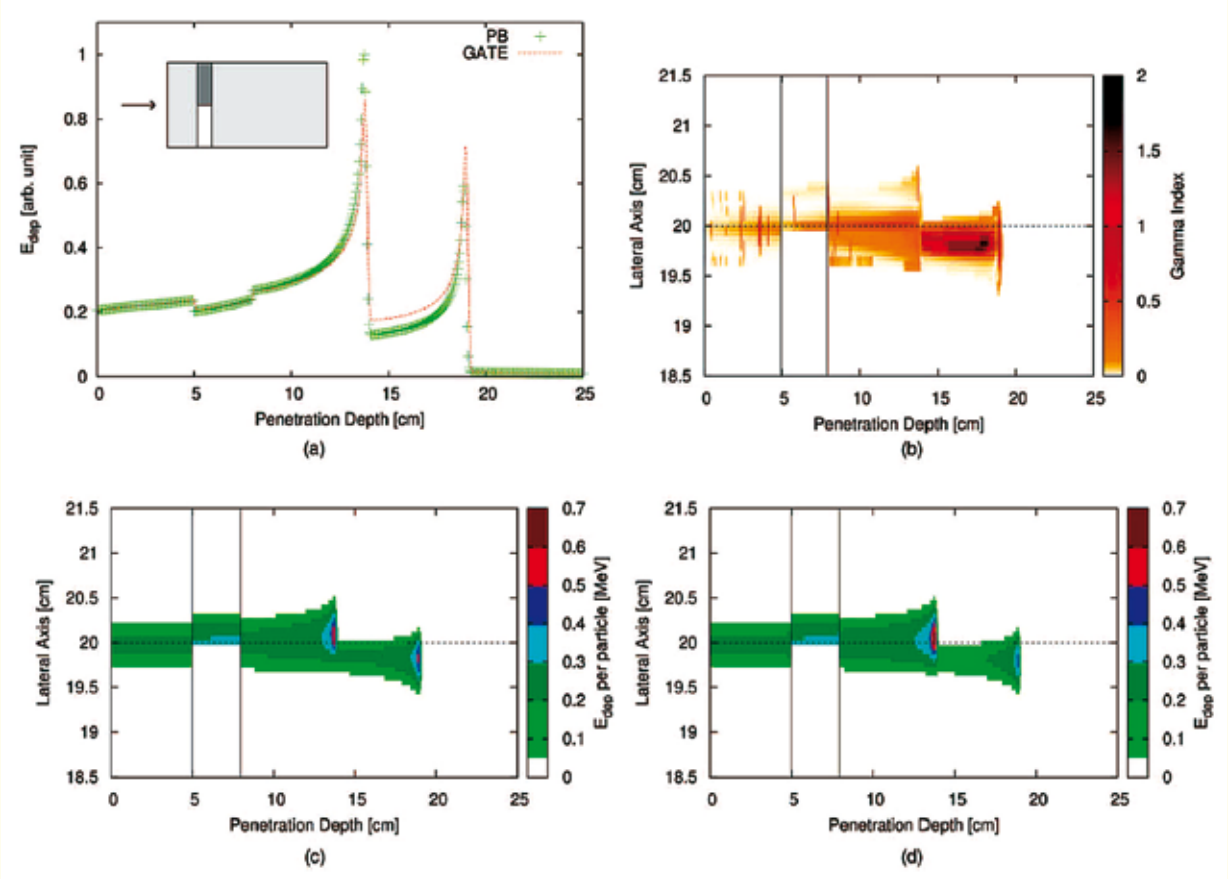

Figure 9.2. Energy deposition of a Gaussian helium ion beam with σ = 2 mm at 150 MeV/A, hitting a water phantom with two 3 cm thick inserts at 5 cm depth. The dark grey area was filled with bone, the white area with air and the light grey areas with water. (a) Longitudinal energy deposition (E_{dep}), lateral energy contributions up to 20 times of the initial sigma were taken into account in the pencil beam calculation. (b) γ -index map, using the 2%/2mm criterion. (c) GATE simulation and (d) the pencil beam calculation results with nine elementary pencil beams per dimension.

driven by dose, organ and volume parameters which in turn specify the treatment intent. In general, the optimisation methods can be classified in terms of single field uniform dose optimisation (SFUD), i.e. field per field optimisation, and the simultaneous optimisation of all treatment fields and beam spots in a composite treatment plan.

The most commonly applied dose calculation algorithm in state-of-the-art TPSs for particle beam therapy are pencil beam models. These models have been shown to deliver sufficient accuracy, high flexibility and high speed, irrespective of particle species. Effects like multiple Coulomb scattering, nuclear interactions and fragmentation can be included, albeit only in a (semi-)empirical manner. To achieve the highest accuracy in dose calculation in the presence of tissue heterogeneities, pencil beams are often subdivided in sub-beams or elementary pencil beams. For dose calculations with passive scattered beams, ray tracing algorithms are also used in the TPS. However, current developments are rendering these models outdated. In Figure 9.2 a dosimetric comparison is shown between a typical pencil beam algorithm and Monte Carlo simulations for a challenging geometry, thus illustrating the suitability of pencil beam algorithms for dose calculation in particle beam therapy.

In addition to the physical dose, radiobiological effects also need to be modelled during dose calculation (see also Chapter 7 on Radiobiology). For low LET particles, such as protons, rather pragmatic approaches are used in clinical practice to include RBE effects, e.g. for protons a generic factor of 1.1 is most commonly applied irrespective of organ, fractionation and energy. The situation is differs greatly for high LET particles like carbon ions. Current practice in carbon ion therapy is very different for scanned beam delivery and passive scattered beams. For the latter, RBE is included via LET dependencies obtained from historical neutron data, while RBE models for scanned beams used in TPS are mostly built on the Local Effect Model (LEM) developed at GSI. The LEM model is an analytical model that accounts for RBE dependencies on dose per fraction, cell type and endpoint. The basic input parameters are alpha-beta ratios of a photon beam for the same endpoints. Although very elegant in its concept, this model suffers somewhat from the limited knowledge of alpha-beta ratios for the vari-

ous tissue types and clinical endpoints with respect to toxicity.

Finally, after a treatment plan has been completed, the resulting dose distribution needs to be assessed and reviewed. Besides the clinical acceptance criteria that focus on tumour doses as well as doses to normal tissues and organs at risk, there are other aspects that require attention. These are, for example, estimated delivery time, scanning patterns and their robustness against organ and patient motion, and effects of uncertainties in RBE on dose distributions. Assessment parameters for the clinical acceptance of a treatment plan are similar to those used in photon beam therapy, i.e. the most common dose volume parameters are applied.

If a treatment plan is accepted, the underlying beam parameters and treatment geometry related parameters, such as table position or gantry position, are transferred to the database of an IT system called Patient Record and Verify System.

9.3 Quality assurance aspects

Treatment planning involves several quality assurance aspects. First of all, a TPS needs to be subjected to periodic quality assurance and quality control procedures. This is a rather complex and workload intensive task which exceeds the scope of this introduction to treatment planning.

As far as patient specific QA is concerned, several aspects require attention in clinical practice. Geometric factors of influence like organ filling status, patient diameter, patient position in the immobilisation device, patient rotations, etc. are verified prior to treatment delivery using imaging equipment. These can be planar or volumetric X-ray based imaging devices mostly located in the treatment room and combined with the beam delivery device. The frequent use of imaging tools to verify and correct patient geometry is called Image Guided Radiotherapy (IGRT). Some IGRT concepts in particle beam therapy are based on pre-positioning and CT located outside the treatment room with a subsequent patient transfer to the treatment rooms.

A treatment-plan-related, and also patient-specific, QA task is to verify that dose delivery is performed as intended. Potential sources of errors and uncertainties are incorrect data transfer from the TPS to the delivery unit, human errors, or shortcomings in the dose calculation of the TPS itself. Methods to perform patient-specific, treatment-plan-related QA range from experimental dosimetry verification in one or more points in a homogenous or anthropomorphic phantom to independent dose re-calculation techniques or in situ dose verification utilising interaction products when particles traverse human tissues, such as beta emitters or prompt gamma rays. Dose reconstruction based on PET imaging of beta activity distributions or single particle detection as mentioned above are currently research topics rather than state-of-the-art QA methods in particle beam therapy.

9.4 Current developments

Developments in treatment planning and dose calculation have focused on various aspects to facilitate the workflow and to improve delivery accuracy. Improvements with respect to dose calculation algorithms concern speed, in which GPU-based algorithm implementation is pursued, dose calculation accuracy, biological modelling and the inclusion of treatment plan robustness in optimisation strategies. Monte Carlo based dose calculation is certainly an issue; however, speed gain with current hardware is also relevant in general concepts like image guided adaptive radiotherapy (IGART) where treatment plans are adapted accordingly to accurately represent the anatomic situation.

Another general trend in radiation oncology is the selective boosting of radio-resistant tumour sub-volumes that can be visualised by molecular imaging techniques. In contrast to current radiotherapy practice, heterogeneous doses are delivered deliberately. This technique is called dose painting and together with scanned beam delivery and high LET particles, ion beam therapy thus offers ideal brushes for dose painting strategies.

From a historical point of view particle beam therapy and photon beam therapy were developed in parallel rather than in synergy. In recent years there has been a clear trend towards closer collaboration between these two communities which has certainly been influenced by the fact that existing standard radiotherapy departments invest in proton beam therapy as a complementary treatment option. In such a setting, combined modality treatments offer new options but also require further research and development. For example, combined modality treatments need to address the challenges arising from temporal changes in anatomy. Examples of research issues that impact TPS development are deformable registration and dose accumulation.

References

[1] M. Goitein, *Radiation Oncology: A physicist's-eye view*, Springer, New York, 2007.

[2] T. F. DeLaney, H. M. Kooy, *Proton and Charged Particle Radiotherapy*, Lippincott Williams and Wilkins, Philadelphia, 2007.

[3] Paganetti H, (editor) *Proton Therapy Physics*, Series in Medical Physics and Biomedical Engineering, CRC Press book, 2011.

[4] International Commission on Radiation Units and Measurements, *Prescribing, Recording, and Reporting Proton-Beam Therapy*, ICRU Report 78, Bethesda, USA, 2007.

[5] International Commission on Radiological Protection, ICRP Statement on Tissue Reactions/Early and Late Effects of Radiation in Normal Tissues and Organs – Threshold Doses for Tissue Reactions in a Radiation Protection Context, ICRP Publication 118, 2012.

10. Boron neutron capture therapy

10.1 Introduction

Boron neutron capture therapy (BNCT) is a dual therapy. First a ^{10}B carrier, with high tumour-cell specificity, is locally, or through the circulatory system, injected into the patient. When the tumour/healthy-tissue ^{10}B concentration ratio has reached the maximum value, the tumour region is irradiated with thermal neutrons. Thermal neutrons have a minor biological effect on living cells. However, they induce an exothermic nuclear reaction in ^{10}B nuclei (see Figure 10.1). Because of the short range of the high-LET nuclear reaction fragments, about 80,000 ionisation events take place inside the ^{10}B-doped living cell giving rise to severe biological damage. The nuclear reaction does not damage the surrounding cells. BNCT is therefore a cellular radiation therapy. Unlike traditional radiotherapy, it can selectively hit the tumour cells, sparing the surrounding healthy tissue.

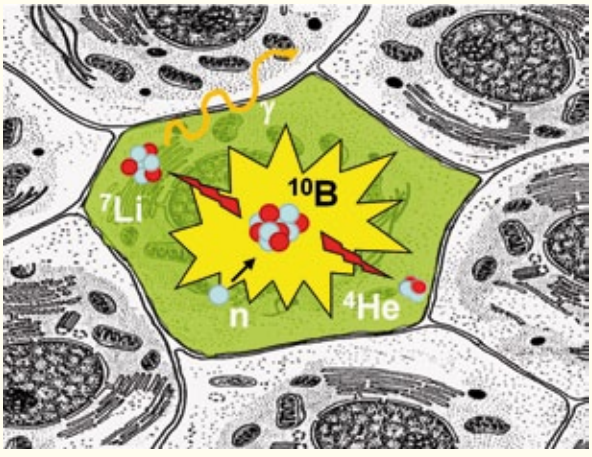

Figure 10.1. Artistic description of BNCT. The ^{10}B atom, previously charged into the tumour cell, undergoes nuclear reaction when it absorbs a thermal neutron. The short-range high-LET reaction fragments destroy the tumour cell.

10.2 BNCT in clinical practice

^{10}B is the isotope widely used for this purpose, being accumulated selectively into tumour cells by several mechanisms. For example, borophenylalanine (BPA) is selectively and preferentially accumulated into tumour cells via the augmented metabolism of amino acids in comparison to normal cells. The first clinical trials with BNCT were initiated in the early 1950s by Farr at the BNL and by Sweet and Brownell at the Massachussets General Hospital by using the MIT Reactor in patients with brain cancer. The disappointing outcomes of these trials were attributable to: i) absence of specific transporters of ^{10}B in the tumour and ii) no difference in concentration of ^{10}B between healthy and pathological tissue. From 1990 to today, many cancers have been treated using BNCT therapy, alone or in combination with other treatment modalities, reporting different results but with evident clinical benefits.

Since 1994, at least 227 patients with glioblastoma multiforme, a form of brain cancer associated with a poor prognosis, have undergone BNCT, in many cases in combination with chemotherapy (such as Bevacizumab or Temozolamide or with external beam radiotherapy, EBRT). The inclusion of BNCT in the therapeutic scheme produced a significant increase of the overall survival rate after 30 months from diagnosis (0% vs. 20% in no-BNCT vs. BNCT group and 0% in no-BCNT vs. 30% in BNCT+EBRT group). Moreover, from 1999, about 165 patients with head and neck cancer were treated by BNCT with a recognised effect from a clinical point of view (reduction of morbidity) and a recovery in overall survival of 38% after 24 months from the date of diagnosis.

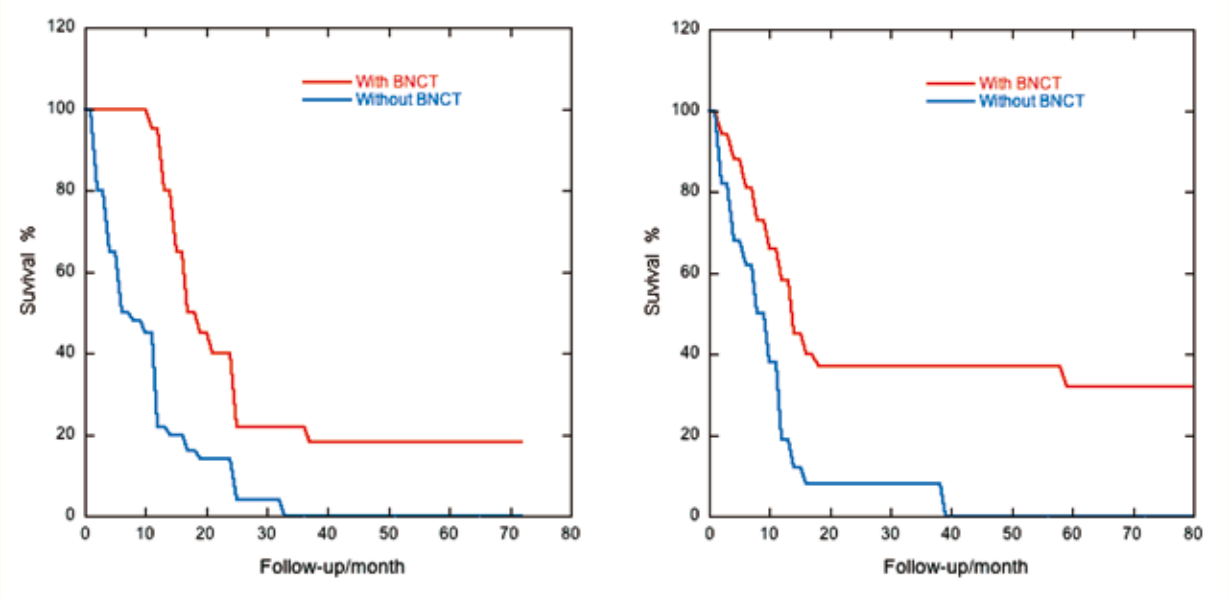

Figure 10.2. Left side, Kaplan–Meier plot of the overall survival for all newly diagnosed glioblastoma treated and not treated with BNCT [from Kawabata *et al*. (2009). Survival benefit from boron neutron capture therapy for the newly diagnosed glioblastoma patients. *Appl. Radiat. Isot.* **67**: S15-18]. Right side, Kaplan–Meier survival plots of patients with recurrent head and neck cancer treated with and without BNCT [from Kato *et al*. (2009). Effectiveness of boron neutron capture therapy for recurrent head and neck malignancies. *Appl. Radiat. Isot.* **67**: S37-42].

Figure 10.2 shows some recent data from the literature concerning glioblastoma and neck cancers.

More than 50 patients with cutaneous melanoma have undergone BNCT with proven effects, especially in the case of relapse in brain or other distant organs.

Many other type of cancer have been treated by BNCT, for example liver metastases from colon cancer, and others under investigations, such as breast and lung tumours.

Nowadays, six centres are treating patients with BNCT (see Table 10.1). All of these centres use neutron beams produced by research nuclear reactors. It is important to underline that the scarce availability of suitable neutron beams and the problematic access to nuclear reactor centres heavily limits the number of BNCT treatments.

Most of the treated tumours with BNCT are glioblastoma multiforme (GB) or squamous cell carcinoma of the head and neck region. The former is very aggressive and is histopathologically characterised by the presence of small areas of necrotic tissue surrounded by anaplastic cells. The latter is conversely less aggressive than GB, although its

Table 10.1. Operative BNCT centres

Centre	States	Neutron source	Neoplasm	N° of treated patients*
Helsinki University Central Hospital, Helsinki, Finland	Europe	FIR-1, VTT Technical Research Centre, Espoo	GB and HN	50 GM 2 AA 31 HN
University of Tsukuba, Tsukuba City, Ibaraki	Japan	JRR-4, Japan Atomic Energy Agency, Tokai, Ibaraki	GB	20 GM 4 AA
University of Tokushima, Tokushima	Japan	JRR-4 (Kyoto University Research Reactor, Osaka)	GB	23
Osaka Medical College and Kyoto University Research Reactor, Kyoto University, Osaka and Kawasaki Medical School, Kurashiki	Japan	KURR	GB, HN, CM	30 GBM 3 AA 7 Men 124 HN
Taipei Veterans General Hospital, Taipei, Taiwan	Republic of China	THOR, National Tsing Hua University, Hsinchu, Taiwan	HN	10
Instituto de Oncología Angel H, Buenos Aires	Argentina	Bariloche Atomic Center	CM and AT	7CM 3 AT

* GM: glioblastoma multiforme; CM: cutaneous melanoma; AA: anaplastic astrocytoma; HN: head and neck cancer; Men: meningioma; AT: anaplastic thyroid cancer

histological characteristics can variously alter the prognosis; for example poorly-differentiated lesions have scarcely five-year survival. Unfortunately, data about histological characteristics of treated head and neck cancer cannot be retrieved from the available literature. Similarly, malignant cutaneous melanoma can show different histological patterns, in particular it can be superficial or deep, with or without lymphatic or vascular invasion.

This targeted therapy has many strengths and weakness. The main advantage is its ability to act directly and specifically on the tumour, both primary or secondary (i.e. metastasis) with a selective effect on the neoplastic cells. Moreover it also has prognostic importance, with a favourable impact on the quality of life and on the overall survival of oncological subjects. The main weaknesses of BNCT are: i) the small number of suitable neutron beams; ii) their location outside the clinical environment; iii) the necessity of a multidisciplinary team (nuclear technology, sophisticated dosimetry, chemistry, biology and medicine); iv) the availability of only two selective molecules for ^{10}B delivery in tumours; v) the lack of randomised trials.

Therefore, as things currently stand, BNCT may be best suited as an adjunctive treatment, used in combination with other modalities, including surgery, chemotherapy, EBRT, which, when used together, may result in an improvement in patient survival.

10.3 BNCT physics

Boron is a metal with two stable isotopes: ^{10}B (19.9%) and ^{11}B (80.1%). The therapy exploits the nuclear reaction $^{10}B(n,\alpha)^{7}Li$. This reaction is very effective in destroying a tumour, providing that a sufficient amount of boron is accumulated in the tumour cell. In fact the two charged particles emerging from the nuclear reaction have high LET (linear energy transfer) and short range, which is smaller than the cell diameter.

The reaction cross section is 3837 barn and the Q-value is +2.79 MeV. The reaction proceeds by two pathways. In the 6.3% of cases the Q-value energy is shared between the α particle (1.78 MeV) and the lithium ion (1.01 MeV). In the 93.7% of cases the reaction leaves the ^{7}Li ion in an excited state, from which it decays immediately to its ground state, emitting a 0.428 MeV gamma ray. The remaining energy is shared between the α particle (1.47 MeV) and the lithium ion (0.84 MeV). The average ranges are 9 μm and 5 μm in tissue for α particles and lithium ions, respectively.

^{10}B has to be carried into or close to the target cell with a drug designed to have a better affinity for tumour cells than the surrounding healthy cells. Two drugs are nowadays available for clinical investigations: BSH (*mercaptoundecahydro-closo-dodecaborate* $Na_2\ ^{10}B_{12}\ H_{11}\ SH$) and BPA (*para-borophenylalanine* $C_9\ H_{12}\ ^{10}BNO_4$). Other drugs are under investigation. For instance, two new drugs, based on a phthalocyanine molecule enriched with 40 ^{10}B atoms and on a porphyrin molecule enriched with 36 ^{10}B, have produced interesting results in mice skin-melanoma studies. Since these molecules are already used in photodynamic therapy (PDT), their use can be envisaged in a BNCT+PDT therapy.

Another element has been proposed for this kind of therapy: gadolinium, which is a metal of the lanthanide series. The natural metal occurs as of five stable isotopes. The ^{157}Gd isotope represents 15.7% of the natural metal and it has a huge thermal-neutron capture cross section (225 kbarn).

The proposed therapy, more properly called **GdNCT**, ought to exploit the capture reaction $^{157}Gd(n,\gamma)^{158}Gd$, which has a positive Q-value of 7.94 MeV. When ^{157}Gd absorbs a thermal neutron, it leaves ^{158}Gd in an excited state. The ^{158}Gd decay produces high energy γ-rays 31% of the time and internal conversion electrons for the remaining 69%. These electrons, the energy of which range from 79 keV to 6.9 MeV, leave vacancies in the orbital electron shells that are filled by higher orbital-level electrons. The ^{158}Gd atom de-excites by emitting X-rays or Auger and Coster-Kronig electrons. While γ-rays and fast electrons transport the energy far from the reaction point, Auger and Coster-Kronig electrons, which have energy of <1 keV, release their energy less than few tens of nanometres from the reaction point. Since ^{158}Gd decay can give rise to an Auger cascade of about 10 electrons, the energy locally released by a single decay is rather high. The high energy density should give rise to high-LET-like biological damage. Gadolinium chelates and cryptates could be used as carriers with very low toxicity. They are indeed already used as contrast agents in MRI (magnetic resonance imaging). This technique is still under preliminary experimental investigation in order to assess its potential advantages with respect to BNCT.

10.4 Accelerator-based neutron sources

Neutron capture therapy (NCT) needs large quantity of thermal neutrons at the tumour site. So

far, only nuclear reactors can supply large quantities of neutrons, but they have several drawbacks. Therefore, low-energy high-intensity particle accelerators have been developed for BNCT since the 1980s. Nowadays, the apparently most advanced project is the neutron source based on the 5MV 30mA RFQ (radiofrequency quadrupole), which was originally developed at the Laboratori Nazionali di Legnaro (Italy) in the framework of the ADS project (accelerator-driven system for nuclear waste transmutation). It successfully passed high power tests in 2012 and it will be the core of a p(5MeV) +Be neutron source of an intensity of more than 10^{14} s^{-1}.

Other running projects are: i) the 30MeV 1mA cyclotron of Kyoto university (Japan); ii) the 2.5MeV 10mA vacuum-insulation tandem accelerator of the Budker Institute (Russia); iii) the 2.4MeV 30mA tandem-electrostatic-quadrupole accelerator of the Argentinean Commission of Atomic Energy; iv) the 3MeV 5mA Dynamitron at the University of Birmingham (UK). In Israel, the SOREQ nuclear centre is designing a 2.0 MeV 10 mA superconductive LINAC.

Particle accelerators are designed to mainly exploit (p,n) neutron reactions by using beryllium or lithium targets, although the possibility to exploit (d,n) reactions is also under investigation.

Lithium

Natural lithium is a metal with two isotopes (^{7}Li 92.5%, ^{6}Li 7.5%) and a melting point at 180.54 °C. It is used in its natural or in its isotopic form ^{7}Li to produce large quantities of fast neutrons of relatively low energy.

The ^{7}Li(p,n)^{7}Be has a Q-value of -1.64 MeV and threshold of 1.88 MeV. The peculiarity of this reaction is its cross section that increases rapidly up to ~ 270 mb within the first 50 keV. At 2.25 MeV there is a broad resonance, which takes the cross section up to 580 mb. Therefore, the neutron yield is very high for proton energies just over the threshold. At E_p = 1.9 MeV the neutron yield is 1.5×10^{10} mC^{-1}, the mean neutron energy is 38.3 keV and the maximum neutron energy is 87.6 keV. However, in order to take advantage of the resonance at 2.25 MeV, proton beams of 2.5 MeV are proposed, which give a neutron yield of 8.8×10^{11} mC^{-1} on a thick natural lithium target. A problematic drawback is the low melting point, which makes difficult handling of this target with the high proton currents (about 10 mA) necessary for performing BNCT in reasonable time (less than 1 hr).

A high-power accelerator-based neutron source based on a liquid-lithium target (LiLiT) and the ^{7}Li(p,n) reaction was developed at SARAF (Soreq Applied Research Accelerator Facility, Israel) as a prototype for use in BNCT. The LiLiT device consists of a high-velocity (> 4 m/s) vertical jet (1.5 mm thick) of liquid lithium (~200 °C) supported by a concave wall. Recent beam tests show that the target dissipates a peak power areal density of 2.5 kW/cm^2 and peak volume density of 0.5 MW/cm^3 with no temperature elevation. The neutron yield for 1.91 MeV protons is $\sim2.5\times10^{10}$ n s^{-1} mC^{-1}. These conservative values demonstrate the feasibility of a full-scale accelerator-based BNCT neutron source based on a liquid-lithium jet target, using a 10-13 mA, 2 MeV proton beam with a radial gaussian distribution sigma ~ 10 mm.

Beryllium

Natural beryllium is a metal with only one isotope (^{9}Be). Because of its high melting point (1278 °C) and good thermal conductivity, it is more suitable for NCT.

With the expression ^{9}Be(p,n)^{9}B several nuclear reactions are usually pointed out. The main one is the two-body reaction ^{9}Be(p,n)^{9}B that proceeds through the formation of the compound nucleus ^{10}B, but it can also proceed through direct charge exchange. The negative Q-value is -1.85 MeV and the threshold energy is 2.057 MeV. However, the isotope ^{9}Be also has the smallest neutron binding energy (1.67 MeV) of any stable isotope. Therefore, both three-body reactions (p,p'n) and indirect (p,p') (n), the neutron production of which proceeds through excited states of ^{9}Be, can occur. Hence the resonant neutron peaks float on a continuous neutron yield, which becomes relatively significant for proton energies bigger than 3 MeV. Recent experimental data give a neutron yield of $3.5 \pm 0.3\times10^{12}$ mC^{-1} for E_p=5 MeV.

The gamma-rays produced by the neutron source are due to the exothermic reaction ^{9}Be(p,α)^{6}Li (Q-value= + 2.125 MeV), which leaves ^{6}Li in the excited state at 3.56 MeV. The gamma yield, due to the decay of ^{6}Li to the ground state, is about 0.1 photon per neutron produced. More gamma rays are produced by the Be target holder and by the beam shifter assembly.

A drawback is the very low permeability of hydrogen in beryllium (about 8 orders of magnitude less than in copper), which gives rise to target swelling with the risk of blistering.

Competing nuclear reactions

Thermal neutrons also cause capture reactions that are not useful in the frame of the targeted therapy, since they transport the reaction energy far from the reaction point. The more important reaction is

hydrogen neutron capture $^{1}H(n,\gamma)^{2}H$, which gives rise to a gamma ray of 2.2MeV of energy. The other key reaction is nitrogen neutron capture $^{14}N(n,p)^{14}C$, which gives rise to a 0.59MeV proton and a 40keV carbon ion. This reaction does not actually transport the energy far from the interaction point, since the ion ranges in tissue are ≤11 μm, but it occurs everywhere, including within healthy cells. Similarly, the reaction $^{40}Ca(n,\alpha)^{37}Ar$ (Q-value +1.748 MeV), which is of interest in irradiated bones.

With fast neutrons other reactions open up. Elastic and radiative reactions are the most important, which generate a background of γ-rays and scattered fast neutrons. Moreover, other nuclear reactions are possible. $^{16}O(n,\alpha)^{13}C$ (Q-value – 2.216 MeV and threshold at 2.36 MeV). $^{14}N(n,\alpha)^{11}B$ (Q-value – 0.158 MeV and threshold at 0.17 MeV). $^{31}P(n,p)^{31}Si$ (Q-value – 0.709 MeV and threshold at 0.73 MeV. $^{40}Ca(n,p)^{40}K$ (Q-value – 0.529 MeV and threshold at 0.54 MeV).

Neutron beam shaping

All the (p,n) reactions produce fast neutrons, which must be thermalised in order to be captured by the ^{10}B atoms and thus be useful to therapy. The original fast neutrons have to be shifted to lower energies in order to ensure that the tissue between the skin and the tumour is able to completely thermalise them. The energy shifter, called also beam shaping assembly (BSA), is a stack of different materials, which appropriately shape, energetically and geometrically, the original fast neutron beam.

Figure 10.3 shows the conceptual design of a thermal neutron source for BNCT. The source (TRIPS) injects into the accelerator (RFQ) a high-intensity proton beam, which is accelerated and then analysed by a 90° magnet. The proton beam impinges the beryllium target, which is in the centre of the BSA. The neutron beam, fully thermalised, emerges from the BSA to treat superficial tumours such as skin melanomas. The BSA size and weight depend on the neutron source spectrum. A BNCT facility which exploits the Li(p,n) reaction needs smaller BSA than a facility which exploits the Be(p,n) reaction, because of the higher neutron energies of the latter.

10.5 Therapeutic neutron beams

Since in BNCT only thermal neutrons are useful, undesirable radiation, which releases energy in healthy tissues upstream and downstream of the tumour site, has to be minimised. The "rule of thumb" to achieve such a minimisation are the IAEA figures of merit for shallow and deep tumours. After having defined the three energetic groups for thermal (E_n<0.5eV), epithermal (0.5eV<E_n <10keV) and fast (E_n > 10keV) neutrons, IAEA recommends the following fluence rates and absorbed dose rates for shallow and deep tumours.

Shallow tumours

$\Phi_{th} \geq 10^{9}$ cm^{-2}s^{-1}

$\Phi_{th}/\Phi_{tot} \geq 0.9$

$\dot{D}_{n\,(epi+fast)}/\Phi_{th} \leq 2\times10^{-3}$ Gy cm^{2}

$\dot{D}_{\gamma}/\Phi_{th} \leq 2\times10^{-3}$ Gy cm^{2}

Deep tumours

$\Phi_{epi} \geq 10^{9}$ cm^{-2}s^{-1}

$\Phi_{epi}/\Phi_{th} \geq 100$; $\Phi_{epi}/\Phi_{fast} \geq 20$

$\dot{D}_{n\,(fast)}/\Phi_{epi} \leq 2\times10^{-3}$ Gy cm^{2}

$\dot{D}_{\gamma}/\Phi_{epi} \leq 2\times10^{-3}$ Gy cm^{2}

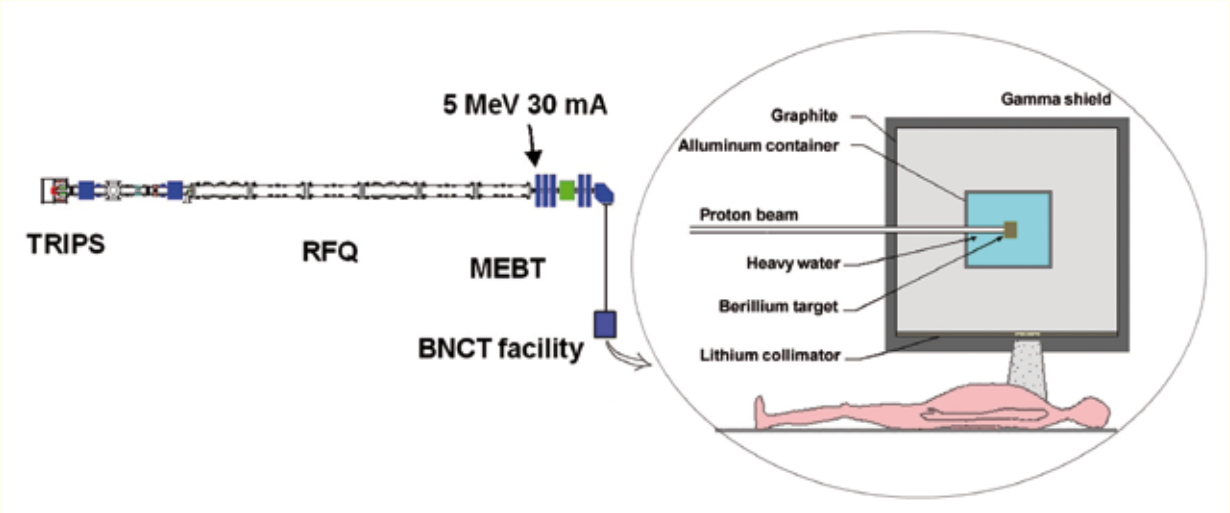

Figure 10.3. Schematic layout of the INFN BNCT irradiation facility for shallow tumours.

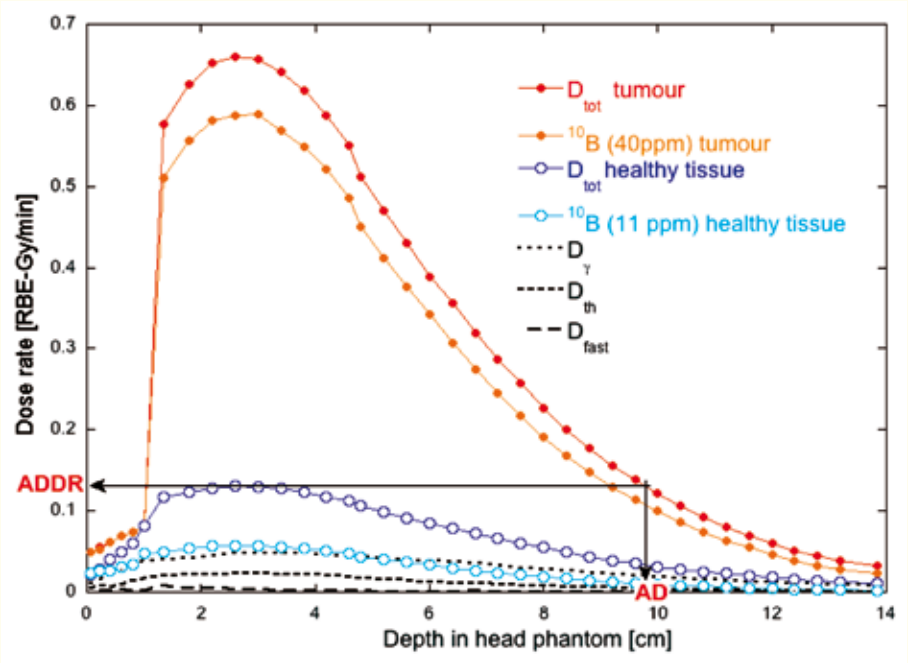

Figure 10.4. Monte Carlo simulations of biological-effective dose rates in glioblastoma tumour and healthy brain tissue, against the depth in a head phantom (J.Esposito, Studio di una sorgente neutronica da fusione per la BNCT, basata su un acceleratore compatto a bassa tensione e su originali materiali traslatori di spettro, PhD thesis, XIV cycle, a.a. 2002, University of Pisa). Different lines point out the different dose-components. The black-line components are common to both the two tissues. The physical doses have been multiplied by appropriate biological weighting factors, which are the same for the two tissues but for the high-LET capture-reaction products (labelled ^{10}B in figure), the weighting factor of which is 3.8 and 1.35 respectively (See reference 3, page 410).

However, although useful for neutron source design, the two figures of merit do not allow for properly assessing the possibility (from the dosimetric point of view) to treat a tumour at a given depth. To this end, a useful tool is to know the *advantage depth* (AD), which is *the depth in tissue at which the dose to tumour equals the maximum dose to the healthy tissue.* In other words, AD is the depth behind which the therapeutic gain (the ratio of tumour-to-healthy-tissue absorbed doses) is less than 1.

In Figure 10.4, Monte Carlo simulations of a BNCT facility, well illustrate the AD concept applied to the biological-effective dose. In Figure 3, together with the total doses, also the dose components are plotted. Only the biological-effective dose due to ^{4}He and ^{7}Li ions, emerging from the ^{10}B capture reactions, is supposed to be different for the two tissues. If we hypothesise that tumour cells have been charged with 40 ppm of ^{10}B, being the healthy-cells ^{10}B concentration of only 11 ppm. The figure shows that the maximum biological-effective dose rate, called ADDR (advantage-depth dose-rate), is 0.13 RBE-Gy/min at 2.6 cm of depth, in healthy brain tissue. The tumour tissue experiences the same dose-rate value at 9.8 cm of depth. Deeper tumours would receive lower dose than the healthy tissue maximum dose. Clearly, the AD value depends on the tumour-to-healthy-tissue ^{10}B concentration ratio (BR), the value of which is 3.6 in the simulation, and on the tumour-to-healthy-tissue RBE ratio with respect to the charge particles emerging from the capture reaction, the value of which is 2.8 in the simulation. Although a precise AD assessment needs a complex approach (Monte Carlo simulations together with microdosimetric data, radiobiological data and ^{10}B concentration assays in the tissues), a thumb rule is to use quasi-thermal neutrons for depths less than 2 cm and epithermal neutrons for deeper depths. However, for small BR-values, epithermal neutrons hardly can treat tumours deeper than 4-5 cm. For higher BR-values (about or more than 4), they can treat tumours as deep as 10 cm in soft tissue.

These considerations are based on the assumption that the ^{10}B concentration is uniform both in tumour and healthy tissue. If it is not, AD can have different values in different parts of the tumour, making the treatment plan rather complex.

Moreover, the RBE of the different radiation components is different. Therefore, monitoring the healthy tissue RBE could be critical for a successful therapeutic plan, since it determines the ADDR value.

Dosimetry and microdosimetry

The actual BNCT dosimetric protocol [1] suggests the use of the well-known twin-chamber method, which uses two ionisation chambers with different neutron sensitivities, for measuring the total absorbed dose and the D_n/D_γ ratio. The thermal neutron fluence, measured by the activation method, is used to calculate the ^{10}B dose. However, the D_n/D_γ ratio is poorly related to RBE. That implies a poor knowledge of the ADDR value.

The RBE at different depths in a phantom can be monitored with tissue-equivalent gas-proportional counters (TEPC). Mini TEPCs of a few millimetres diameter have been constructed, which can be inserted into the patient for in vivo monitoring. A mini detector made of two mini TEPCs, one with

and the other without ^{10}B in the cathode wall, can monitor the RBE for cells with and without ^{10}B [2]. Therefore as for dosimetry, a microdosimetry protocol for BNCT has to be implemented in order to make microdosimetric measurements effective.

10.6 Conclusions

As with conventional radiation therapy, BNCT can achieve its therapeutic effects by inducing damage of nuclear DNA, and endothelial cell damage. Therefore, any tumours can potentially respond to BNCT. If in the past many efforts have been aimed at brain, skin and head-neck cancers, in recent years new tumours have become a target, such as breast cancer, osteosarcoma, lung, pleural mesothelioma, and so on. Moreover, beyond conventional radiation therapy, BNCT can treat infiltrating tumours, minimising damage to healthy tissue.

In order to exploit the large spectrum of BNCT therapeutic possibilities, clinicians need suitable and daily-accessible neutron sources in a clinical environment. This would allow the implementation of more successful clinical protocols, inter-comparisons and randomised studies. Only particle accelerators are able to provide the intense neutron sources that are necessary for BNCT in a clinical environment. The construction of several accelerator-based neutron sources is in progress. The scientific community should support the coordination and the quick completion of neutron sources for accelerator-based BNCT.

Different accelerator-based neutron sources have different radiation components and relative biological effectiveness, which need to be monitored for any significant clinical inter-comparison. Therefore, the use of experimental and theoretical microdosimetric tools is mandatory.

The ^{10}B carrier aspect is less important, since two drugs with good performance are already available. However, new ^{10}B carriers with still higher tumour specificity could expand BNCT potentialities towards deeper tumours. More important is the characterisation of the histological pattern of neoplasms for directly stratifying the effectiveness of neutron treatments or indirectly by testing the in vivo concentration of boron-transporters by functional imaging, such as magnetic resonance imaging (MRI) or positron emission tomography (PET). Future clinical research has to be based on these issues.

More details about BNCT principles and BNCT applications can be found in the recent book edited by W. Sauerwein and colleagues [3].

References

[1] Binns, P.J., *et al.* (2005). An international dosimetry exchange for boron neutron capture therapy, part I: absorbed dose measurements. *Med. Phys.* **32**: 3729–3736.

[2] P. Colautti; D. Moro; S. Chiriotti; V. Conte; L. Evangelista; S. Altieri; S. Bortolussi; N. Protti; I. Postuma. (2013). *Microdosimetric measurements in the thermal irradiation facility of LENA reactor. Applied Radiation and Isotopes*, in press.

[3] W.A.G. Sauerwein, A. Witting, R. Moss, Y. Nakagawa. *Neutron Capture Therapy.* Springer-Verlag Berlin Heidelberg, 2012.

11.
Clinical programme update in particle therapy

11.1 Introduction

Hadrontherapy, i.e. radiation therapy using protons (p), neutrons (n) or heavy ions, has become one of the most sophisticated and attractive approaches in the management of cancer, since it deals with two essential aspects of modern radiation oncology: i) ballistic aspects, that allows optimisation of the dose to the tumour volume, along with maximal sparing of surrounding normal anatomical structures; ii) biological aspects, due to an increased radiobiological effectiveness (RBE) on interposed tissues, related with a high linear energy transfer (LET) along their path. If the ballistic properties are not far different for most particles, i.e. protons and light ions, the biological advantages are only shared by heavier ions, represented nowadays almost exclusively by carbon ions. The interest for particle therapy has paralleled the technological evolution of "conventional" photon (X-ray) therapy: introduction of compact dedicated commercial accelerators in place of former nuclear physics prototypes; development of isocentric rotating gantries that allow sophisticated beam arrangements, and easier patient set-ups (mainly for protons); image guided radiotherapy (IGRT), including mobile target tracking; pencil-beam scanning (continuous or by spots), able to generate intensity modulated proton therapy (IMPT); accurate dose-calculation methods (Monte Carlo) that progressively replace less sophisticated ones (ray-tracing, pencil beam), along with in vivo QA (gamma-prompts, on-line PET). These innovations have considerably stimulated the exploration of new clinical indications, from a few in the early 1980s to more than 60 recorded recently on the PSI website dedicated to protons alone. We summarise below the clinical experience accumulated in proton and carbon ion therapy. Detailed information can be found in recent articles and textbooks [1-4].

11.2 Proton therapy indications

Protons, whose clinical experience exceeds 100,000 patients worldwide, have proven advantages in two settings:

i) Delivering an escalated dose to a "radio-resistant" tumour process, situated close to, or abutting a radiosensitive organ:

- Ocular malignancies, esp. uveal melanomas, represent the main indications in the proton literature, with highly hypofractionated doses being administered to a maximum of 50–60 GyEq *(i.e. Physical dose x estimated RBE of 1.1 for p)*. Remarkable results have been reported by most groups: approx. 95% local control (LC), 80% overall survival (OS), 50% eye-preservation, and sometimes salvage programmes including p re-irradiation.
- Skull base and cervical canal low grade sarcomas: chordomas (CH) and chondrosarcomas (CS) have been extensively explored since the late 1970s. Recent advances have concerned the genetic profile of these malignancies, and the introduction of biological agents in metastatic presentations. But charged particles remain of crucial importance in achieving permanent LC. Optimal dose has been set to about 70 GyEq in CS, and ≥ 75 GyEq in CH. Late failures (i.e. > 10 years) can occur, and make protracted follow-up necessary.
- Spinal, para spinal and sacral sarcomas/CH are particularly challenging conditions due to the cord and/or cauda equina proximities, and the

frequent interposition of metallic surgical material in the beams' path. These lead to a severe selection of patients. Further improvements could be achieved using C-ions (see below).

- Head and neck carcinomas have also long been highly challenging due to the interposition of bone-air cavities, in sino-nasal sites. This introduces uncertainties in dose-distribution. The development of Monte Carlo calculations has made their management much safer. Remarkable results have been achieved esp. in adenoid cystic carcinomas, approaching 80%. But the outcome of malignant gliomas has not been definitely improved despite dose-escalation studies.

ii) Improved sparing of normal tissue from radiation effects:

- In children, this advantage is particularly important, due to the exquisite sensitivity of organs under development. In the mid-1980s, the dramatic improvement of pediatric tumours that followed the introduction of efficient polychemotherapy programmes made RT almost obsolete in the mind of many investigators. Actually RT has remained crucial in most clinical situations, and even gained in popularity when proton facilities became available. Nowadays these indications should be considered a priority. Using protons, one can expect to reduce long term sequelae, esp. those affecting bone growth and brain maturation in youngsters. The potential risk-reduction of radiation-induced secondary malignancies has also been recently addressed.
- In adults, protons have proven beneficial for multiple anatomical organs, such as parotids in ENT sites, or rectum/bowel in pelvic sites, in terms of improved physical dose-sparing. But clinical benefits still remain partially unknown. It is interesting to mention that not only long term side-effects can be spared using particles, but also acute toxicity on mucosa and bone marrow that make them attractive in chemo-radiations combinations. It is also important to stress that optimal "conformality" to the target, along with sparing of critical structures, can only be achieved using modern dose-delivery techniques (see introduction).

11.3 Development of carbon ions indications

The clinical experience has involved approximately 15,000 patients worldwide, mostly in Japan. Biologically, maximal increased RBE is observed in the distal peak, where the tumour is located, and not in the plateau located upstream, where normal tissues are interposed. This makes them highly attractive in the most challenging tumours. But variations are observed according to tissue-type, biological and clinical endpoints, and fractionation of the dose (not to mention alternating types of particles), that make further intensive physical and biological research programmes necessary. The Japanese have derived their C-ion experience from formerly tested neutrons (n), a neutral high-LET particle, which was applied to slow-growing, intrinsically radio-resistant, hypoxic, and/or non- operable malignancies, administered with unusually high doses per fractions. These included salivary, and prostatic primaries (slow growing), and sarcoma/glioma histological subtypes (= radio-resistant). Unfortunately, neutron clinical experiments were discontinued in the mid-1990s, due to the excessive toxicity reported on healthy tissues, related with poor dose-distribution. On another hand, the C-ion dose-profile somewhat similar to protons has stimulated interest for similar indications, with the hope of improving their outcome further: 70–85% LC has been reported in skull base CH, a benefit confirmed in a recent multivariate analysis; 50% OS, in selected cases of pancreatic carcinomas, known for their usual lethal outcome; 80% in unresectable spinal/para spinal sarcomas; 80% in some series of aggressive melanomas (generally not ocular nor cutaneous, but of mucosal origin). Prostate carcinomas have also been largely explored. The European experience, initiated more recently in Germany (Darmstadt, 1997, Heidelberg, 2009), and Italy (Pavia, 2012), has been based on more "conventional" fractionation of the dose (compared with X-rays), that might help put in perspective particles with X-ray therapy. The first randomised trials are also being conducted. There are also C-ion projects under development in Austria (Wiener-Neustadt), and France (Lyon and Caen).

11.4 Perspectives

Recent evaluation by the French ETOILE group in Lyon assessed that protons and C-ions could be beneficial in approximately 12% and 5% of cancer patients respectively. This would represent about 20–25000 new cases per year in countries such as France, Italy or Germany. These values exceed by far the current capacities of hadron-therapy programmes. For protons, facility costs have been substantially reduced over the past few years,

making them relatively "accessible" to major cancer centres. This might favour comparative p vs X-ray evaluations, highly suitable in the context of dramatic technological progress, for both. As for C-ions, it will remain for a long time beyond the scope of most oncological groups, with hopefully the exception of few dedicated centres able to promote advanced research programmes.

References

[1] J. Lundkvist, M. Ekman, S.R. Ericsson, B. Jönsson, B. Glimelius. (2005). Proton therapy of cancer: potential clinical advantages and cost-effectiveness. *Acta Oncol*. **44**: 850–61.

[2] J.S. Loeffler, M. Durante. (2013). Charged particle therapy – optimization, challenges and future directions. *Nat. Rev. Clin. Oncol*. **10:** 411–424.

[3] U. Linz (Editor), *Ion Beam Therapy*. Springer Verlag, Heidelberg, 2012.

[4] T.F. DeLaney, H.M. Kooy (Editors), *Proton and Charged Particle Radiotherapy*. Lippincott Pub, Philadelphia, 2008.

[5] C.M. Charlie Ma, T. Lomax, *Proton and Carbon Ion Therapy*. CRC Press, Taylor & Francis, 2012.

12. Outlook

Despite the heated debate on the cost/benefit ratio, hadrontherapy is rapidly expanding in Europe and Asia. USA, the leading country for the number of proton therapy centres, is now seriously contemplating the construction of a clinical research facility for protons and heavy ions. The superior dose distribution in hadrontherapy compared to conventional X-ray therapy is a consequence of basic nuclear physics. Strict advocates of evidence-based medicine contend that an improved dose distribution does not necessarily lead to improved clinical outcome. However, the current phase I/II clinical results support the rationale of the therapy, especially for tumours localised in proximity of critical organs, unresectable or recurrent tumours, and in general tumours resistant to radiation due to histology, genetic background and/or local microenvironment, including hypoxia. Patients with the highest priority for hadrontherapy are presently those affected by chordomas/chondrosarcomas of the skull base, soft tissue and bone sarcomas, large uveal and mucosal melanomas, and most of the pediatric patients eligible for radiotherapy. The number of patients eligible for hadrontherapy may largely increase if positive clinical evidence emerges from current trials in cancers with high incidence (lung, prostate, breast) or resistant to conventional treatments (renal cell carcinoma, pancreas and liver cancers, glioblastoma), and by including benign diseases, where local control is sufficient. Moreover, radiobiology research could expand the indications for charged particle treatments based on the tumour genetic background.

The contribution of nuclear physics to hadrontherapy has been enormous in the past, and can lead to further breakthroughs in the future.

- Accelerator physics made the treatment possible. Next steps here are the development of smaller and cheaper accelerators and beam delivery systems (gantries), also able to shorten the treatment duration.
- Medical physics is tackling the problem of range uncertainty, one of the main concerns in the treatment of tumours close to critical organs or moving targets, such as non-small-cell lung cancer. Gating, rescanning, and tracking are possible solutions to the problem of the interplay between beam and target movements. A promising alternative is 4D-optimisation, where treatment plans are computed on all 4D-CT phases, incorporating tumour motion and water-equivalent particle path length changes directly.
- Nuclear physicists are developing novel detectors for range verification and particle radiography. Real-time measurement of the 3D dose distribution is important for fast scanning beams and rescanning methods. For example, high-granularity tracking calorimeters for the detection of charged and neutral radiation can be able to determine the Bragg-peak position as well as the lateral 2D dose distribution.
- Biophysical modelling of beam transport and effects is essential for next-generation treatment planning. Monte Carlo methods are largely used for benchmarking of treatment plans, and for *ab initio* modeling of radiation action. The modelling of relative biological effectiveness (RBE) is already a major part of the treatment plan with carbon ions, and is increasingly also becoming an issue in protontherapy.
- Beyond protons and carbon ions there is room for developments in the use of other ions such as He (similar biological effectiveness as protons, but much reduced lateral scattering), oxygen

(possibly useful against very resistant, hypoxic tumours) and neutrons (produced at accelerators for boron neutron capture therapy).

More than 80% of R&D in hadrontherapy is today achieved by commercial companies. One of the important challenges of the coming years will be to develop links with these companies: collaborations, evaluation programmes, share of know-how and expertise, etc. Many fields explored for particle therapy research can have significant feedback in conventional radiotherapy using X-rays or electrons, which still covers over 95% of the treatments.

Nuclear physics will play a major role in the development of particle therapy and Europe can lead this field with existing and future facilities, and extensive expertise in accelerators, detectors, and so forth. The European scientific community involved in hadrontherapy is well represented in the European Network for LIGht Ion Hadron Therapy (ENLIGHT), which for over 10 years has represented an essential network for scientists in different disciplines (physics, biology, engineering, medicine) interested in particle therapy (see http://enlight.web.cern.ch for details). ENLIGHT successfully led several EU FP7 grants such as PARTNER, ULICE, ENVISION and ENTERVISION, with total funding of over 24 M€. ENLIGHT can be the ideal platform to continue this research in Horizon 2020.

List of Contributors (Chapter I)

- **Jacques Balosso,** France – *medical consultant*
- **Guido Baroni,** Italy
- **Marcus Bleicher,** Germany
- **Sytze Brandenburg,** Netherlands
- **Lucas Norberto Burigo,** Brazil
- **Paolo Colautti,** Italy
- **Stephanie Combs,** Germany – *medical consultant*
- **Giacomo Cuttone,** Italy
- **Jürgen Debus,** Germany – *medical consultant*
- **Ludovic Demarzi,** France
- **Jan Dobeš,** Czech Republic – *NuPECC liaison*
- **Marco Durante,** Germany – *convener*
- **Laura Evangelista,** Italy
- **Enrico Fagotti,** Italy
- **Sydney Galès,** France – *convener*
- **Dietmar Georg,** Austria
- **Christian Graeff,** Germany
- **Thomas Haberer,** Germany
- **Jean-Louis Habrand,** France – *medical consultant*
- **Adam Maj,** Poland – *NuPECC liaison*
- **Hamid Mammar,** France – *medical consultant*
- **Alejandro Mazal,** France
- **Samuel Meyroneinc,** France
- **Igor Mishustin,** Russian Federation
- **Pawel Olko,** Poland
- **Annalisa Patriarca,** France
- **Igor Pshenichnov,** Russian Federation
- **Frauke Roellinghoff,** Belgium
- **Dieter Röhrich,** Norway
- **Claas Wessels**, France

Chapter II
Medical Imaging

Conveners: **José Manuel Udias** (Madrid) – **David Brasse** (Strasbourg)

1. Introduction

"A century ago, the living body, like most of the material world, was opaque. Then Wilhelm Roentgen captured an X-ray image of his wife's finger – her wedding ring 'floating' around a white bone – and our range of vision changed for ever". From the words of Bettyann, Holtzmann and Kelves through to the present day, amazing progress has been made in medical imaging. One of the most impressive achievements of the last fifteen years is probably the emergence of molecular imaging.

Multidisciplinary by definition, physicists, biologists, physicians, chemists and mathematicians bring their expertise to observe, characterise and quantify biological processes at the subcellular level in living organisms. Molecular imaging originates from nuclear medicine where single photon emission tomography (SPECT) and positron emission tomography (PET) imaging techniques are used to observe complex biological processes at the early stage of a disease or for therapeutic follow-ups.

The use of radioactive tracers for medical purposes began with Georges de Hevesy in the 1930s. The discovery of technetium at the Berkeley cyclotron and the announcement of the first SPECT machines in 1968 pushed the discipline forward. SPECT rapidly became the most frequently used emission-scanning technology all over the world. The detectors used in SPECT nowadays look quite similar to the ones used at the beginning of this technique. Sodium iodide inorganic crystals, coupled to a matrix of photomultiplier tubes, are well adapted to image the 140 keV photons generated by technetium-99m. The intrinsic performance of most detectors does not impact overall image quality in SPECT, which essentially depends on the collimation stage.

PET began at the same period as SPECT and has overlapped with the other imaging techniques occasionally, but while anatomical imaging modalities such as CT and MR moved under the spotlight of modern clinical practice, PET remained, until very recently, in the shadow. The current success story for PET imaging as an invaluable tool in the clinical routine is due to the combination of several factors,

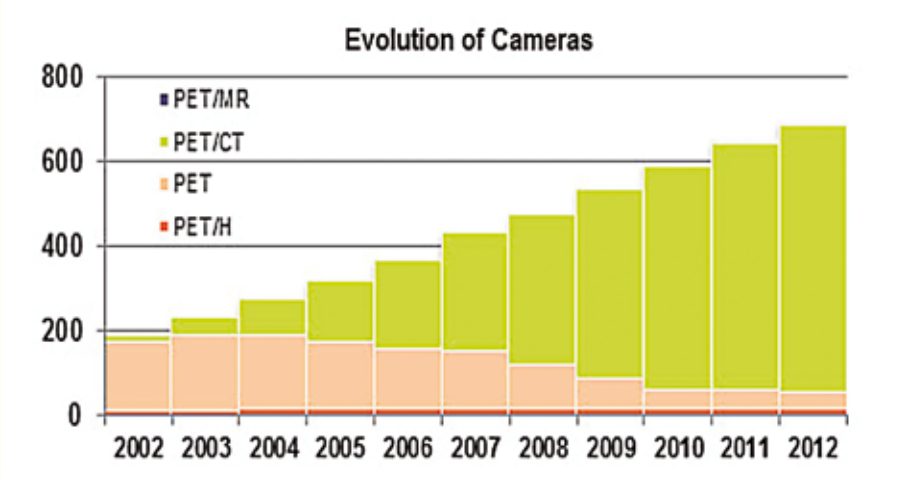

Figure 1. Evolution in the number of PET cameras. It can be seen how PET/CT is now the preferred choice and that the number of PET scanners has sustained a constant growth over the last ten years.

of which improvement in detector performance has in fact played a rather minor role. The need for a "technetium"-like isotope for PET was mandatory. With a half life of almost two hours and ideal physical properties for PET imaging, ^{18}F rapidly became the isotope of choice. However, it requires a well-established network of cyclotron facilities capable of providing radiolabelled compounds at the patient bed. Finding the clinical niche in which PET does not compete with but rather complements other imaging modalities was also a determining factor for the success of PET. The combination with CT promoted PET as the dominant tool in oncology. Johannes Czernin from UCLA, at the 2003 annual DGN meeting, commented that "PET/CT is a technical evolution that has led to a medical revolution".

SPECT and PET imaging techniques are entering a new era, where technical improvements will play an increasingly important role. As an example for SPECT, dedicated cardiac imagers already take full advantage of solid-state detectors. Time-of-flight PET and the combination with MRI will continue to challenge researchers: "PET/MRI is a medical evolution based on a technical revolution", as described by Thomas Beyer.

This chapter highlights state-of-the-art and future prospects of medical imaging, mostly in the field of nuclear imaging. It focuses on new developments and innovations brought by the nuclear physics community. Different sections cover hardware and software developments in clinical and preclinical studies as well as interface applications with other chapters of this booklet.

2.
From nuclear to molecular imaging

2.1 Nuclear imaging techniques

Molecular imaging using radioactive tracers makes use of two distinct types of "camera". Tracers containing a radioactive isotope that decays by the emission of a positron are imaged by a positron-emission tomograph. In tomography, a 3-dimensional image of an object is obtained by combining 2-dimensional images taken at different angles around the object. Tracers emitting gamma rays are imaged by the so-called gamma camera. It is used to take 2-dimensional images and, when positioned on a rotating gantry, allows tomographic imaging (SPECT: single photon emission computed tomography).

2.1.1 Positron emission tomography

A typical state-of-the-art commercial clinical PET scanner contains a few tens of thousands of small scintillation crystals that individually detect the positron annihilation photons emitted by the radiotracers in a patient's body. The detection times are measured very accurately, with a precision of about half a billionth of a second. Data rates are large: typically of the order of a million events per second. Sophisticated algorithms distil 3D images out of the huge data set thus recorded. Images with a spatial resolution of about 4 mm are obtained. A whole body scan with the ^{18}FDG tracer, one of the most common PET procedures, takes about 15 minutes.

The scanner bore of about 70 cm is determined by patient size, the axial length of 20–25 cm is a matter of limiting the costs. Nowadays, all PET scanners are combined with a CT scanner for a quick, easy and accurate determination of the attenuation correction needed for quantitative imaging. Scanners come with a collection of sophisticated data and image analysis options for specific scan procedures and clinical investigations. Ease of use and integration in the clinical workflow are well-developed important features.

2.1.2 PET combined with magnetic resonance imaging

In recent years, commercial systems for clinical use combining a PET and an MRI (magnetic resonance imaging) scanner have become available. First systems allowed the integrated but sequential combination of PET and MRI. The development of silicon-based photosensors, which are insensitive to magnetic fields, have made truly integrated systems possible, first for head scans and most recently for full-body scans. These systems allow simultaneous PET and MRI without quality loss in either imaging modality.

2.1.3 Single photon computed tomography

The physical characteristics of SPECT scanners have not changed much over the past few decades. The originally used scintillation material, NaI, remains adequate for the task, mainly because sensitivity and image resolution are largely determined by the collimator positioned in front of the detector. Collimators are rather simple mechanical devices that were optimised quite a while ago. Nevertheless, SPECT scanner developers have made use of the rapid progress in electronics and computation, improving for example ease of use, stability and reliability.

2.2 Preclinical imaging

During the last decade there has been a growing research interest in the field of "molecular imaging". The necessity of understanding biochemical processes at the molecular level have stimulated

a great advance in technological instrumentation, both in hardware and software, especially for in-vivo studies on small animals, e.g. rats and mice. This field of research is often called "preclinical imaging". Major efforts are devoted towards obtaining higher sensitivity, higher spatial resolution and cheaper and easier to handle instrumentation.

This chapter gives a short overview of the state-of-the-art technologies for the most diffuse molecular imaging techniques, namely, positron emission tomography (PET), single photon emission computed tomography (SPECT), X-ray computed tomography (CT) and MRI (magnetic resonance imaging), as applied to small animals. Finally, multimodality techniques that allow the merging of molecular information with anatomical details, such as PET/CT; SPECT/CT and PET/MR, will be illustrated. These are fields where the technology is rapidly evolving.

2.2.1 Present technology for small animal PET imaging

Functional molecular imaging investigations are performed on small animals, such as mice and rats, down to the cellular level, so as to obtain results on simplified human models before direct study on patients [Massoud and Ghambir, 2009]. The requirements on spatial resolution are much higher than those for clinical scanners, because the dimensions of rats and even more of mice are clearly much smaller than those of human beings. For example, imaging of the rat brain requires a spatial resolution of less than 2 mm full width at half maximum (FWHM). A resolution better than 1 mm (FWHM) would be necessary for the brain of the mouse, whereas a state of the art clinical scanner has a spatial resolution not better than 4 mm (FWHM).

In addition, the available radioactive signal is very weak. In fact, the injected activity in a mouse for brain receptor investigation is typically not greater than 5–10 MBq. Further there are limitations on the maximum volume of injected solution (~10% of the total blood volume). As a consequence high-sensitivity instrumentation is especially required when fast dynamic processes are studied with characteristic times of the same order of the scanning time. All of the above has put stringent requirements on PET scanners for small animals and it has produced copious research in this field.

The design of most small-animal PET instruments is usually based on a miniaturised structure of a clinical scanner with small detector elements surrounding the animal in a small bore ring. Other designs make use of rotating planar detector pairs (see Figure 2). The latter configuration offers a better sampling and image uniformity, but it has severe limitations in terms of dynamic imaging and if very fast throughput is desired.

High-resolution multi-anode photomultipliers tubes (MA-PMT) have been the photodetector of choice for most preclinical scanners. In most solutions the MA-PMTs are coupled to pixilated matrices of scintillators. In this case, the coordinates of the photon interaction are obtained via the "light-sharing" technique, i.e. by calculating the centroid of the light produced by the crystal on the high-granularity position-sensitive PMT. MA-PMTs have undergone a series of improvements (see Figure 3) over the last twenty years, many of which have been partly triggered by the needs of the molecular imaging community: this led to the evolution from early MA-PMTs based on a typical round shape, (up to 10 cm diameter, and a crossed wire anode structure), to second generation (square-shaped metal-channel dynode structure) with a very fine anode granularity. And finally, with the third generation there has been a great improvement in the active area dimensions (up to 5 cm inside) and especially in the active-to-total area ratio (up to about 90%). These 5 cm tubes are based on the metal-channel dynode structure with an anode matrix of 16×16 elements on a 3 mm pitch.

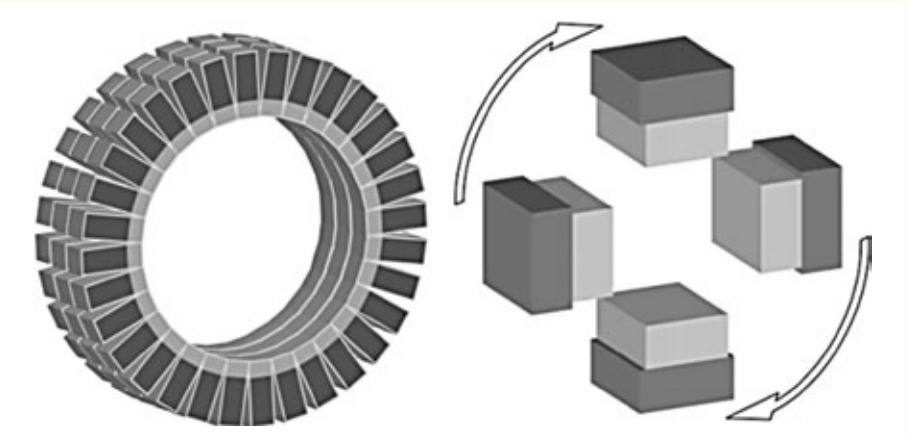

Figure 2. Two different configurations for the construction of a small-animal PET scanner. Left: ring geometry, where the detectors are arranged in rings surrounding the animal. Right: Example of a rotating detectors configuration with four heads, where each one is in time coincidence with the opposite one.

Figure 3. Example of first generation (left, Hamamatsu R2486 with crossed-wire anode structure), second generation (centre, Hamamatsu R8520 with crossed-plate anode structure), and third generation (right, Hamamatsu H8500 with multi-anode structure) MA-PMTs. Images from the Hamamatsu web site: www.hamamatsu.com.

The best readout method for modern MA-PMTs would be independent single anode read-out. To this end, dedicated ASICs have been implemented and are currently used with the H8500 Hamamatsu product in high energy physics. However, in order to limit the cost and complexity of the readout, often the simpler method of resistive chain for both X- and Y-coordinate is adopted, so as to strongly reduce the number of output channels.

More recently, semiconductor photodetectors have become an alternative and more attractive method for the readout of matrices of scintillators. In this case a matrix (either assembled or monolithic) of photoconductors with the same granularity as the scintillator matrix is coupled one to one to the scintillator pixel (no-coding error). Typical examples of this solution are PET inserts to MR, where matrices of small-area avalanche photodiodes (APDs) are used for the parallel readout of the pixilated matrices of a scintillator.

So-called silicon photomultipliers (SiPM) are being characterised and studied by many groups. These photodetectors will definitely not only be used for clinical scanners, but they will replace the so-called block detector. These photodetectors could also be used to reconstruct the centre of mass of the light deposited in a monolithic scintillator, by measuring, with high precision, the centroid of the light spot and also the dimension of the spot, so as to infer depth of interaction (DOI) information.

To maximise the efficiency of PET systems, PET heads should be positioned close to the object, and the thickness of the photon absorber should be at least one attenuation length at 511 keV. With the detector so close to the target, there is a significant contribution of the parallax error to the spatial resolution, and thus many techniques have been developed to obtain DOI information.

The simultaneous improvement of spatial resolution and sensitivity is the challenge of PET imaging. However, these two figures are often mutually opposed, i.e. increasing one could cause the reduction of the other. Every year, new small-animal PET prototypes are produced or proposed by research groups offering or promising even better performance. At the same time, some fully engineered scanners are released as commercial products.

2.2.2 Present technology for small-animal SPECT systems

SPECT systems for small animal imaging are of two main types: the first one makes use of the clinical SPECT configuration, e.g. thallium-doped sodium iodide (NaI:Tl) Anger camera, equipped with a special collimator; the second one consists of dedicated systems based on compact, high resolution detectors, following PET scanner technology.

In both cases, the main feature is the collimator type: contrary to the clinics, where regular arrays of round, square, or hexagonal holes in a high-density medium such as lead or tungsten are used, here the most widely applied collimator solution is the pinhole (or multi-pinhole). With this collimator, one increases the spatial resolution of the imaging system by magnification of the object onto the detector. By using large detectors such as a conventional Anger camera, a very high resolution down to a fraction of a mm is obtained. However, the sensitivity could be very low because of the pinhole configuration. To overcome this problem, multi-pinhole solutions are implemented, but the large magnification produces large projections that may overlap as the number of pinholes increases. The group of Steve Meikle in 2002 has solved the problem of overlapping projections by the use of iterative estimation, originally derived from the coded aperture approach proposed by Harry Barrett in 2001.

As for the second type of small animal SPECT, solid-state detectors provide a promising alternative technology as compact high-resolution gamma cameras. Semiconductor detector technology is the new horizon in dedicated instruments for high-resolution nuclear imaging and such solid-state detectors with direct γ-ray conversion such as CdTe and CdZnTe have been proposed. The requirements for a good detector for SPECT, i.e. high spatial resolution, high energy resolution, and good efficiency for the detection of medium energy γ rays, are only

partially fulfilled by solutions based on scintillators/photomultipliers as in PET, especially due to the low energy resolution of scintillators and the relatively low (25–35%) quantum efficiency of the photodetector. A direct conversion solid state detector offers a much higher quantum efficiency and energy resolution and its granularity is now well within in the range of the necessary high spatial resolution, whereas its intrinsic efficiency does not create a severe DOI contribution, e.g. the mean free path of a 140.5 keV in CdTe is about 2.4 mm.

The major concern for the development of the next generation of PET systems for small-animal imaging is the improvement of sensitivity, always pushing the spatial resolution close to its intrinsic limit. On the other side, small-animal SPECT has almost reached its resolution limit of fractions of a mm. In this case, the main challenge is to increase the sensitivity and especially the field of view to obtain ultrahigh-resolution systems able to visualise the entire animal in one shot.

2.2.3 Small animal CT imaging

Computed tomography (CT) is one of the most widely used techniques of noninvasive diagnosis, which provides a 3D map of the local X-ray attenuation properties of the scanned patient. Dedicated scanners for small animals have been built in the last decades, with the main goal of obtaining a very high resolution, down to tens of microns, and a large field of view so that a scan of the entire animal can be performed in less than one minute. This is obtained by using X-ray tubes with a very small tungsten anode focal spot (~10 micron) and low to medium X-ray energy (30-50 kVp). A large detector, such as magnified CCDs or a CMOS flat panel with a typical pixel size of 50 micron, is used combined with high geometric magnification. The entire system rotates around the animal as in clinical CT in a cone-geometry configuration. Spiral CTs are also implemented. One critical issue for obtaining the design performance is that misalignments in the detectors are kept under strict control during the construction and the use of the CT. This can be done with various techniques, with and without special phantoms. A typical CT image of a mouse is presented in Figure 4.

CT for small animals can operate in step and shoot mode and in continuous mode. The standard way of reconstructing the image employs the Feldkamp algorithm, but iterative methods are being increasingly applied. The main issue with an animal CT is the high dose that is needed for obtaining the requested resolution, i.e. the quantum noise reduction. Hence dose limitation and increase speed of the examination, for instance for angiography studies, are the main topics of research in this field. CT scans have mainly been used in connection with PET images for providing anatomical information to be combined with functional imaging and for calculating the PET attenuation. However, they have also gained importance as a means of investigation *per se* in the field of molecular imaging.

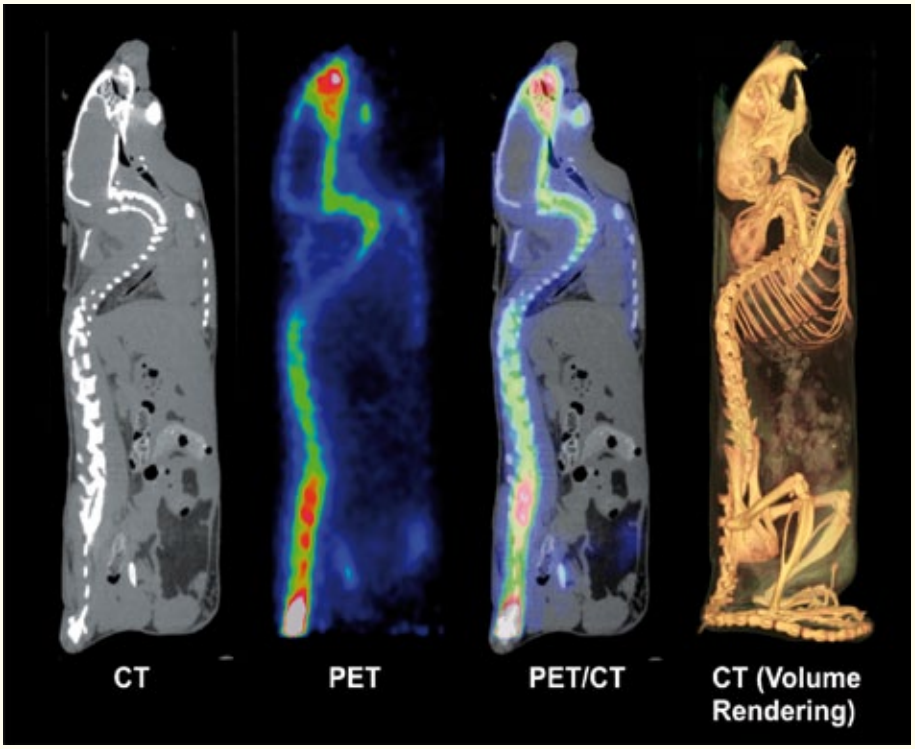

Figure 4. Typical CT image of a mouse: from left to right: CT, PET image (F18-), Fused PET/CT image, CT image volume rendering.

Figure 5. A typical MR system for small animals (Taken from: http://www.weill.cornell.edu/research/cbic/facilities/mri_7tesla.html)

2.2.4 MRI small animal imaging

MRI (magnetic resonance imaging) has become a very useful tool both in the clinical and the preclinical fields. MRI can produce images with excellent contrast between soft tissues and with a very high spatial resolution in 3D. Like other imaging techniques, MRI uses electromagnetic radiation to study districts within the subject. Such radiation is non-ionising, so that it can be considered non-harmful for a human subject. However, the interaction of the RF source to produce the MR image can increase the temperature of the body. The quantity that describes this phenomenon is the SAR (specific absorption rate), measured in W/kg and defined as the RF power absorbed per unit of mass of an object. Hence, in-vivo MR imaging requires that the SAR is maintained below a safety limit. To understand the phenomenon of magnetism of the nucleus, one can think of a mechanical analogy with a mass, electrically charged and rotating around its axis. If the centre of gravity of the charge is not on the axis of rotation, the rotation itself generates a small magnetic field in a certain direction. This phenomenon of rotation is called "spin" and causes the nucleus to possess a magnetic moment μ, which aligns along the direction of an external field (B0). An external RF pulse (the so-called B1 field) can transfer energy to the nucleus that will flip its magnetic moment according to the energy received, typically by 90 or 180 degrees. Within a certain relaxation time, the magnetic moment will return to its stable equilibrium position. The measurement of the relaxation times T1 and T2 gives an insight to the distribution (morphology) and behavior of the hydrogen (i.e. of the water) in the body (physiology). The phenomenon of magnetic resonance can be investigated using different types of nuclei (^{1}H, ^{13}C, ^{19}F, ^{23}Na, and ^{31}P) with an appropriate RF operating frequency to match the Larmor frequency of the nucleus under study. For small animal imaging, MRI is a very versatile technique capable of providing a very high spatial resolution (100 micron or less) for rodents. The strength of the magnetic field may vary from 0.5 to 9.4 T according to the application and of course to the cost of the apparatus. An example of a 7 T system from Bruker is shown in Figure 5. The system has a diameter of clear bore >30 cm.

The impact of MRI in molecular imaging is continuously growing: examples are translation studies for angiogenesis and phenotypic characterisation, dynamic visualisation of tissue perfusion, and many more. The step-up from MRI and MRS has been favoured by high field systems, which allow for a higher signal to noise ratio. The identification of different atomic nuclei provides insights to functional and biochemical information: for instance cell membrane studies, creatine and lactate quantitative studies, etc. The limit of MRI and even more so of MRS is its sensitivity, still in the micromolar range, as compared to PET and SPECT. Thus, the MRS studies with ^{1}H, ^{19}F, ^{31}P and ^{13}C MRS compounds in preclinical research are primarily confined to pharmacodynamic, but not pharmacokinetic studies. With the advent of high field (i.e. 9.4 T) and the advanced shimming high-resolution proton spectra, studies of the mouse brain have been receiving great attention, especially for tumour response and fMRI.

2.2.5 Multimodal approach

2.2.5.1 PET/CT and SPECT/CT

Functional imaging such as PET and SPECT are intrinsically non-morphological techniques. Hence anatomical information is often mandatory to localise precisely the position of the radiotracer. In addition, when quantitative information on small target sites is needed, anatomical images are needed to apply proper corrections for partial volume error. In any case, it is obvious that the information from a morphological imaging technique, such as CT or MR, is of great help for the PET or SPECT image analysis. More and more integrated systems are required in analogy to the clinical area, where a PET/CT is the diagnostic instrument of choice for most investigations. Also in the field of small animal imaging, there are two types of multimodalities, the so-called "tandem configuration", where the two modalities are executed one after the other, sharing the same bed for the animal such as in PET/

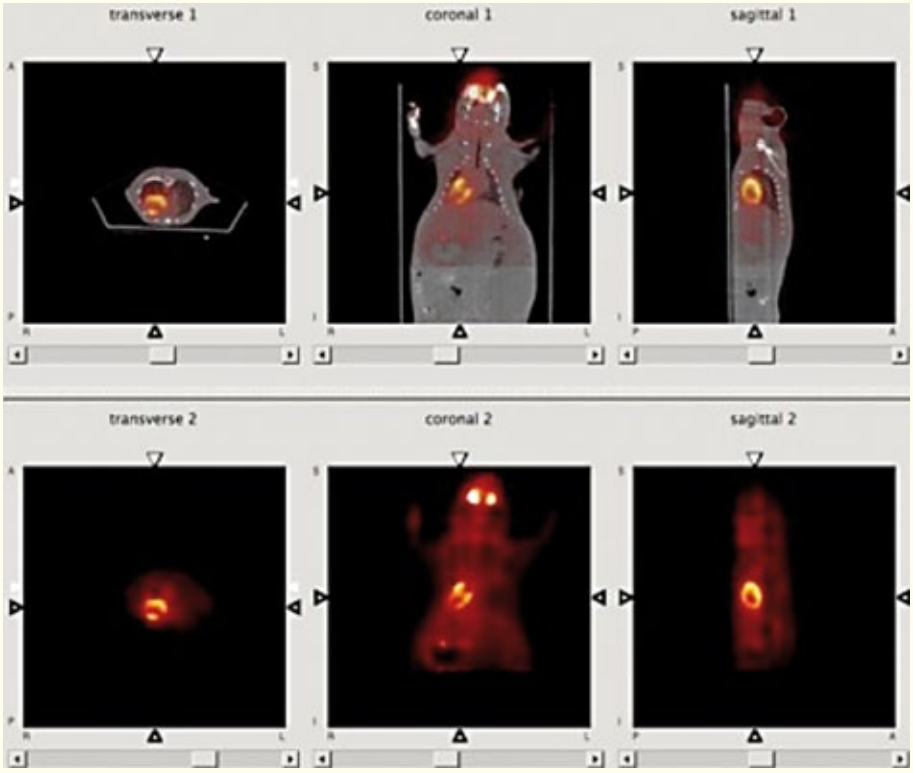

Figure 6. Typical imaging performance on one of the most recent preclinical examples (IRIS, raytest-IVISCAN). Top: PET/CT image obtained with the IRIS PET/CT scanner; bottom: PET image only (courtesy of Panetta D and Salvadori P, IFC-CNR, Pisa, 2013).

CT, SPECT/CT, PET/MR and SPECT/MR, and the truly combined modality, this latter type is only implemented as of today in PET/MR.

In the shadow of the successful application of combined PET/CT scanners in the clinical environment, this technique has been recently transferred to small-animal scanners. In fact, the morphological information from CT can be used to obtain a finer spatial localisation of the radiotracer distribution within the body as well as to obtain the attenuation coefficient map of the object under study for attenuation and scatter correction of the PET images.

CT images are mostly used to improve the emission images. In fact, the emission images are affected by a quantitative error due to the attenuation of radiation by the object under study. Even when this effect is much smaller than for humans, the magnitude of this correction in small animals is non-negligible. For example, in PET the attenuation correction factor is 4.5 for a 40 cm diameter man, and is 1.6 for a 5 cm diameter rat, and 1.3 for a 3 cm diameter mouse. In the CT case, the attenuation coefficients are measured with a continuous X-ray spectrum, ranging from 10 to 70 keV. Hence the CT-energy linear attenuation coefficient (μCT, X) has to be scaled to the 140.5 keV value for SPECT by a linear formula and for PET to 511 keV by a bilinear interpolation. Figure 6 shows typical images obtained without CT (bottom) and with CT corrections and image fusion (top).

2.2.5.2 **PET/MR**

Early diagnosis and therapy are connected to molecular imaging and genetic information. As for molecular imaging, the multimodality approach is becoming increasingly necessary. In fact, the combined systems PET/MR and SPECT/MR have received great attention and development. The advent of new solid state detectors such as APDs, PS-APDs, MPPCs and SiPMs has allowed the insertion of a PET system within the high magnetic field of an MR. It is well known that to have quantitative PET information an attenuation correction must be performed, best made with a CT. This was the reason for introducing PET/CT systems in the clinical, and also in the preclinical, field. As for the MR based attenuation correction, a lot of research has been going on to find the best way to do it: segmentation, brain atlas, and special sequences (i.e. UTE) have been proposed in combined modalities. MRI and PET in the preclinical scenario are now mostly in the same system, either as a PET insert or as a combined structure from the beginning. MRI and PET offer complementary functionality and sensitivity. Simultaneous acquisition capitalises on the strengths of each, providing a hybrid technology that has a significantly greater impact than the sum of its parts. A schematic scheme of the structure of a typical combined system is depicted in Figure 7.

Among the many applications with a combined PET/MR it is worth noting: dynamic studies, MR/PET cross correlation, MR-guided motion cor-

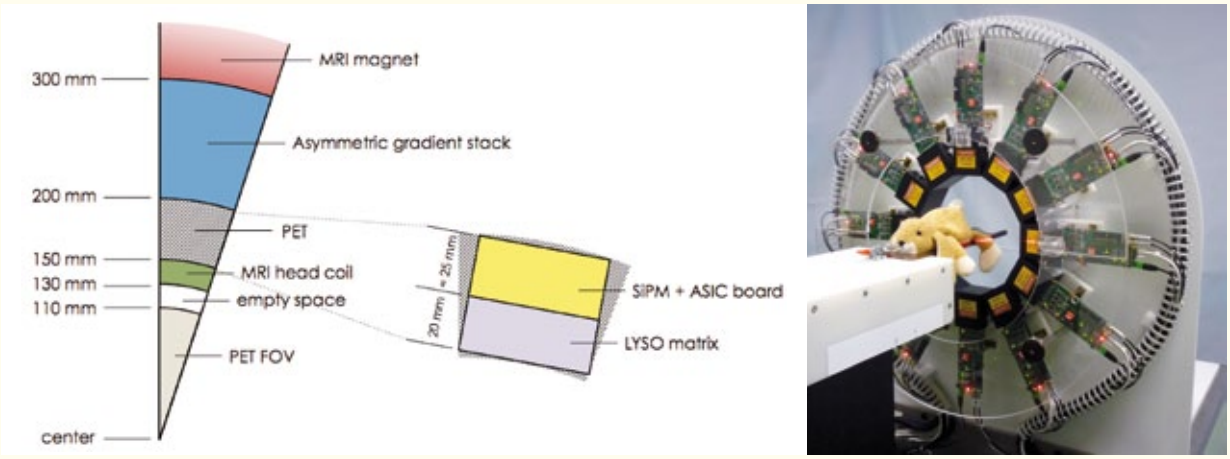

Figure 7. Cross section of the combined PET-MR system proposed for the TRIMAGE PET-MR-EEG project (courtesy of A. Del Guerra, 2013).

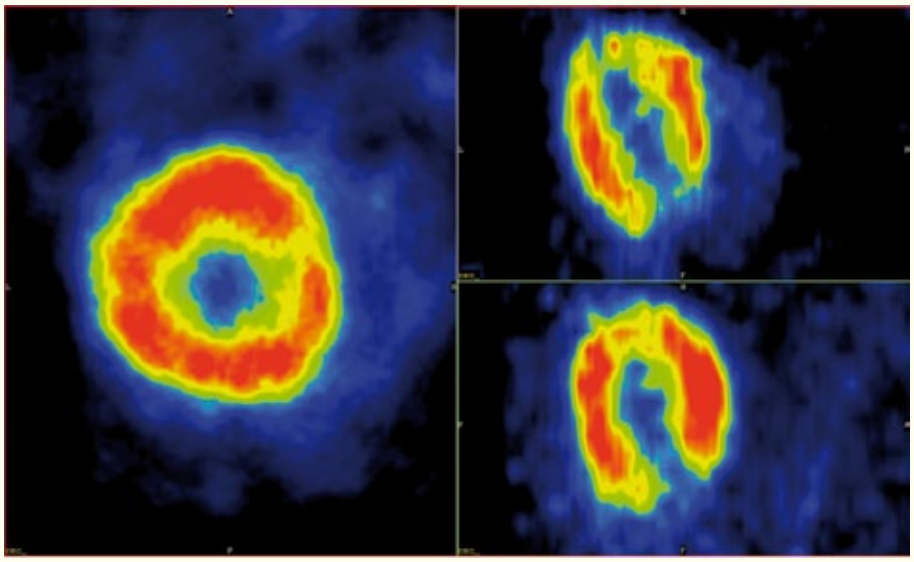

Figure 8. Image of an FDG-injected rat heart obtained in the combined PET-MR MiniPET-3, a SiPM based small animal scanner for molecular imaging developed by MTA Atomki, University of Debrecen (Hungary), ST Microelectronics and Philips Applied Technologies in the frame of ENIAC CSI.

rection of PET and PET image reconstruction. Preclinical PET/MRI scanners based on APDs or magnetically shielded PMTs are on the market. Several detector prototypes based on SiPM are being developed.

3. New challenges

Multi-modality imaging is used to show both the molecular processes taking place in the body and the anatomical location in which they are happening so that, for example, a tumour can be detected using PET imaging and located using CT in a PET/CT scanner. PET/CT was introduced 15 years ago and multi-modality is standard for SPECT and PET machines which are now on sale. Commercially, multi-modality means SPECT/CT or PET/CT.

The new challenge is to combine MR imaging for anatomical location with PET and SPECT. The benefits are to reduce the radiation dose by eliminating the CT scan, and the possibility to use functional MRI as well as simple anatomical MR scans (so that blood flows, for example, can be detected). However, this is technically more difficult because typical SPECT and PET scanners use scintillators with photomultipliers that are incompatible with the intense magnetic fields of modern MR scanners. The rotating gantries used in PET and SPECT can also be affected by the MR magnetic field. Conversely, the PET detectors must not affect the sensitive MR scanner operation either by perturbing the field or introducing electrical noise.

Although PET/MR multi-modal imaging has been in use for a few years it was, until very recently, done sequentially rather than simultaneously. Clearly simultaneous imaging is preferable, for example to avoid motion artefacts between scans, and the first simultaneous PET/MR scanners are now coming on the market (e.g. Philips Biograph mMR). Technology from nuclear physics detector systems is used to overcome the magnetic incompatibility. Some preclinical prototypes used light guides to allow photomultipliers to be located further from the magnetic field, however the more popular route seems to be to use of semiconductor light sensors (APDs or SiPMs) to replace the photomultipliers or to replace scintillators by semiconductor detectors.

The next challenges yet to be solved in the commercial market are to integrate SPECT with MR and to integrate fast detectors for TOF PET in an MR environment for simultaneous operation (sequential TOF PET/MR exists). MR-compatible TOF modules can be made using nuclear physics detectors (fast scintillators with SiPMs) as building blocks for TOF PET/MR. SPECT/MR is far from market while research systems use semiconductor detectors to replace the scintillators either by putting CZT detectors behind the SPECT collimators or else by electronic collimation using a Compton camera made of semiconductor detectors.

These last two (SPECT/MR and TOF PET/MR) are the challenges, where techniques from nuclear physics systems are currently making a difference and enabling the development of new multimodal imaging systems.

3.1 Detector design

Despite the excellent performance reached by PET detectors, there is room for improvements that will also allow non-standard use of PET technology, such as in-beam measurements during particle therapy sessions.

Research is being carried out worldwide in order to improve all the relevant aspects that contribute to the overall performance of a PET scanner: detection efficiency, spatial resolution, depth of interaction measurement, time resolution, compactness, MR compatibility, speed and power consumption.

All the PET components reviewed in the following, as well as the strategic choices in the design

of the global systems, are subject to continuous research and development, with the ultimate goal of providing the most accurate input information to the 3D or 4D reconstruction algorithm.

3.1.1 Scintillators

To be used as a primary photon converter for a PET (fixed photon energy) and a SPECT (wide photon energy range) detector, a scintillating crystal must meet the following requirements:

- high density (i.e. high conversion efficiency);
- high light yield (related to the energy and time resolution);
- short rise time to optimise the time resolution.

The figure of merit that summarises the suitability of a crystal is usually defined as:

$$\eta \sim \varepsilon^2 \sqrt{N/\tau}$$

with ε, N, τ related to the crystal density, light yield and decay time, respectively.

In addition, the technology must provide uniform crystals at a low (acceptable) cost.

The state of the art for PET/SPECT scanners is a set of inorganic crystals, whose properties are summarised in Table 1. LSO and LYSO are the best choice for scanners that also aim at the time of flight measurement. However, the search for new materials that would better meet the requirements for a more efficient and time performance scanner has not stopped and in recent years some new candidates have emerged.

As an optimal timing resolution is related to the photon counting statistics, it requires the capability to trigger at very low threshold, with the performance limit being reached when counting single photons. When these conditions are met, a high light yield and a short rise-time of the scintillating light allow the best measurement of the interaction time, with the theoretical possibility to approach a limit value of about 100 ps.

GAGG crystals have been recently studied as a possible alternative to known scintillators for PET and SPECT scanners: the density, light yield and time resolution are suitable, but suggest a possible marginal improvement rather than a significant step forward.

Plastic scintillators, which would provide a very short decay time, suffer from low stopping power and insufficient optical photon yield. However, novel methods developed in the last few years allow increasing thickness of the plastic detector and at the same time determination of the depth of the interaction of the registered gamma quantum. In addition, thanks to the large solid angle covered by new PET devices under construction, the decrease of the detector efficiency will be compensated by the increase of the acceptance. The small efficiency for the photoelectric effect in organic scintillators worsens the image quality due to a low ability to distinguish between quanta reaching the detector directly and quanta re-scattered in the body of a patient. This drawback is compensated by the selection of only these events for which the energy deposited in the scintillator corresponds to the range close to the maximum of energy which can be transferred to the electron via the Compton scattering process, and by taking advantage of the excellent timing response of organic scintillators, allowing for the effective usage of the TOF technique.

Should the scintillators be engineered with a photonic crystal pattern, the light collection at the surface would be improved. However, despite some promising preliminary results, the technology is still in an early stage.

Table 1. Properties of the most used scintillator in PET and SPECT [Adapted from Lecomte R. *Eur J Nucl Med Mol Imaging* **36**, n° Suppl. 1 (2009): S69–S85.]

	NaI	BGO	GSO	LSO	LYSO	LGSO	LuAP	YAP	$LaBr_3$
Light yield 10^3 ph/MeV	38	9	8	30	32	16	12	17	60
Primary decay time	250	300	60	40	41	65	18	30	16
ΔE/E (%) at 662 keV	6	10	8	10	10	9	15	4.4	3
Density (g/cm³)	3.67	7.13	6.71	7.35	7.19	6.5	8.34	5.5	5.08
Effective Z_{eff}	50	73	58	65	64	59	65	33	46
1/μ@511keV (mm)	25.9	11.2	15.0	12.3	12.6	14.3	11.0	21.3	22.3
PE (%)@511 keV	18	44	26	34	33	28	32	4.4	14

PE: photopeak efficiency

3.1.2 Photon detectors

Once the primary photon conversion efficiency and the secondary photon light yield and collection rate are optimised, a high performance photon detector is required in order to exploit the raw information at best.

Clinical PET and SPECT scanners are typically based on photomultipliers (PMTs), which, despite the high gain, do not meet two important requirements: compactness and magnetic field compatibility.

In recent years, research projects have focused on directly providing digital output.

APDs, that are insensitive to magnetic fields, were used for the first commercial PET/MR scanner; however, their drawbacks (low gain and long rise time) make them unsuitable for high performance TOF-PET.

SiPMs, on the other hand, besides meeting the requirements of compactness and magnetic field insensitivity, present a very interesting advantages: low bias voltage makes them even more attractive than APDs for hybrid PET/MR imaging, while high gain and short rise time make them the best candidates for TOF-PET. The short rise-time and the high level of homogeneity of SiPM matrix components should be compatible with a time resolution that could approach the lower limit of 100 ps. In addition, the high gain could allow single photon counting, which, if the dark count rate is kept under control with active cooling, would make it possible to design a detector that couples continuous crystals to segmented SiPM matrices.

dSiPMs, developed by Philips, are based on the integration within the SiPM sensitive area of basic processing electronics and eliminate the need for external processing. Each micro-cell of the array is connected to an integrated counter and an integrated TDC that provide the energy and time information, respectively. dSiPM coupled to LYSO crystals reach time resolutions as low as 150 ps (FWHM). The various performances of these devices are summarised in Table 2.

Ultra Fast Silicon Detectors (UFSD) are a new promising technology for the improvement of spatial resolution, while keeping a time resolution of the order of 100 ps. Their possible performance limit, however, is in their low gain (5–15), which could deteriorate both the signal to noise ratio and the related time resolution with respect to the nominal expected values. The construction and characterisation of the first prototypes will require special attention to the capability of detecting the first secondary photons emitted in the crystal de-excitation process, which are key to an excellent time resolution. Should this limitation be overcome, UFSD would be an excellent candidate for hybrid PET systems, thanks to their compactness and intrinsic insensitivity to temperature and magnetic fields.

Semiconductor detectors based on CdTe or CdZnTe are solid-state devices that allow the direct conversion of gamma rays to electrical charges. The conversion yield is large with respect to scintillation devices: typically 30000 charges for a 140 keV energy release. As a consequence, the energy resolution is not limited by charge generation statistics but by other phenomena, such as electrical noise or material uniformity. While the best devices achieve better than 2% resolution at 140 keV thanks to an optimised design, typical resolution values by standard systems are close to 5% at 140 keV, a value that can help the development of dual-isotope imaging protocols.

The spatial resolution of these semiconductor detectors can be extremely good, as it is not limited by light spreading and photon statistics, but rather by the readout circuitry. A typical device resolution is of the order of 2.5 mm, but the use of high density readout or sub-pixel positioning electronics allow for an intrinsic resolution of few hundreds of micrometers (200–400μm).

CdTe- or CdZnTe-based detectors are integrated in small modules that couple the semiconductor crystals and the readout electronics on the same

Table 2. The most important parameters of (secondary) photon detectors.

Detector	PMT	APD	(d)SiPM	UFSD
Gain	10^5	50-1000	~ 10^6	5-15
Rise Time (ns)	~ 1	~ 5	~ 1	~ 0.1
Quantum Efficiency (QE) @ 420 nm (%)	~ 25	~ 70	~ 25-75 (PDE)	~ 75
Bias (V)	> 1000	300-1000	30-80	100
Temperature sensitivity (%/K)	< 1	~ 3	1-8	Negligible
Magnetic field sensitivity	Yes	No	No	No

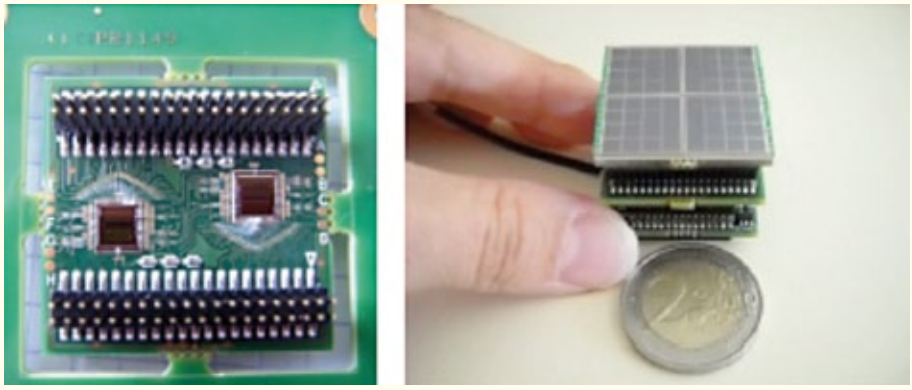

Figure 9. Example of compact front-end electronics to read-out a SiPM matrix.

substrate. System designers have profited from the compactness of such modules to build innovative SPECT tomographs that exploit the modularity to enhance sensitivity and resolution by focusing of a given region of interest. Additionally, these systems also avoid the motion of the camera head around the patient.

3.1.3 Front-end electronics

Front-end electronics is becoming a key enabling technology (KET) for detectors due to the increasing number of channels and the high level of integration that allows reductions in cost and dimensions. A general trend is to integrate more and more functions in ASICs (amplification, filtering, digitisation, signal processing), making them systems on a chip (SoC). These multi-channel ASICs also tend to move closer or even onto the detectors, minimising the connections and improving both performance and reliability. This localisation coupled to the increasing number of channels requires low-power designs, so that the performance and compactness obtained are not spoiled by large cooling systems. The evolution of microelectronics technologies allows this increase of performance together with power reduction and higher operating speeds, an important feature for reducing a patient's exposure, while maintaining high quality resolution.

Such a design is also useful from the point of view of the system performance, since it allows more accurate timing measurements that improve the noise and background reduction and therefore provide better quality images with lower doses delivered to patients.

3.1.4 Module layout

State-of-the-art scanners are based on segmented crystals that collect most of the secondary photons on a single channel, which are then detected by PMTs, APDs or SiPMs, whose signals are processed by dedicated ASICs and FPGAs.

Any change in the detector design is related to possible improvements of the key parameters that describe the overall system performance: efficiency, 3D spatial resolution, time resolution, MR compatibility, compactness, speed and power consumption.

The scintillator, selected according to the figure of merit already discussed, is usually segmented and placed radially with respect to the annihilation volume.

Recently, two alternative designs have been proposed. The segmented crystal could be placed axially, with several long (up to 10 cm) and thin layers: such a design provides an excellent DOI measurement, while the axial position along the crystal is obtained via the light sharing and/or the time difference read on the opposite sides.

The availability of high performance segmented SiPM matrices, with high gain and the possibility to detect single photons, prompted some projects based on continuous scintillator blocks read by segmented matrices. The continuous crystal would allow a cluster reconstruction, with the double advantage of using the cluster size for the DOI measurement and of a multi-sampling of the secondary photon time distribution, which would help improve the TOF measurement. Such an approach strictly depends on the capability to control the SiPM dark count rate, so as to limit the trigger rate and to distinguish contributions to the cluster reconstruction from channels triggered by dark counts. This result can only be achieved with a cooling system that allows a temperature stability within about 1°C.

SiPMs (analogue or digital) are the photon detector of choice for almost every ongoing research project: they are efficient, with very high gain, single photon counting capabilities, very high spatial resolution and excellent timing resolution (with intrinsic resolution among the different cell contributions to a matrix element quite close to 100 ps). They are also compact, compatible with operations in a magnetic field and acceptably priced.

Custom front-end electronics developments mostly focus on optimising the TOF measurement, so as to reach an overall resolution in the 100–150 ps range. If the scintillator rise-time and the pho-

ton detector signal formation time are short enough and the detector uniformity in the time response is good (as it is for the latest SiPM matrices available on the market), the front-end electronics contribution can become the main source that contributes to the system time resolution. Whether the crystal is segmented or continuous, the key to optimise the time resolution is the capability to identify the first photon(s) from the crystal de-excitation and to distinguish them from the spurious dark count signals. With a segmented crystal, the analysis of the rising signal shape is the clue, while in the case of a continuous crystal, where the threshold must be as low as required to detect single photons, the cluster analysis algorithm must be able to distinguish true signals from dark count background events.

An important innovation to real-time data handling could come from the concept of "deferred coincidence". Single events can be routed to a ring network, which provides real-time processing and coincidence determination within the network itself; this simplifies the construction of the overall system and allows its scaling to larger detector arrays.

The need for precise temperature control and uniformity is also being addressed by designing active cooling systems that are very important to keep the system performance constant.

System compactness and MR design compatibility are also provided by the choice of solid-state photon detectors such as SiPMs.

System compactness is particularly important when developing a detector for an endoscopic approach, which, combined with timing resolution, will allow more sensitive, more precise, lower radiation doses and less invasive imaging and intervention on small internal structures and lesions.

Ultimately, all of these features point towards earlier detection and patient-tailored treatment of asymptomatic cancer types.

3.1.5 New detector concepts

Several new approaches to the detection of primary photons originating in the e^+e^- annihilations have been proposed, and are described below.

Resistive plate chambers (RPC) are gaseous parallel plate detectors for charged particles widely used in large-scale high energy physics experiments, and could in principle replace the crystal scintillators, as well as the secondary photon detectors in a PET system.

RPCs provide excellent time (20–30 ps) and spatial resolution (hundreds of microns), work well in strong magnetic fields and are inexpensive, so that large area detectors (~2–3 square metres) can be built, providing a large field of view and increasing the geometrical acceptance with respect to standard PET devices.

The low detection efficiency for 511 keV photons (<30%) is a major drawback, as it implies a much larger number of annihilations to provide statistics comparable to standard PET systems and therefore the dose delivered to the patient will increase.

Still, investigation of RPC-based PET as a candidate for PET/MRI hybrid imaging and in-beam PET measurement is ongoing.

Liquid calorimeters are also being considered as an alternative to standard PET systems. TriMethyl bismuth (TMBi) is an innovative liquid that efficiently converts photons of energy less than 1 MeV through the photoelectric effect. The light produced by a relativistic electron is detected in a time-projection ionisation chamber, supplemented by a photo-detector. The simultaneous detection of light and charge signals leads to a very promising performance in positron-annihilation detection. A spatial resolution of 1 mm^3, a sub-nanosecond timing, and a photon energy resolution of about 10% FWHM are foreseen, with a single interaction (photoelectric) conversion probability above 47%, a value still unsatisfactory when addressing the dose minimisation issue.

To improve the time resolution, the exploitation of the Cherenkov effect, which bypasses the scintillation process and provides almost instantaneous response to incident 511 keV annihilation photons, is being investigated. Cherenkov photons were shown to have significant influence on the rise time of inorganic scintillators – a key-feature for the time measurement and extensive research on this topic might lead to improved time resolution of PET detectors. According to simulations performed by Brunner et al., the intrinsic time resolution could be as low as 30 ps, if appropriate front-end electronics were available.

3.2 Simulation and reconstruction

Contrary to planar imaging, which includes scintigraphy, or radiography, tomographic images are not directly obtained from the measurements, but are the result of the so-called *tomographic* or *image reconstruction* process. Classically, the goal of tomographic reconstruction is to obtain the image of an "object" from its "projections", where the object might be an attenuating medium (CT) or a radioisotope distribution (PET, SPECT or Compton cameras). Tomographic image reconstruction is a process based on mathematical algorithms that

are implemented in computers. Although a mathematical solution for the problem of tomographic reconstruction was first proposed in 1917, the advent of modern computers made CT a reality. Computers are also essential to simulate the complex physical phenomena that underlie the image formation process, such as the behaviour of optical photons within scintillation materials, the radioisotope decay and subsequent radiation emission, etc. Continuously increasing computing power has enabled the development of more sophisticated image reconstruction algorithms, and more detailed and accurate simulations of tomographic systems. In this section, we will present state-of-the-art research and the most recent advances in image reconstruction and simulations.

3.2.1 Image reconstruction

Traditionally, a tomographic image corresponds to a plane section (2D image) of the object under inspection. A volume (3D image) is thus constructed by aligning several reconstructed sections. Nowadays, modern reconstruction techniques can directly provide 3D images (fully 3D reconstruction) and 4D images if time is also taken into account; 4D image reconstruction is particularly useful in cardiac PET and SPECT, or to image regions affected by respiratory motion, and it is essential in dynamic emission tomography, whose goal is to study the concentration of the injected tracer over time.

At present, there are several image reconstruction algorithms, which can broadly be divided into two categories: analytic and iterative reconstruction methods. Analytic reconstruction methods are based on a direct mathematical solution, and are still widely used for CT reconstruction. However, the assumptions on which analytical methods are based usually do not hold in emission tomography.

Compared to analytical reconstruction, the main advantage of iterative methods is their ability to include a more accurate description of the imaging process, which in turn, usually leads to better images. This is particularly the case when the measurements are noisy, or when the imaging device cannot provide uniform or complete sampling (see Figure 8). Therefore, iterative reconstruction methods are preferred in emission tomography, although analytical methods, such as filtered backprojection (FBP) are still used for quantitative image analysis in spite of their limitations.

The goal of iterative reconstruction techniques is to find an image estimate by successive steps. In the last few decades, a wide variety of algorithms have been presented. We refer the interested reader to some excellent reviews (such as that by Defrise & Gullberg 2006).

Most iterative reconstruction techniques share the same 'ingredients': models for the image, the data and the imaging system, an objective function, and an optimisation algorithm. The underlying physics of the image formation and degradation phenomena can be taken into account in the choice and description of the models, as well as in the design of the cost function, as will be described in the following paragraphs.

3.2.1.1 Physics and iterative image reconstruction in emission tomograhy

One of the main strengths of iterative algorithms lies in their ability to include accurate models of the underlying physics, which include the statistical nature of radioactive decay or radiation detection, and the interaction of radiation in matter. The statistical nature is contemplated within the data model. Most commonly used reconstruction techniques are based on a Poisson model; this model naturally leads to the Maximum-Likelihood (ML) criterion to determine which image is the best estimate of the true object.

The behaviour of the imaging device is described within the so-called system response model or system response matrix (SRM). In PET or SPECT, the elements of the SRM correspond to the detection probability of gamma rays originating from a certain location. In the first place, the effects of the geometry and arrangement of the detector elements on the detection (and the collimator in SPECT) should be modeled. The system model can also include a description of crystal penetration effects, cross-talk, inter-crystal scatter, etc. In principle, the more effects that are correctly modeled and included within the SRM, the better the reconstructed image. However, computing the SRM for a certain device can be very challenging given the dimensions of the matrix, which corresponds to NxM, N and M being the number of data and image elements, respectively. For a conventional clinical PET scanner, N can be larger than 10^8, and the image might be composed of several millions of voxels. The more physical effects that are contemplated, the less sparse the SRM becomes. Several techniques have been proposed to compute and handle the SRM. Factorisation of the SRM in several components makes it easier to calculate and store the SRM, and to handle it during the reconstruction. Monte-Carlo simulations have proved to be a very useful tool to compute the whole SRM or several of its components for PET and SPECT. Approaches based on measurements can provide very realistic models for the Point Spread Function. Analytical models usually allow for faster but less accurate

alternatives; analytical comprehensive models have been also proposed, but the computational cost can be prohibitive. In any case, since the factorisation of the system matrix allows the contribution of the various physical phenomena to be calculated separately, different approaches can be combined to calculate the various components of the system response model. Finding a balance between computation cost and model accuracy is currently a very active field of research.

Patient-dependent effects, such as attenuation or scatter, can be also included within the reconstruction process. Attenuation factors, previously obtained from CT, MRI or additional measurements, are built within the SRM. Some attempts have been made to include object scatter within the SRM, for example using Monte-Carlo simulations; however, the most common approach is to use the scatter estimate within the comparison step of the iterative algorithm. In this step, the measured data are compared to the ideal data that would have been measured for an object being described by the last image estimate. For PET, the contribution of accidental coincidences can also be taken into account in the comparison step.

As mentioned above, the increasing number of detection channels and the subsequent need of smaller image elements poses several challenges in the computation and handling of the SRM. Much effort has been expended in the last few years to optimise the balance between accurate models and computational efficiency. A way to avoid the storage of the SRM is to calculate the system model on-the-fly. This approach is usually the one chosen when dealing with "list-mode data", i.e. the measured data are not compressed into histograms (such as sinograms), but are stored accorded to the registration time. List-mode reconstruction makes it possible that the whole information contained in the data is preserved and exploited. This is done usually at the cost of simplified system models, since the latter are calculated on the fly; however, fast but accurate system models for list-mode reconstruction, usually based on analytical approaches, have been proposed lately.

Time information is the key in time-of-flight (TOF) PET, which requires dedicated algorithms to exploit the location constraint for the positron-electron annihilation provided by the time difference in the arrival of the two annihilation photons. This technology, proposed in the 1980s, has been recently translated into clinical PET. In combination with dedicated algorithms, TOF PET allows image quality (in terms of SNR and lesion detectability) to be improved.

Concerning the image model, rectangular voxels are the preferred option. In the last few years, spherical based functions ("blobs") have deserved renewed attention given their ability to reduce image noise, but usually at the expense of higher computational cost. Other potentially interesting alternatives are polar pixels, which allow the symmetries of the imaging device to be exploited, or those based on irregular grids.

The cost function and its optimisation are the 'core' of a reconstruction algorithm. Most widely used techniques are based on the optimisation of the aforementioned ML criterion, the Maximum-Likelihood-Expectation-Maximisation algorithm (MLEM) and its accelerated version Ordered-Subsets-Expectation-Maximisation algorithm (OSEM) being the most popular ones. However, the ML estimation problem is ill-conditioned, which results in unavoidable noise in the data causing noisy images. Noise regularisation is thus needed, which can be achieved through early stopping (before convergence), post-reconstruction smoothing, or by adding a penalty function in the objective function. The latter approach can also be derived if the problem is formulated in a Bayesian framework (Maximum-a-Priori algorithm, MAP). The penalty function (or prior) might also include some anatomical information of the patient obtained from a CT or MRI. Compressed sensing (CS) reconstruction approaches and CS-based total variation (TV) regularisation are earning much interest in the community, especially for CT. TV priors offer a promising alternative to compensate for missing data, such as those arising from gaps between detectors or partial PET ring configurations.

3.2.1.2 **Accelerating iterative image reconstruction**

One of the main drawbacks of iterative image reconstruction is its computational cost. Not only might the calculation of the system response matrix be computer expensive, but also the image reconstruction process as such. Therefore, much effort has been devoted to accelerate the reconstruction process, which remains an active field of research. Some of the proposed approaches rely on parallel computing using clusters, or multicore architectures; the use of graphical processor units (GPUs) has earned much attention in recent years as a cost-effective alternative, especially useful for TOF PET. A completely different approach is to implement the reconstruction within a field programmable gate array (FPGA).

3.2.1.3 **Image quality, quantification and compensation of degradation phenomena in ET**

Tomographic images can be employed for different purposes. PET and SPECT are commonly used for diagnostics and therapy follow-up in clinical routine. More recently, PET images are also used for tumour delineation in radiotherapy planning. At the same time, emission tomography of rodents and larger animals (such as monkeys for neurosciences and pigs for cardiology) is a common tool in biomedical research, or pharmacology. It is obvious that, for any of these applications, the quality of the image should be "as good as possible". On the other hand, the kind of information to be extracted from a reconstructed image depends on the final purpose: visual inspection, lesion detection, quantification of certain physiological parameters, etc. In the end, this purpose will determine which are the main properties or characteristics that a "good image" should exhibit and which, in turn, the reconstruction algorithms of choice should be able to provide.

Quantitative image analysis (quantification) consists of extracting certain parameters of interest from an image, for example tracer uptake. To obtain quantitative information, a linear relationship is required between image voxel values and activity concentration. For this purpose, several effects need to be accounted for; some of these effects are related to the underlying physics and image formation processes and are thus unavoidable, but can be compensated for. This is the case of attenuation and Compton scattering in the patient, Compton scattering in the detectors, partial volume effects, variable spatial resolution across the field-of-view. In PET, accidental coincidences might also be a source of inaccuracy. Truncation artefacts due to limited-angle geometries, or ring artefacts also hinder quantification. Motivated by the advance of novel technologies such as TOF-PET or PET/MR, novel methods able to compensate for attenuation by simultaneously estimating the activity distribution and the attenuation have been proposed.

One main source of image degradation is patient and organ motion. In particular, cardiac and respiratory motion (in thorax or abdominal examinations), and involuntary head motion in brain studies might strongly distort the information content of the images. Several strategies to deal with motion have been proposed (see reviews in Rahmim *et al.*, 2007), which can be grouped into two categories: gating and non-gating methods. In gating methods, the acquired data are split in frames based on an external motion detection system. Assuming that there is little or no motion in the single frame, the frames are reconstructed individually with a standard algorithm. The external signal could be a respiratory belt for respiratory motion or an electrocardiography for a cardiac motion (or both, named "dual gating"). This simple method allows the motion effects on the image to be reduced, but at the cost of increased noise levels (i.e. worsening the signal-to-noise ratio). To overcome these limitations, much research is dedicated to the development of sophisticated non-gating methods, which do not rely on any external signal and, in general, make use of all the acquired data at the same time. The later approach leads to improving the signal-to-noise ratio, as shown in Figure 9. Among these approaches, there are strategies that assess separately motion and image, and other methods that jointly estimate motion and activity distribution (image). Regardless of the motion correction method, accurate quantification requires that the CT map and the PET images are acquired in the same respiratory conditions. In some cases, this is done by acquiring a 4D-CT that entails an increase of dose not justifiable for all the patients. To solve the dose burden of the 4D-CT, the group of Dimitris Visvikis proposed a method to generate dynamic CT images combining a reference CT image and the motion estimation of the 4D-PET.

3.2.2 **Simulations**

Monte-Carlo (MC) simulations have always been a fundamental tool in nuclear and particle physics, and have also become essential for the advancement of emission tomography [Harrison 2012]. MC simulations are often used to optimise the design of novel imaging systems or their components. Simulations are especially useful to examine the effect of a single physical phenomenon or a certain parameter, since the physics in real experiments is very complex and the effects of the underlying physical phenomena cannot be easily isolated.

Simulated data are also cardinal to test and optimise new techniques for data correction, image reconstruction, reconstruction of the interaction position within a detector, etc. Additionally, as mentioned in the former section, Monte-Carlo simulations are also used to calculate the system response model for image reconstruction.

Several multi-purpose packages for photon and particle tracking are being currently employed in emission tomography. Especially relevant ones are Geant4, EGS, MCNP, FLUKA, and Penelope. These packages can provide accurate simulations of the interaction of particles in matter, usually at the expense of large computing times, that might be prohibitive in the case of complex imaging devices. For these cases, dedicated simulation software, spe-

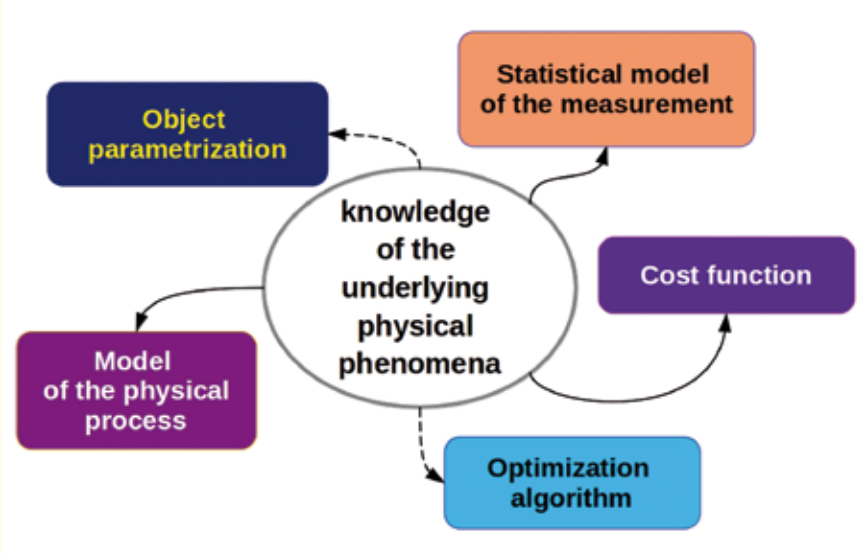

Figure 10. Sketch of statistical-iterative reconstructions. The information on the physical process, plus a statistical model of the measurement, is employed to estimate the data that should be measured in the scanner from a given parameterisation of the object. This estimate is compared to the actual data and a cost function, which may combine differences between estimates and data as well as regularisation criteria, is built and an optimisation function is called to minimise this cost function via modifications of the object.

cially conceived for photon-tracking in emission tomography, is usually preferred. Several packages have been developed for both PET and SPECT, such as GATE, SimSET, GRAY, or GAMOS, GATE and GAMOS being based on a GEANT4 framework. Some packages are PET specific (PETSIM, PET-EGS, PeneloPET, PET-SORTEO, or EIDOLON), whereas SiMIND was originally developed for SPECT. These dedicated packages are usually faster but less flexible than general-purpose ones. Simulating unconventional imaging devices might be difficult or even impossible without modifying the source code; however, for standard devices, they provide a number of interesting features such as detector electronics modelling, complex source and phantom description, or modeling of time-dependent phenomena.

As for image reconstruction, one main issue is to find a trade-off between accuracy and computing time. When speed is the main issue, analytical simulation packages, such as ASIM, might provide the desired performance. On the other hand, effort has been put in to accelerating simulations by parallelising the software or adapting it for distributed computing environments. A very promising alternative is the use of GPUs, which remains an active field of research.

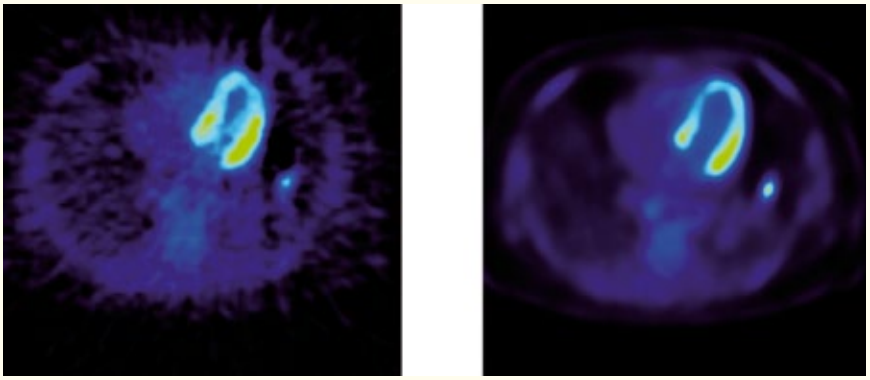

Figure 11. Reconstructed images from a clinical scanner. The data were reconstructed using analytical (left) and iterative (right) reconstruction algorithms.

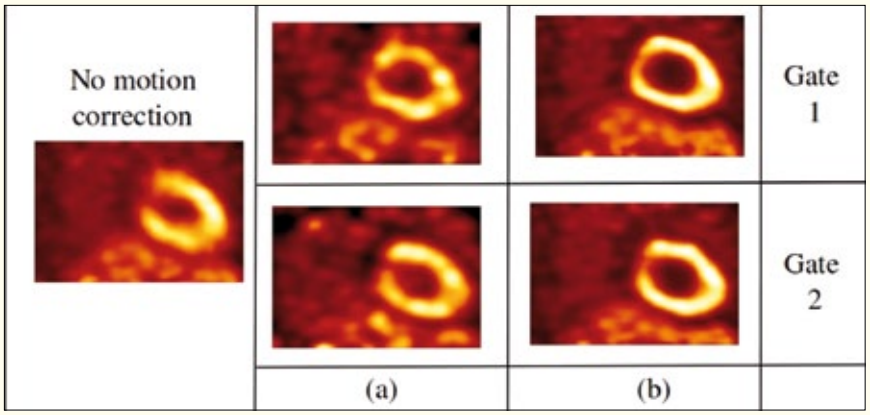

Figure 12. The effect of motion and its correction. Left column: no correction applied. Middle: A gate-based correction is applied. Right: Motion compensation is performed through simultaneous reconstruction of motion and image. The two rows correspond to different gates of very low statistics.

3.3 Photon counting: towards spectral CT

Hybrid pixel arrays applied to X-ray detection might provide a new generation of digital X-ray photon counting cameras that could replace conventional "charge integration" CMOS and CCD cameras used in X-ray computerised tomography (CT). Applied to the detection of X-rays, this technological breakthrough, which was originally developed for the construction of vertex detectors used in high energy physics experiments, can provide spectral information on the X-rays transmitted through an object. Thus, the current advent of X-ray photon counting cameras enables the development of spectral CT: a novel intrinsic anatomical and functional imaging modality that will hopefully open a new door in the field in molecular imaging.

3.3.1 Photon counting with hybrid pixels

Hybrid pixel detectors [Wermes 2005] form a new generation of digital X-ray cameras working in a photon counting mode that can replace conventional "charge integration" CMOS and CCD cameras used in X-ray computerised tomography (CT). This novel approach brings several advantages, such as the absence of dark noise, a high dynamic range and photon energy discrimination.

Hybrid pixel detectors have fulfilled these requirements quite successfully at the LHC at CERN and other nuclear physics experiments.

Hybrid pixels comprise the association of pixelised sensors and readout electronics connected through bump bonds (Figure 13). Usually, the sensor consists of n-type high resistivity silicon of a few hundreds nanometers thick with p^+ pixel implants, but it can also be from different materials of higher effective atomic numbers such as cadmium telluride (CdTe), cadmium-zinc telluride (CZT) or gallium arsenide (GaAs), to provide better photon interaction efficiencies at X-ray energies up to 120 keV. The readout electronics chip (ASIC), which is pixelised at the same pitch as the sensor, is designed using standard CMOS processes.

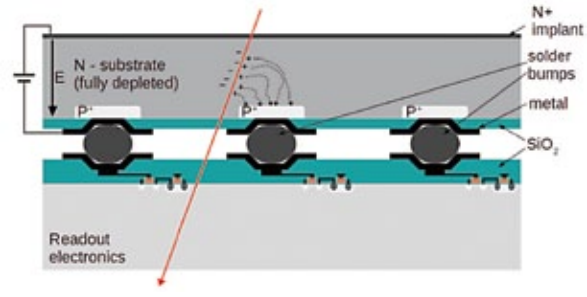

Figure 13. Schematic view of a hybrid pixel detector.

The charges generated by photon interaction in the pixel sensor are collected on the ASIC via the bump bond connection and converted after an amplification stage in either a current or a voltage signal that is compared with one or several adjustable detection thresholds. Signals overcoming the threshold(s) are then stored in a local memory acting as a counter.

Several ASIC designs have already been developed, most of which so far have only one threshold, for the detection of X-rays using hybrid pixels (Table 3).

X-ray cameras consisting of an assembly of one or several modules of pixelised sensors bump bonded with hybrid pixel detector circuits have been built (see e.g. Figure 14) and have been used to pioneer spectral X-ray imaging.

3.3.2 Spectral X-ray imaging

In X-ray CT, the amount of X-ray absorption that induces a useful contrast for imaging depends on

Table 3. Technical specification of some hybrid pixel detector circuits.

	Number of pixels	Pixel size [μm²]	Count rate [counts/pixel/s]	Energy range [keV]	Threshold dispersion (r.m.s.) [e⁻]	Noise (r.m.s.) [e⁻]
Pilatus II	5'820 (60 × 97)	172 × 172	2×10^6	3 – 30	50	125
Eiger	65'536 (256 × 256)	75 × 75	16×10^6	4 – 30	20	180
Medipix2	65'536 (256 × 256)	55 × 55	10^6	5 – 30	360	140
Medipix3 (SPM)	65'536 (256 × 256)	55 × 55	10^6	6 – 30	55	72
XPAD3	9'600 (80 × 120)	130 × 130	10^6	5 – 60	57	130
PIXIRAD	243'712 (512 × 476)	60 hexagonal	10^6	1 – 100	–	50

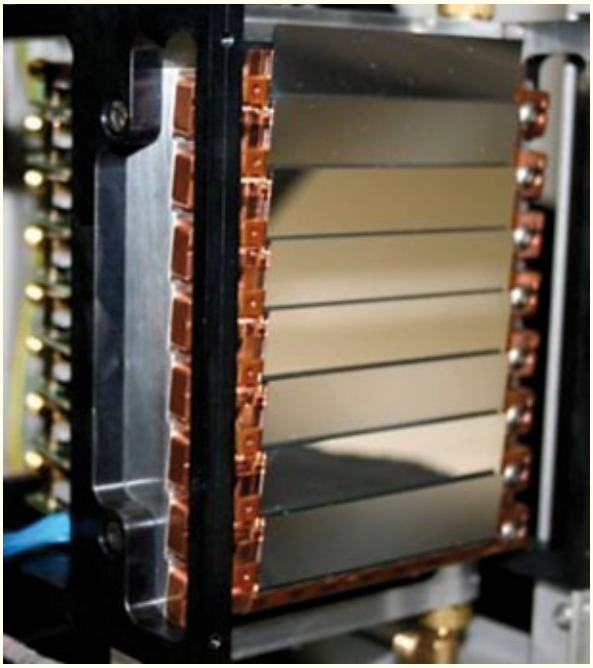

Figure 14. Picture of the XPAD3 camera composed of XPAD3-S ASIC, bump bonded to 500 µm thick silicon sensors to form horizontal modules. Eight modules of seven chips are tiled vertically to form a detector of 11 × 8 cm² composed of more than 500,000 pixels of 130 × 130 µm².

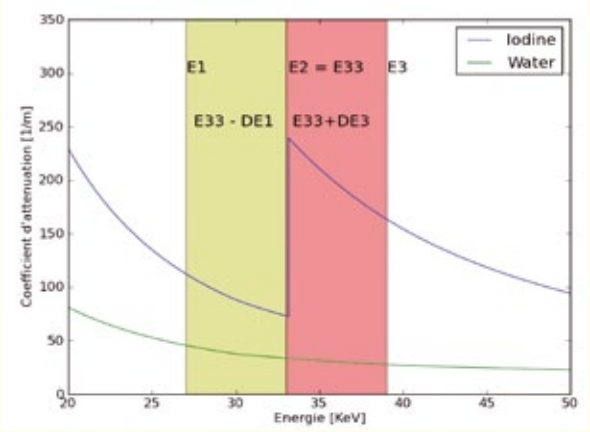

Figure 15. Principle of K-edge imaging of iodine (E_K = 33 keV).

the energy of the X-rays and the density and atomic composition of the matter they penetrate. In the past, several authors have pointed out the benefits of X-ray spectral information in computed tomography. Energy resolving detectors, with two or more energy bins, permit material decomposition thanks to the dependency of the attenuation coefficient on the X-ray energy, which is specific of each element. The increase of contrast-to-noise ratio for a given material can be maximised by choosing the optimal energy bins and/or by performing appropriate image weighting, either at the projection or at the reconstruction image level.

Moreover, when the energy of X-rays reaches the K-shell binding energy of the atoms that compose the traversed matter, the photoelectric absorption probability of X-rays increases sharply. This phenomenon is referred to as the K-edge. It is then possible to sense the atomic composition of matter by analysing these sudden absorption changes with energy. Subtractive analysis of X-ray absorption above and below the K-edge values of selected contrast agents such as yttrium (17 keV), silver (25.5 keV), iodine (33 keV), gadolinium (50 keV) or gold (80 keV) permit the identification of these contrast agents in a CT image.

Indeed, after energy calibration of the pixel, K-edge imaging can be obtained by changing the pixel threshold around the K-shell binding energy E_K of the selected contrast agent. In the case of detector pixels with only one energy threshold, images are acquired with three different thresholds: $E_1 = (E_K - DE_1)$, $E_2 = E_K$ and $E_3 = (E_K + DE_3)$ with DE_1 and DE_3 equivalent to a few keV. Thanks to the increase in absorption associated to its K-shell binding energy (Figure 15), subtraction of images reconstructed within energy windows $(E_2 - E_3)$ and $(E_1 - E_2)$ permit discrimination of the selected contrast agent. If more than two materials have to be quantified, more energy bins must be taken into consideration.

K-edge imaging has been demonstrated using small size (typically built using a single chip or a pair of chips) hybrid pixel detectors, as well as with the larger size XPAD3 camera (Figure 14) that permits scanning of a mouse without detector translation. As an example, Figure 16 shows the result of iodine and silver K-edge imaging of a phantom made of three twisted rubber pipes filled with silver, copper and iodine solutions.

Figure 17 presents maximum intensity projections (MIP) of standard absorption CT and K-edge scans of a mouse injected with 200 µL Iomeron®. A 50 kV, 600 µA X-ray spectrum was generated by a molybdenum anode tube filtered by 100 µm copper; 360 projections of 5 s were reconstructed with the FDK algorithm. K-edge imaging of the mouse suppressed bone structures that do not uptake iodine, while it reveals clearly the mouse kidneys and ureters.

3.3.3 Prospects

In a photon counting camera, every pixel can select X-ray photons above an energy threshold, or within energy windows when pixels have several thresholds, and count every photon individually without adding dark noise. Indeed, this feature cannot be achieved using conventional 'charge integration' CMOS detectors, because it necessitates settling quite a large amount of functions in a small surface that has to be smaller or equal to the pixel sensor surface. This makes a hybrid pixel detector ASIC

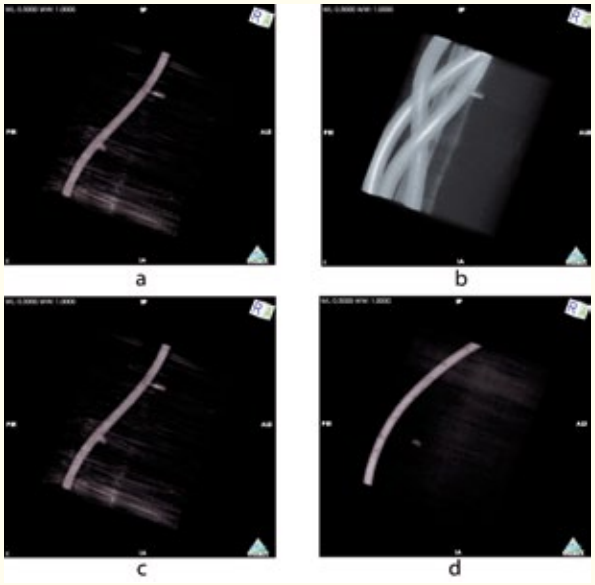

Figure 16. Transverse slice (a) and 3D volume rendering (b) of a phantom made of three twisted rubber pipes filled with Ag, Cu and I solutions. Data presented in (a) and (b) are acquired with a threshold of 25.5 keV and reconstructed using the FDK algorithm. 3D volume rendering of data obtained after subtractive analysis of X-ray absorption above and below the K-edge values of Ag (25.5 keV) and I (33 keV) are shown in (c) and (d), respectively.

quite a complex integrated circuit with several millions of transistor elements. Despite this difficulty, the technology of hybrid pixel detectors with silicon sensors is now rather well mastered and their performance correctly understood and modelled, which makes it possible to develop spectral CT for various applications.

As an example of a prospective application of spectral CT, let us consider glioblastomas, which are aggressive brain tumours with currently no treatment. Vascularisation and inflammation are two possible therapeutic targets whose relative contributions to tumour growth have to be characterised dynamically in vivo. Being able to image longitudinally both the tumour vascularisation and the inflammation would represent an invaluable tool to assess their effects on tumour growth. Markers of tumour vascularisation and inflammation can be labelled with gadolinium and iodine contrast agents used for magnetic resonance imaging (MRI) and CT, or gold nano-particles, which all have K-edges within the energy range of soft X-rays ($E_K = 33$, 50 and 80 keV for iodine, gadolinium and gold, respectively). K-edge imaging of gadolinium, gold and iodine is thus possible by processing subtractive analysis of X-ray absorption above and below their K-edges using X-ray photon counting detectors to select detected X-rays by their energies. As another example, it has been demonstrated that imaging of gold nano-particles can be used to study arterial inflammation and provide information on the composition of atherosclerotic plaque.

Figure 17. (top) MIP of standard absorption CT images. (bottom) MIP of K-edge images.

Nevertheless, X-ray absorption efficiency above 35 keV in silicon is only of a few percent, whereas more than 80% of X-rays interact in cadmium telluride above this energy. Thus the development of CdTe or GaAs hybrid pixel cameras is of utmost importance to address K-edge imaging above the iodine K-edge ($E_K = 33$ keV). At present, the relatively small diameters of CdTe or GaAs wafers do not permit hybridisation of large modules. Furthermore, CdTe wafers are quite brittle and can barely sustain mechanical stress, e.g. due to different dilatation coefficients of the CdTe sensor and the Si integrated circuit. However, given the energy range that is targeted by this new technology, the methodology developed on preclinical models, even using small size detectors, would be easily if not directly transferable to human clinics.

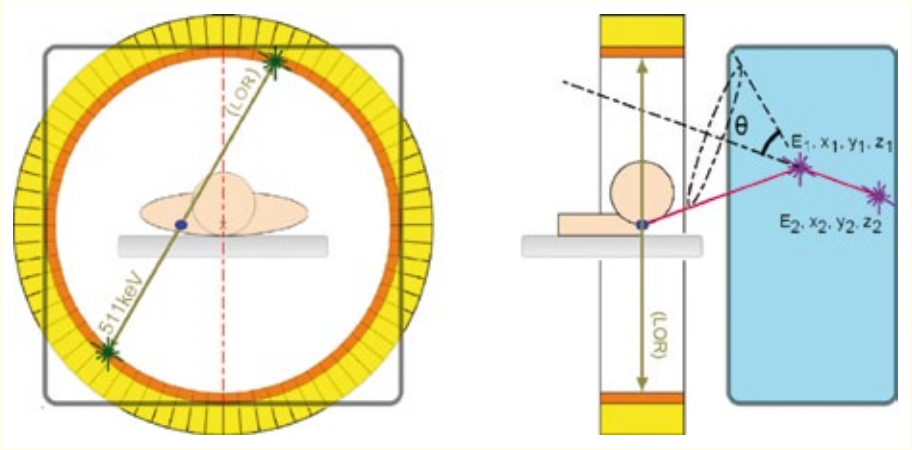

Figure 18. Schematic drawing of the '3γ imaging' principle based on the detection of a line-of-response (LOR) from two positron annihilation photons and a prompt third photon emitted from the excited PET isotope daughter nucleus. In this approach the additional photon is detected in a Compton camera formed by a cryogenic time-projection chamber filled with liquid xenon (from [Oger *et al.*, 2012]).

In summary, photon counting will potentially impact positively "black and white" or grey-scale CT accuracy by improving image contrast and signal-to-noise ratios. Indeed, with 'charge integration' X-ray cameras, the higher the energy of the detected X-ray, the more it will contribute to the formation of the detected signal, whereas with photon counting cameras, every detected photon contributes evenly to the Poisson statistics of the photon count. Hence, image contrast, which results predominantly from the detection of soft X-rays, tends to be better with photon counting CT than with charge integration CT. Furthermore, the rejection of low energy X-rays by photon counting detectors suppresses X-rays that are scattered with large angles and thus also tends to improve image signal-to-noise ratio.

More importantly, it is the ability of photon counting detectors to get spectral information on the detected X-rays that will bring a paradigm shift from "black and white" to "colour" CT. This will permit identification and/or discrimination of multiple contrast agents simultaneously, some of which will be nano-particles labelled with metallic elements identified from by their K-edge signature, and locate those within the anatomic grey-scale CT image, thus providing a large amount of functional information in vivo [Jorgensen *et al.*, 2011].

3.4 Nuclear medical imaging using $\beta^+\gamma$ coincidences: γ-PET

To date, a whole class of potential PET isotopes has been excluded from medical application. These are those where, in addition to the two back-to-back emitted 511 keV β^+ annihilation photons, a third higher-energy γ ray is emitted from an excited state in the daughter nucleus. The resulting extra dose delivered to the patient, as well as the expected increase of background from Compton scattering or even pair creation, has prevented the use of isotopes such as $^{44(m)}$Sc, ^{86}Y, ^{94}Tc, ^{94m}Tc, ^{52}Mn, or ^{34m}Cl. However, provided there is availability of customised gamma cameras, this apparent disadvantage could be turned into a promising benefit, offering a higher sensitivity for the reconstruction of the radioactivity distribution in PET examinations.

Presently two approaches are pursued towards the realisation of a medical imaging system based on β^+-γ coincidences. Both of them draw on the imaging properties of a Compton camera, where the registration of the Compton scatter and absorption kinematics of an incident photon in a suitable detection system (i.e. inelastic scattering of a photon with a (quasi-free) electron) is exploited to reconstruct the source position, within one event restricted to the surface of a cone (see Figures 18 and 19). Determining the intersection of this Compton cone with the line of response (LOR) as defined by the positron annihilation allows a sensitive reconstruction of the decay position of the PET isotope.

In 2004, a project was started in France, aimed at realising '3γ imaging' by combining a PET scanner with a Compton camera based on a cryogenic time projection chamber (TPC) filled with liquid xenon (LXe), acting simultaneously as scatter, absorption and scintillation medium for the additional 3rd photon. A small LXe-TPC prototype has yielded promising results [Oger *et al.*, 2012].

A second, more conventional, experimental approach pursued in several European laboratories utilises solid-state detectors to set up the Compton camera system. Here, double-sided silicon strip detectors serve as a Compton scattering unit, while scintillation crystals (either from well-established materials like BGO or LSO, or from novel scintillators like $LaBr_3$, see Figure 19) act as the photon energy absorber. Such modules could be combined with a ring of PET detectors (similar to the concept illustrated in Figure 18); alternatively a set of several Compton camera modules (as shown in Figure 19) could be arranged to detect either the

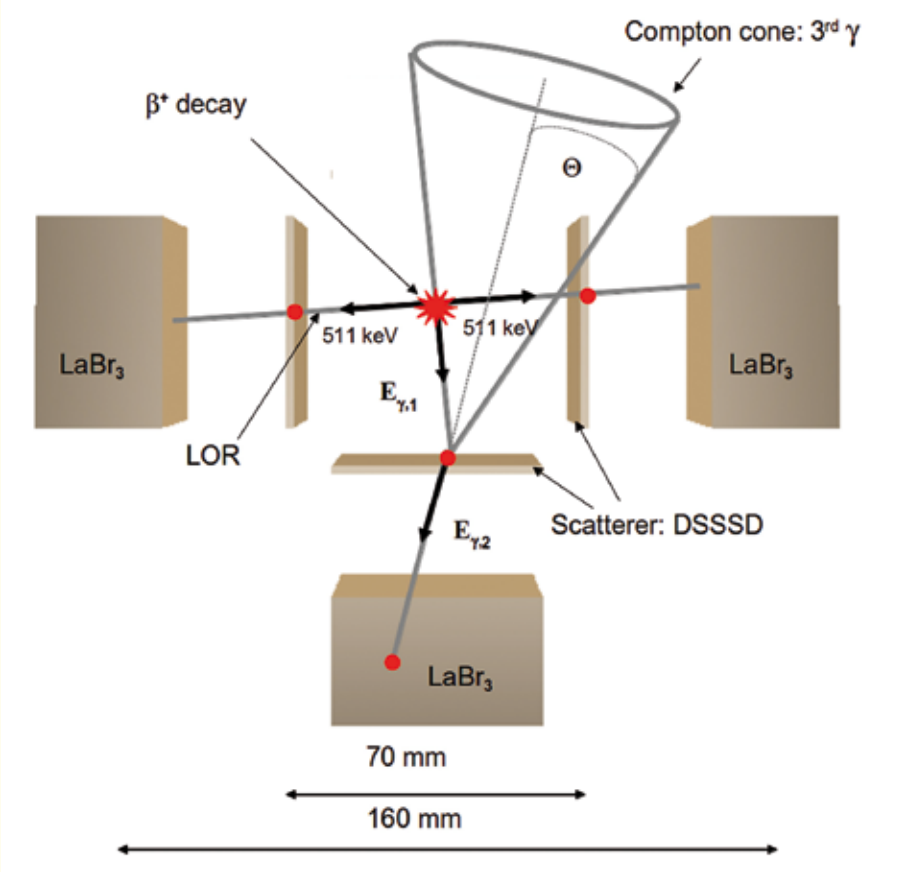

Figure 19. Arrangement of three Compton camera modules to define the LOR from β^+ annihilation in coincidence with the detection of the 3rd photon. Each module consists of a double-sided silicon strip detector (DSSSD) a scatterer and a $LaBr_3$ scintillator as absorber.

β^+ annihilation photons or the additional γ photon in coincidence.

The concept of $\beta^+\gamma$ coincidence imaging ('γ-PET') may open up the possibility to exploit a whole class of new PET isotopes, offering a highly sensitive and highly resolving localisation of the photon source position. The high sensitivity of γ-PET can be illustrated by the setup shown in Figure 19, where already a few tens of reconstructed intersections between the LOR and the direction towards the 3rd photon are sufficient to localise the activity contained in a voxel size of 2x2x2 mm^3 [Lang *et al.*, 2014]. In order to achieve the same with a conventional PET-based analysis, a few thousand LORs would be needed to be reconstructed. Beyond Europe, the topic of 'unconventional' PET isotopes is studied, for example in the US; however, so far no dedicated project to develop a 'γ-PET' detection system has been reported.

Finally, this technique would also provide the opportunity for building a 'hybrid detector', where during hadrontherapy treatment prompt photons could be detected from nuclear reactions of the therapeutic proton or ion beam with the tissue, while in the treatment delayed emission of photons from $\beta^+(+\gamma)$ decay of online produced β^+ emitters ($^{10,11}C$, $^{14,15}O$) could be detected.

4. Interfaces

4.1 Quality control in hadrontherapy

The main physical advantage of charged hadrons (i.e. protons or light ions) in radiation therapy is based on their finite range in tissue, with no or only a minor exit dose after a Bragg peak (see Chapter 1, Hadrontherapy) placed at a given depth depending on the energy at the entrance and the interactions in the path of the beam. However, in clinical practice significant uncertainties remain and the exact position of the beam range is not known with the required precision. Main factors contributing to range uncertainties in the order of several millimetres are summarised in Table 4, in addition to possible slow or fast anatomical changes in the body during or in between fractions. Methods for reducing range uncertainties can be classified in different categories and as a function of the time they are put in operation (Table 5). While pre-treatment dosimetric quality controls and cross calculations are most commonly used in current clinical practice, in vivo verification methods would represent an optimal solution for full exploitation of the advantages afforded by the ion beam.

Table 4. Uncertainty in range [Paganetti 2012].

Source of range uncertainty in the patient	Range uncertainty
Independent of dose calculation:	
Measurement uncertainty in water for commissioning	± 0.3 mm
Compensator design	± 0.2 mm
Beam reproducibility	± 0.2 mm
Patient set up	± 0.7 mm
Dose calculation:	
Biology (always positive)	+ 0.8%
CT imaging and calibration	± 0.5%
CT conversion to tissue (excluding I-values)	± 0.5%
CT grid size	± 0.3%
Mean excitation energies (I-values) in tissue	± 1.5%
Range degradation; complex inhomogeneities	- 0.7%
Range degradation; local lateral inhomogeneities*	± 2.5%
Total (excluding *)	**2.7% + 1.2 mm**
Total	**4.6% + 1.2 mm**

To date several methods of medical imaging in ion beam therapy are being investigated, including within the framework of a dedicated European effort (European NoVel Imaging Systems for ION therapy, http://envision.web.cern.ch/ENVISION/), in order to measure the range of particles in tissue or even directly measure the applied dose in vivo. Positron emission tomography (PET) is currently the only clinically applied method for in vivo range verification during or shortly after irradiation, and its potential benefit for ion tumour therapy has been proven. Further treatment verification methods based on the detection of secondary nuclear reaction products are prompt gamma imaging and charged particle imaging, which are currently under investigation. Another promising imaging tool in particle therapy is ion radiography and tomography, which is intended to be primarily used for position verification and treatment planning, but also can serve as a range verification method. In the following, all of these imaging techniques are presented. They require deep knowledge on nuclear processes as well as substantial abilities in detector design. Apart from challenging reconstruction tasks, the development of such imaging techniques also requires the simulation of the expected distri-

Table 5. Methods for beam range verification.

Family of methods	Name	Method	Short description	accur [mm]	Comm
Virtual	Calculation	Cross calculations	Use of different image data (e.g. dual energy CT) and models (e.g. Monte Carlo vs analytical)	2 - 4	estimation of uncertainty
Physical	Pre-treatment off line	Dosimetry	Dosimetric characterisation with different dosimetric systems	1	measurement in homogeneous media
	Pre or during treatment, upstream	Integrated electronic range verifier	Measurement around the border of the beam, arranged at different water equivalent depths // "transparent" detector (not existing yet)	2	upstream measurements in beam border
	Online in vivo verification	Prompt secondary imaging	Detection of prompt secondaries (prompt gamma, charged particles, neutrons?) emitted during treatment	?	in vivo, nuclear interactions
	Online-offline in vivo verification	PET detection	Detection of tissue activation (C, O,…) by nuclear interactions of the beam using PET imaging in the treatment room or close to it	1-3	in vivo, nuclear interactions
	"1D range probe", "2D radiography" and "3D ion CT"	Measure residual range or energy	Measure of residual range after traversing the body to validate the integrated stopping power and/or to reconstruct images of stopping power ration perform/validate calculations with finite ranges	1	feedback to calculations
	Implanted detector in path or tumour	Measure time pattern from an implanted detector	For modulated passive beams, the time signal of a detector synchronised with the modulator can be used to calculate the residual range	2	need implant
	Implanted detector after the target	Measure signal on the distal range or with higher energy	Implant a detector just after the target (e.g. in a rectum balloon, in a dental mold), measure a low dose at the fall off, or use a higher energy for a short irradiation	1	need implant in critical area or additional dose
Anatomy	Imaging post treatment	Magnetic resonance imaging	Visualisation of variations in images of irradiated tissue	2- 3	post treatment

butions. Therefore, extensive modeling of nuclear and electromagnetic interactions is necessary.

4.1.1 Positron emission tomography in particle therapy

Particles impinging on tissue induce, among others, positron emitters due to nuclear reactions with the atoms of the irradiated tissue. These positron emitters undergo radioactive decay according to their respective half-life, and positrons are released. These positrons annihilate with electrons of the tissue under emission of two annihilation photons with an energy of 511 keV each and an emission angle of approximately 180° (Figure 20). By means of a PET scanner, these annihilation photons can be detected in coincidence. Reconstruction of the measured events results in a 3D β^+-activity distribution.

The measured activity distribution cannot be compared directly to the applied dose distribution, since ß$^+$-activity and dose originate from completely different physical processes.

Thus, a simulation of the expected β^+-activity distribution has to be performed on the basis of the treatment plan, under consideration of the time course of the irradiation and imaging. This calculated β^+-activity can be then compared with the measured distribution. The simulation has to model all physical processes from the electromagnetic slowing down and the nuclear interactions of the impinging ions and further secondary particles with the atoms of the tissue, the induction of

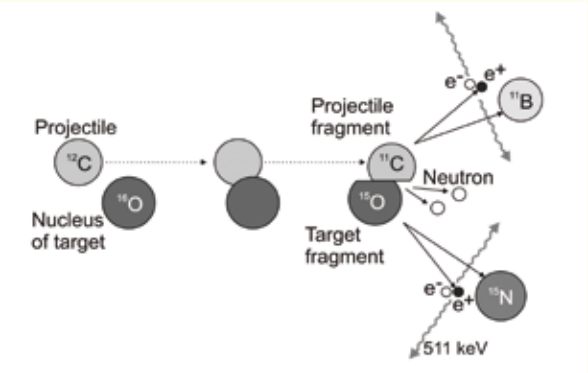

Figure 20. Principle of PET imaging in particle therapy for a ^{12}C ion (projectile) colliding with an ^{16}O atom of the irradiated tissue. Both nuclei may e.g. lose a neutron, resulting in the positron emitters ^{11}C and ^{15}O, respectively. They disintegrate under emission of a positron e$^+$, which annihilates with an electron e$^-$ of the tissue. Annihilation photons with an energy of 511 keV each are emitted.

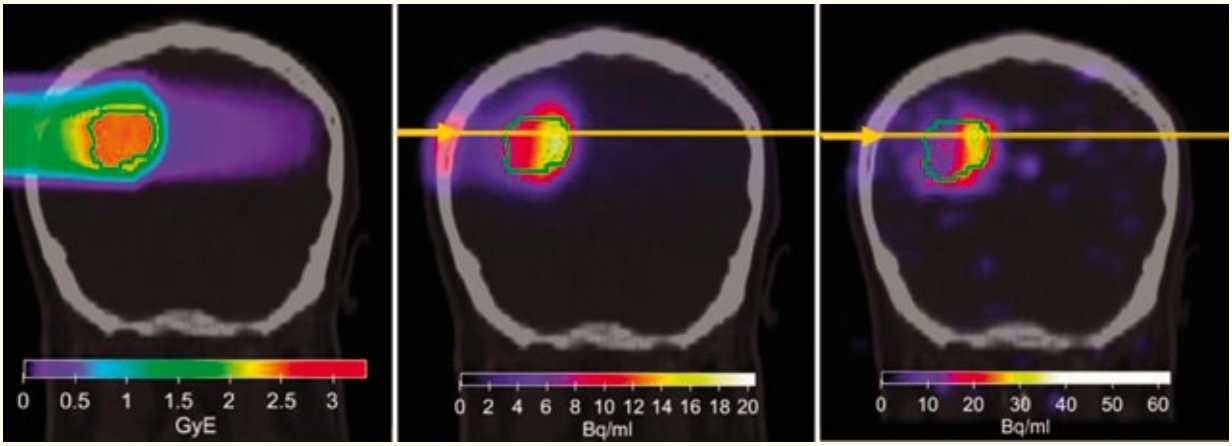

Figure 21. PET activation (right) measured after delivery of the planned carbon ion treatment dose (left) at HIT, in comparison to the corresponding PET MC prediction (middle). The arrow marks an example of good range agreement (adapted from [Bauer 2013] with permission).

positron emitters, the β^+ disintegration and formation of positrons, the thermalisation of positrons and annihilation with electrons, the transport and attenuation of the annihilation photons in the tissue until detection. All these processes require extensive knowledge of electromagnetic and nuclear processes, for example double differential reaction cross sections.

For PET imaging three implementations are investigated, which are described in detail in Shakirin 2011. The first is in-beam PET, which allows the measurement of β^+-activity during irradiation and requires a dedicated PET scanner integrated into the treatment site. The first in-beam PET scanner in clinical use was operated from 1997 to 2008 at GSI, Darmstadt, Germany. Another PET scanner directly integrated into the treatment gantry is located at NCCHE, Kashiwa, Japan, and is commercially available. Furthermore, small prototypes of in-beam PET scanners for research purposes are installed; for example, at HIMAC, Chiba, Japan.

The second modality is in-room PET. Here the PET scanner is located in the treatment room and imaging of the β^+-distribution takes place shortly after irradiation. An in-room PET scanner is investigated at MGH, Boston, USA.

The third modality is off-line PET, where no dedicated PET scanner is required, but conventional diagnostic devices, typically combined with CT scanners, can be used. After treatment the patient is transported to a PET system and the measurement of β^+ activity starts with time delays of several minutes, depending on the location of the scanner. This offline implementation is in clinical use, for example, at HIT, Heidelberg, Germany, and HIBMC, Tatsuno, Japan. An example of clinical application is shown in Figure 21.

Although already implemented in clinics, PET in particle therapy requires more technological and methodological developments. A major issue in future detector developments and a research field of several groups is the use of ultra-fast time of flight (TOF) information for PET monitoring in order to improve image quality. Further investigations are dealing with improvements on the knowledge of reaction cross sections, feasibility of PET for moving targets, application of PET for various other ions interesting for therapy, automatic evaluation of PET measurements, as well as application of PET in unconventional high energy photon therapy.

4.1.2 Prompt gamma ray imaging

During tumour irradiation with particles a large variety of prompt gamma emission occurs. These prompt gamma rays arise from nuclear de-excitation in an energy range of a few MeV. However, besides prompt gamma rays from the excited nuclei, in addition a substantial amount of background arises from other secondary particles, e.g. neutrons, light charged fragments as well as Compton scattered photons (Figure 22). Thus, several imaging modalities are being investigated to shield the background and selectively acquire information from prompt gamma emission.

A first approach is a collimated gamma camera, i.e. a collimator with a hole or a slit in front of a position-sensitive detector. A more advanced system is a multi-slit camera with a collimator with multiple slits in front of the detector. For those kinds of imaging systems, 3D information requires synchronisation with an upstream beam-positioning device such as a hodoscope.

Another possibility of prompt gamma ray imaging entirely independent from the treatment device is a Compton camera, which uses two or more energy- and position-sensitive detectors and, thus, no mechanical collimator is necessary.

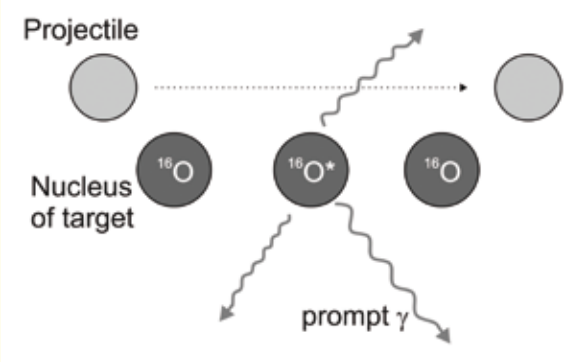

Figure 22. Principle of prompt gamma imaging using the example of a projectile ion colliding with an ^{16}O atom of the irradiated tissue. The target nucleus is excited and de-excites under emission of prompt gamma radiation.

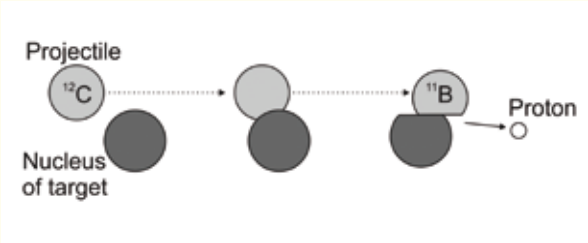

Figure 23. Principle of interaction vertex imaging shown for the collision of a ^{12}C ion with a target nucleus. The projectile ion loses a proton, which leaves the irradiated tissue and is used for imaging.

Improving detection efficiency and background rejection by means of a TOF gamma camera is also under investigation. It is supposed that discrimination between photons and hadrons becomes possible by using the time of flight information, although the time microstructure of the beam can be critical in this respect.

4.1.3 Charged particle imaging

During irradiation with primary ions heavier than protons, lighter projectile fragments are produced in collisions of the incident ions with nuclei of the irradiated tissue (Figure 23). Some of these light fragments have enough energy to leave the patient and can be easily detected. A reconstruction of the trajectory of the emerging charged particles and the intersection with the impinging ion path gives the point of ion– nucleus interaction. By means of a comparison between simulated and measured vertex distributions, the range of impinging ions can be verified. For this method, also known as interaction vertex imaging, a feasibility simulation study has been reported and the first promising measurements on homogeneous targets have been recently performed.

4.1.4 Ion radiography and tomography

Ion radiography enables the direct measurement of the residual range of high-energy low-intensity ions traversing the patient. It may replace X-ray radiography to produce low dose, high density resolution images of the patient at the place of treatment. In terms of pre-treatment verification, the method can be also used to validate in vivo the treatment planning range calibration curve deduced from the X-ray CT, which currently introduces the larger source of range uncertainties due to different physical processes of ion and photon interaction. Tomographic extension of radiographic imaging can enable volumetric images, providing a direct measurement of the ion stopping power ratio relative to water. Due to the weak energy dependence of the stopping power ratio, these images obtained at higher energies than for therapy can be used as a patient model in treatment planning, again eliminating the range uncertainties connected to the usage of calibrated X-ray CT images. Spatial resolution of the method is limited by multiple Coulomb scattering in the patient, which is more pronounced for protons than for heavier ions. However, 1 mm is anticipated to be achievable, even for the more scattering protons. New prototypes are currently under development both for protons and carbon ion beams.

4.2 Mass spectrometry

Mass spectrometry is a technique that was developed more than hundred years ago. It led to epochal discoveries, which laid the foundation to what is now called nuclear and particle physics. At that time it was a key method to explore atomic and subatomic particles, and in 1913 the seminal discovery of isotopes was made: that the chemical elements have constituents of different mass number. Since that time many more building blocks of matter were discovered and analysed in great detail, and besides its wide use and further development in nuclear physics, mass spectrometry found its application as an analytical tool in many fields of science, including chemistry, biology, geology, space science and many others[Mün13]. Besides these natural sciences, where analytical aspects dominate, there are a lot of applications, where mass spectrometry fulfills qualitative and quantitative requirements. These include environment, climate research, health, nutrition, security and many others. Here, we concentrate on health and medicine, with some emphasis on in situ applications. It is the goal of this section to introduce the reader to modern mass spectrometric techniques, sample preparation and present mass spectrometry applications for medical analyses and tissue imaging.

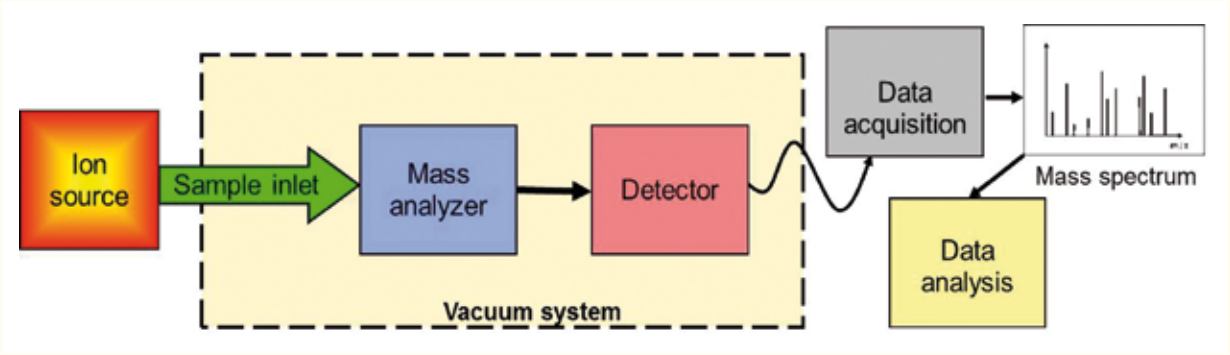

Figure 24. Schematic view of the components present in every mass spectrometer: ion source, mass analyser and detector. The vacuum system ensures that the ion motion does not suffer from collisions with gas atoms or molecules and is governed by the forces of electric and/or magnetic fields; this ensures that the spatial or time-wise separation of different species depends only on their mass-to-charge ratio.

Mass spectrometry

Mass spectrometry (MS) separates and analyses the building blocks and the chemical composition of a substance according to its mass-to-charge (m/z) ratio. Two principal concepts exist to disperse the ions: spatial separation and separation in time. The main elements, common to all mass spectrometers, are depicted in Figure 24: ion source (where the sample under investigation is transformed from its original form to ionised atoms, molecules or clusters), analyser (the central element, which disperses the ions timely or spatially according to their mass-to-charge ratio) and detectors (including data acquisition, storage, graphical display and quantitative analysis systems). Such devices all yield mass spectra, which represent the intensity distribution of the constituents of the sample, sorted according to an increasing mass-to-charge ratio. Today there are many types of ion-source and mass analyser, and a large variety of combinations of these exist, all specialised for certain applications. The most commonly used mass analysers comprise sector field magnets, quadrupole mass spectrometers, ion traps and time-of-flight (TOF) systems.

The performance of a mass spectrometer is characterised by several parameters. The most important ones being **mass range** (the range from the lightest to the heaviest mass that may be analysed, typically this ranges from one mass unit [hydrogen is the lightest chemical element] to a few 10,000 [which is typical for fragments of complex biomolecules like proteins]), **mass resolving power** (the ability to distinguish adjacent masses; this number should be high and ranges for routine operation from ~1,000 to 1,000,000), and **accuracy** (which is the ability to measure the true mass value of a certain species; inaccuracies should not exceed the ppm level). Besides these, other properties like the **sensitivity** of an instrument (the ability to investigate small amounts of sample material), the **dynamic range** (the ability to measure very rare and very abundant species simultaneously) or **scanning or non-scanning operation** (the former samples the mass range stepwise with the necessity of multiple scans to cover the whole mass range, while the latter covers the entire mass range at once) determine the potential for certain applications. Measurement duration as well as repetition rate are further critical properties for some applications.

Some modern instruments provide the capability of tandem-based analyses, the so-called MS/MS technique. With MS/MS sequencing, certain molecules can be selected in a first step, while in a second step the molecule is fragmented and the component pieces detected; by assembling the masses of each fragment, one can deduce the composition and obtain structural information; this works reliably for previously unknown analytes, especially when they are large and/or complex. The structure of complex biomolecules can be derived by this two-step analysis.

Present techniques for medical and imaging applications

Most specific for a certain application are sample preparation, ionisation and inlet techniques. Here, an almost infinite variety of concepts and techniques exist, tailored for the specific physical and chemical properties of the sample and the purpose of the analysis. The goal of all these techniques is to dissolve the sample by the impact of photons (e.g. laser light, which is used in laser ablation ion sources) or energetic particles (e.g. swift ions, which are used in secondary ion mass spectrometry, SIMS) or by desorption (e.g. by microscopic droplets of a solvent) such that it releases microscopic debris from its surface (atoms, ions and molecules), which can be analysed by the mass spectrometer. When such a focused ionising source is rastered in small steps laterally across a sample and for every pixel a mass spectrum is recorded, an "image" can be recorded

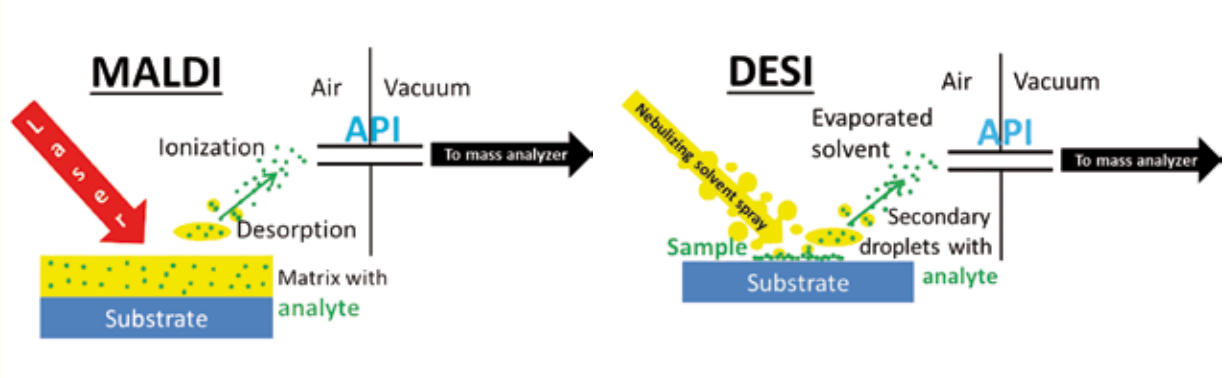

Figure 25. Desorption and ionisation techniques that are widely used in analytical mass spectrometry: matrix-assisted laser desorption ionisation (MALDI, left) and desorption electrospray ionisation (DESI, right). For details see text.

of how the constituents are distributed and structural information is obtained. Biological substances are often processed at ambient air pressure, while the mass spectrometer itself operates in a vacuum vessel; they are connected by an atmospheric pressure interface (API) and the sample fragments are introduced by various transport mechanisms that are simultaneously used to improve the selectivity towards the material of interest, but also to remove the necessity for pre-concentration of samples (enrichment) before analysis.

In imaging mass spectrometry (IMS), the original spatial composition and the integrity of the sample needs to be preserved, and analyte migration, degradation or contamination must be prevented to obtain original information. Figure 25 shows two concepts that are widely used in imaging mass spectrometry: matrix-assisted laser desorption ionisation (MALDI) and desorption electrospray ionisation (DESI). MALDI takes advantage of pulsed laser light impinging on an acidic matrix/solvent combination for extraction, desorption and ionisation of the substance from the surface, while DESI generates ions by a thin jet of electrostatically charged solvent, impinging obliquely on the sample surface. In both cases, the desorbed and charged sample debris are accelerated by an electric field towards the mass spectrometer and collected by its atmospheric pressure inlet system. Both techniques can be applied to basically any human or animal tissue.

Many other methods exist, which cannot be described here. They all have specific strengths and characteristic applicability to individual problems, depending on the sample, environment and purpose. Common to all is the generation of charged sample fragments that can be analysed by the mass analyser.

Present commercial IMS instruments reach a lateral resolution of the order of 10 to 50 micrometres (for comparison: the typical diameter of a mammalian cell is of the order of 5 to 20 micrometres), while research laboratories have reported sub-cellular resolutions down to ~1 micrometre. Typically, the ionising source rasters across the sample and the mass spectra yield characteristic information for each pixel, e.g. on proteins, peptides, lipids, etc. The overall area that can be sampled is in principle unlimited, but in practice depends on the speed of the instrument to record mass spectra and the overall available measurement time, so that typical areas of the order of a few square-millimetres or centimetres can be analysed. Large potential arises with three-dimensional imaging mass spectrometry, 3D-IMS. A stack of IMS images from the analysis of thin slices of three-dimensional objects can provide a detailed and comprehensive 'view' e.g. of an organ, including small tumour biopsies.

Medical applications of mass spectrometry and imaging

Imaging mass spectrometry, where high spatial resolution is combined with mass spectrometric analysis of the sample material, is a versatile and almost universal method to analyse the spatial distribution of analytes in tissue sections. An almost infinitely wide range of applications emerges due to the fact that basically every organic or inorganic material can be "dissolved" to microscopic fragments and ionised. The method is label-free and provides unique features for the analysis of tissues, especially when combined with classical histological stains. It provides specific information on proteins, peptides, lipids, drugs, neuropeptides and drug metabolites and many other biological substances. Since the measurements are performed on biological matrices, they require sensitive, high resolving mass spectrometers with high dynamic range able to handle the complex mass spectra. Medical benefits of MS range from new diagnostics, understanding of illness and its genesis to therapeutic developments. Examples are given in the following.

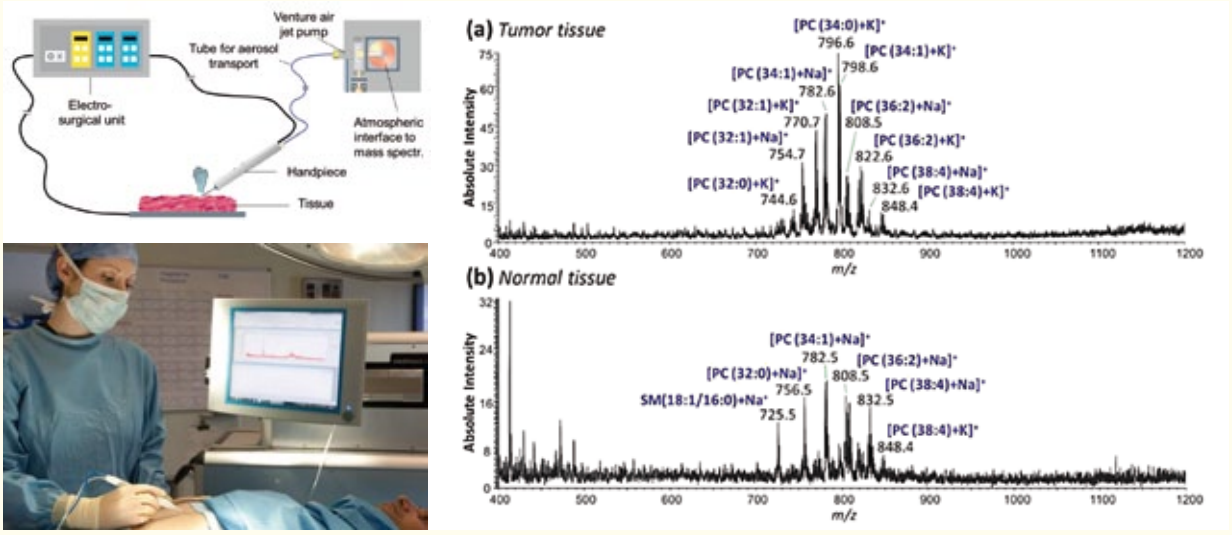

Figure 26. Top left: principle of an electro-scalpel in combination with an Venturi-pump inlet system for mass spectrometric analysis of vaporised tissue (reprinted with permission from Anal. Chem. 82, 7343. Copyright 2010 American Chemical Society). Bottom left: the device in operation during surgery (figure credit: Imperial College London). Right: mass spectra of a cancerous (top) and a healthy (bottom) human bladder tissue show different characteristic patterns (reproduced from *Faraday Discuss*. **149**, 247 by permission of The Royal Society of Chemistry, RSC).

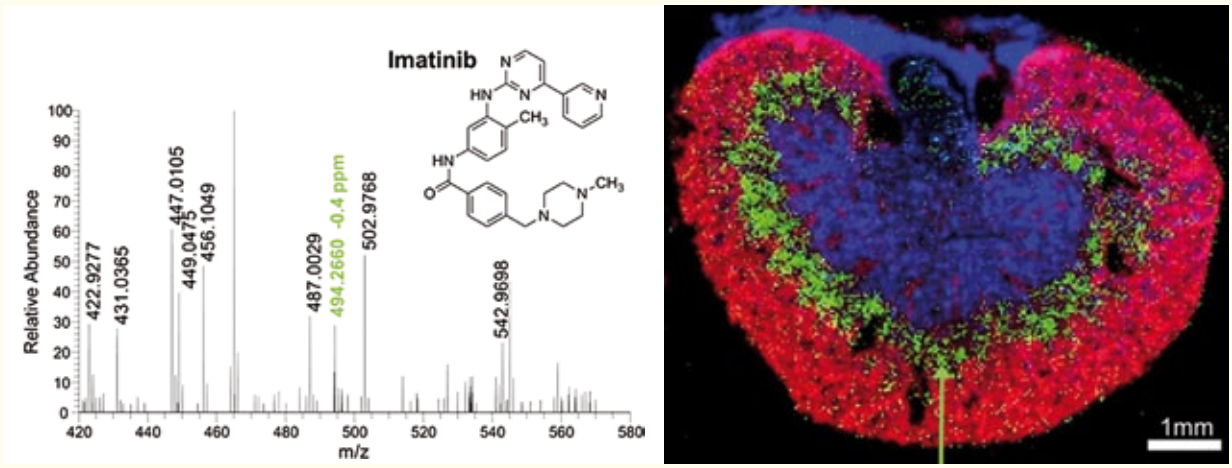

Figure 27. IMS spectra of a mouse kidney after treatment with the anti-cancer drug imatinib. Left: single-pixel mass spectrum of the outer stripe outer medulla; each pixel has an area of about 1/1000 square-millimetre. The green label indicates the mass peak that is characteristic for imatinib (m/z=494.2660). Right: imaging mass spectrometry yields the distribution of different substances in the mouse kidney. The green arrow points to the imatinib distribution, which is concentrated in the outer stripe outer medulla (figures reprinted from ref. [Röm13]).

• Tissue recognition

Very appealing is the potential of mass spectrometry for histology. Typical histological analyses take several hours. For intra-operative cases there exist faster (~30 minutes) but less reliable techniques. Here, fast and precise identification by means of mass spectrometry can be a solution. The tissue material is released by an electro-scalpel and transported into the mass spectrometer: heat is used to cut through the patient's tissue and produces tiny amounts of smoke that is rich in biological information. The "knife" collects some smoke, sucks it into the mass spectrometer and performs an instant mass spectrometric analysis. The obtained mass spectra exhibit different lipid profiles, which are analysed by multi-dimensional principal component analysis. Characteristic patterns indicate whether the cut tissue is cancerous or not. It also allows identification of metastases of various cancer types and to distinguish the original cancer from its metastases by different mass patterns. Figure 26 shows the principle of the electro-scalpel, its application in the operation room and examples of tumour and normal tissue.

• Multi-modal imaging

The above sections illustrate that IMS is a highly valuable method for studying biological samples. However, such samples are invariably complex and a single tissue section contains a large variety of chemical species ranging from salts, amino acids and lipids, to peptides and proteins. Therefore, the use of several different methods, each optimised for different types of molecules, enhances the infor-

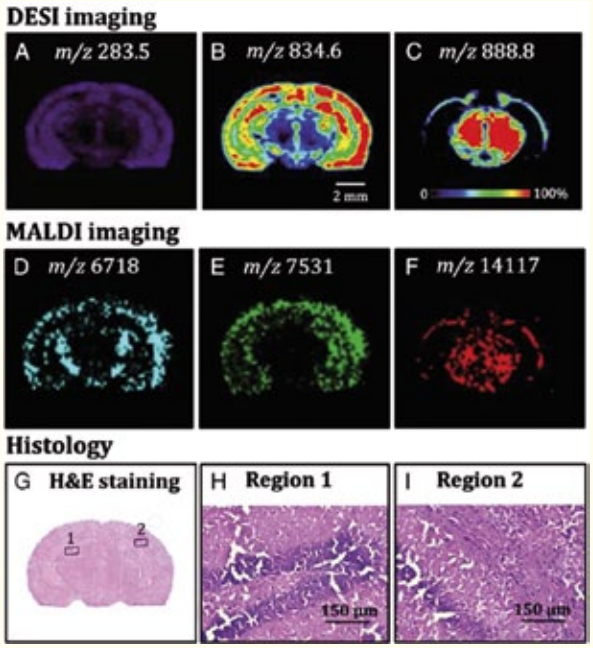

Figure 28. Complementary information on a mouse brain, obtained from different methods. The top and central row show intensity distributions of different lipid species imaged with a DESI source and of different proteins imaged with a MALDI source, respectively; the m/z values refer to various characteristic mass-to-charge ratios. Bottom: classical histological images using hematoxylin and eosin stain (H&E staining). Figure reprinted with permission from *Anal. Chem*. **83**, 8366. Copyright 2011 American Chemical Society.

mation gained by IMS. A good example is tissue samples of the brain, which are ideally suited for mass spectrometry analyses, since many of the relevant neuro-transmitters are either peptides or small molecules. Figure 28 shows an example of multimodal imaging combining conventional H&E staining, DESI imaging mass spectrometry and MALDI imaging mass spectrometry. Each method was carried out on the same tissue slice of a mouse brain. The combination of information from each method provides a unique, complementary perspective by allowing analysis with each technique.

New developments for in situ applications with ultra-high mass resolving power

The growing number of applications and the analytical potential of mass spectrometry has stimulated the development of many different techniques, including miniaturised and portable apparatus for field deployment and use in many daily circumstances. A novel laboratory instrument for research and development is shown in Figure 29: this TOF mass spectrometer, originally developed for nuclear physics and astrophysical precision experiments, is compact, mobile, and it combines an atmospheric pressure interface for universal in situ analyses with ultra-high mass resolving power (in excess of 200,000). Envisaged applications in environment and life-sciences are, e.g.,

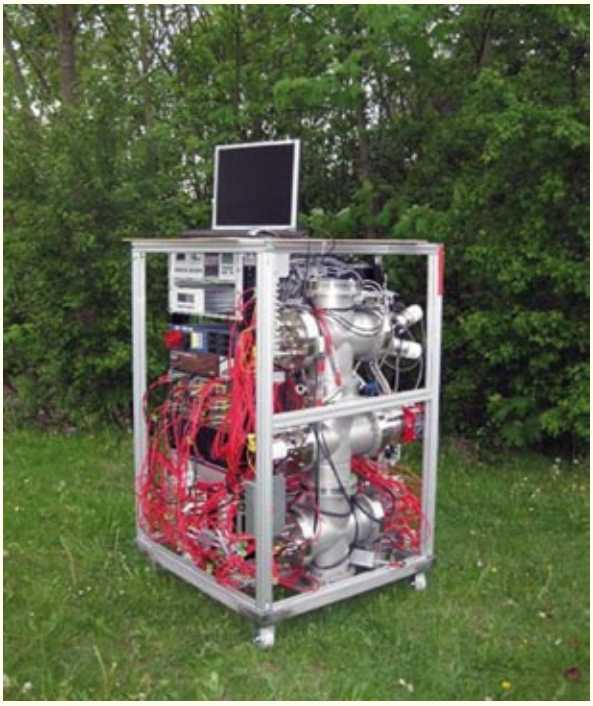

Figure 29. A modern example of a newly developed high-performance TOF mass spectrometer with ultra-high mass resolving power for in situ applications in environment, life-sciences and medicine.

- *wastewater monitoring:* contamination of water with pharmaceuticals and personal care products are of increasing concern and represent a threat to wildlife and humans,
- *detection and identification of food contaminants:* there are numerous and steadily increasing numbers of contaminants, e.g. pesticides, natural toxins, veterinary drugs, food additives, adulterations or food-packaging migrants, that need to be identified and quantified, and
- *security:* the possibility of deployment of biological weapons by terrorists is an existing threat and effective detection and countermeasures are necessary.

The hitherto unrivalled combination of ultra-high mass resolution, MS/MS, non-scanning broad-band, IMS and in situ capabilities provides new analytical opportunities that will stimulate new field applications. These developments are a living example of how mass spectrometry methods and instruments, devised for nuclear physics experiments, continue to stimulate and cross-fertilise new applications in medicine and neighbouring fields.

5. Outlook

Medical imaging in general, and nuclear medicine in particular, for which detection of radiation emitted by the atomic nucleus is involved, has experienced and continues to exhibit evolution at exponential speeds. In the past, this evolution has largely benefited from technologies developed and tested in the experimental nuclear physics battleground, and it seems that this trend will only increase in the future. The maturity of the nuclear imaging sector can be seen by the fact that while in the past most nuclear detector technologies employed in the medical field, such as PMT and scintillators, were borrowed from the experimental nuclear physics knowledge base, nowadays new technologies are being pursued by the demanding medical industry, where the rate of technological evolution has never been so fast and new techniques are translated into biomedical research and clinical use within the year.

Nuclear physics groups have always been aware that their work in radiation detection, simulations, electronics, and data processing, might find application in nuclear medicine. But today we realise that our activities in these two fields are not only complementary and synergetic, but that their pace of development is very different. Nuclear physics experiments may take several years to design, fund, set up, run and analyse data. In the nuclear imaging arena, though, trends and technologies are being introduced, tested and dismissed at high speed. One can assess this by attending every year the leading conferences in the nuclear imaging instrumentation sector, such as the IEEE Medical Imaging Conference, and witnessing how the trends of previous year have been discarded and new ones are in the spotlight.

The urge to evolve nuclear imaging detectors is dynamising the activity of nuclear physics groups, while, on the other hand, mid-term stability in the scientific goals needed to face multi-national nuclear physics experiments, makes it possible to train and shape the best technicians, doctors, researchers and in general experts in technology for nuclear detection. There are many examples of researchers trained in nuclear physics groups doing basic research, who have later pursued successful careers in the medical imaging industry.

This chapter has provided a glimpse of how nuclear physics research has been involved in the advance of medical imaging and, more interestingly, how our current efforts are paving the way for the imaging technologies of tomorrow. X-ray spectral CT, PET/MRI scanners, devices for quality control of hadrontherapy, to name a few, will be commonplace in the most up-to-date clinical practice in a few years.

We have seen that multimodality in nuclear imaging has taken a big step forward in the last decade. This has mostly been driven by the introduction and widespread acceptance of PET/CT units in clinical practice, especially in oncology, and more recently by the deployment of simultaneous PET/MRI systems. In the preclinical field combined modalities are diffused and necessary, since the active groups are typically in academia where they can find the resources and knowledge to implement and develop the most highly sophisticated molecular imaging technologies available today. Just to address the hardware side, novel scintillators, photodetectors and DAQ systems have received a great boost from these activities, thus demonstrating the cross-fertilisation between the fundamental research in detector and technology carried out in nuclear physics groups and their application in molecular imaging.

We have also noticed that advances in instrumentation for medical imaging should be accompanied by corresponding advances in image reconstruction and modeling, in order to fully exploit the improved performance of novel devices and provide increased image quality. For this purpose, accurate models of the image formation and degradation processes should be developed for each scanner or prototype. These models should rely on a profound knowledge of the underlying physical phenomena and their interconnection. Increasing computing power and advances in computer technology should make feasible the implementation of these models as a part of image reconstruction, requiring the involvement of highly specialised experts, very often trained through participation in nuclear physics experiments.

This chapter reflects the fact that inside the nuclear physics community, research and development activities in medical imaging detector development coexist, at times even within the same research group. These developments prove that, even if from the outside it appears that basic nuclear physics activities are far from real world application, they in fact continue to provide the best field to test new technologies in detector, electronics and processing. Moreover, they help to obtain critical mass to interface with the medical imaging industry. We feel more than ever that it is our duty to help and promote the translation of developments from our nuclear physics laboratories and basic nuclear science experiments into practical tools for the clinical and preclinical environments.

References

[1] Bauer, J.; Unholtz, D.; Sommerer, F.; Kurz, C.; Haberer, T.; Herfarth, K.; Welzel, T.; Combs, S. E.; Debus, J. & Parodi, K. (2013). Implementation and initial clinical experience of offline PET/CT-based verification of scanned carbon ion treatment. *Radiother. Oncol.,* **107**(2):218–26.

[2] Defrise, M. & Gullberg, G. T. (2006). *Image reconstruction.*, *Phys Med Biol* **51**: R139–R154.

[3] Harrison, R. (2012). In: Grupen, C. & Buvat, I. (Ed.), *Simulation of Medical Imaging Systems: Emission and Transmission Tomography*, Springer Berlin Heidelberg.

[4] S.M. Jorgensen, D.R. Eaker and E.L. Ritman. (2011). "Biomedical spectral X-ray imaging; promises and challenges," in *Medical Applications of Radiation Detectors*, edited by H.B. Barber, H. Roehrig and D.J. Wagenaar, Proc. of SPIE, vol. **8143**, 814302.

[5] C. Lang *et al.* (2014). Sub-millimeter nuclear medical imaging with high sensitivity in positron emission tomography using $\beta^{+}\gamma$ coincidences, JINST 9 P01008. doi:10.1088/1748-0221/9/01/P01008.

[6] Massoud, T.F., Gambhir, S.S. (2003). Molecular imaging in living subjects: seeing fundamental biological processes in a new light. *Genes Dev.* **17**:545.

[7] T. Oger *et al.* (2012). A liquid xenon TPC for a medical imaging Compton telescope, *Nucl. Instr. Meth.* A **695**: 125.

[8] Paganetti H. (2012). Range uncertainties in proton therapy and the role of Monte Carlo simulations. *Phys. Med. Biol.* **57**:R99–R117

[9] Rahmim, A., Rousset, O., & Zaidi, H. (2007). Strategies for motion tracking and correction in PET. *PET Clinics*, **2**(2), 251–266.

[10] N. Wermes, "Pixel detectors for tracking and their spin-off in imaging applications," Nucl. Instrum. Meth. A541:150-165,2005

[Mün13] G. Münzenberg, Int. J. Mass Spec.349-350 (2013) 9-18: "Development of mass spectrometers from Thomson and Aston to present"

[Röm13] A. Römpp *et al.*, Histochem. Cell Biol. 139 (2013) 759–783: "Mass spectrometry imaging with high resolution in mass and space"

List of Contributors (Chapter II)

- **Faiçal Azaiez,** France
- **David Brasse,** France
- **Piergiorgio Cerello,** Italy
- **Christophe de La Taille,** France
- **Alberto Del Guerra,** Italy
- **Peter Dendooven,** Netherlands
- **Wolfgang Enghardt,** Germany
- **Fine Fiedler,** Germany
- **Ian Lazarus,** United Kingdom
- **Guillaume Montemont,** France
- **Christian Morel,** France
- **Alex Murphy,** United Kingdom
- **Josep F. Oliver,** Spain
- **Katia Parodi,** Germany
- **Marlen Priegnitz,** Germany
- **Magdalena Rafecas,** Spain
- **Christoph Scheidenberger,** Germany
- **Paola Solevi,** Spain
- **Peter G. Thirolf,** Germany
- **Irene Torres-Espallardo,** Spain
- **Jose Manuel Udias,** Spain

Chapter III
Radioisotope Production

Conveners: **Ulli Köster** (ILL) – **Marie-Claire Cantone** (Milano)

Introduction

The field of nuclear medicine covers all medical uses of open radioactive sources emitting ionising radiation that are introduced into the patient for the purpose of diagnostics or therapy.

Every year over 30 million nuclear medicine procedures are performed worldwide. These include diagnostic procedures to detect, localise or stage the progression of an illness, decisive parameters for the choice of treatment options, as well as therapeutic procedures where radionuclides capable of selectively targeting the sites to the treated are used, either in elemental form or bound to appropriate molecules.

The application of closed radioactive sources (brachytherapy) is formally part of the field "radiology" but has much in common with nuclear medicine and will therefore also be covered.

Radionuclides are the essential fuel that drives all nuclear medicine applications. With few exceptions the required radionuclides are not present in natural decay chains but have to be produced by artificial transmutation, driven by projectiles delivered by accelerators or nuclear reactors. Historically all medical radionuclides were initially produced at nuclear physics facilities. Today production at dedicated "medical cyclotrons" coexists with complementary production at multi-purpose research reactors and accelerators.

This chapter will illustrate which radioisotopes are needed for what type of applications, how they were produced historically and today and how radioisotope production keeps profiting from tight synergies with other nuclear physics activities. An outlook is given for promising "novel" radioisotopes with improved properties for certain applications.

1. Properties of radioisotopes for nuclear medicine

Over the last decades more than 3000 radioactive isotopes have been discovered at nuclear physics facilities. Many are very short-lived or extremely difficult to produce, but several dozen have properties that make them potentially useful for nuclear medicine. What are the crucial selection criteria that could allow a radioisotope to find an application in nuclear medicine?

i) *Nuclear decay properties:* Radioactive isotopes may emit different types of ionising radiation and the applications in nuclear medicine will differ accordingly. In general, longer range, more penetrating radiation is used for imaging purposes since it can be detected outside the patient's body while shorter range radiation is used therapeutically to deposit a maximum amount of energy within a defined region, (see Figure 1.1). Ideally imaging isotopes should not emit short range radiation, to minimise the dose for the patients. On the other hand therapeutic isotopes, which are administered at high activities, should not emit intense hard gamma radiation to minimise shielding requirements in the handling of the radiopharmaceuticals and to prevent isolation of the patients.

ii) *Half-life:* Upon introduction in the patient, the radioisotope should live long enough to reach its destination and not much of it should decay earlier. If not available from so-called generators the half-life should be long enough to avoid excessive decay losses during transport between production and use. On the other hand it should not be too long-lived either to avoid useless radiation burden to the patient, e.g. after an imaging procedure has been completed. Even for radioisotopes that are rapidly excreted shorter half-lives may be preferable to prevent long-term waste-handling issues for the hospital.

iii) *Chemical properties:* Different medical applications require very different chemical properties. Noble gases are well suited to be inhaled and exhaled for lung ventilation studies but they cannot form stable bonds to biomolecules that are required for many other applications. Halogens can relatively easily form such bonds, but they may suffer in vivo from dehalogenation, i.e. a breaking of the bonds. Radiometals (group 7, trivalent, etc.) coupled to an appropriate molecule find a wide range of applications. Free, unlabelled alkaline earth metals and rare earth metals act as bone seekers.

iv) *Ease of large scale production:* There may be isotopes that fulfill perfectly the first three conditions but that are difficult to be produced at the required quality in large scale. Under these circumstances they may still be used in smaller quantities for laboratory experiments, e.g. to understand and optimise the mechanism of new radiopharmaceuticals, while a more conventional radioisotope is applied clinically.

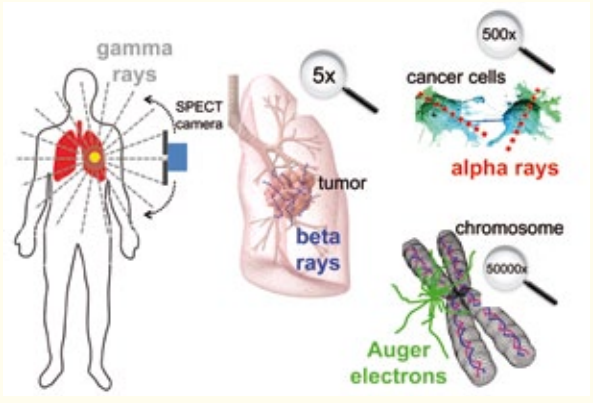

Figure 1.1. The alphabet of ionising radiation, with ranges varying from nanometres to decimetres in the human body.

1.1 Radioisotopes for imaging

1.1.1 Scintigraphy and SPECT

Gamma cameras for the 2D imaging method scintigraphy and the corresponding 3D method SPECT (single photon emission computed tomography) detect gamma rays or X-rays that are sufficiently energetic to leave the patient's body without excessive attenuation. Thus photon energies above 70 keV are suited for humans, while for imaging in small animals that is often used for (radio-)pharmaceutical development lower energies (down to 30 keV) may suffice. Gamma cameras and SPECT detectors rely on collimation to achieve position resolution. This imposes a high energy limit for the used photons, or else the collimators would become less efficient or too thick, reducing resolution or overall detection efficiency respectively. Figure 1.2 demonstrates in simplified form that photons between 100 and 200 keV are ideal for gamma cameras and SPECT. Table 1.1 shows an overview of the radioisotopes most frequently used for imaging with gamma cameras or SPECT.

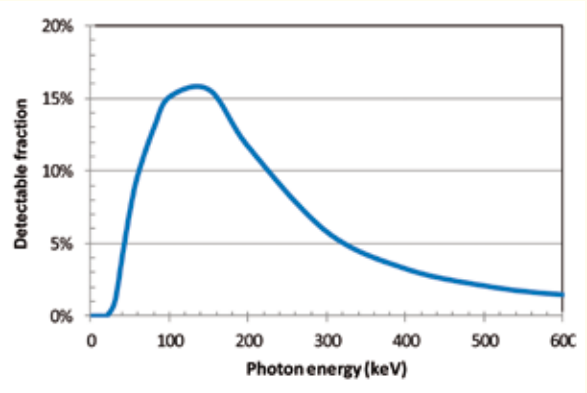

Figure 1.2. Product of transmission through 10 cm soft tissue and 0.2 cm aluminium (detector encapsulation) and photopeak efficiency in a 1 cm thick NaI crystal as function of photon energy.

^{99m}Tc

It happens that there is one isotope that fulfils well the optimisation criteria discussed above for a large variety of applications: the isomer ^{99m}Tc. It emits gamma rays of 141 keV, close to the ideal energy for SPECT. It decays by an internal transition to ^{99g}Tc ($T_{1/2}$=0.2 million years) that is so long-lived that it can be regarded as stable for practical purposes. No beta radiation is emitted. The 6 hour half-life makes it suitable even for more complex chemical labelling procedures. Most importantly, it is easily available from ^{99}Mo/^{99m}Tc generators (see below).

Given these favourable properties of ^{99m}Tc, over time a multitude of technetium compounds has been developed for a large variety of nuclear medicine applications:

- ^{99m}Tc-phosphates and diphosphonates (e.g. MDP: methylene diphosphonate) are used for bone imaging, mainly to detect bone metastases from prostate or breast cancer. Bone mineral consists of carbonated hydroxyapatite, i.e. mainly calcium and phosphate. Consequently bone building cells show high uptake of phosphates and bone metastases lead usually to a strong enhancement of the uptake in their surroundings. Consequently ^{99m}Tc-MDP will enrich close to bone metastases and make them visible by planar scans with gamma cameras. For observation of small lesions the SPECT technique provides better resolution, see Figure 1.3.
- ^{99m}Tc-sestamibi and ^{99m}Tc-tetrofosmin are used to measure myocardial blood flow during a stress test and at rest, allowing diagnosis of myocardial infarcts and coronary artery disease.

Table 1.1. Isotopes typically used for SPECT imaging. IT stands for internal transition from an isomer, EC for electron capture and β^- for beta-minus decay. I_γ gives the number of emitted gamma rays or X rays relative to the total number of decays. ^{131}I and ^{177}Lu are therapeutic isotopes but also emit gamma rays that allow monitoring of the in vivo distribution.

Radio-nuclide	Half-life (h)	Eγ (keV)	I_γ (%)	Decay type
Ga-67	78	93 185	42 21	EC
Kr-81m	0.004	190	64	IT
Tc-99m	6	141	89	IT
In-111	67	171 245	91 94	EC
I-123	13	159	83	EC
Xe-133	126	81	38	β^-
Tl-201	73	70 167	59 10	EC
I-131	192	364	82	β^-
Lu-177	161	113 208	6 10	β^-

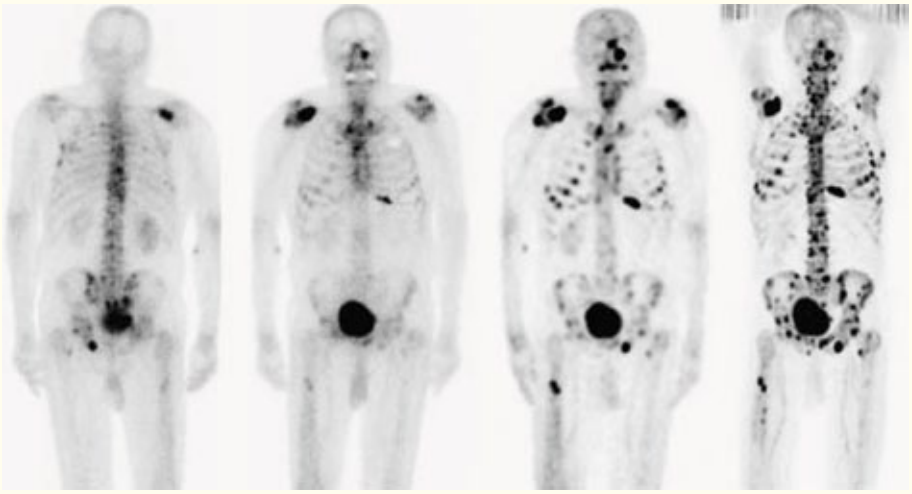

Figure 1.3. Bone metastases observed after injection of ^{99m}Tc-MDP on a planar scan (left) and a SPECT image (middle) compared to a ^{18}F-fluoride PET image (right). Reprinted by permission of SNMMI from Even-Sapir E *et al.*, *J Nucl Med* 2006; **47**: 287. Figure 1.

- $^{99m}TcO_4^-$ (pertechnetate) behaves similarly to iodide anions, i.e. it will enrich in the thyroid and is used for thyroid imaging to detect thyroid cancer or other thyroid malfunctions.
- Various ^{99m}Tc compounds (DMSA, DTPA or MAG3) allow assessment of kidney function.
- ^{99m}Tc-MAA (macro aggregated albumin) are aggregates used for lung perfusion studies to detect pulmonary embolism.
- Technegas consists of ^{99m}Tc attached to carbon aerosols. These can be inhaled and exhaled and serve for lung ventilation studies.
- ^{99m}Tc is also used for labelling of leukocytes to detect sites of infection or inflammation, e.g. in cases of fever of unknown origin.
- Additional ^{99m}Tc compounds are in clinical use or under development for a variety of applications.

Today the second-most universal SPECT isotope is ^{123}I: As iodide it is ideal for thyroid uptake measurements and for thyroid imaging as an alternative to ^{99m}Tc-pertechnetate. ^{123}I-ioflupane is a cocaine analogue with high affinity to the dopamine transporter used in brain imaging for diagnosis of Parkinson's disease. ^{123}I-iodohippurate serves for renal function measurement and renal imaging and ^{123}I-MIBG (m-iodobenzylguanidine) for detection of neuroblastoma and adrenal gland tumours.

^{133}Xe and generator-produced ^{81m}Kr are alternatives to Technegas for lung ventilation studies. Here the beta-minus emission of ^{133}Xe does not cause major radiation dose due to relative rapid exhalation.

^{201}Tl can be used for myocardial imaging as an alternative to ^{99m}Tc-MIBI but the attenuation corrections are higher (see Figure 2), leading to lower quality images, and due to the longer half-life the radiation dose is higher too.

Free gallium ions behave iron-like in the human body and are bound in areas of rapid cell division (tumours) and inflammation sites. Thus gallium scans (with ^{67}Ga) or indium scans (where ^{111}In is labelled to removed leukocytes, then reinjected) are used to localise inflammation sites. Labelled to a suitable peptide (e.g. octreotide) ^{111}In also serves for peptide receptor detection [Mae11].

The in vivo distribution of some therapeutic isotopes such as ^{131}I or ^{177}Lu can also be monitored by gamma cameras. In addition to these clinically used isotopes some other SPECT isotopes are used for R&D applications. Often the prime selection criterion is their chemical property, e.g. to study the in vivo behaviour of a given chemical compound or as complementary imaging isotope belonging to the same chemical element as a promising therapeutic isotope.

The administration of elements like gallium or thallium might appear surprising at first glance since these elements are known to be toxic in macroscopic amounts. However, one has to realise that while the activities used are in the range of tens to hundreds of MBq, this corresponds just to trace quantities of few nanograms, i.e. many orders of magnitude below levels where chemical toxicity would appear. It is the extreme sensitivity of nuclear detection techniques that assures safe use of such a large variety of substances and many could not be used with non-nuclear techniques in larger concentrations.

1.1.2 Positron emitters for PET

Desirable properties of positron emitters for PET are high branching ratio for positron emission ($BR_{\beta+}$), no or low emission of gamma rays, limited positron energy to assure stopping and annihilation close to the point of emission, as well as suitable half-life and chemical properties for the application in question (Table 1.2 and Table 1.3).

Similarly to ^{99m}Tc for SPECT, here these conditions converge for many applications of one isotope: ^{18}F. It has $BR_{\beta+} = 99.8\%$ with a short average range in water of only 0.6 mm. Fluoride can be rapidly

Table 1.2. Common short-lived PET isotopes and their average positron range in water. $I_{\beta+}$ gives the number of emitted positrons relative to the total number of decays.

Radio-nuclide	Half-life (h)	$BR_{\beta+}$ (%)	E_{mean} (MeV)	Range (mm)
C-11	0.34	99.8	0.39	1.1
N-13	0.17	99.8	0.49	1.5
O-15	0.03	99.9	0.74	2.4
F-18	1.83	96.7	0.25	0.6
Ga-68	1.13	89.1	0.83	2.8
Rb-82	0.02	95.4	1.48	5.4

and stably linked to many organic compounds, e.g. by replacing OH^- groups. Low projectile energies are sufficient for production, enabling use of compact accelerators for in situ production (see below). On the other hand the ease of producing larger quantities of ^{18}F at medical cyclotrons allows compensation for a certain amount of decay losses during transport, thus permitting delivery to more remote locations (many hours transport time, compared to 1.8 h half-life).

By far the dominant ^{18}F compound in clinical use is FDG (fluorodeoxyglucose). It is a modified glucose that is taken up in cells after phosphorylation but cannot be metabolised. Thus it stays trapped in the cell sufficiently long to enable PET imaging. Many malignancies show an enhanced glucose metabolism and are therefore detected in a FDG scan. In addition FDG may detect infection sites and can be used for glucose metabolism studies in the brain.

Injected as simple fluoride salt (NaF) solution, the fluoride anions are bone-seeking, making them a PET alternative to ^{99m}Tc-bone scans (see Figure 1.3).

^{18}F-labelled fluorothymidine (FLT) serves as marker for cell proliferation. It is accumulated in cancer cells that are rapidly proliferating and which therefore generate new DNA that includes thymidine as one of the nucleosides. PET scans with FLT can serve for very early validation of response to therapies or to adapt the therapy accordingly.

Many more ^{18}F compounds have been developed or are under development. They are used in oncology as alternatives to FDG for imaging of specific cancers or for apoptosis imaging to follow therapeutic progress of cancer treatment. Several compounds allow for beta-amyloid plaque imaging for the detection of Alzheimer's disease.

^{11}C is short-lived ($T_{1/2}$=20 min) which makes its processing more challenging but it can be labelled to a variety of organic molecules. Various ^{11}C compounds are available for brain imaging of neuroreceptors in a variety of neurological and psychiatric diseases.

^{15}O ($T_{1/2}$ = 2 min) and ^{13}N ($T_{1/2}$ = 10 min) are very short-lived and are used as simple compounds (^{15}O-water or ^{13}N-ammonia respectively) for myocardial perfusion studies as PET alternatives to ^{99m}Tc or ^{201}Tl. Production has to be located very close to the PET scanner.

Still shorter-lived ^{82}Rb ($T_{1/2}$ = 75 seconds), obtained from a $^{82}Sr/^{82}Rb$ generator and injected as simple Rb^+ cation, is another alternative for cardiac imaging. In heart perfusion studies it showed improved specificity and accuracy compared to the usual SPECT isotopes and minimises, due to its short half-life, radiation exposure to the patient. Thus this isotope is extremely promising, but at present demand outpaces ^{82}Sr production capacities.

^{68}Ga ($T_{1/2}$ = 68 min), obtained conveniently from a long-lived ^{68}Ge generator, is increasingly used and is predicted to become the "^{99m}Tc equivalent for PET". As a small trivalent ion it can be stably labelled to many biomolecules by using macrocyclic chelators. At present it is the main PET isotope used for peptide receptor imaging. Fixed to carbon aerosols as "Galligas" it allows lung ventilation studies with PET, as an alternative to the corresponding SPECT tracers.

Not all applications can be covered with short-lived isotopes. Larger biomolecules such as antibodies or antibody fragments show relatively slow biokinetics of the order of many hours to days. Consequently longer-lived PET isotopes are required to follow the uptake dynamically or to perform imaging once the optimum uptake has been reached.

At present ^{64}Cu, ^{89}Zr and ^{124}I are the preferred isotopes to be coupled to antibodies for immuno-PET while ^{44}Sc is well suited for mid-sized molecules such as peptides.

Copper is special since it has two redox states (I and II) with a transition potential very close to the difference between hypoxic versus norm-oxic tissue regions. Certain tumours may become hypoxic, i.e. show lower oxygen concentrations than usual. This is often associated with more aggressive types of cancer and with a higher resistance of cancer

Table 1.3. Overview of longer-lived PET isotopes.

Radio-nuclide	Half-life (h)	$BR_{\beta+}$ (%)	E_{mean} (MeV)	Range (mm)
Sc-44	3.97	94.3	0.63	2.0
Cu-64	12.7	17.6	0.28	0.7
Br-76	16.2	55	1.18	4.7
Y-86	14.7	31.9	0.66	2.1
Zr-89	78.4	22.7	0.40	1.1
I-124	100	22.8	0.82	2.9

cells against treatment by radiation since the so-called oxygen enhancement effect is reduced [see Hadrontherapy, Chapter 7.2]. For optimum treatment planning it is therefore necessary to identify such hypoxic areas. Cu-II bound in the compound ATSM (diacetyl-bis(N4)-methylthiosemicarbazone) reaching hypoxic regions may be reduced to Cu-I upon which it leaves the compound and stays internalised in the cell. Consequently the higher concentration of the respective Cu positron emitter makes hypoxic regions visible. Copper has four diagnostic PET emitters with different half-lives: ^{60}Cu ($T_{1/2}$=24 min), ^{61}Cu ($T_{1/2}$=3.3 h), ^{62}Cu ($T_{1/2}$=9.7 min) and ^{64}Cu ($T_{1/2}$=12.7 h). The shorter-lived ones are also useful to measure myocardial and renal perfusion.

The Q-value for β^+ decay affects inversely the half-life and the branching ratio for positron emission versus competing electron capture decay. Hence, most positron emitters have either long half-lives ($T_{1/2}$) *or* abundant positron emission probability ($BR_{\beta+}$) but not both. A way around the unfavourable relation between $T_{1/2}$ and $BR_{\beta+}$ are in vivo generators where a longer-lived nuclide decays to a shorter-lived positron emitter with strong positron emission: ^{44m}Sc ($T_{1/2}$ = 2.4 d) → ^{44}Sc ($BR_{\beta+}$ = 94%), ^{134}Ce ($T_{1/2}$ = 3.2 d) → ^{134}La ($BR_{\beta+}$ = 64%) and ^{140}Nd ($T_{1/2}$ = 3.4 d) → ^{140}Pr ($BR_{\beta+}$ = 51%). One can thus combine the favourable half-life of the mother with the high positron branching ratio of the daughter, provided that the daughter nucleus remains after the decay of the mother nucleus in the targeting compound or the targeted region, respectively.

It is interesting to note that even one neutron-rich isotope can be detected by PET! A tiny fraction of the beta-minus decay of the therapeutic isotope ^{90}Y proceeds via an excited 0^+ state, that decays partially via internal e^-e^+ pair creation, thus leading to the emission of 3×10^{-5} positrons per decay, just enough for PET imaging of therapeutic ^{90}Y activities (~GBq) (see Figure 1.4).

In some isotopes (see Table 1.4) positron emission is accompanied by prompt gamma ray emission. Abundant emission of energetic gammas is usually a drawback since this "useless" radiation increases the radiation burden to the patient, the shielding requirements for transport and handling and may induce background in the imaging. Mainly due to

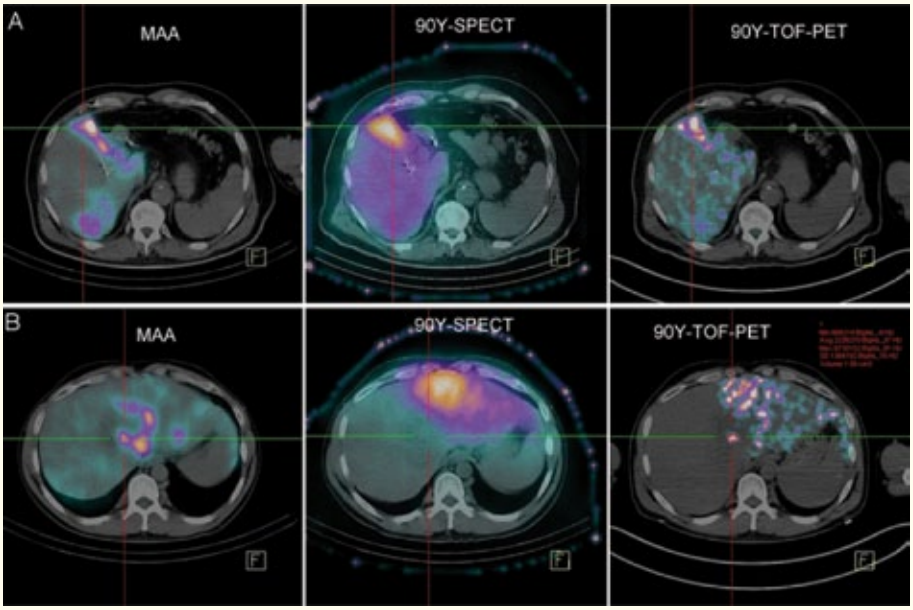

Figure 1.4. Different imaging techniques at the example of two patients (A on top, B on bottom) that were treated with ^{90}Y microspheres for radioembolisation of hepatic tumours. The left image shows ^{99m}Tc-MAA prior to treatment, the middle image ^{90}Y-Bremsstrahlung-SPECT and the right ^{90}Y-TOF-PET. The images were taken from Figure 7 of Th. Carlier *et al.*, *EJNMMI Research* 2013; **3**: 11 (Springer Open Access Licence, Creative Commons Attribution Licence).

Table 1.4. $BR_{\beta+\gamma}$ gives the number of positrons emitted together with gamma rays relative to the total number of decays.

Radio-nuclide	Half-life (h)	$BR_{\beta+\gamma}$ (%)	E_{mean} (MeV)	Range (mm)	Eγ (keV)	I_γ (%)
Cl-34m	0.53	54.3	0.84	2.8	2127	43
Sc-44	3.97	94.3	0.63	2.0	1157	100
Mn-52	134	29.6	0.24	0.6	744 936 1434	91 95 100
Y-86	14.7	31.9	0.66	2.1	628 1077 1153	33 83 31
Tc-94	4.9	10.5	0.36	1.0	703 850 871	100 96 100
Tc-94m	0.87	70.2	1.07	3.7	871	94
I-124	100	12	0.82	2.1	603	61
Tb-152	17.5	12	1.08	3.5	344	65

these drawbacks, none of these isotopes is much used at present.

3-photon-cameras (also called γ-PET) are under development (see Chapter 2, Imaging, section 3.4.) that will be capable of detecting the gamma ray in coincidence with the two 511 keV annihilation gammas. Every event can then provide 3D information of the localisation, i.e. many fewer events are required for full 3D mapping compared to intersecting "lines of response" in usual PET. Correspondingly imaging becomes possible with much lower activities, effectively reducing the dose to the patient. Prospects for routine availability of 3-photon-cameras in clinics will be determine the long-term fate of these promising PET isotopes. It should be stressed that most of these isotopes are of high interest for clinical applications since established synthesis and labelling methods exist for radiopharmaceuticals of these elements (technetium, iodine, trivalent metals) and several of these isotopes could serve as imaging isotopes in a "matched pair" of the theranostics approach (see below): ^{44}Sc, ^{86}Y, ^{124}I, ^{152}Tb.

1.2 Radioisotopes for therapy

1.2.1 Gamma emitters

Gamma emitters may be used for external beam radiation therapy (EBRT). Intense collimated gamma ray sources of ^{60}Co, ^{137}Cs or ^{192}Ir are used for this purpose. Today this technique is mainly applied in emerging countries where the alternative electron accelerators providing Bremsstrahlung are less widespread.

Sealed radioactive sources can be used in or close to the body, for example close to a tumour, for a "loco-regional" treatment dubbed "brachytherapy". A certain dose can be applied either by brief exposure to intense sources (HDR, high dose rate) or long exposure to weaker sources (LDR, low dose rate).

In HDR brachytherapy the required dose is given in a short time (minutes) by a very intense source (for example 370 GBq of ^{192}Ir). After positioning an applicator, the source is rapidly introduced from a shielded storage position to the selected position via a catheter ("afterloader"), then pulled back into the storage position. Very compact sources (e.g. metal disks or wires containing ^{60}Co, ^{153}Gd, ^{169}Yb or ^{192}Ir) are required for this application.

In LDR brachytherapy the source remains for days or weeks or even permanently in the body. Short-range radiation (X-rays, low-energy gamma rays and beta particles) is preferred to minimise unnecessary dose outside of the treatment area. Longer-lived isotopes such as ^{103}Pd, ^{125}I, ^{131}Cs or the beta emitter ^{32}P are fixed in form of "seeds" (needles) or "stents" (tubes) or specially shaped applicators. Seeds are frequently used for treatment of prostate cancer; radioactive stents may prevent restenosis (repeated clogging of arteries).

Treatment of primary and metastatic liver cancer by SIRT, a variant of brachytherapy, is rapidly gaining clinical importance. SIRT stands for "selective internal radioembolisation therapy". Liver metastases are mainly supplied via the hepatic artery while normal liver cells are mainly supplied by the portal venous blood. Thus one can block the supply line of the cancer by radioembolisation. Here either small radioactive spheres containing either the high energy beta emitter ^{90}Y (TheraSphere or SIR-Spheres respectively) or the beta- and gamma emitter ^{166}Ho or colloids (lipiodol) containing one

of the beta emitters ^{188}Re, ^{131}I or ^{90}Y are injected via a catheter into the hepatic artery that is supplying the cancer (Figure 1.5). The microscopic radiation sources are then preferentially delivered to the well-perfused cancer and will irradiate it selectively.

Daily use of antimatter

Antimatter is nowadays familiar to many people thanks to its central role as powerful weapon in science fiction films and novels such as "Angels and Demons". Less known is the fact that antimatter is actually used daily in the bodies of thousands of patients to display cancer and other illnesses via PET imaging. In this regard, antimatter-emitting radionuclides might be thought of as the "angel" that helps to defeat the "demon" that is cancer.

1.2.2 Beta emitters

In HDR brachytherapy the high energy beta emitter ^{188}Re is used alternatively to low energy gamma ray emitters. ^{188}Re is applied in liquid form at high activity concentration to inflate balloon catheters placed into arteries to prevent restenosis. Lower activities of ^{188}Re are applied as "cream" to treat non-melanoma skin cancer.

Radiosynoviorthesis (or radiation synovectomy) makes use of the intra-articular injection of colloids containing radioisotopes to treat severe inflammations (e.g. arthritis) of the flexible joints. Pure beta emitters without gamma ray emission (or with weak gamma ray emission) are employed where the beta energy is adapted to the size of the joint: ^{90}Y with higher beta energies for large joints like the hip or the knee, ^{186}Re with medium beta energies for mid-sized joints like the elbow and ^{169}Er for small joints in the fingers.

While the therapies discussed so far are so-called *loco-regional*, i.e. the radioisotope or compound is simply injected into the right place, we come now to *systemic therapies*, where a radiopharmaceutical is administered orally or injected intravenously or intraarterially, from where it will be distributed throughout the body (i.e. to the whole "system") and locally enriched by various mechanisms.

The first targeting mechanism exploited was *metabolic targeting* of thyroid cells. These are characterised by an enhanced iodine uptake and can be targeted by ^{123}I or ^{124}I for diagnostic purposes or by ^{131}I for therapy. Often thyroid cancer cells maintain their affinity to iodine, even when growing as metastases elsewhere. Thus high ^{131}I activities are used to treat even metastatic thyroid cancer. Also in certain forms of "benign" thyroid diseases such as thyrotoxicosis and goitre (Graves' and Plummer's disease), ^{131}I is used for ablation of excess tissue.

^{131}I-MIBG is a molecule used for metabolic targeting of neuroblastoma. Good therapeutic response has been observed as a first line therapy or combined with other therapy modalities.

Many cancers (prostate cancer, breast cancer, etc.) frequently develop in a later stage painful bone metastases. Compared to normal, slowly growing bone, the bone metastases often show an enhanced metabolism of calcium and phosphates. This can be exploited to target them with bone-seeking radioisotopes. Chemical homologues of calcium, such as ^{89}Sr or ^{223}Ra, as well as phosphates or bisphosphonates carrying ^{32}P or stable complexes of radioactive metals (^{117m}Sn, ^{153}Sm, ^{186}Re, ^{188}Re) show an enhanced uptake in the bone metastases and are used for palliative therapy [Lew05].

For targeted therapy of tumours such as PRRT (peptide receptor radionuclide therapy) or RIT (radioimmunotherapy) today mainly the isotopes ^{90}Y, ^{131}I and ^{177}Lu are used; others are under evaluation. These isotopes differ in beta range (see Table 1.5) and their (bio-)chemical properties. ^{131}I shows abundant emission of hard gamma rays requiring more shielding and often an isolation of the patients during treatment. Therefore for applications other than thyroid treatments today radiometals are preferred when these can be labelled to the vectors.

Beta particles have low linear energy transfer (<1 keV/µm), therefore usually many "hits" are required to induce apoptosis of a cancer cell. In larger metastases with uneven perfusion not every cell can be directly reached by the injected radiopharmaceuticals. Hence, the "cross-fire effect" from beta emission in neighbouring directly targeted cells helps to achieve a more evenly distributed dose. On the other hand, shorter-range betas cause less cross-fire to adjacent healthy cells. Thus, depending on the average size and perfusion of metastases beta emitters with lower or higher energy, or mixtures of both, are preferred. Very large metastases are clearly better targeted by non-nuclear medicine methods (surgery or EBRT). In the past new therapies such as RIT had to make their first demonstration of effectiveness in clinical trials with patients for which first line therapies had failed. Consequently the patients often showed advanced stages of disease with larger metastases. Still, RIT with Zevalin (^{90}Y-ibritumomab), Bexxar (^{131}I-tositumomab), ^{131}I-rituximab and ^{177}Lu-rituximab showed excellent results in therapy of lymphoma, while gastro-entero-pancreatic neuroendocrine tumours (GEP-NET) are successfully treated with PRRT using the

Table 1.5. Typical beta-emitting isotopes used for therapeutic applications with mean and maximum beta energies and ranges in water. Major gamma rays (>5% abundance) are given.

Radio-nuclide	Half-life (d)	E_{mean} (MeV)	E_{max} (MeV)	Range max (mm)	E_γ (keV)	I_γ (%)
P-32	14.3	0.7	1.71	8		-
Sr-89	50.6	0.59	1.5	7		-
Y-90	2.7	0.93	2.28	11		-
I-131	8.0	0.18	0.81	3.3	284 364 637	6 82 7
Sm-153	1.9	0.22	0.81	3.3	103	29
Ho-166	1.1	0.67	1.85	9	81	7
Lu-177	6.7	0.13	0.50	1.7	113 208	6 10
Er-169	9.4	0.10	0.35	1.0		-
Re-186	3.7	0.35	1.07	4.6	137	9
Re-188	0.7	0.76	2.12	10	155	16

radiolabelled somatostatin-analogues ^{90}Y-/^{177}Lu-DOTA-TOC and ^{90}Y-/^{177}Lu-DOTA-TATE. Thus, today radionuclide therapies are increasingly recognised as the optimum form of therapy for several indications (Figure 1.5). Correspondingly PRRT and RIT can now be extended to patients at earlier stages with smaller metastases or even as prophylactic treatment preventing the proliferation of individual cancer cells that might be released during surgical removal of a tumour. For such applications short-range radiation is preferred. This explains the present trend towards low-energy beta emitters (^{177}Lu) or even shorter-range alpha emitters (see below).

^{131}I, the useful devil

The isotope ^{131}I dominates the short-term radiotoxicity of fission products. Following the reactor accident in Chernobyl an increase of 16000 thyroid cancer cases and 25000 other cancers is expected in Europe until 2065, i.e. within 80 years from the accident [Car06]. On the other hand the very same isotope is extremely useful in treating thyroid cancer and hyperthyroidism. Patients with thyroid problems profit from ≈800 000 treatments with ^{131}I worldwide every year [UNSCEAR2008].

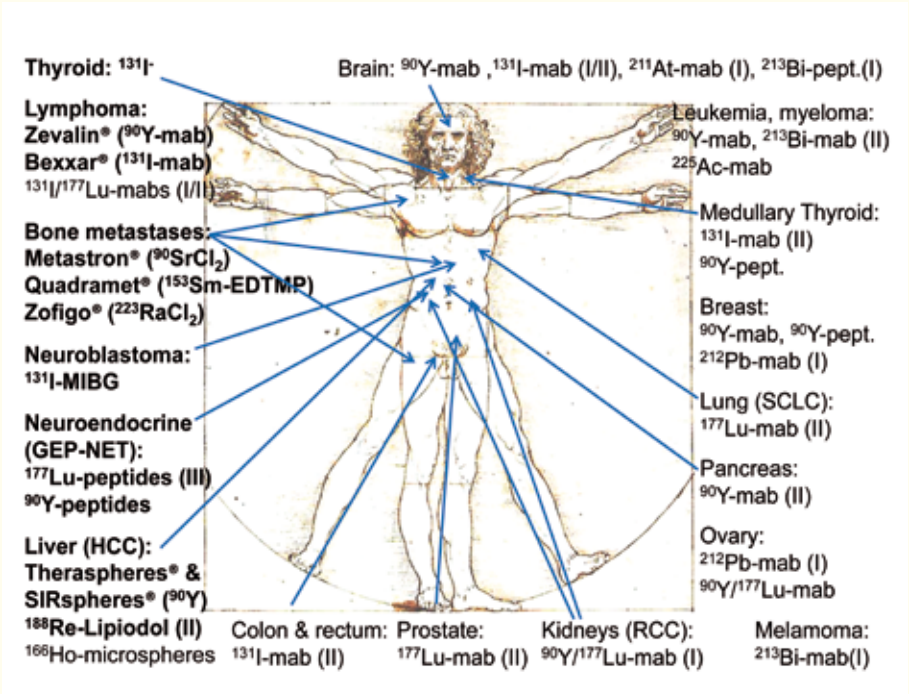

Figure 1.5. Therapeutic radiopharmaceuticals in clinical use or clinical trials (phase I, II or III in parentheses). Radiopharmaceuticals that were already used for many hundreds or thousands of patients are marked in bold.

1.2.3 Alpha emitters

The therapeutic potential of alpha particles has long been recognised. The availability of naturally occurring or artificially produced alpha emitting radionuclides greatly facilitates attempts to implement this modality in the treatment of cancer and other diseases (Figure 1.5). For the relevant range of alpha particle energies (4–9 MeV) the linear energy transfer (LET) is of the order of 100 keV per micron. This high LET value is responsible for the intense damage that alpha radiation produces in both healthy and malignant cells. However, it also implies that their range in biological tissue is limited to less than 0.1mm. In this section we describe the various therapeutic approaches consistent with this range limitation as well as attempts to overcome it and to considerably increase the scope of treatable malignancies.

The main mechanism of cell inactivation by alpha particles is the high concentration of double strand breaks induced to the DNA of the cell. In fact, in most cases no more than a few alpha particles passing through the nucleus are enough to permanently inactivate it. Like all high LET radiations the biological effect of alpha particles does not require the action of free radicals. Thus, it is not dependent on the oxygenation state of the cell (as oxygen plays a crucial role in mediating free radical damage). Hypoxic cells, found in poorly perfused regions in solid tumours, are nearly as sensitive to alpha radiation as cells with normal oxygen levels. This is in marked contrast to low-LET radiation (electrons and photons) for which the dose required for the inactivation of hypoxic cells may be larger by a factor of 2–3 compared to that required to inactivate well oxygenated ones. Unlike low-LET radiation whose biological effectiveness is highly dependent on the dose rate, the effect of alpha particles is nearly independent of the rate of dose delivery. In addition, the biological effectiveness of alpha particles is significantly less dependent on the age of the cell in the mitotic cell cycle, than that of low-LET radiation. Finally, the type of DNA damage caused by alpha particles is less amenable to the available DNA repair mechanisms.

Quantitative investigation of the effects of alpha particle irradiation on cancer cells (as well as on living cells in general) is perforce done by in vitro experimentation. One of the simplest and most direct methods in use is clonogenic assay. A monolayer of cells seeded and grown on an appropriate substrate is subjected to a known flux of alpha particles. Following the irradiation the cells are removed and seeded again in a highly diluted concentration. Those cells that have survived and retained the ability to unlimited reproduction form colonies (a colony is defined as consisting of at least 50 cells), providing a direct measure of the survival probability. The relationship between the surviving fraction SF and the applied dose D is found to be well represented by an exponential function $SF = \exp(-D/D_0)$, where D_0 is a phenomenological parameter characteristic of the cell line involved. It is referred to as the mean lethal dose and its magnitude is typically around 1 Gy. Note, that for low LET radiation, such as photons and electrons, the corresponding dependence is more complex, involving a quadratic term of D in the exponential. This is a consequence of the nature by which damage incurred to the cell nucleus leads to its death.

The mean lethal dose translates to a rather small number of alpha particle hits per cell. Since the number of hits per cell obeys a Poisson distribution, the averaging procedure combines cells with varying numbers of hits, including a fraction of cells not hit at all. It is therefore interesting to be able to observe the effect on cells hit by a precise, well defined number of alpha particles. This can be achieved by microbeam facilities (see Chapter 1 Hadrontherapy, section 3.3).

One of the oldest medical applications using alpha emitters dates back to the beginning of the twentieth century. Rheumatoid diseases (such as arthritis) were treated by exposing patients to the 3.8 day half-life radon gas (^{222}Rn). This was done either by bathing for about 20 minutes in a water bath with a radon concentration of 0.3–3 kBq per litre, or by exposure in caves or in man-made galleries containing about 30–150 kBq of radon per cubic metre of air. A large number of controlled clinical trials have established the long-term anti-inflammatory effect of this treatment. It is, in fact, still practised in central Europe rather widely despite warnings by medical and regulatory bodies of the long term carcinogenic danger involved.

Another long and extensive therapeutic use of alpha emitters was the treatment of ankylos-

From waste to cancer treatment

^{212}Pb is a promising isotope for targeted alpha therapy (via its alpha emitting daughter ^{212}Bi) and an example of a radioisotope extracted from naturally occurring minerals, and thus not requiring artificial transmutation. In 2013 AREVA opened a dedicated facility in Limoges (France) to extract ^{212}Pb from stocks of ^{232}Th "waste" for medical purposes and a clinical trial is ongoing to use this ^{212}Pb for treatment of intra-abdominal cancers.

ing spondylitis (AS), a chronic and debilitating inflammatory rheumatic disease, by ^{224}Ra-chloride injection. ^{224}Ra is an alpha emitter whose half-life is 3.66 days and is produced by the decay of its parent ^{228}Th (1.91 years half-life). It had been in use in Germany from 1948 until 2006. Radium, characterised by its calcium-like chemistry, has a tendency to concentrate in the bones, where the sequence of alpha decays slows down the process of skeletal deformation and alleviates the pain which generally accompanies the condition. In a recent study only mild side effects were observed. It was concluded that the injection of ^{224}Ra is an effective and safe treatment for AS.

Radium: diffusion makes the difference

Medical applications of radium radioisotopes were investigated as soon as the new element was discovered. For decades ampoules with long-lived ^{226}Ra and its decay chain were an important radiation source for medicine. Later ^{224}Ra was explored for targeted alpha therapy in bones but it was recognised that due to diffusion of the ^{220}Rn daughter (half-life of 55 seconds) part of the alpha decay chain was translocated elsewhere, reducing the selectivity of targeting. When switching from ^{224}Ra to neighbouring ^{223}Ra, the corresponding daughter ^{219}Rn is more short-lived (4 seconds half-life) and nuclear chemists at Oslo University demonstrated that most will decay before diffusing away. Based on successful clinical trials the radiopharmaceutical Xofigo ($^{223}RaCl_2$) was approved in the USA and Europe in 2013. It has great prospects for therapy of bone metastases.

The tendency of radium to concentrate in the bones is the basis for the development of a new radio-pharmaceutical, ^{223}Ra-chloride (Alpharadin/Xofigo), for the treatment of bone metastases of various cancers such as castration-resistant prostate cancer (CRPC), breast or lung cancers. The alpha emitter ^{223}Ra has a half-life of 11.4 days and is obtained from the decay of ^{227}Ac (21.8 years half-life) through its daughter ^{227}Th (18.7 days half-life). ^{223}Ra preferentially targets regions of new bone growth which are quite often centred around metastases. A series of preclinical studies on laboratory animals has established its basic targeting premise and provided input related to safety considerations and efficacy expectations needed for clinical trials. The first human clinical studies on CRPC patients not only confirmed the bone targeting of the pharmaceutical but also defined the safe dose range. In addition, some pain relief and survival prolongation amongst patients was noticed. Following initial positive indications a major phase III study was undertaken, enrolling over 900 CRPC patients whose selection was subject to strict acceptance criteria. An interim analysis of this trial (referred to as ALSYMPCA) revealed an increase of life expectancy in the ^{223}Ra-treated group which was later confirmed by an expanded follow-up: the median survival of the treated group was 14.9 months compared to 11.3 months in the placebo group [Par13]. In 2013 regulatory approval of the drug (brand name Xofigo) was obtained in the US and in Europe.

The radium therapies discussed so far are used for metabolic targeting of bone metastases, exploiting their enhanced uptake of calcium and chemical homologues. To target other types of cancer a more elaborate targeting strategy is required, namely use of targeting vectors, i.e. cancer-specific biomolecules that will carry an attached radioisotope as payload to its destination. Its realisation relies on monoclonal antibodies or peptides which preferentially seek the malignant cells. These "cell-seekers" are tagged with a therapeutic (or, for that matter, diagnostic) agent which acts on the targeted cell. This agent can be some variant of chemotherapy or radiotherapy or possibly some biologically active compound. The most natural choice for this type of application is tagging with radioactive isotopes. Amongst these, alpha emitters are the most potent and promising; in fact, the advantage of alpha emitters over gamma and beta emitters has been demonstrated in specially designed preclinical trials. This specific modality is referred to either as "targeted alpha therapy" (TAT) or "alpha radioimmunotherapy" (α-RIT) when antibodies are used as targeting vectors.

For such applications radium isotopes are not useful since they cannot be stably linked to the targeting vector. Instead other chemical elements such as terbium, astatine, bismuth, lead, etc. are required. See Table 1.6 for an overview of therapeutic alpha emitters.

An important feature of alpha decay is the significant recoil energy that the daughter nucleus experiences upon emission of an alpha particle: 100 to 160 keV for the cases shown in Table 1.6. This exceeds chemical binding energies by orders of magnitude and will usually result in a delabelling from the targeting vector. Hence, a large fraction of the daughter isotopes will be released and, depending on their lifetime, chemical properties and biochemical environment may move more or less far away from the primary target cell. Therefore the fate of these daughter activities is an issue to be considered.

Table 1.6. Overview of alpha emitters used in nuclear medicine. Isotopes decaying mainly by beta-decay are shown in slanted letters.

Radio-nuclide	Half-life	Daughters	Half-life	Cumulative α/decay	E_α mean (MeV)	Range (μm)
Tb-149	4.1 h			0.17	3.97	25
Pb-212	*10.6 h*	Bi-212 Po-212	1.01 h 0.3 μs	1	7.74	65
Bi-212	1.01 h	Po-212	0.3 μs	1	7.74	65
Bi-213	*0.76 h*	Po-213	4 μs	1	8.34	75
At-211	7.2 h	Po-211	0.5 s	1	6.78	55
Ra-223	11.4 d	Rn-219 Po-215 *Pb-211* Bi-211	4 s 1.8 ms *0.6 h* 130 s	4	6.59	>50
Ra-224	3.66 d	Rn-220 Po-216 *Pb-212* Bi-212	56 s 0.15 s *10.6 h* 1.01 h	4	6.62	>50
Ac-225	10.0 d	Fr-221 At-217 *Bi-213* Po-213	294 s 32 ms *0.76 h* 4 μs	4	6.88	>50
Th-227	18.7 d	Ra-223 Rn-219 Po-215 *Pb-211* Bi-211	11.4 d 4 s 1.8 ms *0.6 h* 130 s	5	6.45	>50
U-230	20.8 d	Th-226 Ra-222 Rn-218 Po-214	0.51 h 38 s 35 ms 0.16 ms	5	6.71	>50

In Table 1.6 one can observe two distinct classes of alpha emitters: the first comprises those decaying to a stable daughter or to radioisotopes that emit only beta or gamma rays. The latter give no radiologically significant dose, i.e. their uncontrolled release can be tolerated.

The second class decays to alpha emitting daughters, i.e. one mother decay result in a decay chain of 4 to 5 alphas until stable or radiologically insignificant daughters are reached. Very short-lived daughters (μs to ms) will decay locally before diffusing very far but longer-lived daughters (seconds to hours) might diffuse away. Depending on the application this unavoidable spread might be acceptable or not (see below). Strategies to control and limit the release of daughter nuclides by scavengers or by incorporating the primary nuclide into lipids or carbon nanotubes are under exploration.

The "single alpha" emitters do not have the problem of daughter activities but are mainly short-lived. Bismuth can be labelled with well-known chelating agents (e.g. DOTA), but both isotopes (^{212}Bi and ^{213}Bi) have short half-lives ($T_{1/2} \leq 1$ h). Therefore they have mainly been used in combination with peptides that have sufficiently quick uptake and with antibodies seeking blood cancer cells. More preclinical and clinical studies have been performed with ^{213}Bi since it is conveniently available from a ^{225}Ac/^{213}Bi generator.

Anti-CD33 antibody labelled with ^{213}Bi has shown a significant reduction of leukemic blast cells in AML patients [Jur02]. Other promising studies with ^{213}Bi labelled antibodies and peptides have been performed for treatment of leukaemia, melanoma, metastatic breast, ovarian and gastric cancer and even outside oncology, such as serious fungal, bacterial and even viral diseases [Dad09].

The drawback of the short half-life of ^{212}Bi might be overcome when using the beta-decaying ^{212}Pb as an "in vivo generator". A phase I clinical trial with ^{212}Pb-TCMC-Trastuzumab in patients with HER-2 positive intraperitoneal cancers is ongoing.

Another "longer-lived" alpha emitter is ^{211}At. The difficulty of its application resides more in its (bio-) chemistry. Astatine is a heavier homologue of the halogen iodine, but it is also close to the metalloids. For therapeutic applications it is essential to ensure a stable bond to the targeting vector to minimise in vivo delabelling. Efforts are ongoing to improve the understanding of astatine chemistry by experiments with trace quantities supported by computational chemistry [Cha11]. Interestingly, the ionisation potential of astatine, one of the fundamental atomic properties of an element, was only experimentally determined by laser spectroscopy with astatine iso-

topes produced at ISOLDE (CERN) [Rot13]. This value can now serve as experimental benchmark to support "in silico" design of astatine compounds for nuclear medicine applications.

^{211}At-labelled antibodies have been used clinically for treatment of brain cancer [Zal08]. Phase I trials for treatment of prostate cancer micrometastases and of neuroblastoma with ^{211}At labelled antibodies are under preparation.

Preclinically ^{211}At-labelled antibodies have been used against acute myeloid leukaemia as well as cancers of the ovary and intestine.

A particular case is ^{149}Tb (4.1 hours half-life). It is the only clinically useful alpha emitter below lead with the well-known chemical properties of a lanthanide. This can serve for direct comparison of the radiobiological effectiveness of alpha versus beta radiation (of ^{161}Tb or chemically similar ^{177}Lu). First preclinical studies have been reported [Bey04,Mue12] but so far this interesting isotope is only available at the ISOL facilities ISOLDE (CERN) and ISAC (TRIUMF).

Clinical trials employing ^{225}Ac-labelled antibodies (HuM195 and Lintuzumab) against leukaemia are ongoing; preclinically other types of cancer are being targeted with ^{225}Ac-labelled vectors. $^{227\text{Th}}$-labelled trastuzumab is being studied preclinically against breast and ovarian cancer and ^{230}U has been proposed as another long-lived alpha emitter.

Most of the research over the last decade has comprised preclinical experiments treating murine cell lines in mice and human derived cell lines in nude mice. While several clinical trials investigating the safety and efficacy of α-RIT show promising results in the treatment of malignancies characterised by isolated cells or microscopic cell clusters, such treatments generally fail against solid tumours. This is largely because of physical barriers which exist in solid tumours (such as the elevated interstitial fluid pressure) that preclude the efficient extravasation and the subsequent dispersion of the blood-borne targeting molecules inside the tumour. This in turn leads to a highly heterogeneous dose distribution with numerous "cold spots" in the tumour mass. While some of these barriers may be partially overcome by direct intra-tumoral injection of the targeting molecules, this option has yet to be validated by clinical trials.

A method that makes a virtue of the necessity to consider the diffusion of daughter isotopes to deliberately enhance the range of action in solid tumours has been proposed recently [Ara07]; it is termed diffusing alpha-emitters radiation therapy (DART) and it can be conceptually classified as a brachytherapy method. The basic idea is to treat tumours by intra-tumoral implantation of specially prepared radioactive sources of relatively low activity, which continually release short lived α-emitting atoms from their surface. As these atoms spread inside the tumour by the combined effects of interstitial diffusion and vascular convection, they deliver a well-localised high radiation dose through their α-decays, leading to massive tumour cell destruction. Since the α-emitters begin their journey in the intratumoral cellular space and no molecular targeting mechanism is involved, their subsequent distribution throughout the tumour may be expected to be less affected by the obstacles that hinder systemic α-RIT. Cell destruction must extend continuously over a few millimetres about the source (two orders of magnitude higher than the α-particle range in tissue) for DART to be therapeutically relevant. If this is the case, tumours may be treated by deploying a finite number of sources at a typical spacing of a few millimetres, similar to brachytherapy. In other words, DART overcomes the limitations imposed by the short range of α-radiation by introducing intermediate agents (the diffusing atoms) that take the α-particles' lethal energy away from the source.

The diffusing atoms are released from the source by recoil of a daughter atom during the α-decay of a parent isotope. Thus, the source consists of parent α-emitting atoms embedded closely below its surface, at a depth that prevents them from entering the tumour themselves, but allows considerable release of their recoiling daughters. To implement the idea, one uses the α-decay chain beginning with ^{228}Th (1.91 year half-life) that serves as a generator for the production of ^{224}Ra. The source – a thin conducting wire (0.3–0.5 mm diameter) carrying a small activity of ^{224}Ra embedded in the wire surface – is inserted through a fine-gauge needle into the tumour. Once inside the tumour and over a period determined by the ^{224}Ra half-life (3.66 days), the source releases, by recoil, ^{220}Rn (55.6 seconds half-life), ^{216}Po (0.15 second half-life) and ^{212}Pb (10.6 hours half-life) atoms, while the remaining atoms of ^{224}Ra stay below its surface. ^{220}Rn, a noble gas, diffuses in the extra- and intra-cellular space near the source with no chemical interactions, occasionally entering and leaving the porous network of tumoral blood vessels. It contributes two α-particles through its own decay and through that of its exceedingly short-lived daughter ^{216}Po, which disintegrates essentially at the same point. ^{212}Pb enters the tumour either by directly recoiling from the source or following the decay of ^{216}Po away from the source, giving rise to a third α-particle: it β-decays to ^{212}Bi (60.6 minutes half-life), which either α-decays to ^{208}Tl (3 minutes half-life) or β-decays to ^{212}Po (0.3 microseconds half-

life), which then α-decays to stable ^{208}Pb. Due to the relatively long half-life of ^{212}Pb its atoms travel to significant distances from the source and are partially taken out of the tumour by the blood. ^{212}Pb cleared from the tumour through the blood redistributes at low concentration throughout the body.

In a series of preclinical experiments on mice bearing both murine and human derived cell lines the basic premise of this approach was validated. The response of subcutaneously injected tumours in all mice models ranged from the slowing down of tumour growth to the complete cure of the animal. Considerable prolongation of life expectancy related to a decrease of the metastatic load in the lungs was also routinely observed. DART, whose implementation is technologically rather simple, is now poised for its first-in-man clinical trial. If successful, it may provide a low-cost and easily transportable additional mode of "high-LET brachytherapy".

1.2.4 Auger electron emitter

The logical progression of the increase in selectivity from beta to alpha emitters would be Auger electron emitters. Low-energy Auger electrons have a very short range of nm to µm and high linear energy transfer. If they are brought close to the cell's nucleus they may be extremely effective in inducing double strand breaks but they are rather harmless while outside of non-targeted cells. Thus the selectivity of very targeted delivery agents that will specifically internalise into cancer cells is maximised. Auger emitters such as ^{117m}Sn, ^{125}I, ^{161}Tb, ^{193m}Pt or ^{195m}Pt are very promising, but it is still challenging to find suitable internalising agents [Kas11].

Auger electron therapy, a long-term project

In 1927 (briefly after the discovery of Auger electrons) the radiation therapy pioneers Claudius Regaud and Antoine Lacassagne concluded: *"The ideal agent for cancer therapy would consist of heavy elements capable of emitting radiations of molecular dimensions, which could be administered to the organism and selectively fixed in the protoplasm of cells one seeks to destroy. While this is perhaps not impossible to achieve, the attempts so far have been unsuccessful."* After three generations of R&D in biotechnology, radiobiology and Auger emitter production methods, we are now closer than ever to finally realising this early dream.

1.3 Radiotracers for biokinetics and pharmaceutical R&D

Radioisotopes are not necessarily used solely for imaging or therapy, they may also serve as radiotracers for quantification of certain in vivo processes (metabolic activity, etc.) by external counting of samples (blood, urine, exhaled air). Here detection is very efficient and consequently activities administered in small amounts are sufficient. The isotopes ^{3}H, ^{14}C, ^{32}P, ^{45}Ca, ^{51}Cr, ^{57}Co, ^{59}Fe, ^{75}Se, etc. are used for this purpose.

In basic pharmaceutical R&D in addition to SPECT or PET studies with small animals, molecules marked with ^{3}H, ^{14}C or ^{32}P are also frequently used for radiotracer studies in cell colonies or small animals. For example the ground-breaking work on key regulators of the cell cycle that was rewarded the Nobel prize in physiology and medicine in 2001 is largely based on radioassay techniques employing ^{31}P.

2. Production methods and facilities

2.1 Nuclear reactions

A large diversity of nuclear reactions can be used for radioisotope production. For a comparison of different methods one has to consider not only the producible quantity, but two additional properties that are essential for nuclear medicine applications:

a) The specific activity

The specific activity of a radioisotope, usually expressed in units of GBq/mg or Ci/mg, is a measure of the activity per mass. A given amount of pure shorter-lived isotopes has obviously a higher activity than the same amount of longer-lived isotopes. However, for practical purposes one has to consider that the radioisotopes are often "diluted" by admixtures of stable ("cold") isotopes of the same element that have no therapeutic effect. For metabolic targeting of thyroid or bone metastases very high specific activity is not required. Instead the radioisotope is often diluted on purpose to avoid an atypical in vivo behaviour of ultratrace quantities.

On the other hand for tumour cell types that have only few selective sites (peptide receptors or antigens respectively) it is crucial to use radioisotopes with very high specific activity. Else the selective sites would be blocked with tumour-seeking agents carrying cold isotopes that have no therapeutic effect.

Pure radioisotopes are called "carrier-free" and radioisotopes accompanied by a lot of stable isotopes are called "carrier-added" (c.a.).

In the tables, in addition to the usual unit GBq/mg, we also give R as the atomic ratio of radioactive isotopes over all (radioactive plus stable) isotopes.

Depending on the use, not only stable isotopes of the same element may be interfering but also those of chemically similar elements (e.g. other lanthanides) or other elements (e.g. iron) that interfere in the labelling process. Therefore one often defines as "effective specific activity" the ratio of activity over the mass of all interfering elements.

b) Radioisotopic purity

While specific activity is a measure of stable impurities, radioisotopic or radionuclidic purity measures the absence of admixtures of unwanted radioisotopes. In particular admixtures of very long-lived radioisotopes should be avoided to avoid unnecessary dose to the patient and extra burden on facility waste handling in the hospital.

2.1.1 Neutron capture

Neutron capture on stable targets usually leads to slightly neutron-rich isotopes that decay by beta-minus emission. The only positron emitter of clinical relevance that could in principle be produced by neutron capture is ^{64}Cu.

If other reactions (such as destruction of the target or product by nuclear reactions) do not interfere significantly, then the specific activity achievable by a one-step transmutation reaction is given by:

$$S = \frac{N_A}{A} \cdot \sigma \cdot \phi \cdot \left(1 - \exp\left(-\frac{\ln(2) \cdot t_{irr}}{T_{1/2}}\right)\right)$$

where N_A is Avogadro's constant, A the atomic mass, $T_{1/2}$ the half-life of the product, σ the cross-section for transmutation of the target into the product, Φ the neutron flux density and t_{irr} the irradiation time.

Thus high neutron flux *and* a high capture cross-section are essential to achieve a high specific activity by converting a large fraction of the stable target into the wanted radioisotope. Only ^{60}Co, ^{153}Sm, ^{169}Yb and ^{177}Lu can be produced with

appreciable specific activity ($R > 0.05$) in this way.

To optimise specific activity often the target material is enriched in the useful target isotope and depleted in other stable isotopes that do not contribute to the production of the desired radioisotope. Enrichment is performed via ultracentrifugation of gaseous compounds, electromagnetic mass separation or selective laser dissociation or laser ionisation respectively. Most of these techniques are costly and complex, therefore the cost of highly enriched target material can contribute substantially to the overall cost of the produced radioisotopes. The tables show the natural isotopic abundance of the target isotopes as an indication of the difficulty of obtaining highly enriched material.

In principle specific activity could also be increased after irradiation by physical mass separation of the radioisotope from remaining stable isotopes. However, all the mentioned enrichment techniques would be even more costly to implement if radioactive material has to be handled; the methods take time (decay losses!) and have an overall efficiency well below unity (loss of valuable radioisotopes).

Chemical separation methods are generally more efficient than physical ones, but the isotopes produced by neutron capture belongs to the same element, i.e. is chemically identical to the target isotope. However, in certain cases neutron capture does not produce the final radioisotope directly but a radioactive precursor that decays by beta decay to the wanted isotope. Thus the final radioisotope differs chemically from the target and can therefore be chemically separated. This *indirect production* usually leads to products in so-called "non-carrier-added" (n.c.a.) quality, which are often de facto "carrier-free" if no stable impurities of the product isotope were present in the target material and other chemicals used.

If the intermediate isotope is short-lived, a single separation is performed after decay to the longer-lived desired radioisotope. If the intermediate isotope is longer-lived it may serve as *generator* for repeated separations of the daughter. After each separation new daughter activity will grow in and can be separated again. Such generators are particularly interesting since short-lived isotopes can be extracted again and again, even many half-lives after the end of irradiation. Hence, generators are essential to make shorter-lived isotopes easily available at remote places (see section 2.1.6).

In certain cases (^{166}Dy, ^{188}W, ^{195m}Ir) the required radioisotopes can only be reached from a stable target by two consecutive neutron captures. A particularly high neutron flux is required to bypass

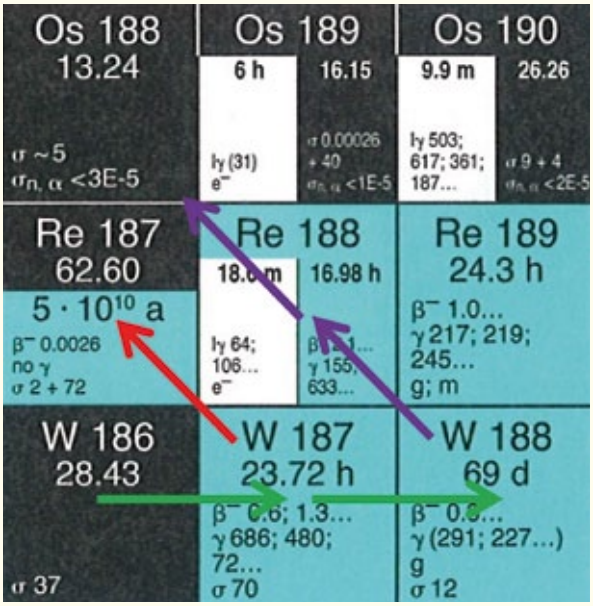

Figure 2.1. Example of a double neutron capture reaction leading from stable ^{186}W to the generator isotope ^{188}W.

efficiently the intermediate shorter-lived isotope (see Figure 2.1). The specific activity of the product produced by double neutron capture increases roughly in proportion to the square of the neutron flux; therefore irradiation positions with particularly high neutron flux are required to produce high specific activity isotopes via double neutron capture.

2.1.2 Fission

Fission of actinide targets efficiently produces neutron-rich isotopes with atomic masses ranging from about 85 to 150. Most frequently thermal neutron capture of ^{235}U is used, but fast neutron-induced fission or photo-fission of ^{238}U are also being considered. The product elements differ chemically from the actinide target and can be chemically separated from all other products except other isotopes of the same element, thus leading to relatively high specific activity. Today mainly ^{99}Mo ($R \approx 0.1$), ^{131}I ($R \approx 0.5$) and ^{133}Xe ($R \approx 0.1$) are produced by fission.

2.1.3 Proton induced reactions

Proton induced reactions such as (p,n) and (p,α) dominate for low proton energies (≈5–15 MeV) and are essential for production of most PET isotopes with compact accelerators. Additional reaction channels such as (p,2n), (p,3n) or (p,4n) are opened at consecutively higher proton energies. Thus 30 MeV protons are usually employed to make good use of the (p,2n) excitation functions and 70 MeV protons to exploit (p,4n) reactions. Also (p,2p) reactions for the production of neutron-rich isotopes such as ^{47}Sc or ^{67}Sc require protons of several tens of MeV. Finally with protons of 100 MeV or

more, spallation becomes possible that allows the population of isotopes further away from the target. Spallation with GeV protons produces a large variety of products which gives the method more universality but also makes the subsequent separation steps more challenging. Chemical separation cannot remove radioisotopic impurities of the same element, but sometimes a combination of chemical separation with suitably chosen irradiation and decay times leads to products of sufficient purity, e.g. for ^{67}Cu (the longest-lived copper isotope remaining after decay of all shorter-lived ones). Also generator isotopes of reduced radioisotopic purity are often acceptable since the chemical selectivity of the generator provides an additional purification step.

Physical mass separation in combination with chemical element separation is possible, e.g. on-line with the ISOL method at ISOLDE (CERN), but it is presently not in commercial use. However, it is of great interest for R&D applications to provide quick access to unusual radioisotopes before a conventional production scheme has been set up or for applications requiring particularly high specific activity, e.g. systematic studies of dose–effect relationships as function of specific activity.

Most isotopes can be made by a number of different nuclear reactions, differing not only in projectile energy and the target material isotope, but also in the mass and charge of the projectile. When it comes to practical, economical high yield and high purity production the choice of projectile most often favours protons. For a given projectile energy, protons have, compared to heavier projectiles, the lowest energy loss and the largest range in targets. At comparable production cross-sections the highest production yields per beam current unit or, more importantly, per beam power unit are therefore often achieved with protons. Thus proton-induced reactions are generally preferred whenever the required stable target isotopes are readily available and can be bombarded in a suitable chemical form. It is an obvious fact that all major diagnostic isotopes for nuclear medicine imaging (SPECT and PET) are most efficiently and simply made by proton bombardments: ^{11}C, ^{13}N, ^{18}F, ^{67}Ga, ^{111}In, ^{123}I and ^{201}Tl. The only important exception to this rule is ^{99m}Tc, that *can* be made efficiently and pure by proton bombardment on ^{100}Mo, but still is made far more economically and in a much more readily available way from reactor-derived ^{99}Mo.

2.1.4 Light ion induced reactions

For certain isotopes that cannot be reached easily by proton-induced reactions, heavier projectiles are warranted. The main alternatives to protons are deuterons and alpha particles. Triton and ^{3}He bombardment is considered too expensive or technically challenging to warrant large scale use, while the heavy ion reactions (Li and heavier projectiles) populate many exit channels, thus reducing the available yield in each channel and the resulting radionuclidic impurity is impaired if no additional measures are taken.

The ^{14}N(d,n)^{15}O reaction uses natural nitrogen where ^{14}N is abundant (99.6%) rather than expensive enriched ^{15}N (0.4% natural abundance) required for the corresponding ^{15}N(p,n)^{15}O reaction.

Also the ^{20}Ne(d,α)^{18}F reaction makes use of non-enriched targets instead of requiring highly enriched ^{18}O for the ^{18}O(p,n)^{18}F reaction. When traces of stable F_2 are added to the gas target the produced ^{18}F will be readily available in form of fluorine (F_2), an advantage for certain subsequent chemical processes compared to the fluoride (F^-) produced in water targets.

In other cases deuteron induced (d,2n) reactions lead to the same target–product combinations as (p,n) reactions but may provide higher yields, e.g. for ^{44m}Sc production from ^{44}Ca targets.

Alpha-induced reactions provide access to products with two protons more than the target. Thus, the reaction ^{209}Bi(α,2n)^{211}At is the only direct way to this promising alpha emitter since no stable polonium targets exist for alternative (p,xn) reactions.

2.1.5 Other reactions

Neutron-induced reactions like (n,n'), (n,2n), (n,p) or (n,α) give access to additional products or higher specific activities compared to standard reactions, but only in a few cases are these reactions regularly used for radioisotope production. The same applies to photon induced reactions such as (γ,γ'), (γ,n) or (γ,p).

2.1.6 Radionuclide generators

The optimum half-life of an imaging isotope for diagnostic purposes is given by the time it takes to achieve a representative biodistribution. This can be as short as few seconds for lung ventilation or cardiac perfusion studies. Longer-lived isotopes can be used for the same purpose but they may lead to enhanced radiation doses to the patient if a fraction of the radioisotope remains longer in the body (not an issue for ventilation studies). Hence, to minimise dose one should select the shortest-lived isotopes compatible with a given application.

On the other hand the use of very short-lived isotopes challenges the chain from production, via handling to injection into the patient. Indeed isotopes like 2 minute ^{15}O are used for PET imaging,

but only a few nuclear medicine departments are equipped with appropriate "bedside cyclotrons" or rapid transport systems from the central cyclotron to the PET imaging room and even with this equipment the logistical challenge is significant and decay losses are unavoidable, i.e. far more radioactivity has to be produced than that which is actually used.

Radioisotope generators are an elegant way out of the dilemma of contradicting half-life requirements for use in patients and logistics. Here a longer-lived mother isotope is produced that decays continuously to the wanted shorter-lived daughter isotope (Figure 2.2). The mother isotope is loaded onto a "generator" and is usually chemically bound to stay there quasi-infinitely. After sufficient daughter isotopes have accumulated by decay of the mother isotope, the daughter which has chemical properties different from the mother is extracted ("eluted") from the generator. After each separation new daughter activity will grow in and can be separated again. Such generators are particularly interesting since short-lived isotopes can be extracted again and again, even many half-lives after the end of irradiation. Hence, generators are essential to make shorter-lived isotopes easily available at remote locations. The most prominent example is the ^{99}Mo/^{99m}Tc generator. Without its invention that enabled the introduction of an excellent SPECT isotope to remote places, nuclear medicine would probably have not reached the importance it has today.

A convenient side effect of a generator is the additional chemical separation step during elution, performed just before use. This added separation step (in addition to a separation performed before or during loading of the generator) provides often enhanced radionuclidic purity and high specific activity of the product.

The price to pay for the convenience of radioisotope generators is often more challenging production. Most of the mother isotopes are slightly more "exotic", i.e. further away from stable isotopes and their production requires more effort compared to direct production of the imaging isotopes. Hence, nuclear reactors with particularly high neutron flux are required to produce efficiently the generator isotopes ^{166}Dy, ^{188}W or ^{229}Th and larger accelerators that provide more energetic projectiles are required to produce efficiently ^{68}Ge, ^{82}Sr, etc.

Radioisotope generators are often called a "cow" from which the wanted product can be "milked". If milk were as perishable as some radioisotopes are, it would indeed be better to transport the cow to the customer rather than the milk.

Various chemical methods are used for the separation of mother and daughter isotopes: liquid chromatography, liquid–liquid extraction, sublimation, distillation, gas–liquid systems, etc. From the user perspective it is more interesting to classify the generators according to the half-life of mother and daughter isotopes respectively:

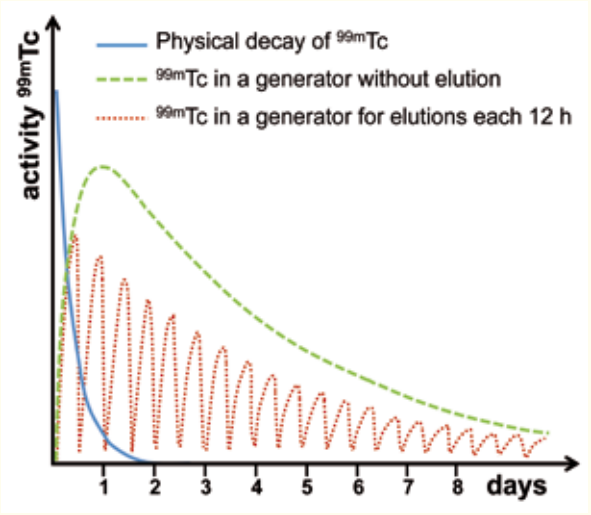

Figure 2.2. ^{99m}Tc activity (blue) available from a ^{99}Mo/^{99m}Tc generator as function of time in comparison to the decay of ^{99m}Tc produced directly (green).

a) Generators with short-lived daughter isotopes

These generators are placed close to the end user, i.e. in the nuclear medicine department, to minimise decay losses after "milking the cow". If the decay product is very short-lived (5 s ^{191m}Ir, 13 s ^{81m}Kr, 75 s ^{82}Rb), the product is used in a simple chemical form as provided by the generator and the generator is connected more or less "directly" to the patient, leaving no time for a quality control step before use. Hence, a stringent quality assurance scheme has to be respected where the quality of the eluted product is tested regularly (e.g. daily) before use of the generator for humans.

Somewhat longer-lived products (such as 68 min ^{68}Ga, 45 min ^{213}Bi or even 10 min ^{62}Cu) can be used for simple chemical processing. The chemical reactants are either readily supplied to the nuclear medicine departments in the form of "kits" which are simply mixed with the eluted or preprocessed product isotope, or the generator is directly attached to an often automated radiochemical process system.

b) Generators with longer-lived daughters

Longer-lived daughters can be shipped to remote customers without excessive decay losses. Therefore it is often more convenient to centralise the generator operation and the subsequent quality control steps. Hence generators providing ^{90}Y, ^{223}Ra or ^{225}Ac are always kept in central locations that have the

required handling permits for the long-lived mother isotopes. Future ^{44}Ti/^{44}Sc generators that could provide ^{44}Sc without a local cyclotron would probably also remain at central distributors.

^{99m}Tc with 6 hours half-life is at the boundary of groups 1 and 2 In Europe and Japan ^{99}Mo/^{99m}Tc generators are distributed to end users where they are eluted when needed. Alternatively the generators can be placed at central radiopharmacies where they are regularly eluted, then the product is dispensed in the required amounts and shipped to the customer on demand. This model is mainly practised in the US and Canada. The logistics effort is clearly smaller in the former case (weekly dispatch of radioactive packages versus shipping daily or several times per day) while the latter system can make more efficient use of the mother isotope if the end users have irregular use of an own generator and if decay losses during distribution of ^{99m}Tc remain acceptable.

Another boundary case is the therapeutic isotope ^{188}Re ($T_{1/2}$=17 hours) that can either be eluted from distributed or central ^{188}W generators or even be produced daily by neutron capture on stable ^{187}Re targets in nuclear reactors.

The misjudged generator

In 1957 radiochemists at the Brookhaven National Laboratory developed a method to make a simple and reliable generator for the supply of ^{99m}Tc, at the time just one radioisotope of a "strange" chemical element not present in nature. Filing of a patent was refused by the BNL patent office with the argument *"the product will probably be used mostly for experimental purposes in the laboratory"* and *"We are not aware of a potential market for technetium-99 great enough to encourage one to undertake the risk of patenting"* [Ric82]. Today such ^{99}Mo/^{99m}Tc radioisotope generators are the workhorses of nuclear medicine and 30 million patient doses of ^{99m}Tc are eluted every year.

c) In-vivo generators

Certain isotopes have good properties for imaging or therapy respectively but are simply too short-lived to be brought to their destination in the human body in time before they decay. In certain cases a longer-lived mother isotope can be injected into the patient that will localise as required, then decay to the short-lived daughter that emits the desired radiation. In contrast to ex vivo generators where the mother and daughter isotopes should have sufficiently different chemical properties to enable an efficient separation, for in vivo generators similar chemical properties are required to ensure that the daughter remains at the intended place where the mother isotope was delivered. In particular one has to verify that the nuclear decay does not break chemical bonds which could lead to uncontrolled release of the daughter from the delivery vehicle (chelator). This issue is particularly problematic for alpha emitters where the violent recoil may break even strong chemical bonds. Details are discussed in the section on therapeutic alpha emitters.

^{188}W/^{188}Re generator

^{188}Re can be eluted once or several times daily from a ^{188}W/^{188}Re generator. With 69 days half-life of ^{188}W these generators can be used for several months, thus giving convenient in-house access to a therapeutic isotope. This explains why ^{188}W/^{188}Re generators are particularly popular in emerging countries where a just-in-time delivery network of short-lived isotopes does not always exist. Tungsten is a chemical homologue of molybdenum and rhenium is a homologue of technetium; hence the separator technology (adsorption on acid alumina column) is identical to the well-known Mo/Tc generator. Moreover the labelling chemistry of the eluted ^{188}Re corresponds to that of ^{99m}Tc, making ^{188}Re often the prime choice for therapeutic applications (even if the decay parameters of other isotopes might be slightly better for a given application). ^{188}W/^{188}Re generators providing high activity in little elution volume are particularly convenient since time-consuming radiochemical post-concentration steps are not required. However, ^{188}W of relatively high specific activity (≥ 1 Ci/g) is required that has to be produced in high flux reactors.

^{82}Sr/^{82}Rb generator

The ^{82}Sr/^{82}Rb generator has been used in nuclear cardiology for more than 20 years in the USA. As an analogue of potassium, ^{82}Rb is extracted by the myocardium and allows evaluation and quantification of myocardial perfusion in patients with suspected coronary disease. As a short lived ($T_{1/2}$ = 75s) positron emitter, ^{82}Rb presents several advantages as compared to monophotonic emitters such as ^{99m}Tc and ^{201}Tl:

- Better correction of the attenuation of photons in the tissues leading to fewer false positive results for overweight patients and women with large and dense breasts
- The possibility for quantification
- Shorter duration of the examination (rest and stress examinations can be made in about 30 min)
- Lower radiation dose to the patients

Due to its short half-life, rubidium cannot be efficiently produced as a direct product but is obtained using the ^{82}Sr/^{82}Rb generator. ^{82}Sr ($T_{1/2}$=25.5 d) is produced using high energy protons (> 40 MeV). Below this energy, no ^{82}Sr can be produced. The target is made of rubidium. Rubidium chloride (RbCl) or rubidium metal are used as targets. In both cases, the nuclear reaction of interest is the (p,4n) reaction which has a cross section of about 100 mb. Large production of ^{82}Sr requires high intensity beams (> 100 μA). After irradiation, an extraction and purification of the ^{82}Sr is needed. This product is then sent to the generator manufacturer to fill the generator which consists of a shielded stannic oxide resin on which the strontium is adsorbed. This resin has the properties to retain strontium isotopes and not rubidium isotopes. When a dose of ^{82}Rb is needed, sterile NaCl is injected through the column and the ^{82}Rb is eluted. The solution containing ^{82}Rb is then ready to be injected to the patient. A generator typically contains 4 GBq and can be used for between 4 and 6 weeks depending on the number of injected patients.

^{68}Ge/^{68}Ga generator

The ^{68}Ge/^{68}Ga generator is mainly used in oncology for positron emission tomography imaging. To do so, the ^{68}Ga must be attached to a vector molecule which targets the cancer cells. The big advantages of ^{68}Ga are related to its high positron branching ratio (89%) and its chemical properties that allow a rapid and efficient coupling via chelators to biologic molecules. Due to its half-life ($T_{1/2}$= 68 min), ^{68}Ga is well suited for use with peptides and several applications have been developed to be used in imaging of neuroendocrine tumours.

^{68}Ga can be produced directly using a (p,n) reaction on enriched ^{68}Zn targets but most often ^{68}Ga is eluted from generators. ^{68}Ge ($T_{1/2}$=271 d) is produced using proton beams below 30 MeV on a gallium target, either in elemental form or as Ni-Ga alloy. In the first case, the target melts under irradiation (T_{melt}=37°C) and liquid gallium which is very corrosive must be contained in a niobium container. Despite this, corrosion and cracks can be observed leading to target destruction from time to time. The other solution presents the advantage of increasing the melting temperature and allows safer irradiation especially in the case where the target is placed behind the rubidium target to take advantage of the remaining energy of the protons during ^{82}Sr production. After irradiation, the germanium is extracted and purified before shipment to the generator manufacturer.

Different generator designs exist nowadays based on TiO_2, SnO_2 or organic resins. Up to 3.7 GBq of ^{68}Ge can be loaded on a generator. Elution is performed using HCl solutions. To meet radiopharmaceutical requirements, in some cases, the eluted solution from the generator passes through an additional purification module (post processing module).

^{44}Ti/^{44}Sc generator

Scandium is the lightest rare earth and can be easily attached via chelators to biological vectors. The medium half-life ($T_{1/2}$=3.9 h) of the positron emitter ^{44}Sc makes it interesting to label peptides or antibody fragments.

^{44}Sc can be directly produced through (p,n) and (d,2n) reactions on ^{44}Ca or obtained from a ^{44}Ti/^{44}Sc generator. The long-lived ^{44}Ti ($T_{1/2}$=60 y) can be produced in (p,2n) reaction on ^{45}Sc or by spallation of V, Fe or Cu. Thus ^{44}Ti can be extracted from beam dumps that have been irradiated for long time with high energy protons.

^{225}Ac/^{213}Bi generator

^{213}Bi is an alpha emitter that can be used for targeted alpha therapy. Several studies have been performed with this isotope at the preclinical as well as clinical level. Leukaemia, brain tumours and Non-Hodgkin's Lymphoma are among the different types of cancer that have been studied.

Actinium-225 is currently obtained from the decay of 7340-years ^{229}Th. Thorium-229 originates from ^{233}U as the first alpha decay daughter, and both nuclides are members of the extinct neptunium series. ^{233}U, which has a fission characteristic similar to that of ^{235}U, was produced as part of the US molten salt breeder reactor research programme and is currently stored at ORNL. ^{229}Th is not easily available and only small quantities are available for medical applications. Another approach consists of using ^{226}Ra (T1/2= 1600y) as target material irradiated by protons, neutrons or gamma rays to produce ^{225}Ac directly or as a decay product of ^{225}Ra. But as for ^{229}Th, the availability is restricted and the manipulation of large amounts of ^{226}Ra is tricky.

In recent years, several laboratories have been working on producing ^{225}Ac from proton irradiation of a ^{232}Th target in high energy accelerators. In this case, the proton energy must be at least 100 MeV.

^{212}Pb/^{212}Bi generator

^{212}Bi is an alpha emitter with a half-life of 61 min. Alpha particles are emitted directly from the ^{212}Bi in 36% of the case or after the beta decay to ^{212}Po (T1/2=0.3μs). It is obtained through the decay of ^{212}Pb ($T_{1/2}$=10h) and the ^{212}Pb/^{212}Bi is used as an in vivo generator. A phase I clinical trial is currently

ongoing in the US for breast cancer expressing the HER-2 antigen using the trastuzumab antibody. In order to transport the ^{212}Pb to hospitals, a ^{224}Ra/^{212}Pb generator is provided. ^{224}Ra is extracted in turn from ^{228}Th decay and the ^{228}Th stems from ^{228}Ra retrieved from the natural decay chain of thorium. Thus ^{212}Pb is a generator isotope deriving from a generator which in turn derives from a generator...

2.2 Production facilities

The two main tools to produce medical isotopes, research reactors and accelerators, are complementary offering a large set of radioisotopes for nuclear medicine applications. Figure 2.3 shows the main steps from the raw material to the separated radiochemical solution ready for labelling.

2.2.1 Radioisotope production in nuclear reactors

Certain research reactors provide a high neutron flux that allows the production of large quantities of radioisotopes for medical and other applications.

The generic term "research reactor" covers various types of reactors that are not primarily aimed at electricity production. There are often prototypes of new reactor concepts (e.g. reactors with fast neutron spectrum, molten salt reactor, etc.), reactors for studying certain aspects of reactor physics or accident scenarios, neutron sources for intense extracted neutron beams that serve for neutron scattering and fundamental neutron physics and irradiation reactors which have in-pile irradiation positions with high flux for test irradiations of materials (fuel elements, components of existing and future reactor types), for neutron transmutation doping of semiconductors and finally for radioisotope production. Some reactors provide in-pile irradiation positions *and* extracted neutron beams while the first listed types of research reactors are usually distinct.

Power reactors are aimed at efficient conversion of heat to electricity. Therefore the coolant is extracted at high pressure and high temperature which require appropriate construction materials. The neutron flux in the reactor is deliberately limited in the design to avoid a combination of thermo-mechanical stress with high radiation damage. The massive pressure vessels of most power reactors are built for the entire lifetime of the reactor and cannot be exchanged.

Research reactors that aim at the highest possible neutron fluxes are optimised antipodal to power reactors. The aim is to produce the maximum useful neutron flux at limited thermal power generation (Table 2.1). Therefore the fuel elements and the entire core are far more compact. Only a few kg up to tens of kg of uranium are used, but this lower mass is compensated by higher enrichment of the "useful" fissile ^{235}U. Today generally so-called LEU (low enriched uranium with <20% enrichment of ^{235}U) is used for most research reactors while those providing the highest neutron flux require higher enrichment (up to 93%). The tiny mass of fuel and the relatively low thermal power contributes to the exceptional inherent safety of research reactors.

There is no straightforward ranking of the suitability of different research reactors for radioisotope production. Due to very different core designs the maximum neutron flux does not scale with the nuclear power and even for comparable maximum flux the effectively usable flux varies strongly with the available irradiation positions. Reactors with

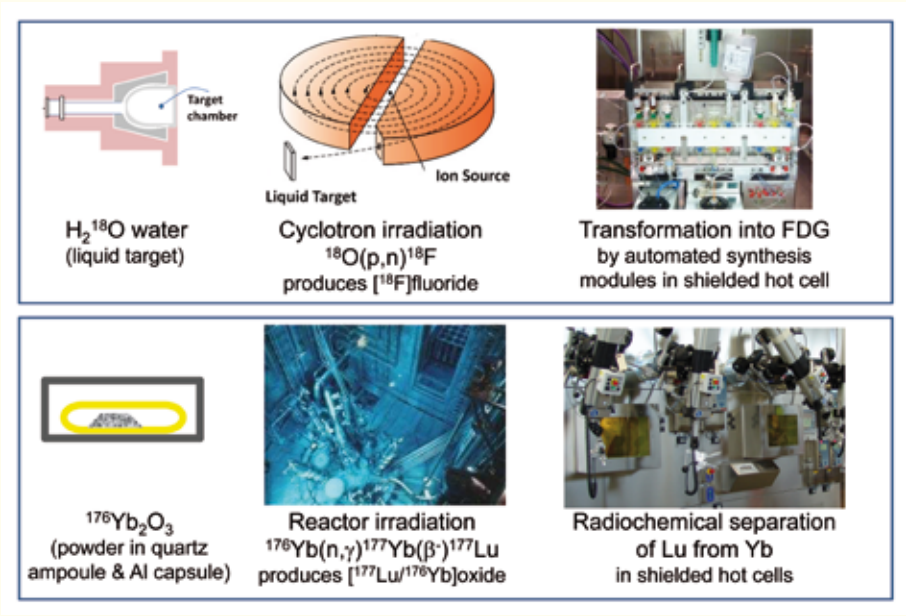

Figure. 2.3. Typical process steps for accelerator or reactor produced isotopes at the example of ^{18}FDG and ^{177}Lu.

Table 2.1. Prominent research reactors that are used for radioisotope production [RRDB]. The maximum unperturbed thermal neutron flux that is usually accessible for production of medical radioisotopes is given.

Research reactor	Laboratory	Location	Thermal flux (10^{14} cm^{-2} s^{-1})	Power (MW)
HFIR	ORNL	Oak Ridge, USA	25	85
BOR-60	SSC RIAR	Dimitrovgrad, Russia	20 (fast)	60
SM-3	SSC RIAR	Dimitrovgrad, Russia	19	100
RHF	ILL	Grenoble, France	15	58
BR2	SCK-CEN	Mol, Belgium	10 (tank), 3.6 (pool)	100
HFR	NRG	Petten, Netherlands	4.5	45
MURR	Univ. Missouri	Columbia, USA	4.5	10
HANARO	KAERI	Daejeon, South Korea	4	30
SAFARI	NECSA	Pelindaba, South Africa	4	20
NRU	AECL	Chalk River, Canada	4	135
FRM2	TUM	Garching, Bavaria	4 (fast), 1.3 (th.)	20
OSIRIS	CEA Saclay	Saclay, France	2.7	70
OPAL	ANSTO	Lucas Heights, Australia	2.5	20
Maria	Polatom	Świerk-Otwock, Poland	2.5	30
RA-3	CNEA	Ezeiza, Argentina	2.4	10
BRR	KFKI	Budapest, Hungary	1.7	10
LVR-15	NRI	Řež, Czech Republic	1.4	10

a single compact fuel element (e.g. HFIR, RHF, FRM2) have a very high neutron flux just outside the core (at 10 to 20 cm distance) and inside the hollow fuel element (e.g. flux trap in HFIR). Reactors with multiple fuel elements (e.g. BR2, HFR, NRU) do not reach the same peak flux but provide far more irradiation positions distributed over a larger volume.

For radioisotope production it is essential that the targets can be easily introduced into the irradiation position and recovered after irradiation.

The easiest access is in "pool-type reactors" where the reactor core and control rods are situated at the bottom of an open reactor pool. A water layer of 6m or more acts as an efficient radiation shield. Thus operators can access the top of the pool during reactor operation and load and unload the irradiation positions from the top with long manipulators or fishing lines.

At higher power efficient cooling of the core requires a faster water flow. Therefore the core is situated in a closed cooling circuit operated at higher water pressures of a few bar up to few tens of bar. In a "tank reactor" the moderator is placed in the same pressure vessel as the core. Alternatively only the core is placed in a pressure vessel but the surrounding elements stay in an open pool: a "tank in pool reactor". Heavy-water moderated reactors also use this concept to enclose the precious heavy water in a tank and thus separate it from the light water in the surrounding pool.

When producing radioisotopes in tank reactors the samples have to be loaded into and removed from the tank while the tank is not under pressure, i.e. when the reactor is not operating. Thus, such irradiation positions are suitable for production of longer-lived radioisotopes with half-lives commensurate with the operation cycles of the reactor. Alternatively the tank has to be equipped with dedicated inserts to introduce and remove the irradiation samples during reactor operation.

The difficulty of accessing positions close to the core during operation together with the very long operation cycles are, together with the lower neutron flux, the main reasons why power reactors are not used for production of medical isotopes. Conceptual studies have been performed for ^{99}Mo production in boiling water reactors and CANDU reactors but so far none of these projects has demonstrated economic feasibility.

The technical challenges for radioisotope production targets in nuclear reactors are quite different from cyclotron targets. Unlike charged particle beams the simple passage of thermal neutrons through a target does not heat the latter significantly. However, the heating by gamma rays from the reactor core (several W/g close to the core

Table 2.2. Radioisotopes produced directly by neutron capture reactions.

Product isotope	Half-life	Target isotope	Natural abundance %	Specific activity	
				$\Phi = 10^{14}$ cm^{-2}s^{-1} GBq/mg	$\Phi = 10^{15}$ cm^{-2}s^{-1} GBq/mg
^{32}P	14.3 d	^{31}P	100	0.3	3
^{60}Co	5.27 a	^{59}Co	100	14	30
^{64}Cu	12.7 h	^{63}Cu	69	4.3	40
^{89}Sr	50 d	^{88}Sr	83	0.004	0.04
^{90}Y	64 h	^{89}Y	100	0.8	8
^{99}Mo	66 h	^{98}Mo	24	0.08	0.8
^{103}Pd	17 d	^{102}Pd	1.0	1.9	18
^{117}Sn	13.6 d	^{116}Sn	15	0.003	0.03
^{153}Sm	46.3 h	^{152}Sm	27	80	640
^{166}Ho	26.8 h	^{165}Ho	100	21	200
^{169}Er	9.4 d	^{168}Er	27	0.8	8
^{169}Yb	32 d	^{168}Yb	0.13	190	260
^{177}Lu	6.65 d	^{176}Lu	2.6	470	1500
^{186}Re	3.72 d	^{185}Re	37	35	300
^{188}Re	17 h	^{187}Re	63	24	230
^{192}Ir	73.8 d	^{191}Ir	37	70	90
^{193}Pt	4.33 d	^{192}Pt	0.78	0.6	6
^{195}Pt	4.02 d	^{194}Pt	33	0.009	0.02

of high flux reactors) and the self-heating of the sample (mainly for fissile targets that reach kW/g power) provide significant heat load. Thus fissile samples or irradiation positions close to the reactor core usually require forced convection for sample cooling.

Finally the self-shielding effect of materials with high neutron capture cross-sections has to be considered. Nuclear reactors are inherently equipped with advanced systems for nuclear safety: multiple safety barriers including the building, massive biological shielding, tight supervision of gaseous and liquid effluents, etc., assure safe management of the radioisotope inventory of operating and used reactor cores. The activities, dose rates and radiotoxicities of samples irradiated for radioisotope production usually represent only a minor fraction of the respective values of the reactor core. Therefore nuclear reactors are naturally predestined for safe production of large activities of radioisotopes.

Table 2.2 shows a list of radioisotopes produced directly by neutron capture. The maximum achievable specific activity (saturation activity) was calculated for thermal neutron fluxes of 10^{14} and 10^{15} cm^{-2}s^{-1} respectively. Experimental values may differ due to additional resonance capture of epithermal neutrons. In certain cases (e.g. ^{60}Co) the irradiation time would be impractically long (many years) to reach saturation activity, thus in reality shorter irradiation times are used for higher throughput.

In the indirect route the final quality (n.c.a.) does, to first order, not depend on the neutron flux. With higher flux the yield (i.e. the activity produced per mass of target material) will rise, but even at lower flux the quality of product will remain the same. However, in reality it becomes more challenging to achieve a higher separation factor (more stable target material has to be removed) and the requirements of the chemical purity of target material and chemicals

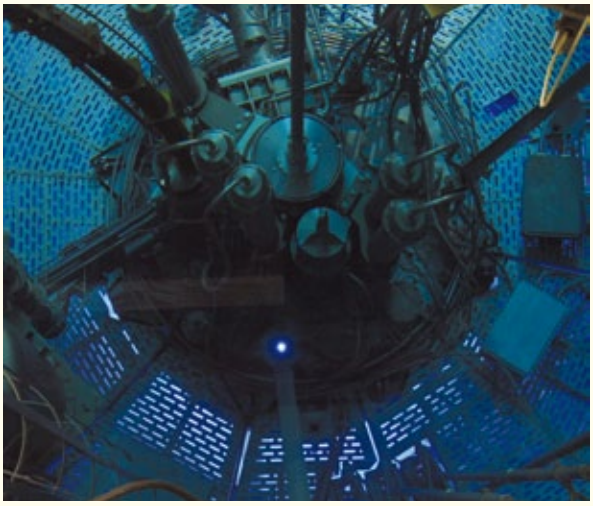

Figure 2.4. Top view of the central part of ILL's reactor seen through 7.5 m of light water. The heavy water tank in the middle is surrounded by a light water pool. The bottom of the latter is "illuminated" by Cherenkov light. The bright blue point below the centre of the image is the V4 thimble tube providing at its bottom a thermal neutron flux of 1.5×10^{15} cm^{-2}s^{-1}. It can be manually loaded and unloaded with irradiation shuttles during reactor operation.

Table 2.3. Radioisotopes produced indirectly by neutron capture reactions.

Product isotope	Half-life	Target isotope	Natural abund. %	Inter-mediate isotope	Half-life	$\Phi = 10^{14}$ cm^{-2}s^{-1}			$\Phi = 10^{15}$ cm^{-2}s^{-1}		
						T_{irr} d	T_d d	Yield GBq/mg	T_{irr} d	T_d d	Yield GBq/mg
Production via (2n,γ) reactions											
^{166}Dy	3.4 d	^{164}Dy	28	^{165}Dy	2.35 h	10	1	2	5	1	100
^{188}W	69.8 d	^{186}W	28	^{187}W	0.99 d	100	10	0.002	50	10	0.1
Indirect production via (n,γ)β$^-$											
^{47}Sc	3.3 d	^{46}Ca	0.004	^{47}Ca	4.5 d	10	1	0.5	10	1	5
^{125}I	59.4 d	^{124}Xe	0.10	^{125}Xe	17 h	7	7	6	4	7	20
^{131}I	8.0 d	^{130}Te	34	^{131}Te	25 min	28	2	0.1	28	2	1
^{131}Cs	9.7 d	^{130}Ba	0.11	^{131}Ba	12 d	7	7	0.7	7	7	7
^{161}Tb	6.9 d	^{160}Gd	22	^{161}Gd	4 min	14	0.5	0.4	14	0.5	4
^{177}Lu	6.7 d	^{176}Yb	12.8	^{177}Yb	1.9 h	14	1	0.6	14	1	4
^{199}Au	3.1 d	^{198}Pt	7.2	^{199}Pt	31 min	7	0.5	0.7	7	0.5	7
^{227}Ac	21.7 a	^{226}Ra	0	^{227}Ra	42 min	100	30	0.02	28	30	0.03
Indirect production via (n,f)											
^{99}Mo	2.8 d	^{235}U	0.72			7	1	5.7			
^{131}I	8.0 d	^{235}U	0.72			7	12	0.7			
^{133}Xe	5.3 d	^{235}U	0.72			7	7	3			

Figure 2.5. Typical sizes of IBA cyclotrons providing proton energies of 11, 18, 30 and 70 MeV from left to right.

used in the separation process rise since traces of stable impurities become relatively more important for a batch with lower activity. Table 2.3 shows a list of radioisotopes produced indirectly by neutron capture reactions. The achievable yields (GBq of product isotope per mg of 100% enriched target isotope) were calculated for thermal neutron fluxes of 10^{14} and 10^{15} cm^{-2}s^{-1} respectively. Experimental values may differ due to additional resonance capture of epithermal neutrons. Typical irradiation and decay times were chosen to keep co-produced radioisotope impurities at an acceptable level.

As for other indirect production routes the neutron flux is not very relevant for the quality of produced radioisotopes. Large scale industrial production is performed in high flux reactors at neutron fluxes ranging from 5×10^{13} to 2×10^{14} cm^{-2}s^{-1}. Irradiation in still lower fluxes is possible (e.g. for local or regional supply of ^{99}Mo with medium-flux reactors) but leads to a less efficient use of the ^{235}U targets. Still higher fluxes are not favourable since the cooling of the fissile targets gets increasingly difficult.

Not every research reactor is equipped for irradiation of massive fission targets. This requires additional investments such as forced cooling, local monitoring of fission gas release, additional shielding and correspondingly heavy equipment for handling the heavily shielded transport containers.

2.2.2 Medical isotope production by accelerators

Today two types of particle accelerator are used for radioisotope production; cyclotrons and to a lesser degree linear accelerators, but new developments are underway.

Advanced Cyclotron Systems Inc. (ASCI), Richmond, Canada
Advanced Biomarkers Technology (ABT), Louisville, TN, USA
Best Cyclotron Systems Inc. (BCSI), Vancouver, Canada
China Institute of Atomic Energy (CIAE), Beijing, China
Efremov Institute (NIIEFA), St. Petersburg, Russia
GE Healthcare, Uppsala, Sweden
Ion Beam Applications (IBA), Louvain-la-Neuve, Belgium
KIRAMS, Seoul, Korea
PMB Alcen (formerly EuroMeV), Peynier, France
SIEMENS Healthcare, Erlangen, Germany
Sumitomo, Tokyo, Japan

Table 2.4. Cyclotron manufacturers

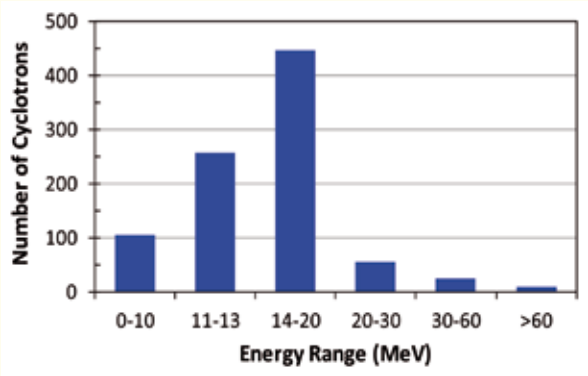

Figure 2.6. Number of cyclotrons operational worldwide in 2013 against their maximum proton beam energy.

Cyclotrons

Most of the beam driven facilities use a cyclotron. They are commercially available from several providers worldwide, see Table 2.4 [Sch11]. The size is compact and plug power needs are modest (Figure 2.5). Available beam currents are in the 10 μA to 1 mA range.

Figure 2.6 shows the number of cyclotrons operating for medical isotope production as a function of their maximum proton energies world-wide in 2013 [Sch13].

Intense proton beams are conveniently produced by cyclotrons, in particular by negative ion machines that accelerate H^- ions which are stripped to H^+ for extraction. The predominance of cyclotrons is a direct consequence of the dominance of proton-induced reactions for radioisotope production. Moreover the required proton energies are in most cases modest. The PET isotopes (except generators) are invariably accessible with protons below 11–19 MeV, while almost all the SPECT isotopes can be produced by 30 MeV protons. This fact has lead to the present fleet of "medical" and "industrial" cyclotrons.

Cyclotrons are able to accelerate protons and at reduced performance also light ions. For singly charged ions the maximum ion energy scales with 1/A, A being the mass number.

Ion Linacs

Compared to cyclotrons the contribution of linear ion accelerators to medical isotope production is rather small. Some proton linacs at large accelerator facilities like BNL Brookhaven, LANSCE (LANL Los Alamos) or MMF (INR Troitsk) produce medical isotopes that require higher energy protons than available from standard medical cyclotrons. Dedicated medical ion linacs have been developed by ACCSys, Pleasanton, CA, USA.

A compact 7 MeV proton system is optimised for PET isotope production (Figure 2.7). It consists of an ECR (electron cyclotron resonance) ion source, a 4-vane RFQ (radio frequency quadrupole) and an Alvarez – DTL (drift tube linac). A mobile version installed on a truck has been available since 2007. An extended version for light ion acceleration is under development.

In Europe and in Japan, compact ion linacs have been developed for A/q ratios up to 3. All these linacs driven by multi-cell cavities deliver beams at a constant final beam velocity, that means at a con-

Figure 2.7. A 7 MeV Proton linac for PET isotope production from ACCSys. [http://www.accsys.com]

Figure 2.8. View of the 7 A×MeV linac at the cancer therapy centre HIT, Heidelberg, Germany.

Figure 2.9. 325 MHz prototype CH – cavity accelerating from 11.7 MeV to 24.3 MeV within a tank length of 2.9 m.

stant energy per nucleon. The maximum accepted A/q ratio is given by the design (Figure 2.8). The 7 A×MeV $^{12}C^{4+}$ linac (217 MHz) developed by GSI Darmstadt and IAP Frankfurt, Germany, serving as injector at the Heidelberg Ion Therapy centre HIT, consists of an ECR ion source, a 1m 4-Rod RFQ and a 3.7 m IH-DTL. This 21 MV injector has since been reproduced for four other therapy centres. This design might become attractive for medical isotope production too as it can be adapted to other end energies or max. A/q values by industry.

A new development towards compact 100 A×MeV linacs is another H- type drift tube structure, the cross-bar CH structure. A 70 MeV, 25 m long linac based on that technology is under development within the GSI FAIR project at IAP Frankfurt in cooperation with GSI Darmstadt, Germany (Figure 2.9) [Cle11].

Comparison of cyclotron with ion linac installations

The two sections above show very clearly that cyclotrons significantly dominate in medical isotope production. The reasons are:

- Very compact design at most of the requested beam energies
- Long experience by commercial manufacturers
- Low rf power requirements significantly reduce investment and operation costs

The natural limitations in beam current at cyclotrons are no problem in most cases.

Recent technical improvements in linac design have reduced the size and/or rf power requirement by a factor of 3–5, but the linac rf power needs are still about an order of magnitude higher when compared to cyclotrons.

Cases where linac solutions might be superior to cyclotrons are:

- Helium anions exist only in a metastable atomic state and production of He^- beams has very low efficiency. Therefore negative ion cyclotrons are not competitive for producing alpha beams. In positive ion cyclotrons the extracted beam currents are usually limited by beam losses on the septum. Linacs can accelerate intense beams of helium and heavier projectiles more efficiently.
- The plug power efficiency of linacs increases with the beam current. Hence linacs are more competitive for very high currents (mA). However, such currents can only be used with appropriate target technology and are only of interest for longer-lived radioisotopes that can be distributed from a centralised production facility over a wider region to many end-users.
- Mobile light weight solutions as realised by ACCSys for PET isotope production on a truck are in competition with very compact low-energy cyclotrons.
- Further drastic price reductions of solid state power amplifiers, as has been observed in the last 10 years, could reduce the difference in investment costs more in favour of linacs.

New developments for ion beam production

Electrostatic accelerators play at present no role in radioisotope production (except for injectors into cyclotrons or linacs), but the Tandem accelerator principle is currently being revisited by a joint activity of Oxford University, STFC and SIEMENS Healthcare. Their novel development of the Cockcroft Walton design is known as the ONIAC, a compact, high-current H^- Tandem Accelerator with onion like shaped electrodes [Bea11] that could serve as a low-energy proton and deuteron accelerator for local "point of demand" production of PET and SPECT radionuclides (Figure 2.10). However, the concept is challenged by the development of very compact low energy cyclotrons (<8.5 MeV protons) [Jen12], but these operate with lower beam currents.

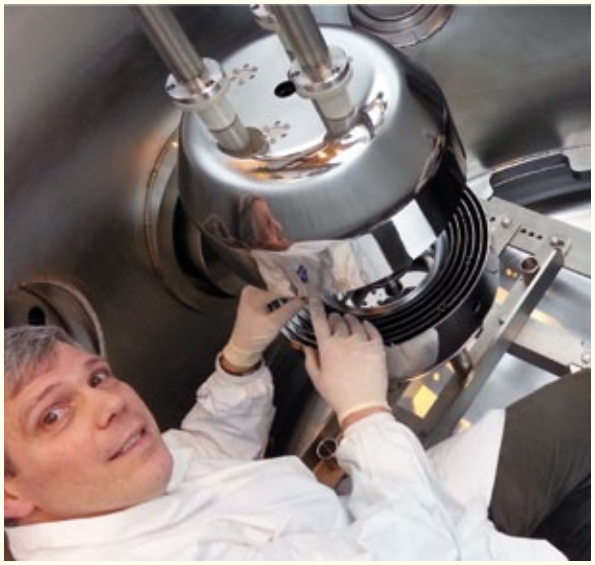

Figure 2.10. A prototype ONIAC electrostatic accelerator.

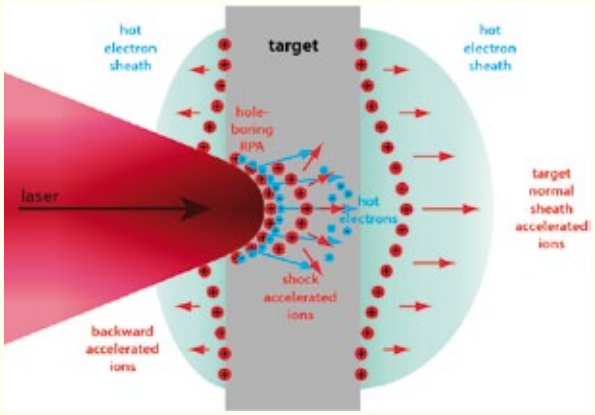

Figure 2.11. Advanced approaches to high intensity laser-driven ion acceleration (courtesy of Andreas Henig, PhD thesis, LMU Munich, 2010)

Another trend is acceleration behind thin foils hit by an intense, well focused laser beam (Figure 2.11) [Led10]. Proton beam energies ranging from some MeV to some tens of MeV have been achieved but the energy spectrum is usually quite wide. While hadrontherapy requires very precise beam energies, a wider energy distribution is usually acceptable for production of radioisotopes. First proof-of-principle experiments have demonstrated that the PET isotopes ^{18}F and ^{11}C could be produced at activities of the order of ~1 MBq per laser shot when using the highest possible irradiance available at the large VULCAN petawatt laser [Led10]. However, only a few laser shots per day are possible with such a machine.

More compact "table top" lasers are required for practical production purposes and a few Bq per laser shot have been obtained with 100 TW lasers [Led10]. Once such lasers can operate with a higher repetition rate (kHz), saturation activities suitable for clinical applications (~GBq) could be reached. Given that the technological development of high power lasers follows a kind of Moore's law it is possible that in future table-top lasers could complement conventional accelerators.

A potential advantage of laser accelerators is that only the (compact) target area may get activated and need radiation shielding, and not the machine (laser) itself. However, more R&D is needed to solve open issues such as efficient coupling of the radioisotope production target to the primary laser target given the large beam divergence.

Neutron beams

The most apparent neutron source is the nuclear fission reactor providing thermal neutrons with well suited fluxes for isotope production. Significant fluxes of fast neutrons are available in a few dedicated fast reactors (BOR60) or in irradiation positions in the core or very close to the core of multi-purpose irradiation reactors (SM3, HFIR, BR2, FRM2). Since these irradiation positions are located inside the pressurised primary cooling circuit, access is less straightforward. Often they can only be loaded and unloaded during a reactor stop. This limits the efficient application to longer-lived radioisotopes with half-lives comparable to the duration of the reactor cycles.

There are also alternative neutron sources driven by accelerators. One has to recognise that not any of these projects is optimised to medical isotope production as a priority. However, these projects may give a hint on options to be further developed and optimised for medical isotope production. Main concepts are:

- Proton and deuteron accelerators up to a few MeV to generate neutrons by the (p,n) – and (d,n) process, respectively, with targets like ^{9}Be or ^{7}Li as operated at FZK on a single ended electrostatic accelerator, under construction in Frankfurt with a 2 MeV rf linac.
- Deuteron acceleration up to 40 MeV and breakup reaction on target: under construction at SPIRAL2 at GANIL, Caen, France (see Figure 2.12) and SOREQ, Israel.
- Spallation neutron sources irradiate heavy targets with protons of several hundred MeV energy. Initially neutrons of several MeV energy are generated which can be subsequently moderated to thermal energies. Thus spallation neutron sources can provide slow neutron spectra similar to fission reactors but in addition also higher energy (>10 MeV) spallation neutrons. Today a thermal neutron irradiation position at the spallation neutron source SINQ at Paul Scherrer Institut, Villigen, Switzerland is used for production of experimental

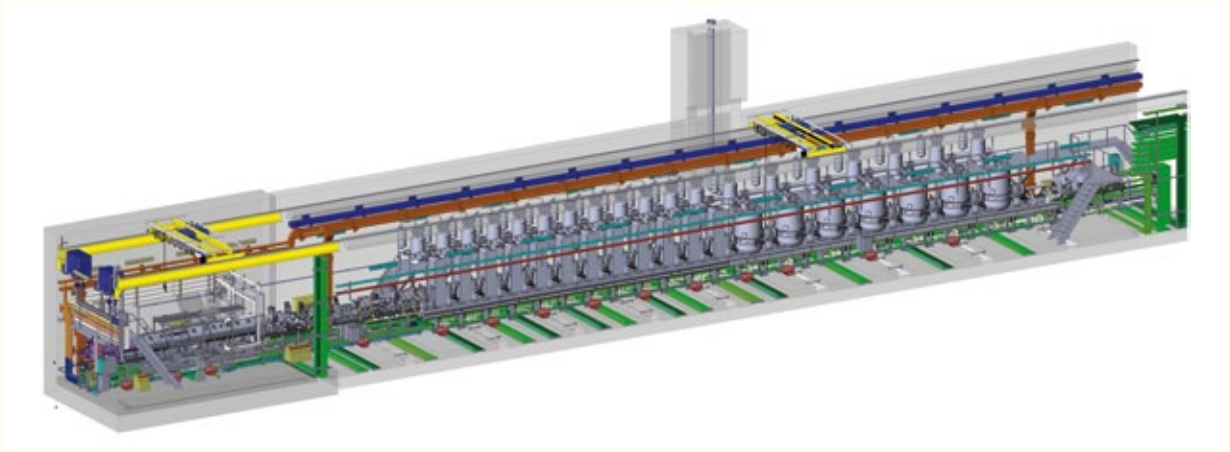

Figure 2.12. The light and heavy ion LINAC of the SPIRAL2 project at GANIL, Caen, France. It will be capable of delivering up to 5 mA deuteron beams at 40 MeV as well as light and heavy ion beams with up to 1 mA current at up to 14.5 MeV per nucleon.

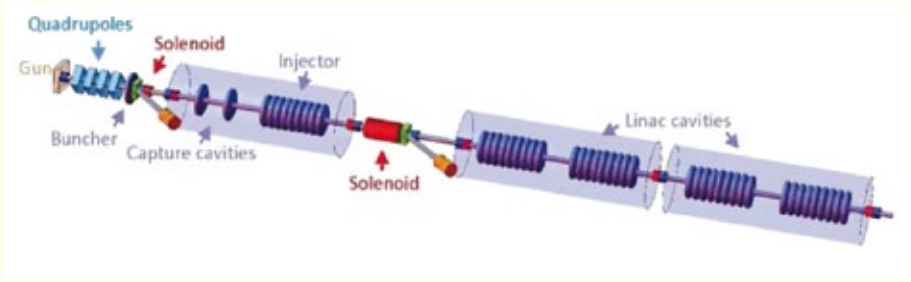

Figure 2.13. The 50 MeV electron linac at TRIUMF, Vancouver, Canada. Each 9-cell cavity will provide up to 10 MV at a length of 1 m.

radioisotopes. There is potential for radioisotope production by fast neutron irradiation ports in the future EURISOL and ESS facilities.

- While the time-averaged neutron flux of pure spallation neutron sources is generally lower than that of the highest flux research reactors, it can be further boosted by combination with a fissile core in so-called accelerator-driven subcritical (ADS) reactors. The future European ADS facility MYRRHA at SCK-CEN Mol in Belgium will provide very competitive thermal and fast neutron fluxes for radioisotope production and is foreseen to eventually replace the BR2 reactor for routine radioisotope production.

Gamma induced nuclear reactions

Electron beam generated Gamma rays via Bremsstrahlung can also be used directly for isotope production; (γ,n) reactions induced by 10 to 50 MeV electron beams and leading to isotopes like ^{103}Pd, ^{67}Cu or ^{111}In are being studied at Kharkov. Gamma rays can also be used to induce photo-fission, e.g. at ALTO-IPN Orsay and in the ARIEL project at TRIUMF where a 50 MeV electron linac will provide 10 mA of electron beam (see Figure 2.13).

A general drawback of gamma-ray induced reactions is their low cross-section, generally considerably lower compared to neutron-induced reactions. Moreover, in matter an incident gamma-ray beam will rapidly evolve to an equilibrium of gamma-rays and energetic electrons, the latter causing important energy deposition. Hence, as for charged particle beams the gamma ray fluxes usable with thick targets are inherently limited by the power that can be dissipated. Consequently the specific activity of radioisotopes produced in (γ,n) reactions is inherently limited. A possibility to overcome this limitation is the use of intense quasi-monoenergetic gamma beams to induce (γ,γ') or (γ.n) reactions resonantly at the appropriate energies. Such gamma beams can be produced by Compton backscattering of laser light from relativistic electron beams, e.g. at the future ELI-NP facility. Provided suitable resonant transitions are found, such a production will not compete in quantity with conventional radioisotope production but can give access to specific cases providing higher specific activity (e.g. ^{195}Pt(γ,γ')^{195m}Pt) or more efficient transmutation of special rare and/or radioactive targets, e.g. ^{226}Ra(γ.n)^{225}Ra as a source for the promising ^{225}Ac generator for targeted alpha therapy [Hab11].

2.3 Targetry for radionuclide production

The term "targetry" usually denotes complex systems for production of radionuclides via bombardment with charged particles (protons, deuterons, ^{3}He, α

etc.). Targets may be irradiated in all three phases – solid, liquid and gas. Charged particle beams are indispensable for production of all radionuclides used for positron emission tomography (PET) and many radionuclides for single photon emission computed tomography (SPECT) and for therapeutic purposes (e.g. α- and Auger emitters). The majority of accelerator-produced radionuclides is obtained in non-carrier-added quality. This parameter is undoubtedly very favourable for production of labelled compounds with high specific activity desirable for PET/SPECT diagnostics.

A target system should be optimised with respect to:

- physico-chemical form of the irradiated material (co-determines maximum applicable beam power, target processing and possible recycling of enriched materials)
- efficient cooling (co-determines maximum applicable beam power; it is provided not only by cooling systems, but also by mutual position of beam and target)
- design and automation (facilitates target handling and minimises personnel's radiation burden, allows for optimal recycling of enriched material, in particular gases)
- monitoring of parameters during irradiation (beam current, flow, pressure or temperature of cooling media, pressure in gas targets)

In the case of medical radionuclide production, much attention must be paid to optimising the yield while maintaining an acceptable radionuclidic purity by taking into consideration target enrichment. Another issue that must be solved is the optimal chemical form of a radionuclide resulting from its separation from the target matrix: it must be compatible with further production of a radiopharmaceutical. Finally, presence of chemical impurities in the target matrix and chemicals used for target processing must not exceed levels that could disturb labelling or cause toxic effects. Since many parameters, e.g. radionuclidic purity, are measured after the release of a radiopharmaceutical for use (it is in particular true for short-lived radionuclides), the whole production process must be validated and each batch of target material tested prior to regular production. Due to the routine character of radionuclide production for nuclear medicine, economic aspects play an important role in the choice for a complex solution of a target system, too.

For a given radionuclide and given production route there are four parameters available to increase the activity obtained at the end of irradiation:

- Enrichment of target isotope and use of pure element instead of its compounds.
- Entrance energy and the total beam energy loss in the target.
- Duration of bombardment.
- Beam current.

Enrichment applies to all polyisotopic elements and is directly related to economic aspects and technical feasibility. It improves yield and usually also the radionuclidic purity; on the other hand, it requires primary investment in expensive material, not always available, and its effective recycling. In many cases, it is the only way to accomplish radionuclidic purity that meets criteria for application in humans (e.g. production of ^{18}F from water highly enriched in ^{18}O, production of ^{123}I from highly enriched ^{124}Xe or ^{123}Te, and direct production of ^{99m}Tc from ^{100}Mo). Recycling is easiest in the case of gases, where cryogenic pumping allows for almost quantitative recovery of the enriched material (e.g. ^{82}Kr for production of ^{81}Rb or ^{124}Xe for production of ^{123}I). In contrast, recycling of solid targets is usually based on wet chemistry that results in losses of at least a few percent of the original amount. Liquids, like $H_2[^{18}O]$ for production of ^{18}F, can also be recycled quite effectively; however, losses are slightly higher than for gases. Among the chemical forms of target matrices naturally pure elements dominate, in particular metals with good thermal conductivity and sufficiently high melting points, or inert gases. However, sometimes oxides or other compounds of a target isotope display much better properties than the element itself (e.g. TeO_2 with ca 6% of Al_2O_3 forms a glassy material with much better thermal resistance than elemental ^{124}Te used for production of ^{124}I; enriched $^{76}SeO_2$ is also more suitable for production of ^{76}Br than elemental ^{76}Se and Cu_3As for the production of the same ^{76}Br via ^{3}He activation of monoisotopic arsenic).

The increase of the total beam energy loss in the target allows for better utilisation of the integral below the excitation function, but it has certain limits. The maximum available beam energy, e.g. compact cyclotrons for production of PET radionuclides, is limited to ≈19 MeV protons. A higher beam energy loss requires a thicker target layer, i.e. more material, often expensive, and more efficient cooling due to higher heat dissipation in the target layer. Finally use of a wider energy range may increase the production of radionuclidic impurities.

The time of bombardment (irradiation time) is also strongly related to production costs, since cyclotron operation is rather expensive. For shorter-lived medical radionuclides, irradiation longer

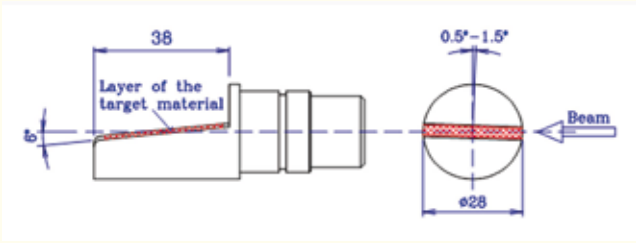

Figure 2.14. Example of a multipurpose internal slanted solid target with extremely low angle suitable for production of e.g. ^{67}Ga, ^{111}In or ^{201}Tl (Nuclear Physics Institute AS CR, v.v.i., Řež) [Leb05].

Figure 2.15. Liquid target (left) and its niobium chamber (right) for production of ^{18}F that can be also operated as solution target for production of ^{68}Ga or ^{86}Y (Nuclear Physics Institute AS CR, v.v.i., Řež).

than 1–2 half-lives generally brings little profit. For radionuclides with a half-life significantly longer than the irradiation time, the produced activity is almost directly proportional to the irradiation time.

Maximisation of the final variable, the beam current, is limited by the accelerator performance and by the targetry. Modern compact cyclotrons supply beams up to 1 mA. Due to this fact, the maximum applicable current is determined rather by the design and construction of a target system combined with the properties of the target layer.

There are several ways to classify targets and target systems. The most widespread are:

- According to their location with respect to the cyclotron (external or internal). Linear accelerators always use external targets.
- According to the phase (solid, liquid, gas).
- According to the position with respect to the beam (perpendicular or slanted, fixed or rotating).

Internal targets are located directly in the cyclotron chamber, and thus limited to solid targets. They can be designed as slanted targets with extremely low angles. An example is shown in Figure 2.14. Typical examples of internal slanted targets are production systems for ^{67}Ga, ^{111}In, ^{201}Tl or ^{211}At.

Modern compact cyclotrons accelerate protons and deuterons as negative ions and extract the beam via the stripping method, which results both in high efficiency and in flexible energy, varied by the stripper foil position. They usually offer only external target positions, either closely attached to the vacuum chamber (leaving practically no possibility to modify the beam parameters), or located at the end of a beam line whose elements allow for shaping the beam. The external location enables installation of all kinds of target systems, i.e. also liquid and gas targets, and application of helium cooling on solid target matrices or entrance windows.

The phase of the target matrix strongly influences the target's characteristics. Solid targets are preferably metallic layers with the best possible thermal contact with their backing. They are, therefore, frequently prepared by electroplating, vacuum evaporation or sputtering on a metallic backing with the best possible thermal conductivity. Some thick perpendicular targets have no backing and are directly cooled from the back during processing, only the activated layer is etched and used for separation of a radionuclide, and the target can then be re-used several times (e.g. irradiation of ^{nat}Ni with low energy deuterons for production of ^{61}Cu). Metals with poor thermal conductivity and/or low melting points, or non-metallic elements are often converted to their oxides, or more rarely to other inorganic compounds or alloys.

Liquid targets (see Figure 2.15) are usually metal chambers of a few millilitres volume closed by an entrance window. Recently, an interesting variation on liquid targets have attracted the attention of researchers: solution targets. These were successfully used for the pilot production of e.g. ^{86}Y from a concentrated solution of $^{86}Sr(NO_3)_2$ or ^{68}Ga from a concentrated solution of $^{68}ZnCl_2$, or for the production of ^{89}Zr from $^{89}Y(NO_3)_3$ solutions.

Gas targets are medium-pressurised vessels (usually at 5–15 bars) with a volume of a few tens of millilitres (see Figure 2.16). The shape of the target body is very often conic in order to compensate for the gradual increase of the beam diameter due to beam straggling in the gas filling, while minimising the chamber volume to spare enriched gas (e.g. ^{82}Kr for production of ^{81}Rb and ^{124}Xe for production of ^{123}I).

Operation and processing of both liquid and gas targets can be easily automated, including recycling of enriched filling. It significantly reduces radiation burden and shortens the whole process, something that is particularly favourable for short-lived radionuclides.

Another aspect related to targetry is the positioning of a target in the beam, as this affects the

Figure 2.16. Disassembled external gas target system filled with highly enriched ^{82}Kr for production of ^{81}Rb (top) and its position on an external beam line of the cyclotron U-120M (bottom); a similar target filled with ^{124}Xe is used for production of ^{123}I (Nuclear Physics Institute AS CR, v.v.i., Řež).

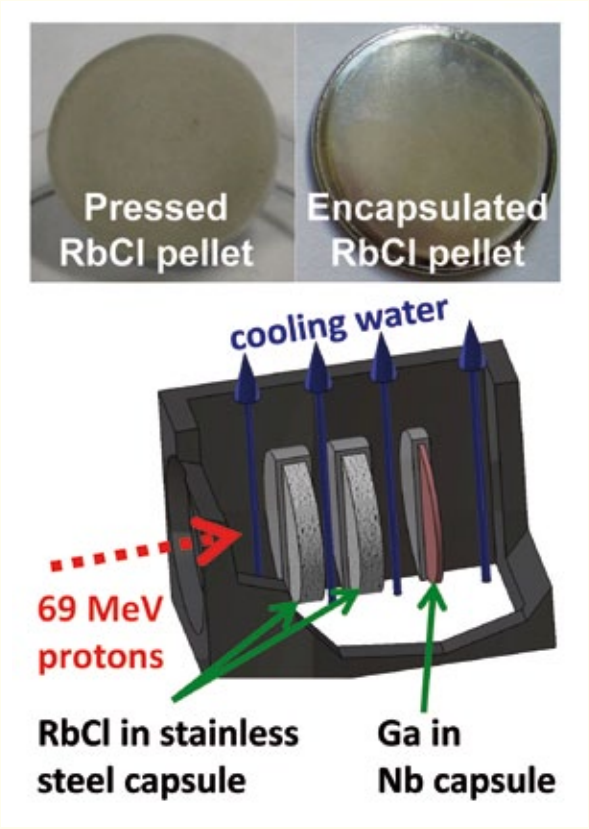

Figure 2.17. Example of an external perpendicular solid target system with 4π water cooling of two stainless steel capsules with RbCl targets for ^{82}Sr production and an additional niobium capsule with a Ga target for ^{68}Ge production (ARRONAX Nantes).

cooling efficiency and the necessary amount of target matrix. Slanted targets (also called tangential or grazing angle targets) are a good choice for solid targets irradiated with high currents. Small angles project the beam diameter on a larger target surface, thereby reducing the heat power per unit of area and the target thickness required for optimal beam energy loss. Both factors improve cooling and increase the maximum applicable beam current, especially for target matrices of low thermal conductivity. Cyclotron production of ^{99m}Tc would require external slanted, high-current targetry that can dissipate up to 12 kW of heat. Automated transport of the irradiated target to processing in hot cells is obviously mandatory in such cases.

For completeness, we mention the possibility of rotating the target or the beam to spread the power deposition over the target surface.

In routine cyclotron production of medical radionuclides, the incident projectile energy only rarely goes beyond 40 MeV, except for cases such as ^{82}Sr production (see Figure 2.17). This means that only a few reaction channels that potentially contribute to formation of significant radionuclidic impurities are opened. With rising projectile energy, more and more reaction channels are opened leading to a mixture of different product nuclei. This allows the system to range further from the valley of beta-stability thereby forming more exotic radionuclides. But the gain in usable target thickness and higher product yield is accompanied by a reduction in selectivity. In the extreme case of very high projectile energy (GeV protons) very thick targets (tens of g/cm^2) can be irradiated and via fragmentation, spallation and fission reactions virtually all isotopes from hydrogen up to the target element are produced simultaneously. In this case, it is necessary to combine mass separation with chemical separation to be able to extract single radionuclides. In the so-called isotope separation on-line (ISOL) method even very short-lived isotopes are accessible; moreover this method provides radionuclides of almost carrier-free quality.

3. Examples and specific topics

3.1 Examples of success of nuclear medicine applications versus conventional (non-nuclear) treatments

SPECT and PET imaging play an important role in the correct staging of disease and, for certain cancer types, also in the early detection of recurrence. Correct disease staging helps to avoid needless operations which might be aggravating for the patient and are costly for the healthcare system. The clinical value and cost-effectiveness of myocardial perfusion imaging has been reviewed, for example, in [Mar08] and application of PET and PET/CT in cancer management is discussed in [Buc10].

Gastroenteropancreatic neuroendocrine tumours (GEP-NET) frequently show overexpression of peptide receptors that can be targeted by radiolabelled somatostatin analogues. This so-called PRRT (peptide receptor radionuclide therapy) is today considered the best systemic treatment option for surgically unremovable GEP-NET. Clinical phase II and III trials were performed with ^{90}Y and ^{177}Lu labelled DOTATOC and DOTATATE. The results of these treatments, for example with ^{177}Lu-DOTATATE, compare very favourably with alternative (chemotherapeutic) treatments: median progression-free survival of 32 months vs. 3 to 18 months [Kwe08]. Side effects are mild and reversible and quality-of-life of the patients is improved [Kha11].

Lymphoma is a blood cancer affecting the white blood cells. B cells show overexpression of the CD20 antigen that can be targeted by appropriate antibodies. Zevalin (^{90}Y-ibritumomab) has demonstrated excellent results in a randomised phase III trial of patients with advanced follicular lymphoma that were either treated by an induction treatment (chemotherapy) plus Zevalin or the induction treatment alone. Treatment with Zevalin showed a complete remission rate of 87% after 3.5 years [Mor08]. Median time to next treatment was 8.1 years for patients treated with Zevalin versus 3.0 years for the control group [Mor13]. Promising results were also obtained in trials using Zevalin or Bexxar as first line therapy of lymphoma [Bod13]. Bexxar (^{131}I-tositumomab) is an alternative radioimmunotherapy that is mainly employed in the USA but not in Europe due to radiation protection restrictions requiring longer hospitalisation and isolation after ^{131}I treatment.

Medullary thyroid carcinoma is a rare form of thyroid cancer that does not respond to normal radioiodine treatment. Apart from surgical extraction of visible metastases no durable treatment options exist for this type of cancer. Treatment with ^{131}I-anti-CEA antibody provided an overall survival of 110 months versus 61 months for the control group [Cha06].

Standard treatment of colorectal cancer that has developed liver metastases is surgical resection of the metastases but additional chemotherapy did not show improved survival. A small trial demonstrated that additional treatment with ^{131}I-labetuzumab provides an improved survival of 58 months versus 31 months in the control group [Lie07].

Bone metastases occur frequently in the late stage of prostate cancer and other cancers. Deaths from prostate cancer are often due to bone disease and its complications. The definition of "symptomatic skeletal event" covers very serious events such as spontaneous bone fractures or spine compression leading to paralysis, severe pain requiring external beam therapy for pain management or tumour-related orthopaedic surgical intervention. These events are decisive for the quality of life of a cancer patient.

The alpha emitter Xofigo ($^{223}RaCl_2$) used against bone metastases from metastatic prostate cancer demonstrated in a recent phase III clinical trial a median overall survival benefit of 3.8 months (14.9 versus 11.3 months) [Par13]. The time to the first "symptomatic skeletal event" was 15.6 versus 9.8 months [Par13], a significant gain in particular when considering the impact on the quality of life. No other therapy modality has provided similar success in this disease. In 2013 Xofigo was approved for sale in the USA and Europe. At present new trials are underway where the treatment is not stopped after six cycles (previous trial) but continued in regular intervals and where combination treatments with other drugs are explored. It is expected that these modifications could further improve the outcome.

3.2 Statistics of radionuclide use in Europe: evolution and trends

In the previous chapters we discussed a large variety of nuclear medicine procedures and the methods that are used to produce the relevant radionuclides. However, in present clinical practice the frequency of use is highly variable. Making an assessment of possible future trends in radionuclide needs requires first of all a comprehensive view of the past and present use. Unfortunately, regular and detailed data on the number of nuclear medicine procedures and consumed radionuclides is only available for few European countries. The DDM2 project [DDM2] made a huge effort to gather precise data for the frequency, employed activity and radiation doses for the most important diagnostic procedures in Europe. It is thus the best publicly accessible data source for a comprehensive comparison provided some caution is taken in the interpretation.

The year of data collection varied considerably between the countries participating in DDM2, ranging from 2004 (for the UK) to 2011. This may induce a strong bias for procedures and radionuclides with rapidly changing consumption. For example, in most countries the use of PET doubled within three to six years, hence the bias due to the differing reference years can reach a factor two to four. Also ^{99m}Tc consumption may differ significantly before, during and after the ^{99}Mo crisis.

Where possible the data taken from the DDM2 draft report were complemented with additional, more recent data obtained from national sources. See "Contributors" at the end of this chapter for a listing of persons and institutions that provided valuable input. No data was available for Belgium. Thus, as approximation the Belgian contribution to the European average was estimated taking the same per capita use as Luxembourg. This appears justified since data from the previous Dose Datamed 1 project (1998-2002) show that Belgium had similar or higher per capita use of nuclear medicine procedures than Luxembourg.

For FR, IT and UK the number of PET procedures in 2010 was updated from [Ste11], even if the methodology of this reference is not fully traceable.

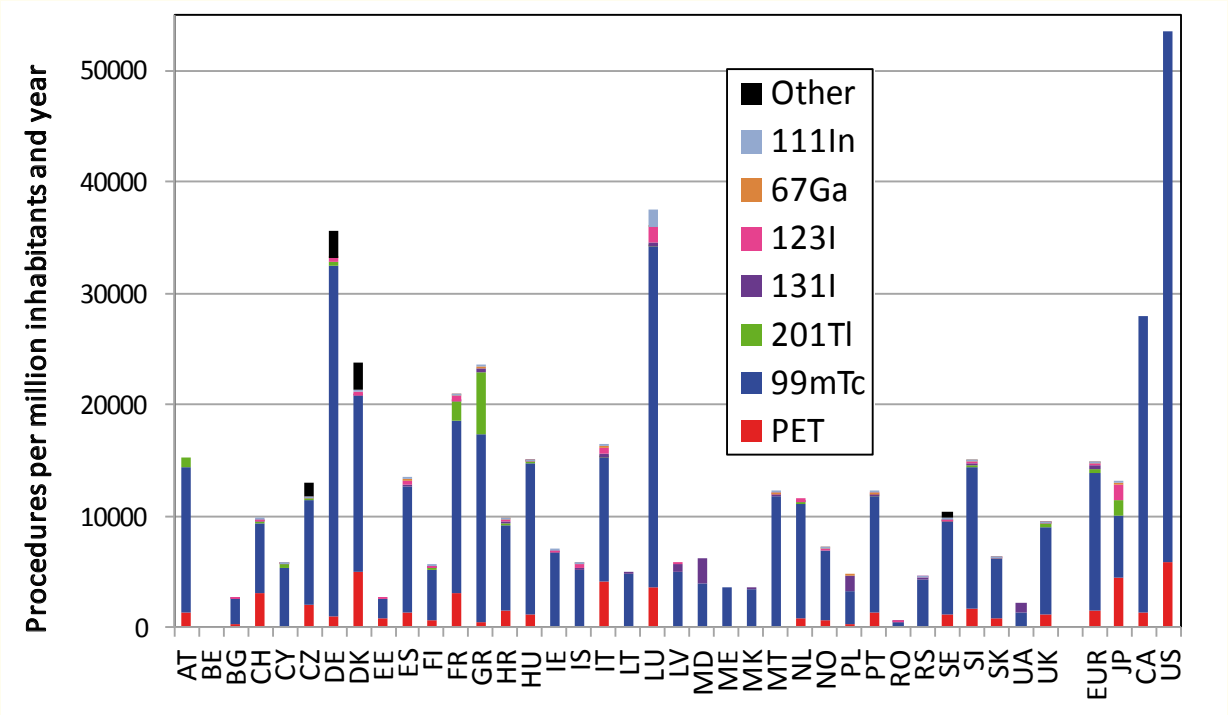

Figure 3.1. Use of diagnostic radioisotopes in European countries, Japan, Canada and the USA.

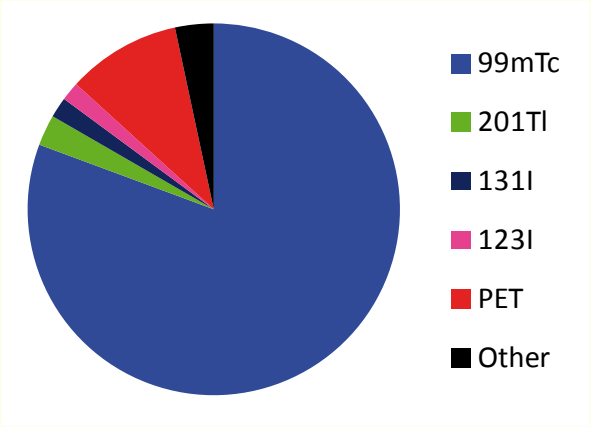

Figure 3.2. Cumulative distribution of radionuclides used in Europe.

Figure 3.1 shows the number of diagnostic nuclear medicine procedures as a function of radionuclide in Europe, the United States and Canada (both only PET and ^{99m}Tc) and Japan. Figure 3.2 shows the European average which is dominated by 80% ^{99m}Tc and about 10% PET isotopes. For certain countries "other" also contains diagnostic procedures that use small activities of radiotracers for ex vivo counting (see section 1.3).

In addition statistics were collected for therapeutic radionuclides which were not covered by DDM2. Again a country-dependent bias cannot be excluded since certain procedures (such as SIRT and radiosynovectomy) are not always included.

Detailed time series covering five or more consecutive years are so far only available for a few countries: CH, CZ, DE (only stationary hospital patients), DK, EE, ES, GR, LV, MK, SI and Bavaria as well as the non-European comparator Japan. These data cover less than 20% of the European population base and do not allow determination of a meaningful arithmetic average. Still, some trends are evident and consistent in most of these countries.

Overall there is a continuous rise in nuclear medicine procedures, in particular in countries with cost-conscious healthcare systems that are orienting their healthcare expenses towards cost-effective diagnostic and therapeutic procedures. However, the evolution varies considerably for different radioisotopes.

Among single photon emitters the use of ^{123}I has risen over the last decade, while a decline is observed for ^{201}Tl and, even more pronounced, for ^{133}Xe and ^{67}Ga. In lung ventilation studies ^{133}Xe is being replaced by Technegas or ^{81m}Kr respectively and ^{67}Ga is being replaced as an inflammation marker by PET tracers or ^{99m}Tc labelled leucocytes. The use of ^{201}Tl for myocardial perfusion imaging is declining despite recent replacement effects during the ^{99m}Tc crisis. The corresponding ^{99m}Tc radiotracers (MIBI and Tetrofosmin) provide often superior imaging results and give a lower radiation dose to patients.

The number of PET procedures showed a rapid rise in the last decade (about 20% per year) that is correlated with the number of installed PET scanners. Certain PET radiopharmaceuticals have unique properties (FDG, FLT, and so forth) while others can provide superior results with respect to the corresponding SPECT tracers (^{68}Ga vs. ^{111}In, ^{18}F- vs. ^{99m}Tc-phosphonates, etc.). Thus, whenever new PET scanners are installed they are soon extensively used. Based on the countries where detailed statistics are available, more than 90% of PET procedures are performed with ^{18}F-tracers, and these are largely dominated by FDG. Next are ^{11}C-tracers and ^{68}Ga that showed the most rapid rise among PET isotopes in recent years. ^{82}Rb, a PET tracer for myocardial perfusion, does not yet show up in European statistics since ^{82}Sr/^{82}Rb generators are only available at a

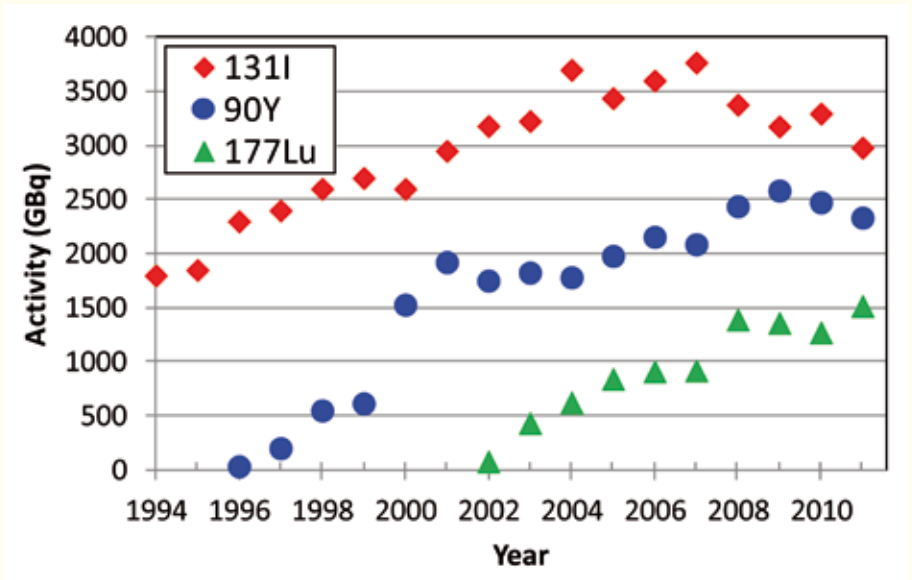

Figure 3.3. Evolution of the use of the three most important therapy isotopes in Switzerland.

few European hospitals. It is clearly a supply-limited issue: if more generators become available more ^{82}Rb will be used (see section 3.7).

Therapy procedures are still largely dominated by ^{131}I for thyroid treatment. As an example for the temporal evolution of the use of therapy isotope, Figure 3.3 shows data from Switzerland where excellent statistics are available from the FOPH (Federal Office of Public Health). Moreover, the University Hospital of Basel is one of the European pioneers in novel radionuclide therapies: ^{90}Y-DOTATOC, first for treatment of gliomas (by locoregional administration) then for neuroendocrine tumours, later complemented by ^{177}Lu-DOTATOC. Zevalin (^{90}Y-ibritumomab) and ^{177}Lu-rituximab are used for treatment of lymphomas. The statistics of this "early adopter" can thus provide guidance for the future of therapeutic radionuclides in other countries, once the corresponding radiopharmaceuticals become approved for regular use.

To summarise the future prospects of radionuclide isotopes for nuclear medicine: the most important rise in relative terms is expected for newly approved PET and SPECT tracers and even more for new therapeutic radionuclides. Many of these are so far only available in a few hospitals in the frame of clinical trials. Once approved as certified radiopharmaceuticals they can be applied in more hospitals and more countries. Thus in the next decade the worldwide use of ^{90}Y (for SIRT, PRRT and RIT), ^{177}Lu (for PRRT and RIT) and of ^{223}Ra (for bone metastases) is expected to rise rapidly and might eventually overtake that of ^{131}I.

3.3 ^{99}Mo/^{99m}Tc supply issues: reactor vs accelerator

Today the worldwide supply of ^{99}Mo relies on a limited number of research reactors and processing facilities. Its production is essential for providing nuclear medicine with ^{99m}Tc in the form of ^{99}Mo/^{99m}Tc generators. Technetium-99m itself is used in more than 80% of diagnostic nuclear imaging procedures. These applications represent approximately 30 million examinations worldwide every year. Therefore, a weekly ^{99}Mo production of about 10.000 Ci '6-day' calibrated (i.e. 6 days after the end of processing) is required to supply North America (53%), Europe (23%), Asia (20%) and the rest of the world (4%). The 10.000 Ci '6-day' calibrated represents a ^{99}Mo activity of about 85.000 Ci (3100 TBq) to be produced at the end of irradiation, depending on the time needed for processing and shipment. Given the short half-lives of ^{99}Mo (66 hours) and its daughter ^{99m}Tc (6 hours), a continuous supply of ^{99}Mo/^{99m}Tc generators to hospitals or central radiopharmacies is required (Figure 3.4).

Today only eight research reactors are involved in the large scale production (>95% of world supply) of ^{99}Mo: NRU (Canada), HFR (The Netherlands), BR2 (Belgium), OSIRIS (France), SAFARI (South Africa), MARIA (Poland), LVR-15 (Czech Republic) and OPAL (Australia). They irradiate highly (HEU) and/or low enriched uranium (LEU) targets from which the ^{99}Mo is subsequently extracted in four processing facilities: AECL/NORDION (Canada), MALLINCKRODT (The Netherlands), IRE (Belgium) and NTP (South Africa). Worldwide ^{99}Mo production is presently being converted from HEU to LEU targets to address non-proliferation policy issues*.

The main actors in the supply chain (research reactors, processing facilities and ^{99}Mo/^{99m}Tc generator manufacturers) are represented in the Reactor and Isotopes Working Group of the Association of Imaging Producers and Equipment Suppliers (AIPES). Their priority is to achieve optimal coordination of their operating periods to ensure a secure supply of ^{99}Mo worldwide. However, the current

* It has to be stressed that it is indeed a pure policy issue and *not a real proliferation risk* since one ^{99}Mo production target contains just 4 grams of ^{235}U while many thousands of such targets would be needed to make a nuclear bomb.

Figure 3.4. The pathway of the produced ^{99}Mo/^{99m}Tc from the irradiation facilities to the users.

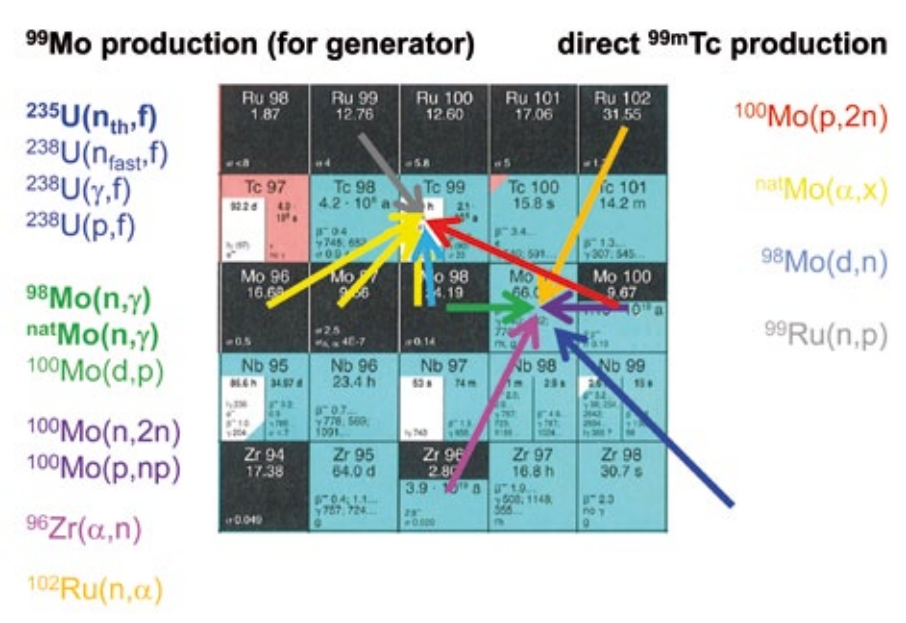

Figure 3.5. Selection of nuclear reactions leading to ^{99}Mo or ^{99m}Tc respectively.

Back to the roots

The chemical element technetium was discovered in 1936 by Carlo Perrier and Emilio Segrè who separated technetium isotopes chemically from a molybdenum foil that had served as deflector (and became thereby irradiated) in Ernest Lawrence's famous cyclotron. Over recent decades ^{99m}Tc, the workhorse of nuclear medicine, was exclusively produced in nuclear reactors. Today nuclear physicists are in the process of industrialising an alternative method to produce ^{99m}Tc for Canada by... irradiating molybdenum foils in cyclotrons.

fleet of research reactors is ageing and some of them are expected to stop irradiating targets for ^{99}Mo production within the decade.

Since 2008 several severe shortages have been experienced in the supply of ^{99}Mo and ^{99m}Tc [Pon10]. For this reason, the High-Level Group on the Security of Supply of Medical Radioisotopes (HLG-MR) was created in 2009 by the OECD/NEA. Practical measures – near, medium and long term – have been identified for a reliable supply, including significant changes in the economic structure [NEA11]. Six principles have been established to address the key issues for a secure supply of ^{99}Mo/^{99m}Tc, including the implementation of full-cost recovery, reserve capacity, etc. [NEA12].

Furthermore, in 2012 the European Commission created the "European Observatory on the Supply of Medical Radioisotopes" to support actions relating to urgent issues concerning the ^{99}Mo/^{99m}Tc supply chain that directly impact on healthcare needs. Europe is planning to develop replacement irradiation capacity based on conservative production technologies (fission of ^{235}U), involving the challenging conversion to LEU targets by 2015. The FRM-II reactor (Garching, Bavaria) is developing an irradiation capacity for the irradiation of LEU targets from 2015. The OSIRIS reactor is scheduled to shut down at the end of 2015, but will be replaced in 2017 by the JHR reactor that is currently under construction in Cadarache (France). Other replacement projects are currently being investigated such as PALLAS (The Netherlands) and MYRRHA (Belgium) to replace HFR in 2022 and BR2 in 2023, respectively [Kri13]. In the meantime the annual irradiation capacity of BR2 is being increased. In Australia ANSTO is building a large ^{99}Mo separation plant to fully exploit the production capability of the OPAL reactor. Other countries like Russia, China, Argentina, Brazil and the Republic of Korea have also projects for the construction of new reactors and new ^{99}Mo processing facilities which would be commissioned in the period 2016 to 2018.

The recent supply shortages also raised interest in alternative production routes of ^{99}Mo and ^{99m}Tc. Besides ^{235}U fission in nuclear reactors the following major options were identified (Figure 3.5):

- Production of ^{99}Mo by neutron activation of ^{nat}Mo or ^{98}Mo via the ^{98}Mo(n,γ) reaction.
- Direct cyclotron production of ^{99m}Tc via the ^{100}Mo(p,2n) reaction.
- Cyclotron production of ^{99}Mo in ^{100}Mo(p,pn), ^{100}Mo(p,2p), ^{98}Mo(d,p) or ^{100}Mo(d,t) reactions.
- Photofission ^{238}U(γ,f) or the photonuclear reaction ^{100}Mo(γ,n) resulting in ^{99}Mo.
- Neutron induced fission of ^{235}U by accelerator-driven neutron sources.
- Production of ^{99}Mo in the ^{100}Mo(n,2n) reaction.

Non-fission routes have the advantage of radioactive waste reduction since mainly or only ^{99}Mo is produced but no fission products. On the other hand, they result in low specific activity of ^{99}Mo where the ^{99}Mo is typically diluted with a thousand times more stable molybdenum compared to fission production and most of these routes prefer or require highly enriched ^{98}Mo or ^{100}Mo respectively. These drawbacks stimulated interest in the study of suitable generator matrices with high sorption capacity and low breakthrough of ^{99}Mo [Das13] as well as in efficient recycling of ^{98}Mo or ^{100}Mo respectively.

The ^{100}Mo(p,2n) reaction allows cyclotron production of ^{99m}Tc. Using high-current cyclotron targets, one could obtain up to 2 TBq of ^{99m}Tc at the end of irradiation (proton energy 24 MeV, beam current 500 μA, irradiation time 6 h). Assuming another 6 hours for target processing, packing, quality control and transport, one could provide up to 1 TBq of ^{99m}Tc to nuclear medicine departments, i.e. typically the daily need of a large metropolitan area. The Government of Canada has decided that the NRU reactor – a major player in the supply chain – will stop its global ^{99}Mo production in 2016. To cover domestic needs the Canadian Government has funded efforts to establish the feasibility of accelerator production of ^{99}Mo and ^{99m}Tc respectively. Thus one consortium, led by the Canadian Light Source, is working on the photonuclear reaction ^{100}Mo(γ,n)^{99}Mo driven by 40 kW electron accelerators. Two consortia (led by TRIUMF and ACSI respectively) are preparing a fleet of existing and new cyclotrons plus the related target and Tc extraction technology for direct ^{99m}Tc production via the ^{100}Mo(p,2n)^{99m}Tc reaction. The joint use of the same cyclotrons for production of ^{99m}Tc (during the night) and PET radionuclides (during the morning and day) helps reduce investment and operation costs. The optimum proton energy (between 16 and 30 MeV) for ^{99m}Tc production is still under debate [Leb12]. The ^{99m}Tc yield increases with energy but the specific activity of ^{99m}Tc decreases and might become too low for the labelling of certain kits [Qai14].

Various projects are underway in the USA to set up domestic ^{99}Mo/^{99m}Tc production. The most advanced project will irradiate natural Mo or enriched ^{98}Mo in the MURR reactor in Columbia (Missouri). As for cyclotron production, the ^{99m}Tc will be extracted from this low specific activity ^{99}Mo with automated two-column selectivity inversion generators. A longer-term project aims at also using the photonuclear reaction ^{100}Mo(γ,n) ^{99}Mo.

Another project proposes critical LEU solution reactors, so-called aqueous homogeneous reactors. These have to be kept critical for a couple of days, then the produced high specific activity ^{99}Mo is extracted from the liquid core.

A variant is the SHINE (Sub-critical Hybrid Intense Neutron Emitter) project that aims at using electrostatic accelerators to send an intense (100 mA) low energy (300 keV) deuteron beam onto a tritium gas target for production of 14 MeV neutrons that irradiate in turn undercritical LEU solutions to produce ^{99}Mo.

It should be noted that the boundary conditions for ^{99m}Tc use are significantly different in various regions. In North America the ^{99}Mo/^{99m}Tc generators are placed in radiopharmacies which extract the ^{99m}Tc and ship it to the end users. Thus a change of generator technology or a switch to direct ^{99m}Tc production is easier to implement since it affects only the radiopharmacies but not directly the end users. However, in Europe and other regions the ^{99}Mo/^{99m}Tc generators are shipped to the end users without intermediate radiopharmacies. Hence, cyclotron production of "instant ^{99m}Tc" would require a radical change of the distribution logistics: one or more daily shipments of ^{99m}Tc instead of a once weekly delivery of a generator. Hence, in particular for remotely located users with fewer patients per day, there is a risk that transport costs may far exceed production costs of ^{99m}Tc.

^{99m}Tc is in the middle of the chart of nuclides, surrounded by stable isotopes. Consequently there are many possible nuclear reactions that result in formation of ^{99m}Tc or its precursor ^{99}Mo. However, only a small fraction of these reactions can be seri-

Megatons to Megacuries

With the end of the cold war and the signature of the nuclear disarmament treaties between the US and the Soviet Union, many nuclear warheads had to be dismantled. To ensure truly irreversible disarmament 20,000 warheads, each containing on average 25 kg of highly enriched uranium, were dismantled and the nuclear contents "mixed" with natural uranium to produce fuel for nuclear power stations. In addition to this famous "Megatons to Megawatts" programme, disarmed warheads also serve as fuel for high flux reactors and as targets for ^{99}Mo production. Every year several ten kg HEU are used for ^{99}Mo production targets and several hundred kilograms for fuel elements of high flux reactors producing medical isotopes. Thus, disarmament helps medical isotope production and the latter contributes to durable disarmament!

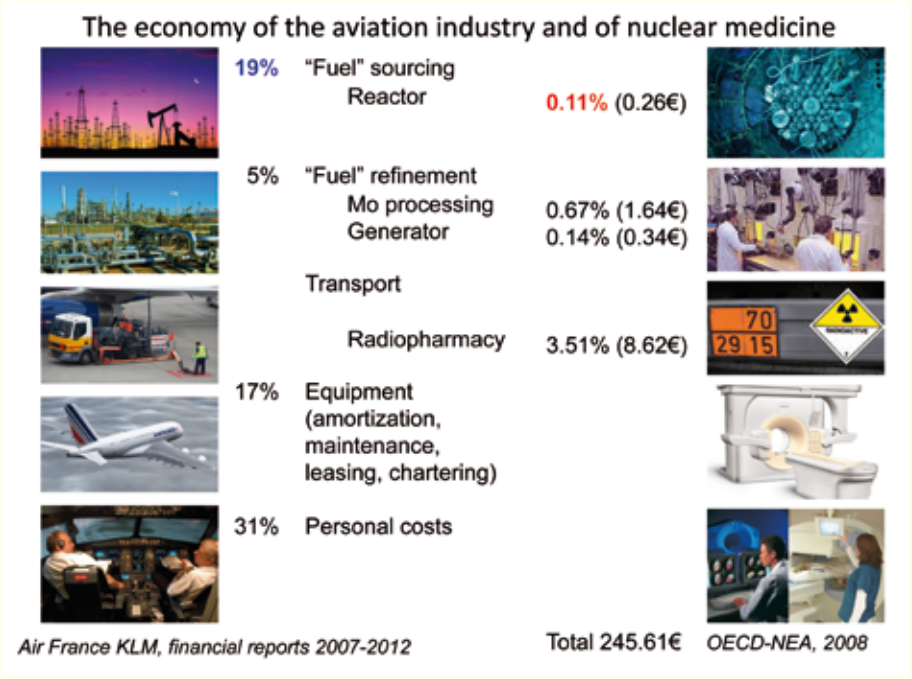

Figure 3.6. The economy of nuclear medicine compared to the aviation industry. The numbers for nuclear medicine were taken for an average ^{99m}Tc scan from [NEA10], while for the aviation industry costs an average from 2007 to 2012 was taken from the annual reports of Air France/KLM and the refinery margin for kerosene (from www.eia.gov) was averaged from 1995 to 2011.

ously considered for industrial production. Before a new method can contribute to industrial radionuclide production it has to be demonstrated that its product satisfies the established quality criteria and often the new method has to be included in the drug master files of the respective radiopharmaceuticals. The administrative effort of validating and adding a new method is only justified if it can contribute substantially to regional or global demand. The huge demand for ^{99m}Tc puts this hurdle quite high. Secondly a new method has to demonstrate that it is economically viable, an aspect directly related to the market value of the radionuclide.

Economic issues of radionuclide production

Nuclear medicine is today recognised as an essential and cost-efficient method of supporting a variety of disciplines in medicine or achieving therapeutic success where other methods fail. Nuclear medicine uses high tech equipment (SPECT-CT, PET-CT, PET-MR, etc.), requires specific "fuel" (the radionuclides) that is carried by special dangerous goods transporters to its destination and needs highly trained experts (medical doctors, nuclear medicine technicians) to provide regular and safe service to millions of users. It is instructive to compare this situation to the aviation industry that also uses high tech equipment (airplanes), specific "fuel" (kerosene) that is brought by dangerous goods transporters to its destination and highly trained experts (pilots, air traffic controller, etc.) to provide regular and safe service to millions of users. Note that both activities are highly regulated, subject to various supervisory bodies and the personnel involved are often exposed to enhanced radiation doses while exercising their profession. Figure 3.6 shows a comparison of the cost distribution in both fields.

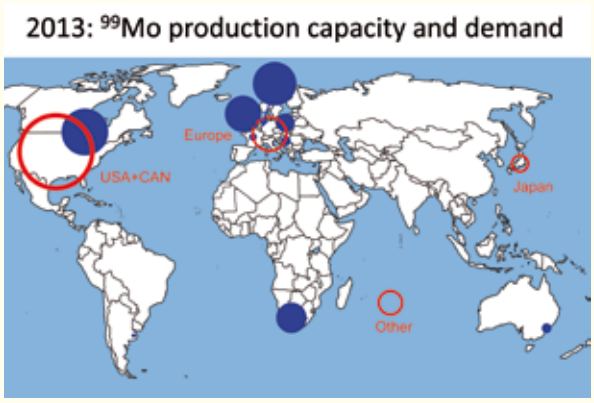

Figure 3.7. Present ^{99}Mo production capacity and demand. The diameter of the blue circles is proportional to the annual production capacity of the reactors (BR2 and HFR shifted for visibility) and the diameter of the red circles is proportional to the consumption in a given region.

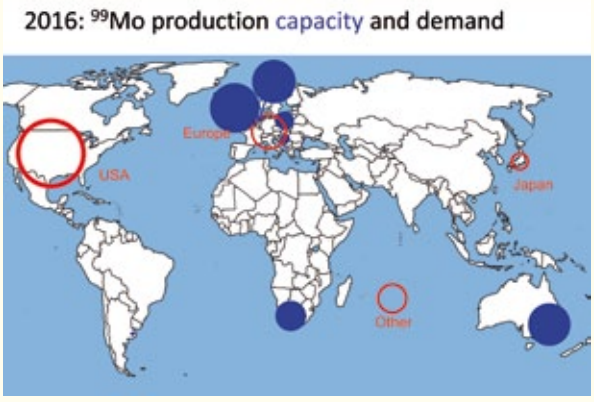

Figure 3.8. Expected ^{99}Mo production capacity and demand end of 2016. Canada is assumed self-sufficient by cyclotron production of ^{99m}Tc, reducing the demand for ^{99}Mo accordingly. At present it cannot be judged reliably which of the proposed US projects can be operational by 2016.

While "fuel" costs represent about a quarter of the expenses in aviation, in nuclear medicine they are less than 1% in the case for ^{99m}Tc scans. This suggests that perhaps the value of radionuclides, the "fuel" in nuclear medicine, is not widely appreciated. In many countries the radionuclides used in a nuclear medicine procedure are not reimbursed directly, but are considered as a simple auxiliary material similar to disposable syringes, plasters of bandages. It is mainly this economic aspect, and not physical or technical problems, that has been the root cause for occasional radionuclide supply disruptions in the past. When discussing the prospects of other promising radionuclides that have advantageous properties for the patient, for radiation protection issues, and for overall cost-effectiveness, it must be made clear that these cannot be introduced or reach the use they deserve unless the essential value of radionuclides in nuclear medicine therapies is better recognised and acknowledged by healthcare systems!

It is noteworthy that the average OECD costs of a ^{99m}Tc diagnostic procedure given above are largely exceeded in countries with different structures of the healthcare system such as the USA, Japan, Switzerland, Germany and some Scandinavian countries. Interestingly none of these countries supports at present their own ^{99}Mo or ^{99m}Tc production. Therefore there appears (see Figures 3.7 and 3.8.) a clear risk that in times of global undersupply the market would favour delivery to certain "non-producers" if no political action is taken.

3.4 Theranostics

As Paracelsus, a cofounder of modern medicine, had already recognised in 1538: "All things are poison and nothing is without poison. Only the dose makes that a thing is not poisonous." This principle applies in particular for all cancer therapies: in general a low dose does not cause a durable therapeutic effect since the cancer cell's repair mechanisms recover from small damage completely. A sufficiently high dose can destroy all cells without the possibility of recovery. With medium doses a proportion of the cells may be destroyed, while a proportion are repairable. Rising doses provide higher therapeutic effect but also higher side effects. Any therapy tries to stay in the middle range, the so-called "therapeutic window" where a good therapeutic effect is achieved with acceptable side effects. More targeted ("selective") therapy allows better concentration of the poison on the cancer cells, thus the curves of therapy effect and side effects are better separated and the therapeutic

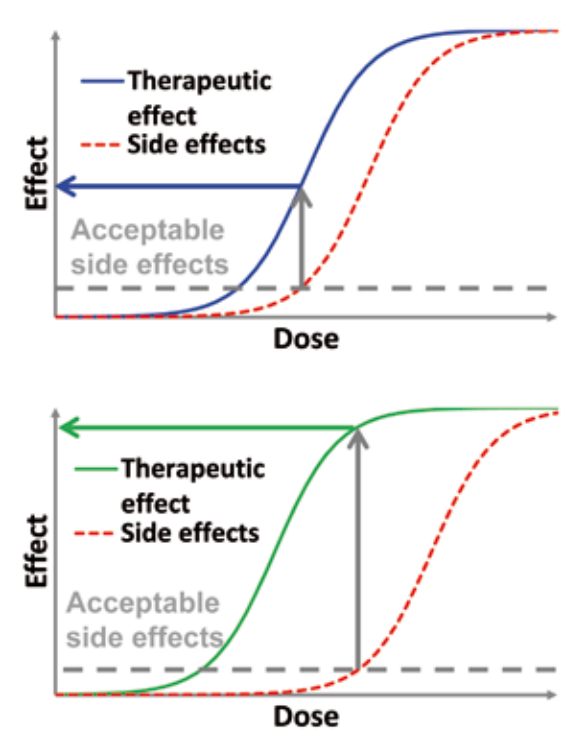

Figure 3.9. A more selective pharmaceutical (right side) provides a larger therapeutic window, i.e. gives better therapeutic results at a dose that causes acceptable side effects.

window becomes wider (Figure 3.9). Thus, at a given therapeutic result the side effects are reduced or at a given level of side effects the therapeutic success can be improved respectively. Thus highly selective therapy is best for the patients. These general considerations are valid for all types of therapy, but in particular for nuclear medicine therapies.

The abundance of certain tumour markers may differ from one patient to another. Therefore it is crucial to verify before a selective therapy that the required marker is present in sufficient abundance. This is done by injecting a PET or SPECT isotope coupled to the targeting vector in question. Thus uptake into the tumour can be visualised and unwanted excessive uptake in healthy tissue can be excluded. Only after this verification the therapy dose consisting of a therapeutic isotope coupled to the same targeting vector is injected. This ensures that only those patients are treated who will most likely benefit from the treatment. PET even enables a quantitative analysis of the scout dose, i.e. the concentration of the targeting vector in the tumour and in dose-limiting organs can be quantified and used to adapt the therapy dose individually, thereby making optimum use of the therapeutic window. This method of personalised medicine is called theranostics (from 'therapy based on diagnostics') [Bau12]. Also for non-radioactive therapeutics it would be preferable to know the tumour uptake before the treatment, but without radioactive probes this is

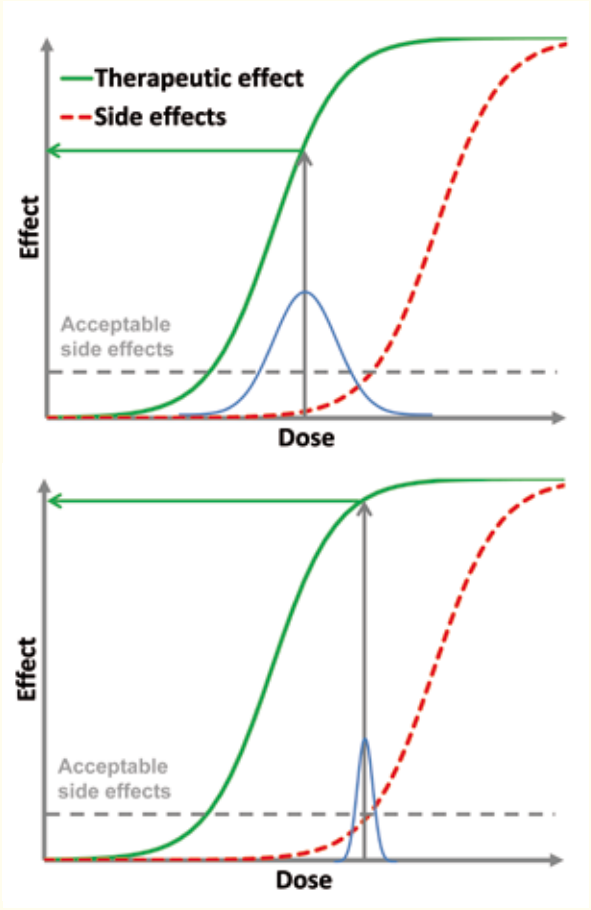

Figure 3.10. Principle of theranostics: the distribution of pharmaceuticals varies from patient to patient, thus for a given administered amount (mass of normal pharmaceuticals, activity for radiopharmaceuticals) the resulting dose scatters correspondingly (blue curve). With patient-specific theranostics the scatter of the dose is reduced and a better therapeutic effect can be achieved.

difficult to realise non-invasively (i.e. without surgical sampling). Thus the use of radioactive probes allowing non-invasive studies represents a decisive advantage of nuclear medicine.

In clinical trials the maximum tolerated dose (MTD) is determined as the amount that does not lead to excessive side effects and is fixed for the clinical application. This concept will obviously lead *on average* to an under-treatment and thus to a reduction of the therapy success. The distribution of pharmaceuticals varies from patient to patient (see Figure 3.10). By measuring the real distribution in an *individual patient* before the therapy, the administered amount can be tailored accordingly to achieve the optimum dose and improve the success of the therapy.

Obviously the theranostics approach relies on the fact that the scout dose of the imaging isotope and the therapeutic dose behave the same way in vivo. Ideally one should use radioisotopes of the same element to ensure identical biochemical behaviour. This explains the particular interest for so-called "matched pairs" of one diagnostic and one therapeutic isotope of the same element. Real matched pairs are ^{123}I (SPECT) or ^{124}I (PET) with ^{131}I (β^-) or ^{125}I (Auger), ^{86}Y (PET) with ^{90}Y (β^-), ^{61}Cu or ^{64}Cu (PET) with ^{67}Cu (β^-), ^{44}Sc (PET) with ^{47}Sc (β^-) or ^{203}Pb (SPECT) with ^{212}Pb (α). There is even one element with a "matched quadruplet" that covers all decay modes used in nuclear medicine: ^{152}Tb (PET) or ^{155}Tb (SPECT) with ^{161}Tb (β^- plus Auger) or ^{149}Tb (α). If real matched pairs are not available one often resorts to "nearly matched pairs" of radioisotopes from chemically similar elements, e.g. ^{99m}Tc (SPECT) with ^{186}Re or ^{188}Re (β^-), ^{111}In (SPECT) or ^{68}Ga (PET) with ^{90}Y (β^-) or ^{177}Lu (β^-). However, the degree of chemical resemblance has to be validated by in vivo experiments for every targeting vector and chelator combination. Some element dependencies have indeed been observed. Since the uptake can also be followed to a certain degree by SPECT or planar gamma cameras, therapeutic isotopes that also emit low intensities of imageable gamma rays (^{153}Sm, ^{166}Ho, ^{177}Lu, ^{186}Re, ^{188}Re, ^{211}At) allow monitoring of the biodistribution with the therapeutic dose. Usually such therapies are fractionated into smaller administered activities that are repeated regularly. Thus deviations in the uptake can be compensated for in the subsequent treatment cycle.

3.5. ^{177}Lu, a showcase for nuclear physics and radiochemistry

With a convenient half-life of 6.65 days, a low beta energy (0.13 MeV mean) and range (< 2mm) and a low abundance of SPECT imageable gamma rays ^{177}Lu has excellent nuclear decay properties for a therapeutic isotope. Moreover lutetium has the lowest ionic radius among all lanthanides, ensuring particularly stable labelling with macrocyclic ligands. This makes it an optimum isotope for applications including RIT, PRRT and other targeted radionuclide therapies. Even successful use for treatment of bone metastases has been reported.

Direct production of c.a. ^{177}Lu by neutron capture on enriched ^{176}Lu targets in high flux reactors provides a specific activity of about 20 Ci/mg at the moment of production. Thus, after delivery the ratio of radioactive ^{177}Lu to total Lu is about 1:6 to 1:8. This seems sufficient for present PRRT applications and treatment of bone metastases but certain RIT would profit from higher specific activity and preclinical PRRT experiments demonstrated improved targeting with higher specific activity.

In the direct production of c.a. ^{177}Lu a 0.1% branch of the neutron capture reaction leads not to the "useful" $7/2^+$ ground state of ^{177}Lu ($T_{1/2}$=6.65 d)

but to the longer-lived 23/2$^-$ high-spin isomer ^{177m}Lu ($T_{1/2}$=160 d). Thus c.a. ^{177}Lu contains at least 10^{-4} relative activity of ^{177m}Lu, or more when the decay of ^{177g}Lu during transport is considered. When treated with ^{177}Lu for systemic therapy (PRRT or RIT), patients will rapidly excrete the excess activity via urine. The latter is separately collected in nuclear medicine departments of hospitals and only released after sufficient decay (>>10 half-lives) when the remaining activity has dropped below the free limit. Given the long half-life of ^{177m}Lu it would be impractical to keep the waste water for many years to let ^{177m}Lu decay.

A long and tedious challenge for chemists

Ytterbium was first chemically separated, and thus discovered as a new chemical element, in 1878. It took nearly thirty years until chemists managed to separate the chemically very similar lutetium from ytterbium, thus demonstrating its existence as separate element. In 2007, a century after discovery of lutetium, a large-scale radiochemical separation was developed that now allows clean separation of hundreds of patient doses ^{177}Lu from grams of irradiated ytterbium within hours.

Thus, depending on the free limit and local legislation concerning radioactive waste, in certain countries sewage water of nuclear medicine departments that contains c.a. ^{177}Lu cannot be disposed of easily. This may represent a serious bottleneck for the application of this promising radioisotope.

Fortunately ^{177}Lu can also be produced by an *indirect production* path. Here the spin selection rules of beta decay ensure that 9/2$^+$ ^{177}Yb decays only to the wanted ground state and does not populate the high-spin state ^{177m}Lu. Hence, n.c.a. ^{177}Lu is virtually free of ^{177m}Lu and solves the "administrative" waste problem.

In addition to a suitable nuclear reaction and decay path, indirect production also requires a powerful radiochemical separation method. The Lu/Yb separation is particularly challenging since these are neighbouring, chemically very similar lanthanides. After ytterbium was first chemically separated, and thus discovered as a new chemical element, by Jean-Charles Galissard de Marignac in 1878, it took nearly thirty years before three chemists (Georges Urbain, Carl Auer von Welsbach and Charles James) managed independently to separate the chemically very similar lutetium from ytterbium, thus demonstrating its existence as separate element. It was not until the 1990s that large-scale chemical separation of pure lutetium became possible, thus enabling production of LSO crystals for PET instrumentation. In 2007, a century after the discovery of lutetium, large-scale radiochemical separation was developed that now allows separation of hundreds of patient doses of pure ^{177}Lu from grams of irradiated ytterbium within hours. Today irradiations of massive ^{176}Yb targets by a network of several research reactors (FRM2 Munich, BR2 Mol, ILL Grenoble, HFR Petten, SAFARI Pelindaba, etc.) followed by radiochemical separation at ITG Garching assures a regular supply of n.c.a. ^{177}Lu in GMP quality.

It is interesting to compare reactor-based production and accelerator-based production in the example of ^{177}Lu. In principle all (n,γ) reactions could be replaced by (d,p) reactions with the same target/product combination. However, the (d,p) cross-sections are generally lower and so are the deuteron currents available from accelerators and sustainable by the targets. For indirect production paths the final product populated by (n,γ)β$^-$ is also accessible directly by (d,n) reactions. The excitation functions for ^{176}Yb(d,p) and ^{176}Yb(d,n) were recently measured [Man11]. Even if 0.1 mA of deuteron current is sustained over one week on a highly enriched metallic ^{176}Yb target, only about 80 GBq of ^{177}Lu would be produced. Irradiating the same target (about 2 g mass) for a week in a thermal neutron flux of 10^{14} cm^{-2}s^{-1} would produce ten times more ^{177}Lu. Therefore accelerator production with (d,p) and (d,n) reactions is not competitive if the same isotope can be produced in research reactors.

3.6 Synergies of nuclear medicine and nuclear physics

Since its "inception", nuclear medicine has been tightly interwoven with nuclear physics and radiochemistry. Today's use of nuclear medicine directly uses numerous achievements in nuclear physics and radiochemistry, among these more than a dozen outstanding discoveries and techniques that were recognised by Nobel Prizes in Physics and Chemistry.

When the effects of ionising radiation were discovered, these were rapidly introduced into medical practice for treatments via brachytherapy (in French still called Curie therapie) with ^{226}Ra sources. The sudden need for large quantities of ^{226}Ra (a decay product of ^{232}Th present in minerals like Pechblende) triggered the development of a real radiochemical "industry" for large scale separation of gram amounts of ^{226}Ra. In turn the industrial availability of this material enabled new, more complex experiments that required stronger radiation sources. The close collaboration of nuclear physicists and nuclear

medicine and radiology physicians enabled many of the ground-breaking discoveries of the 20th century:

- Discovery of the neutron by Chadwick.
- Discovery of artificial transmutation by Joliot-Curie.
- Szilard-Chalmers reaction (at a hospital).
- The discovery of neutron moderation and its use for more efficient transmutation by Fermi was based on a Rn/Be source with the ^{222}Rn recovered from medical ^{226}Ra sources.
- Later on the ^{99}Mo/^{99m}Tc generator and FDG were developed at the Brookhaven National Laboratory.
- The presently used labelling methods for ^{18}F were developed at the Nuclear Research Centre Jülich.

Nuclear medicine is a relatively young sub-specialisation of medicine. Although its roots can be traced all the way back to George Hevesy's centennial discovery of the tracer principle in 1913 and some of the first medical applications taking place in both the United States and in Europe in 1920–1930, the main breakthrough came in the wake of the Manhattan programme and the "Atoms for Peace" concept. In his famous speech in 1953 president Eisenhower invited the formation of what was to become the IAEA, including in this call not only anti-proliferation and nuclear power measures, but also:

"The more important responsibility of this atomic energy agency would be to devise methods whereby this fissionable material would be allocated to serve the peaceful pursuits of mankind. Experts would be mobilised to apply atomic energy to the needs of agriculture, medicine and other peaceful activities."

During the following years, nuclear medicine developed rapidly into an important sibling to diagnostic radiology. This is normally seen as the result of the many research reactors in the world capable of satisfying the needs of the medical world for diagnostic and therapeutic radioisotopes. Although some early pre-1960 work was done with radium-derived activity and cyclotron-produced neutron-rich isotopes (^{32}P, ^{24}Na, etc.) it was only after the advent of the many research reactors that radioactive isotopes became available at a large scale and on demand. The IAEA soon played a major role in the development of this production capacity by support of research and training programmes, by conferences and by the important publication programme. Within this context, it is worth remarking that the IAEA's effort towards nuclear medicine was initiated outside the medical world, and strangely enough justified by the threat posed by the invention of nuclear weapons.

This advance of nuclear medicine driven by scientific and technological developments from basic physics and most notably from the various national laboratories is seen as a general pattern, which is worth remembering when considering the future role of nuclear physics.

Very important examples of developments in basic science driving medical advance can be noted:

- The development of the cyclotron. This universal workhorse of medical isotope production originated at the University of California Radiation Laboratory and the entire field of cyclotron design and isotope-producing targetry evolved rapidly during the period of the Manhattan programme.
- The gamma camera and the well counter came in the 1950s from Hal Anger working in the same group as the Radiation Lab.
- While the PET scanner concept emerged more or less directly from the medical physics world and under inspiration from CT development, it can be strongly argued that the present day block-ring PET and PET/CT detector development had strong roots in the vast detector arrays of nuclear physics.
- PET/MRI integration had important input from the detector groups at CERN, Fermilab etc.

On the basis of this pattern it can be reasonably argued that the medical field and in general the health of the public has been and will continue to be advanced by important spin-offs from fundamental research in nuclear and particle physics. It seems an almost universal truth that the experimental scientist in basic physics sooner or later starts to think of medical applications. This 'food chain' of innovation into medicine and healthcare should be recognised throughout the EU.

From nuclear physics to medicine and back

The discovery of natural radioactivity, of methods to extract strong sources of isotopes like ^{226}Ra and ^{210}Po and derived neutron sources, and the use of such sources for medical purposes (at the time mainly brachytherapy) triggered the development of a veritable radiochemical industry that provided these isotopes en masse. Frequently nuclear physicists profited from the well equipped medical faculties by borrowing such sources for their research. Discoveries like the production of artificial radioisotopes through neutron activation by Enrico Fermi or the Szilard-Chalmers separation method would not have occurred so quickly without this close synergy. In turn the nuclear physics discoveries quickly found medical applications.

The role of nuclear medicine and PET in pharmaceutical discovery and development

The complexity of instruments, the methods applied, and the underlying structure of training, production capacity and scanner development is now driven by clinical applications. However this infrastructure still supports development of new pharmaceuticals. New pharmaceuticals are by themselves very important for future healthcare and economic growth.

From the outset, diagnostic nuclear medicine and its companion science of clinical physiology have relied upon quantitative measurements of tracer level compound concentrations, unperturbed and in vivo, in man as well as in animals. In the modern PET scanner this quantitative aspect is combined with good spatial resolution and anatomical registration and very high sensitivity. PET radiochemistry based on ^{11}C or ^{18}F allows in vivo measurements of even picomolar concentrations of almost any organic compound.

This has made PET a very important tool in the discovery, development and approval process of modern pharmaceuticals. No other imaging modality can compete with the sensitivity of these nuclear medicine techniques, and the pharmaceutical industry is embracing PET centres in universities to utilise the strength of the technology. Some big pharmaceutical companies even have their own PET departments.

3.7 Joint exploitation of research reactors and accelerators for research and radioisotope production

Only one nuclear reactor worldwide carries isotope production as its main purpose in its name, the HFIR (High Flux Isotope Reactor) in Oak Ridge. However, the isotopes produced at HFIR serve a variety of applications (^{252}Cf for neutron sources, used for bore hole probes in the petrol industry, actinide isotopes for superheavy element research, isotope batteries for satellites, etc.) with medical isotopes (^{188}W, ^{186}Re, ^{117m}Sn, etc.) representing only a minority of the irradiated volume.

Also TRIGA (Training, Research, Isotopes, General Atomic) reactors carry 'isotopes' in their name and indeed part of the fleet of over 40 TRIGA reactors operating worldwide contribute to local and regional radioisotope supply for medicine, in particular in emerging countries.

Other research reactors with less explicit names (HFR, BR2, NRU, SAFARI, MURR and many more) usually serve a variety of purposes at the same time (materials research with irradiated samples, certification of fuel elements, production of industrial isotopes, transmutation doping of silicon, etc.) where medical isotope production is an important but not exclusive use.

Certain research reactors (FRM2, RHF at ILL, OPAL at ANSTO, ORPHEE at LLB, etc.) serve mainly to supply extracted neutron beams that are used for neutron scattering, an important technique where the neutrons serve as a probe for fundamental and applied studies in condensed matter physics, chemistry, biology, materials science, etc. However, these reactors also have in-pile irradiation positions that are used for radioisotope production.

The project to operate two MMIR (MDS Medical Isotope Reactors, previously known as MAPLE) in Canada failed due to technical, regulatory and political problems, but also faced economic problems when it became clear that radioisotope production for medicine alone could not cover the rising project costs. Given this historic precedent it seems today evident that the model of shared use of multipurpose reactors is more efficient and sustainable. Consequently it has been adopted for future facilities (RJH, MYRRHA, PALLAS).

Historically the accelerators of many nuclear physics labs were used to produce new radioisotopes for medical applications before sufficient dedicated medical cyclotrons became available. Today there are still a number of interesting radioisotopes whose production is not covered by medical cyclotrons and thus the joint exploitation of nuclear physics accelerators helps to fill these gaps.

One example is the production of ^{82}Sr that requires protons of more than 60 MeV for efficient use of the $^{85}Rb(p,4n)$ and $^{87}Rb(p,6n)$ reactions. The accelerators of the US DOE laboratories Brookhaven National Laboratory (BNL) and Los Alamos National Laboratory (LANL) were essential in the development of a regular supply chain for ^{82}Sr.

At BNL a linear accelerator is used as proton injector for the Booster synchrotron that can fill the Alternating Gradient Synchrotron (AGS) and ultimately the Relativistic Heavy Ion Collider (RHIC). The LINAC supplies polarised or unpolarised protons to the booster for nuclear physics experiments and the NASA space radiobiology programme. Excess proton beams with energies between 66 and 202 MeV are diverted to the Brookhaven LINAC Isotope Producer (BLIP) station for production of ^{82}Sr, ^{68}Ge and other radioisotopes.

At LANL a 100 MeV proton beam can be branched off from the linear accelerator that is providing 800 MeV protons to the LANSCE spallation neutron source. The 100 MeV protons are sent to the

Isotope Production Facility (IPF) for regular production of ^{82}Sr, ^{68}Ge and many more radioisotopes.

TRIUMF, Canada's National Lab for nuclear and particle physics has as part of its mandate the application of physical techniques for medicine and research in basic life sciences. In keeping with this effort TRIUMF has a strong collaboration with the University of British Columbia (UBC) Department of Medicine and the BC Cancer Agency. A commercial radioisotope manufacturer, Nordion, is co-located at the site where they operate 3 cyclotrons producing a number of products, including ^{201}Tl, ^{123}I, ^{111}In, ^{103}Pd, ^{67}Ga and other isotopes. TRIUMF's 500 MeV cyclotron is designed to extract multiple proton beams of varying energies and intensities, thus the production of ^{82}Sr at 70-90 MeV can be performed simultaneously with ongoing physics experiments in two other locations. In addition there is an active proton therapy programme where patients are treated for ocular melanoma. TRIUMF's nuclear medicine programme is actively pursuing new labelling technologies and radionuclide targetry to support its collaborators and maintain a national and international presence in these research arenas.

iThemba LABS (formerly known as the National Accelerator Centre), a National Facility of the National Research Foundation of South Africa, was designed from the outset to be a multidisciplinary facility for basic and applied nuclear physics research, radiotherapy with protons and neutrons, and radionuclide production. These three main disciplines share the beam from the K=200 separated sector cyclotron (SSC) while a commercial 11 MeV PET cyclotron is exclusively used for radioisotope production. Radionuclide production that receives about 40% of the SSC beam time allocation shares during the week a 66 MeV proton beam with neutron therapy while for proton therapy dedicated scheduled blocks are earmarked. Three bombardment stations, of which two can be simultaneously operated, are routinely used for the production of ^{123}I, ^{82}Sr, ^{68}Ge, ^{67}Ga, ^{22}Na and ^{18}F. The maximum beam current on the vertical beam target station is currently 300 μA and up to four targets can be bombarded simultaneously.

At the Institute of Nuclear Research of the Russian Academy of Sciences in Troitsk, Russia, proton beams of 94 MeV to 158 MeV can be diverted from the linear accelerator that is driving the Moscow Meson Factory. ^{82}Sr is produced routinely and production of ^{117m}Sn, ^{225}Ac, ^{223}Ra, ^{109}Cd, ^{72}Se, etc. has been demonstrated.

While ^{82}Sr was produced in the last decades exclusively at five nuclear physics facilities, clinical trials demonstrated impressively the added value of ^{82}Sr and today demand outpaces by far the production capacity. This triggered the development of additional dedicated and shared facilities.

The 70 MeV cyclotron ARRONAX in Nantes, France, can provide simultaneously two proton beams with up to 375 μA each to produce ^{82}Sr, ^{68}Ge plus other medical isotopes (^{64}Cu, ^{67}Cu, ^{44}Sc, ^{47}Sc, etc.). In addition this accelerator is used for scientific research in radiolysis and nuclear physics (cross-section measurements) [Had11].

From injectors for injectors

^{82}Rb, a short-lived positron emitter, showed improved specificity and accuracy compared to the usual SPECT isotopes in heart perfusion studies and, due to its short half-life (75 seconds), a minimisation of radiation exposure to the patient. With an automated system it is eluted from ^{82}Sr/^{82}Rb generators and directly injected into the patients. Production of ^{82}Sr requires energetic protons (>60 MeV) that are not available from usual medical cyclotrons. For long time all five ^{82}Sr producers worldwide were therefore nuclear physics accelerators and so-called injector accelerators for nuclear or high energy physics laboratories respectively. With rising demand for this promising isotope the first dedicated ^{82}Sr production machines are now coming on-line.

Multiple beams from a new 70 MeV cyclotron at Legnaro National Laboratory, Italy, will drive simultaneously the radioactive ion beam facility SPES and several stations for medical isotope production (LARAMED).

Recently Zevacor Molecular, USA, announced the purchase of a 70 MeV proton cyclotron which will be the first such machine fully dedicated to commercial radioisotope production.

Paul Scherrer Institute (PSI) in Villigen, Switzerland, operates two cyclotrons in series: the so-called Injector 2 which accelerates 2.5 mA proton beams to 72 MeV that are injected into the Ring Cyclotron and post-accelerated to 590 MeV. The Ring Cyclotron feeds the Swiss Muon Source (SμS) with six beamlines available for experiments using muons as sensitive local magnetic probes, and SINQ, a continuous spallation neutron source providing neutrons for neutron scattering, neutron radiography, neutron physics experiments and radioisotope production by (n,γ) reactions. Via a beam splitter part of the 72 MeV proton beam can be sent into the radionuclide production vault. PSI currently pro-

duces ^{44}Sc, ^{64}Cu and ^{161}Tb regularly to aid its users to further research in radiopharmacy and medicine.

Another example where nuclear physics installations play a significant role is the production of alpha emitter ^{211}At. Only few modern cyclotrons (e.g. ARRONAX) can be operated in negative *and* positive ion mode, the latter being essential for efficient acceleration of alpha beams that are required for the ^{209}Bi(α,2n) reaction. However, nuclear physics heavy ion cyclotrons usually operate in positive ion mode and can therefore accelerate alpha beams.

At the Heavy Ion Laboratory of the University of Warsaw the K=160 heavy ion cyclotron serves nuclear physics experiments, but also produces ^{211}At. The ^{211}At is then extracted from the irradiated Bi samples at the Institute of Nuclear Chemistry and Technology where new methods of binding ^{211}At directly or using silver coated TiO_2 nanoparticles to substance P are tested. Substance P is a peptide with high affinity to the receptors of glioma cancer cells. Recently the K=160 cyclotron was complemented by a PETtrace medical cyclotron, intended mainly for a regular supply of PET radiopharmaceuticals.

The nuclear physics cyclotrons at Oslo University, Řež, Debrezen, etc. can also be exploited to produce ^{211}At and thus complement production at the few medical cyclotrons accelerating alpha beams (mainly in Copenhagen, Hannover and Orleans).

The linear accelerator of the new SPIRAL2 facility will have the capability of supplying alpha beams at tunable energy with up to 1 mA current. It has the potential for large-scale production of ^{211}At and other medical radioisotopes.

The isotope separation on-line facility ISOLDE at CERN provides over 1000 different radioisotopes in non-carrier-added quality by combining universal production via 1.4 GeV proton induced reactions with chemically selective ion sources and on-line mass separation. It gives access to high purity radioisotopes for R&D purposes in saturation activities up to ≈1 GBq. Thus promising radioisotopes that cannot be easily produced by established production methods can be supplied for fundamental research in radiobiology and preclinical studies before a dedicated production method has been developed.

Several disciplines (nuclear and atomic spectroscopy, mass measurements, nuclear astrophysics, nuclear solid state physics, etc.) depend on beams from this unique facility. Therefore radioisotopes for medical applications are only available a few times a year.

To overcome this restriction a new project called MEDICIS is now under construction. It will make use of the protons that have traversed the ISOLDE targets for additional beam dump irradiations of appropriate materials. After irradiation these targets are recovered and the radioisotopes of interest are recovered by off-line isotope separation. Thus the great choice of high quality ISOLDE isotopes will become available much more frequently.

TRIUMF has also recently embarked on feasibility studies for the production and isolation of radiotherapeutic isotopes using the ISOL technology as part of its ISAC science programme. Present efforts are aimed at the spallation production of ^{211}At. Additional α- and β-emitting isotopes are under consideration.

3.8 Examples of spinoffs from nuclear physics laboratories

The Cyclotron Research Centre of the University of Louvain-la-Neuve, Belgium, is well known in the field of nuclear physics as the birthplace of post-accelerated radioactive ion beams by first coupling two cyclotrons, a Cyclone 30 cyclotron providing protons for producing radioisotopes and a Cyclone 110 cyclotron for post-acceleration of these radioisotopes. This Cyclone 30, first operating in 1986, was also the prototype of a new powerful and compact type of negative ion cyclotron for medical radioisotope production. Yves Yongen founded in the same year the spinoff company IBA (Ion Beam Applications) that subsequently developed smaller (11 MeV and 18 MeV) and larger (70 MeV, 230 MeV) cyclotrons plus other accelerator types. Today IBA is the world-leading producer of accelerators and associated equipment for radioisotope production, hadrontherapy and industrial applications of sterilisation and ionisation. Today he IBA group has 1300 employees, revenues of 215 M€ and has installed and services over 600 accelerators world-wide. IBA Molecular, the radioisotope production branch co-owned by IBA, operates 36 production sites in Europe and Asia and 13 radiopharmacies in the USA with about 800 employees.

The nuclear physics laboratory TRIUMF in Vancouver, Canada, has a long tradition of hosting on-site medical radioisotope production and was the origin of several spinoff companies supplying medical applications. Based on TRIUMF's technology developed for its 500 MeV negative ion cyclotron (the largest cyclotron in the world), ACSI (Advanced Cyclotron Systems Inc.) built in 1987 the high power cyclotron TR30, the first industrial cyclotron to deliver over 1 mA of extracted proton beams. Later the programme was complemented by the more compact TR-19 and TR-24 cyclotrons (still carrying TR in the name to acknowledge the

TRIUMF technology). In response to the "molybdenum crisis" ACSI launched in 2009 a project, today known as "CycloTec", that aims to meet a good fraction of Canada's ^{99m}Tc needs by production in a National Cyclotron Network by 2015.

GANIL in Caen, France, accelerates heavy ions for nuclear physics experiments and interdisciplinary applications. Key for the availability of intense beams of highly charged ions is the ECR (electron cyclotron resonance) ion source invented by Richard Geller. In 1991 the spinoff company PANTECHNIK was created from a cooperative agreement with IN2P3/CNRS and patent licences of GANIL to commercialise ECR ion sources and related beam diagnostics equipment, beam lines and turnkey solutions. PANTECHNIK is the world leader for ECR ion sources with permanent magnets or superconducting coils for low and high charge state ion beams. Today over 60 ECR ion sources from PANTECHNIK are in use world-wide, of which one third are for medical applications, delivering intense $^{4}He^{2+}$ beams to IBA XP cyclotrons and carbon and proton beams for hadrontherapy accelerators at HIT, CNAO, MedAustron, Siemens and Kirams.

Advanced Accelerator Applications (AAA) is a European pharmaceutical group founded in 2002 as a spinoff from the European Organisation for Nuclear Research (CERN), to develop innovative diagnostic and therapeutic applications and products. AAA focuses on molecular imaging, in particular the production of PET radiopharmaceuticals, and on radionuclide therapy for the personalised treatment of serious diseases. AAA's CEO Stefano Buono, a nuclear physicist, had worked for 10 years with Carlo Rubbia at CERN on the ARC (Adiabatic Resonance Crossing) method that was then further developed by AAA. After 10 years of existence AAA currently has 16 production and R&D facilities that manufacture and commercialise both diagnostic and therapeutic nuclear medicine products, and over 260 employees in 10 countries (France, Italy, Germany, Switzerland, Spain, Poland, Portugal, Israel, USA, Canada).

References

[Ara07] Arazi L *et al.* (2007). Treatment of solid tumors by interstitial release of recoiling short-lived alpha emitters. *Phys Med Biol* **52**: 5025.

[Bat06] Bateman TM *et al.* (2006). Diagnostic accuracy of rest/stress ECG-gated Rb-82 myocardial perfusion PET: comparison with ECG-gated Tc-99m sestamibi SPECT. *J Nucl Cardiol* **13**: 24.

[Bau12] Theranostics, gallium-68, and other radionuclides: A pathway to personalized diagnosis and treatment; recent results in cancer research. Eds Baum R, Rösch FP. Springer (2012).

[Bea11] Beasley P, Heid O. Progress towards a novel compact high voltage electrostatic accelerator. Proc of PAC 2011 Conf, New York, USA, p. 1876.

[Bey04] Beyer GJ *et al.* (2004). Targeted alpha therapy in vivo: direct evidence for single cancer cell kill using 149Tb-rituximab. *Eur J Nucl Med Mol Imaging* **31**: 547.

[Bod13] Bodet-Milin C *et al.* (2013). Radioimmunotherapy of B-cell non-Hodgkin's lymphoma. *Front Oncol* **3**: 177.

[Buc10] Buck AK *et al.* (2010). Economic evaluation of PET and PET/CT in oncology: evidence and methodologic approaches. *J Nucl Med* **51**: 401.

[Car06] Cardis, E. *et al.* (2006). Estimates of the cancer burden in Europe from radioactive fallout from the Chernobyl accident. *Int J Cancer* **119**: 1224.

[Cha06] Chatal JF *et al.* (2006). Survival improvement in patients with medullary thyroid carcinoma who undergo pretargeted anti–carcinoembryonic-antigen radioimmunotherapy: A collaborative study with the French Endocrine Tumor Group. *J Clin Oncol* **24**: 1705.

[Cha11] Champion J *et al.* (2011). Assessment of an effective quasirelativistic methodology designed to study astatine chemistry in aqueous solution. *Phys Chem Chem Phys* **13**: 14984.

[Cle11] Clemente G et al. (2011). Development of room temperature crossbar-H-mode cavities for proton and ion acceleration in the low and medium beta range, *Phys Rev ST Accel Beams* **14**: 110101.

[Dad08] Dadachova E. (2008). Radioimmunotherapy of infection with Bi-labeled antibodies. *Curr Radiopharm* **1**: 234.

[Das13] Dash A, Knapp Jr FF, Pillai MRA. (2013). ^{99}Mo/^{99m}Tc separation: An assessment of technology options. *Nucl Med Biol* **40**: 167.
[DDM2] Study on European population doses from medical exposure. Dose Datamed 2 draft report from 25.1.2013. http://ddmed.eu
[Hab11] Habs D, Köster U. (2011). Production of medical radioisotopes with high specific activity in photonuclear reactions with γ -beams of high intensity and large brilliance. *Appl Phys B* **103**: 501.
[Jen12] Jensen M. (2012). Particle accelerators for PET radionuclides. *Nucl Med Rev* **15** Supp C:C9.
[Jur02] Jurcic JG *et al.* (2002). Targeted alpha particle immunotherapy for myeloid leukemia. *Blood* **100**: 1233.
[Kas11] Kassis AI *et al.* (2011). Molecular and cellular radiobiological effects for Auger emitting radionuclides. *Radiat Prot Dosim* **143**: 241.
[Kha11] Khan S et al. (2011). Quality of life in 265 patients with gastroenteropancreatic or bronchial neuroendocrine tumors treated with [^{177}Lu-DOTA0,Tyr3]octreotate. *J Nucl Med* **52**: 1361.
[Kri13] Krijger G *et al.* (2013). The necessity of nuclear reactors for targeted radionuclide therapies. *Trends Biotechnol* **31**: 390.
[Kwe08] Kwekkeboom DJ *et al.* (2008). Treatment with the radiolabeled somatostatin analog [^{177}Lu-DOTA0,Tyr3]octreotate: toxicity, efficacy, and survival. *J Clin Oncol* **26**: 2124.
[Leb05] Lebeda O *et al.* (2005). A new internal target system for production of ^{211}At on the cyclotron U-120M, *Appl Radiat Isot* **63**: 49.
[Leb12] Lebeda O *et al.* (2012). Assessment of radionuclidic impurities in cyclotron produced ^{99m}Tc. *Nucl Med Biol* **39**:1286.
[Led10] Ledingham KWD, Galster W. (2010). Laser-driven particle and photon beams and some applications. *New J Phys* **12**: 045005.
[Lew05] Lewington VJ. (2005). Radioisotopes for the palliation of metastatic bone cancer: a systematic review. *J Nucl Med* **46** Supp **1**:38S.
[Lie07] Liersch T *et al.* (2007). Update of carcinoembryonic antigen radioimmuno-therapy with ^{131}I-labetuzumab after salvage resection of colorectal liver metastases: comparison of outcome to a contemporaneous control group. *Ann Surg Oncol* **14**: 2577.
[Mae11] Maecke HR, Reubi JC. (2011). Somatostatin receptors as targets for nuclear medicine imaging and radionuclide treatment. *J Nucl Med* **52**: 841.
[Man11] Manenti S *et al.* (2011). Excitation function for deuteron induced nuclear reactions on natural ytterbium for production of high specific activity ^{177g}Lu in no-carrier-added form for metabolic radiotherapy. *Appl Radiat Isot* **69**: 37.
[Mar08] Marcassa C *et al.* (2008). Clinical value, cost-effectiveness, and safety of myocardial perfusion scintigraphy: a position statement. *Eur Heart J* **29**: 557.
[Mor08] Morschhauser F *et al.* (2008). Phase III trial of consolidation therapy with yttrium-90-ibritumomab tiuxetan compared with no additional therapy after first remission in advanced follicular lymphoma. *J Clin Oncol* **26**: 5156.
[Mor13] Morschhauser F *et al.* (2013). ^{90}Yttrium-ibritumomab tiuxetan consolidation of first remission in advanced-stage follicular Non-Hodgkin Lymphoma: Updated results after a median follow-up of 7.3 years from the international, randomized, phase III first-line indolent trial. *J Clin Oncol* **31**: 1977.
[Mue12] Müller C *et al.* (2012). A unique matched quadruplet of terbium radioisotopes for PET and SPECT and for α- and β-radionuclide therapy: an in vivo proof-of-concept study with a new receptor-targeted folate derivative; *J Nucl Med* **53**: 1951.
[NEA10] OECD/NEA. The supply of medical radioisotopes. Review of potential Molybdenum-99/Technetium-99m production technologies. 2010.
[NEA11] OECD/NEA. The supply of medical radioisotopes: the path to reliability. 2011.
[NEA12] OECD/NEA. A supply and demand update of the Molybdenum-99 market. 2012.
[Par13] Parker C *et al.* (2013). Alpha emitter radium-223 and survival in metastatic prostate cancer. *New England J Med* **369**: 213.
[Pon10] Ponsard B. Mo-99 supply issues: report and lessons learned, European Nuclear Society, ENS RRFM 2010 Transactions.
[Qai14] Qaim SM *et al.* (2014). Evaluation of excitation functions of ^{100}Mo(p,d+pn)^{99}Mo and ^{100}Mo(p,2n)^{99m}Tc reactions: Estimation of long-lived Tc-impurity and its implication on the specific activity of cyclotron-produced ^{99m}Tc. *Appl Radiat Isot* **85**: 101.
[Reg27] Regaud C, Lacassagne A. (1927). La radiosensibilité envisagée dans ses manifestations generales. *Radiophysiologie et Radiothérapie* **1**: 95.

[Ric82] Richards P, Tucker WD, Srivastava SC. (1982). Technetium-99m: An Historical Perspective. *Int J Appl Radiat lsot* **33**: 793.
[Rot13] Rothe S et al. (2013). Measurement of the first ionization potential of astatine by laser ionization spectroscopy. *Nature Comm* **4**: 1835.
[RRDB] IAEA's Research Reactor Database (RRDB). http://nucleus.iaea.org/RRDB
[Sch11] Schmor P. (2011). Review of cyclotrons for the production of radioactive isotopes for medical and industrial applications. *Rev Accel Sci Techn* **4**:103.
[Sch13] IAEA Directory of cyclotrons used for radionuclide production in member states, 2013 update by Schlyer DJ, pers comm.
[Ste11] Stevens Anthony, Development of PET in Western Europe, presented at EANM 2011.
[UNS08] Sources and effects of ionizing radiation. UNSCEAR 2008, volume II: Scientific Annex D, Effects due to radiation from the Chernobyl accident. UN New York, 2011.
[Zal08] Zalutsky MR *et al.* (2008). Clinical experience with α-particle–emitting 211At: treatment of recurrent brain tumor patients with ^{211}At-labeled chimeric antitenascin monoclonal antibody 81C6. *J Nucl Med* **49**: 30.

List of Contributors (Chapter III)

- **Marie-Claire Cantone,** Italy – *convener*
- **Ferid Haddad,** France
- **Sotirios Harissopoulos,** Greece
- **Mikael Jensen,** Denmark
- **Ari Jokinen,** Finland – *NuPECC liaison*
- **Itzhak Kelson,** Israel
- **Ulli Köster,** France – *convener*
- **Ondrej Lebeda,** Czech Republic
- **Bernard Ponsard,** Belgium
- **Uli Ratzinger,** Germany
- **Thierry Stora,** Switzerland
- **Ferenc Tarkanyi,** Hungary
- **Piet Van Duppen,** Belgium – *NuPECC liaison*

Valuable input was received from Paul Beasley (Siemens Healthcare) José Benlliure (University of Santiago), David Brasse (IPHC), Marc Garland (DOE), Tom Ruth (TRIUMF), Lucia Sarchiapone (LNL), Paul Schaffer (TRIUMF), Peter Thirolf (LMU), Nick van der Meulen (PSI), Erik Van Lier (ACSI) and Etienne Vermeulen (iThemba labs).

We are very grateful to the following individuals and organisations for providing statistical data on the use of radionuclides in nuclear medicine:
Juan Carlos Alonso Farto (SEMNIM, Spain) Bernard Aubert (IRSN France), Ursula Bär (Federal Statistical Office, Germany), Dieter Cernohorski (Federal Office of Economics and Export Control, Germany), Panicos Demitriades (Department of Labour Inspection, Cyprus), Andrejs Dreimanis (State Environmental Service, Latvia), Marisa España Lopez (H.U. de la Princesa, Madrid), Cécile Etard (IRSN France), Jörg Kotzerke (DGN & TU Dresden, Germany), Leszek Krolicki (Medical Univ. of Poland), Reto Linder (Federal Office of Public Health, Bern, Switzerland), Dietmar Noßke (Federal Office for Radiation Protection, Germany), Sigrid Richter (Bavarian State Office for Environment), Anthony Samuel (Mater Dei Hospital, Malta), Elena Shubina (Environmental Board, Estonia), Damijan Škrk (Slovenian Radiation Protection Administration), Pedro Teles (IST/ITN Portugal), Gertrud Vierkant (Federal Statistical Office, Germany), Stavroula Vogiatzi (Greek Atomic Energy Commission) as well as the State Institute for Drug Control Czech Republic, the State Institute of Radiation Protection Denmark, the Japan Radioisotope Association, and Informe del Consejo de Seguridad Nuclear al Congreso de los Diputados y al Senado Spain.

Annexes

Annex I: **Contributors**

- **Faiçal Azaiez** (France)
- **Jacques Balosso** (France)
- **Guido Baroni** (Italy)
- **Marcus Bleicher** (Germany)
- **Angela Bracco** (Italy)
- **Sytze Brandenburg** (Netherlands)
- **David Brasse** (France)
- **Lucas Norberto Burigo** (Brazil)
- **Marie-Claire Cantone** (Italy)
- **Piergiorgio Cerello** (Italy)
- **Paolo Colautti** (Italy)
- **Stephanie Combs** (Germany)
- **Giacomo Cuttone** (Italy)
- **Jürgen Debus** (Germany)
- **Christophe de La Taille** (France)
- **Alberto Del Guerra** (Italy)
- **Ludovic Demarzi** (France)
- **Peter Dendooven** (Netherlands)
- **Jan Dobeš** (Czech Republic)
- **Marco Durante** (Germany)
- **Wolfgang Enghardt** (Germany)
- **Laura Evangelista** (Italy)
- **Enrico Fagotti** (Italy)
- **Fine Fiedler** (Germany)
- **Sydney Galès** (France)
- **Dietmar Georg** (Austria)
- **Christian Graeff** (Germany)
- **Thomas Haberer** (Germany)
- **Jean-Louis Habrand** (France)
- **Ferid Haddad** (France)
- **Sotirios Harissopulos** (Greece)
- **Mikael Jensen** (Denmark)
- **Ari Jokinen** (Finland)
- **Itzhak Kelson** (Israel)
- **Gabriele-Elisabeth Körner** (Europe)
- **Ulli Köster** (France)
- **Ian Lazarus** (United Kingdom)
- **Ondrej Lebeda** (Czech Republic)
- **Hamid Mammar** (France)
- **Adam Maj (**Poland)
- **Alejandro Mazal** (France)
- **Samuel Meyroneinc** (France)
- **Igor Mishustin** (Russian Federation)
- **Guillaume Montemont** (France)
- **Christian Morel** (France)
- **Alex Murphy** (United Kingdom)
- **Josep P. Oliver** (Spain)
- **Pawel Olko** (Poland)
- **Katia Parodi** (Germany)
- **Annalisa Patriarca** (France)
- **Bernard Ponsard** (Belgium)
- **Marlen Priegnitz** (Germany)
- **Igor Pshenichnov** (Russian Federation)
- **Magdalena Rafecas** (Spain)
- **Uli Ratzinger** (Germany)
- **Frauke Roellinghoff** (Belgium)
- **Dieter Röhrich** (Norway)
- **Christoph Scheidenberger** (Germany)
- **Sabine Schott** (France)
- **Paola Solevi** (Spain)
- **Thierry Stora** (Switzerland)
- **Ferenc Tárkányi** (Hungary)
- **Peter G. Thirolf** (Germany)
- **Irene Torres-Espallardo** (Spain)
- **José Manuel Udias** (Spain)
- **Nick van der Meulen** (Belgium)
- **Piet Van Duppen** (Belgium)
- **Claas Wessels** (France)

Annex II: NuPECC Committee

Chair:

- **Angela Bracco**
  Milano (Italy)

Members:

- **Faiçal Azaiez**
  Orsay (France)
- **Maria Borge**
  Madrid (Spain)
- **Gheorghe Cata-Danil**
  Bucharest (Romania)
- **Philippe Chomaz**
  Gif-sur-Yvette (France)
- **Jan Dobeš**
  Řež (Czech Republic)
- **António Fonseca**
  Lisboa (Portugal)
- **Jens Gaardhøje**
  Copenhagen (Denmark)
- **Sotirios Harissopulos**
  Athens (Greece)
- **Tord Johansson**
  Uppsala (Sweden)
- **Ari Jokinen**
  Jyväskylä (Finland)
- **Klaus Jungmann**
  Groningen (The Netherlands)
- **Bernd Krusche**
  Basel (Switzerland)
- **Marek Lewitowicz**
  Caen (France)
- **Adam Maj**
  Krakow (Poland)
- **Đuro Miljanić**
  Zagreb (Croatia)
- **Alexander Murphy**
  Edinburgh (United Kingdom)
- **Eugenio Nappi**
  Bari (Italy)
- **Paul Nolan**
  Liverpool (United Kingdom)
- **Joakim Nystrand**
  Bergen (Norway)
- **Günther Rosner**
  Darmstadt (Germany)
- **Christelle Roy**
  Strasbourg (France)
- **Raimond Snellings**
  Utrecht (The Netherlands)
- **Horst Stöcker**
  Darmstadt (Germany)
- **Hans Ströher**
  Jülich (Germany)
- **Piet Van Duppen**
  Leuven (Belgium)
- **Jochen Wambach**
  Darmstadt (Germany)
- **Wolfram Weise**
  ECT* Trento (Italy)
- **Eberhard Widmann**
  Wien (Austria)
- **György Wolf**
  Budapest (Hungary)

Observers:

NPB/EPS:

- **Klaus Peters**
  GSI Darmstadt (Germany)

NSAC:

- **Don Geesaman**
  Argonne (USA)

ANPhA:

- **Yanlin Ye**
  Beijing (China)

NuPECC Scientific Secretary:

- **Gabriele-Elisabeth Körner**
  c/o Physik-Department E12
  Technische Universität München
  85748 Garching – Germany
  Tel: +49 172 89 15 011 / +49 89 2891 2293
  Email: sissy.koerner@ph.tum.de

European Science Foundation:

- **Jean-Claude Worms**
  Head of Science Support Office
- **Nathalie Geyer-Koehler**
  Administrative Coordinator

European Science Foundation
1 quai Lezay-Marnésia – BP 90015
67080 Strasbourg Cedex – France
Tel: +33 3 88 76 71 48
Email: ngeyer@esf.org

- **^{18}FDG:** Fluorodeoxyglucose with radioactive ^{18}F.
- **α/β ratio:** A measure of tissue radiosensitivity provided by the ratio of the two parameters used to describe the radiation effects (E) as a function of the dose (D): $E=\alpha D+\beta D^2$. A high α/β ratio implies a small sparing for fractionation, and is common in early responding normal tissues (e.g. skin and colon) and many tumours. On the other hand, a low α/β ratio corresponds to a strong reduction of the effect with fractionation, and is generally observed in late responding tissues (e.g. lung and kidney).
- **Advantage-depth dose-rate (ADDR):** In BNCT, it is defined at the depth in tissue where a tumour receives the same equivalent dose rate of the normal healthy tissue. Deeper tumours would receive a lower dose-rate than the normal tissue.
- **APDs:** Avalanche photodiodes (PS-APD: position-sensitive APD).
- **API:** Atmospheric pressure interface.
- **ASIC:** Application-specific integrated circuit.
- **BGO:** Bismuth germanium oxide.
- **BNCT:** Boron neutron capture therapy.
- **Bq (Becquerel):** SI unit of activity. 1 Bq = 1 decay per second.
- **Brachytherapy:** Introduction of closed sources, that emit (short-range) ionising radiation, into the body or close to the body. Formerly a discipline closer to radiology than to nuclear medicine.
- **Bragg peak:** Region where charged particles release most of their energy in matter. It is very close to the range of the particle in the target.
- **CCD:** Charged coupled device.
- **CdTe:** Cadmium telluride.
- **CdZnTe:** Cadmium zinc telluride.
- **Ci (Curie):** A unit of activity that is still used in nuclear medicine. 1 Ci = 37 GBq, 1 mCi = 37 MBq.
- **CMOS:** Complementary metal–oxide–semiconductor.
- **CNAO:** Centro Nazionale Adroterapia (http://www.cnao.it).
- **CPO:** Centre de Protonthérapie Orsay (http://protontherapie.curie.fr/).
- **CS:** Compressed sensing image reconstruction.
- **CT:** Computed tomography. Several X-ray transmission scans are taken at different angles rotated around a single axis and numerically combined to a 3D view. This provides a morphological image of the body.
- **CZT:** Cadmium zinc telluride.
- **Cyclotron:** A type of particle accelerator in which charged particles accelerate outwards from the centre along a spiral path.
- **DESI:** Desorption electrospray ionisation.
- **DOI:** Depth of interaction.
- **Dose:** Energy deposited per unit mass by ionising radiation. It is measured in gray (Gy). 1 Gy = 1 J/kg.
- **Dose equivalent:** Physical dose corrected for the biological effectiveness. Since radiation with different LET have different biological effects, physical dose must be multiplied by the RBE to account for radiation quality. In therapy, the product of the physical dose x RBE is generally expressed in gray-equivalent (GyE) or Gy(RBE).
- **Dose rate:** Dose delivered per unit time (usually in Gy/min).
- **ENLIGHT:** European Network for Light Ion Therapy (http://enlight.web.cern.ch/).
- **Fractionation:** The therapeutic radiation dose is very high (up to 60–70 Gy), but is normally delivered in daily fractions of approximately 2 Gy for effective sparing of the normal tissue.
- **FBP:** Filtered backprojection.
- **FFAG:** Fixed-field alternating gradient synchrotron.
- **FPGA:** Field programmable gate array.
- **FWHM:** full width at half maximum.
- **GAGG:** $Gd_3Al_2Ga_3O_{12}$ based scintillator.
- **GaAs:** Gallium arsenide.
- **GPU:** Graphical processor unit.
- **GSI:** Helmholtz Centre for Heavy Ion therapy (www.gsi.de).
- **HIT:** Heidelberg Ion Therapy Centre (http://www.klinikum.uni-heidelberg.de/Willkommen.113005.0.html).
- **IGRT:** Image-guided radiation therapy.
- **IMPT:** Intensity modulated proton therapy.
- **IMRT:** Intensity modulated radiation therapy.
- **IMS:** Imaging mass spectroscopy.
- **Interplay:** Inhomogeneity in treatment plan caused by the uncorrelated motion of the scanning beam and of the target organ.
- **kVp:** Peak kilovoltage.
- **Linear energy transfer (LET):** Energy deposited per unit track in the tissue by charged particles. It is generally measured in kilo-electronvolt per

micron in tissue (keV/μm). LET depends on the ion charge and velocity.

- **Linear-no-threshold (LNT):** The model commonly adopted by the International Regulatory Agencies to extrapolate the radiation risk at low doses. It is assumed that the cancer risk is always directly proportional to the absorbed dose.
- **LC:** local control.
- **Lesion:** Any abnormality in the tissue of an organism.
- **LSO:** Lutetium oxyorthosilicate (Lu_2SiO_5).
- **LXe:** Liquid xenon.
- **LYSO:** Lutetium yttrium orthosilicate (cerium-doped)($Lu_{1.8}Y_{0.2}SiO_5(Ce)$).
- **MALDI:** Matrix-assisted laser desorption ionisation.
- **MA-PMT:** Multi-anode photomultiplier tube.
- **MAP:** (Bayesian framework) maximum a-priori algorithm.
- **MBq:** Millions of becquerel (millions of radioactive decays per second).
- **MC:** Monte Carlo
- **MIP:** Maximum intensity projection
- **ML:** Maximum likelihood (statistical technique).
- **MLEM:** Maximum-likelihood-expectation-maximisation algorithm.
- **MPPC:** Multi-pixel photon counter.
- **MR:** Magnetic resonance.
- **MRI:** Nuclear magnetic resonance imaging provides a morphological image with better soft tissue contrast than CT and no radiation burden. However, it cannot be used directly for attenuation correction of PET or SPECT.
- **MRS:** Magnetic resonance spectrograph.
- **MS:** Mass spectroscopy.
- **MS/MS:** Two stage 'tandem' mass spectroscopy.
- **Multi-modality imaging:** combination of different imaging modalities such as PET/CT, PET/MR, SPECT/CT, ultrasound, etc.
- **NIRS:** National Institute for Radiological Sciences (http://www.nirs.go.jp).
- **Normal tissue complication probability (NTCP):** Probability of inducing early or late morbidity with the radiation treatment.
- **Nuclear medicine:** Medical discipline using open radiation sources in the human body for diagnostic or therapeutic applications.
- **OS:** Overall survival.
- **OSEM:** Ordered-subsets-expectation-maximisation algorithm.
- **PET:** In positron emission tomography the emitted positrons annihilate, producing two 511 keV gamma rays emitted back to back. Coincident detection provides the line of response. Detection of many such events allows computation of the 3D distribution of the positron emitters, i.e. functional imaging.
- **PET/CT and SPECT/CT:** combination of PET and CT or SPECT and CT into a single device for improved combination of functional and morphological images. The CT scan also helps attenuation correction.
- **PMT:** Photomultiplier tube.
- **PRRT:** Peptide receptor radionuclide therapy uses therapeutic radionuclides linked to peptides that target specific peptide receptors which are overexpressed on the cancer cells.
- **PTCOG:** Particle Therapy Co-Operative Group (http://ptcog.web.psi.ch/).
- **PSI:** Paul Scherrer Institut (www.psi.ch).
- **Range:** Distance that a charged particle reaches in a target before losing all its initial energy and stopping. The range depends on the type of particle, on its initial energy and on the material through which it passes. In CPT, the energy of the beam must be high enough to reach deep-seated tumours.
- **RECIST:** Response evaluation criteria in solid tumours is a set of published rules that define when cancer patients improve ("complete or partial response"), stay the same ("stable disease") or worsen ("progressive disease") during treatments.
- **RPC:** Resistive plate chamber.
- **Relative biological effectiveness (RBE):** The ratio of the dose D_R of a reference radiation (typically γ- or X-rays) and D_t of a test radiation (e.g. neutrons, protons, heavy ions etc.) that produce the same biological effect. It depends on several factors including the dose, dose-rate, biological endpoint, radiation test LET, tissue etc.
- **RFQ:** Radio frequency quadrupole.
- **RIT:** Radioimmunotherapy uses therapeutic radionuclides linked to antibodies that target specific antigens which are overexpressed on the cancer cells.
- **SAR:** Specific absorption rate.
- **SBRT:** Stereotactic body radiation therapy.

- **Scanning:** Delivery of a pencil particle beam into the target. 2D scanning is achieved by magnetic stirrers, and the depth is changed either by active energy changes or by passive attenuators.
- **Scintigraphy** is a functional imaging technique providing 2D planar images of a gamma emitter distributed in the body registered with a gamma camera. Position resolution is achieved via suitable collimators.
- **SiPM:** Silicon photomultipliers (dSiPM: digital SiPM).
- **Sparing effect:** When the same radiation dose is delivered in multiple fraction, at intervals of several hours (typically 1 day), the biological damage is generally reduced (sparing effect). Fractionation is used in radiotherapy to avoid severe normal tissue morbidity. The sparing effect depends on the fractionation scheme, tissue (α/β ratio), dose/fraction, and radiation quality.
- **SPECT:** Single photon emission computed tomography. 2D scintigraphic images from different directions are combined to compute a 3D image for functional imaging with improved spatial resolution.
- **Spread-out-Bragg-peak (SOBP):** The Bragg peak is too narrow to cover large tumours, and must therefore be widened by passive or active superimposition of beams with different energy.
- **SRM:** System response matrix.
- **Target volumes in radiotherapy:**
  Gross tumour volume (GTV): Tumour volume visible in the radiological imaging of the patient.
  Clinical target volume (CTV): GTV+ plus a margin for sub-clinical disease spread which therefore cannot be fully imaged.
  Internal target volume (ITV): CTV+ margins to include target motion.
  Planning target volume (PTV): CTV+ a margin for uncertainties in planning, positioning, or treatment delivery.
  Organ at risk (OAR): Volume of an organ close to the tumour which should be spared to avoid side effects.
  The treatment planning is finalised to increase the dose to the PTV (high TCP) keeping as low as possible the dose to the OARs (low NTCP).
- **TCP:** Tumour control probability. Probability of killing the primary tumour.
- **TEPC:** Tissue equivalent proportional chamber.
- **Theranostics:** A modality of personalised medicine where individual patients are first tested with a diagnostic procedure (e.g. SPECT or PET) to judge the probable response to a therapy before the latter is applied. This assures that only probable responders are treated, thus improving the ratio of overall success vs side-effects.
- **TOF:** Time of flight.
- **Tomograph:** A device used for imaging in sections.
- **TPC:** Time projection chamber.
- **TPS:** Treatment planning system.
- **TV:** (CS based) total-variation approach to image reconstruction.
- **UFDS:** Ultrafast silicon detectors.
- **WEPL:** Water-equivalent path length.

ISBN: 978-2-36873-008-9
Printing: Ireg Strasbourg

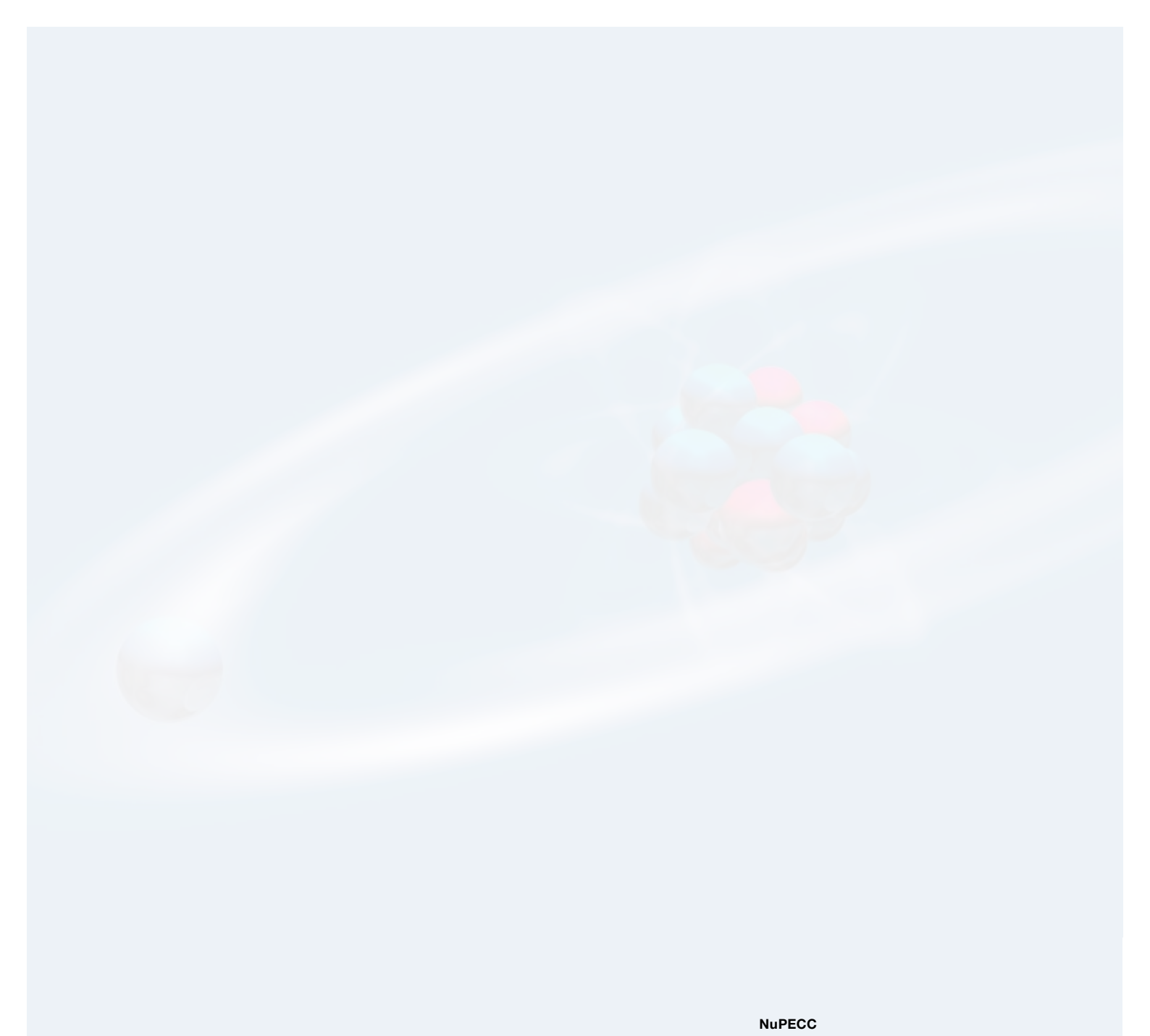

NuPECC

Professor Angela Bracco
NuPECC Chair
Università degli Studi di Milano
Dipartimento di Fisica and INFN sez. Milano
Via Celoria 16 • 20133 Milano • Italy
Tel: +39 02 50317252
Email: bracco@mi.infn.it

Dr Gabriele-Elisabeth Körner
NuPECC Scientific Secretary
c/o Physik-Department E12
Technische Universität München
85748 Garching • Germany
Tel: +49 172 89 15 011 / +49 89 2891 2293
Email: sissy.koerner@ph.tum.de

www.nupecc.org

European Science Foundation

1 quai Lezay-Marnésia • BP 90015
67080 Strasbourg cedex • France
Tel: +33 (0)3 88 76 71 00
Fax: +33 (0)3 88 37 05 32

www.esf.org

April 2014 – Print run: 2 000
Graphic design: Dans les villes, Strasbourg